ISSN 0031 - 9465

PHYTOPATHOLOGIA MEDITERRANEA

Plant health and food safety

Volume 65 • No. 2 • August 2026

The international journal of the
Mediterranean Phytopathological Union

FIRENZE UNIVERSITY PRESS

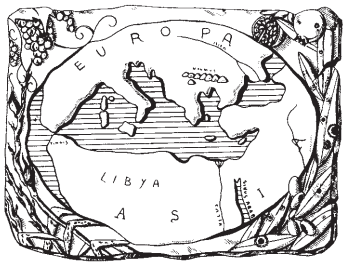

PHYTOPATHOLOGIA MEDITERRANEA

Plant health and food safety

The international journal edited by the Mediterranean Phytopathological Union
founded by A. Ciccarone and G. Goidànich

Phytopathologia Mediterranea is an international journal edited by the Mediterranean Phytopathological Union. The journal's mission is the promotion of plant health for Mediterranean climate and regions, safe food production, and the transfer of knowledge on diseases and their sustainable management.
The journal deals with all areas of plant pathology, including epidemiology, disease control, biochemical and physiological aspects, and utilization of molecular technologies. All types of plant pathogens are covered, including fungi, nematodes, protozoa, bacteria, phytoplasmas, viruses, and viroids. Papers on mycotoxins, biological and integrated management of plant diseases, and the use of natural substances in disease and weed control are also strongly encouraged. The journal focuses on phytopathology and closely related fields in the Mediterranean agro-ecological regions. The journal includes three issues each year, publishing Reviews, Original research papers, Research notes, New or unusual disease reports, News and opinion, Current topics, Commentaries, and Letters to the Editor.

EDITORS-IN-CHIEF

Laura Mugnai – University of Florence, DAGRI, Plant pathology and Entomology section, P.le delle Cascine 28, 50144 Firenze, Italy
Phone: +39 055 2755861
E-mail: laura.mugnai@unifi.it

Richard Falloon – New Zealand Institute for Plant & Food Research (retired)
Phone: +64 3 337 1193 or +64 27 278 0951
Email: richardefalloon@gmail.com

CONSULTING EDITOR

G. Surico, DAGRI, University of Florence, Italy

EDITORIAL BOARD

J. Armengol, Universidad Politécnica de Valencia, Spain
S. Banniza, University of Saskatchewan, Canada
A. Bertaccini, Alma Mater Studiorum, University of Bologna, Italy
A.G. Blouin, Plant & Food Research, Auckland, New Zealand
R. Buonaurio, University of Perugia, Italy
N. Buzkan, Imam University, Turkey
T. Caffi, Università Cattolica del Sacro Cuore, Piacenza, Italy
I.L.P.M. da Conceição, University of Coimbra, Portugal
U. Damm, Senckenberg Museum of Natural History Görlitz, Germany
A.M. D'Onghia, CIHEAM/Mediterranean Agronomic Institute of Bari, Italy
A. Eskalen, University of California, Davis, CA, United States
T.A. Evans, University of Delaware, Newark, DE, USA
A. Evidente, University of Naples Federico II, Italy
M. Garbelotto, University of California, Berkeley, CA, USA
S. Gargouri, INRAT-Tunisi, Tunisia
L. Ghelardini, University of Florence, Italy
V. Guarnaccia, University of Turin, Italy
P. Kinay Teksür, Ege University, Bornova Izmir, Turkey
S. Kumari, ICARDA, Terbol Station, Lebanon
A. Lanubile, Università Cattolica del Sacro Cuore, Piacenza, Italy
M. Masiello, National Research Council, (CNR), Bari, Italy
L. Mostert, Faculty of AgriSciences, Stellenbosh, South Africa
J. Murillo, Universidad Publica de Navarra, Spain
J.A. Navas-Cortes, CSIC, Cordoba, Spain
L. Palou, Centre de Tecnologia Postcollita, Valencia, Spain
E. Paplomatas, Agricultural University of Athens, Greece
I. Pertot, University of Trento, Italy
A. Picot, Univerisité de Bretagne Occidental, LUBEM, Plouzané, France
D. Rubiales, Institute for Sustainable Agriculture, CSIC, Cordoba, Spain
J-M. Savoie, INRA, Villenave d'Ornon, France
A. Siah, Yncréa HdF, Lille, France
A. Tekauz, Cereal Research Centre, Winnipeg, MB, Canada
D. Tsitsigiannis, Agricultural University of Athens, Greece
J.R. Úrbez-Torres, Agriculture and Agri-Food Canada, Canada
J.N. Vanneste, Plant & Food Research, Sandringham, New Zealand
M. Vurro, National Research Council (CNR), Bari, Italy
A.S Walker, BIOGER, INRAE, Thiverval-Grignon, France
M.J. Wingfield, University of Pretoria, South Africa

DIRETTORE RESPONSABILE

Giuseppe Surico, DAGRI, University of Florence, Italy
E-mail: giuseppe.surico@unifi.it

EDITORIAL OFFICE STAFF

DAGRI, Plant pathology and Entomology section, University of Florence, Italy
E-mail: phymed@unifi.it, Phone: ++39 055 2755861/862
Editorial Assistant - **Sonia Fantoni**
Editorial office staff - **Angela Gaglier**

PHYTOPATHOLOGIA MEDITERRANEA

The international journal of the Mediterranean Phytopathological Union

Volume 65, August, 2026

Firenze University Press

Phytopathologia Mediterranea. The international journal of the Mediterranean Phytopathological Union
https://www.fupress.com/pm
ISSN 0031-9465 (print) | ISSN 1593-2095 (online)
Published three times a year

Editor-in-Chief:
Laura Mugnai, University of Florence, Italy
Richard Falloon, New Zealand Institute for Plant & Food Research, New Zealand

Direttore Responsabile: Giuseppe Surico, University of Florence, Italy
Iscritto al Tribunale di Firenze con il n° 4923 del 5-1-2000

© 2026 Author(s)

Content license: except where otherwise noted, the present work is released under Creative Commons Attribution 4.0 International license (CC BY 4.0: https://creativecommons.org/licenses/by/4.0/legalcode). This license allows you to share any part of the work by any means and format, modify it for any purpose, including commercial, as long as appropriate credit is given to the author, any changes made to the work are indicated and a URL link is provided to the license.

Metadata license: all the metadata are released under the Public Domain Dedication license (CC0 1.0 Universal: https://creativecommons.org/publicdomain/zero/1.0/legalcode).

Published by Firenze University Press

Firenze University Press
Università degli Studi di Firenze
via Cittadella, 7, 50144 Firenze, Italy
www.fupress.com

Phytopathologia Mediterranea
The international journal of the
Mediterranean Phytopathological Union

Firenze University Press
www.fupress.com/pm

New or Unusual Disease Reports

First report of camellia ring spot associated virus 3 in *Camellia japonica* in Europe

Francesco DESIDERIO[1], Myeonghwan KWAK[2], Eui-Joon KIL[2], Giuseppe PARRELLA[3,*]

[1] *Institute for Bioscience and Bioresources, National Research Council (IBBR-CNR), 90146, Palermo, Italy*
[2] *Department of Plant Medicals, Gyeongkuk National University, 36729 Andong, Republic of Korea*
[3] *Institute for Sustainable Plant Protection, National Research Council (IPSP-CNR), 80055 Portici (NA), Italy*
*Corresponding author. E-mail: giuseppe.parrella@cnr.it

Summary. Numerous viruses have been described in camellia, often found in association, and a variety of symptoms have been associated with these infections. In this study, a plant with chlorotic spots, including complete yellowing of the leaves, was subjected to high-throughput sequencing (HTS). Three viral contigs were identified by HTS, and complete genome sequences of a new isolate of camellia ring spot associated virus 3 (CRSaV-3) were determined using nested PCR to bridge the gap between discontinuous contigs. The new CRSaV-3 isolate shared the highest percentage of nucleotide identity (87.1%) with the American isolate CJ5_676. This represents the first report of CRSaV-3 in symptomatic camellia in Europe and, since only this virus was diagnosed, for the first time it was possible to reliably associate the symptoms observed in camellia to a specific CRSaV-3 isolate.

Keywords. CRSaV-3, High Throughput Sequencing, leaf variegation, chlorotic ringspots, virus detection.

OPEN ACCESS

Citation: Desiderio, F., Kwak, M., Kil, E.-J., & Parrella, G. (2026). First report of camellia ring spot associated virus 3 in *Camellia japonica* in Europe. *Phytopathologia Mediterranea* 65 (2): 191-196. doi: 10.36253/phyto-17185

Accepted: June 1, 2026

Published: July 12, 2026

© 2026 Author(s). This is an open access, peer-reviewed article published by Firenze University Press (https://www.fupress.com) and distributed, except where otherwise noted, under the terms of the CC BY 4.0 License for content and CC0 1.0 Universal for metadata.

Data Availability Statement: All relevant data are within the paper and its Supporting Information files.

Competing Interests: The Author(s) declare(s) no conflict of interest.

Editor: Arnaud G Blouin, Institut des sciences en production végétale IPV, DEFR, Agroscope, Nyon, Switzerland.

ORCID:
FD: 0000-0002-9555-3737
GP: 0000-0002-0412-4014
MK: 0009-0008-9662-9044
E-JK: 0000-0002-7256-3879

INTRODUCTION

Camellias (*Camellia* spp.) are important evergreen flowering plants in the *Theaceae* family, known for tea, oil camellia, and ornamental types. They are native to China and Japan and grows naturally in forests at altitudes of around 300–1,100 metres. There are over 250 species, with *C. japonica, C. reticulata, C. sasanqua*, and their hybrids being widely grown as garden ornamental plant, although *C. japonica* is preferred for its variety of flower colours, shapes, and blooming seasons (Macoboy and Mann, 1998). In Italy, the first specimen of the plant arrived in 1760 and was planted in the "English Garden" of the Royal Palace of Caserta. It was a gift, a token of love, from Admiral Nelson to Lady Emma Hamilton, the wife of the English ambassador to the Bourbon court of Naples (Monda, 2017).

Most of the new camellia cultivars come from crosses, but they are mainly propagated from cuttings, making them susceptible to accumulate viral infections. Symptoms of these infections varying from foliar mottle, mosaic, ringspots to foliar and flower variegations. The pattern of affected plant tissue also is irregular on the whole plant, since some branches show symptoms, others do not, and symptoms may not appear every year. Moreover, in the same plant different sizes and shapes of light-green and/or yellowish spots on the leaves are frequently observed. These foliar symptoms have always been associated with mixed infections involving two or more viral entities, making it difficult to attribute them to a single virus. Attempt to associated specific symptoms to a single viral entity were proposed in Zhang *et al.* (2020) based on comparative analysis of symptoms from several and multiple infected camellias. In 2018, a geminivirus, camellia chlorotic dwarf-associated virus (CaCDaV), was found associated to camellia chlorotic dwarf disease (Zhang *et al*., 2018), while in 2019, in USA, three betaflexivirus, camellia ringspot associated virus 1, 2 and 3 (CRaV-1, CRaV-2 and CRaV-3) were found in mixed infection and associated to chlorotic ringspot symptoms of *C. japonica* (Liu *et al*., 2019). Recent analysis of samples from affected plants from Italy using the high-throughput sequencing (HTS) technique revealed a complex group of viruses from the *Betaflexiviridae* and *Fimoviridae* families. Particularly, two new emaravirus species were identified, named camellia japonica associated emaravirus 1 and 2 (CjEV1 and CjEV2), were found only in symptomatic plants, while the betaflexiviruses identified were associated to camellia ringspot associated virus 1 and 2 (CRaV-1 and CRaV-2) (Peracchio *et al*., 2020). Using the same approach, new viruses were identified in China from camellias with various symptoms, provisionally named camellia chlorotic ringspot viruses (CaCRSVs, genus *Fimoviruses*), camellia yellow ringspot virus (CaYRSV, genus *Idaeovirus*), camellia-associated badnavirus (CaBaV), and camellia-associated marafivirus (CaMaV) (Zhang *et al*., 2020). In the same work, tea plant necrotic ring blotch virus (TPNRBV), previously detected in *C. sinensis* (Hao *et al*., 2018), has also been detected. Overall, a clear-cut picture correlating with precision, symptoms observed in *C. japonica* with a specific virus is still far to be complete. In the present study, we used HTS to analyse the virome of a *C. japonica* plant displaying yellow spots, yellow mottling up to yellowing in some leaves and colour-breaking of flowers (Figure 1). These symptoms

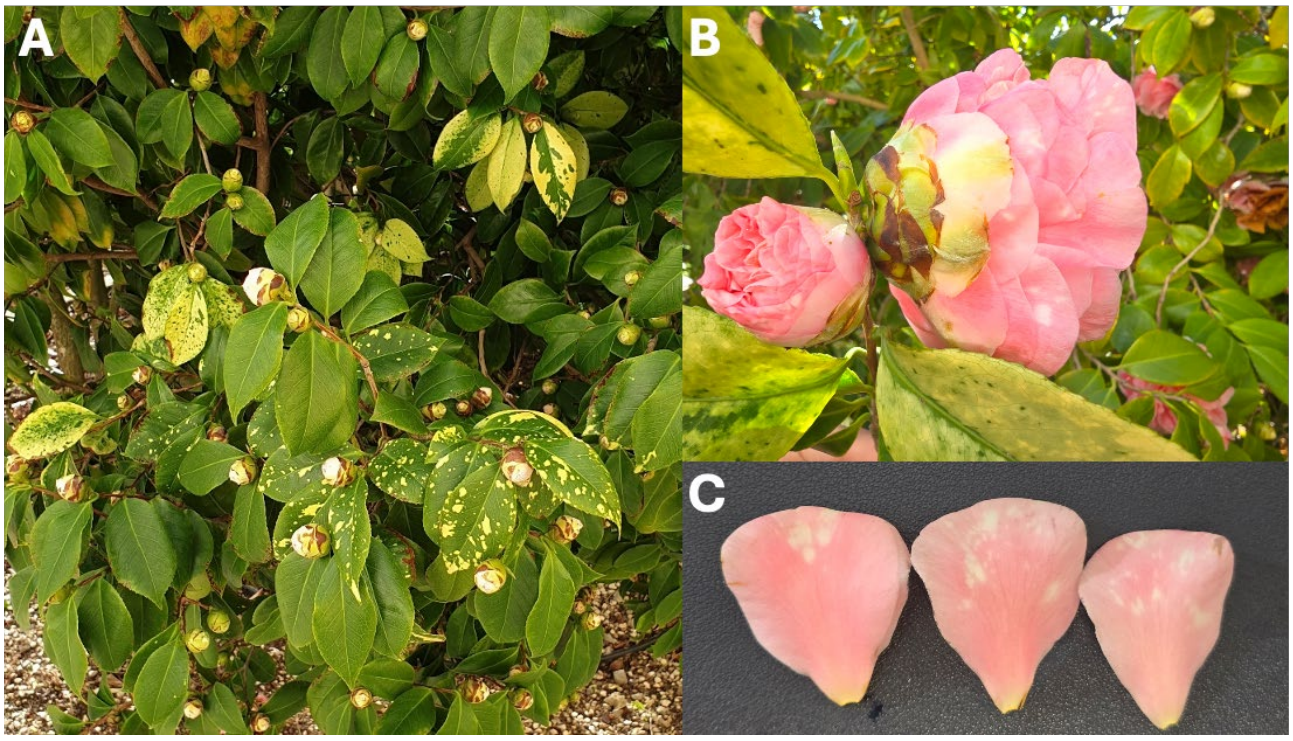

Figure 1. Camellia plant analysed in this study, showing leaf symptoms in some branch, consisting in yellow spots, yellow mottling up to yellowing (A) and colour-breaking of flowers (B and C).

were associated to only one virus for which a detection method was also proposed.

MATERIALS AND METHODS

Sample collection

In May 2020, during a tourist visit to the villa Campolieto, considered one of the most beautiful villas on the so-called "Golden Mile", an historic and cultural stretch of 18th-century Italian baroque architecture, located between Ercolano and Torre del Greco municipalities (Campania region, Italy), a camellia plant was noted for its evident viral leaf symptoms. Symptomatic leaf samples were kept in clean bags on ice and brought to the Portici section of the Institute for Sustainable Plant Protection of National Research Council (IPSP-CNR). Part of the fresh samples were used for RNA extraction and submitted to HTS, while the remaining part was annotated in the IPSP-CNR virus collection and kept in calcium chloride at 5 °C.

RNA isolation, library preparation and HTS analyses

Total RNA was extracted from 100 mg of fresh leaves (50 mg in the case of petals), by pooling 0.5 × 0.5 cm leaf pieces obtained from four different leaves of the same plant, using the NucleoSpin RNA Plant kit (Macherey-Nagel, Düren, Germany). The purified RNA (80 ng/ml) was used to construct cDNA libraries with the TruSeq Stranded Total RNA Library Prep Kit with Ribo-Zero Plant (Illumina, San Diego, CA, USA). The resulting cDNA libraries were sequenced on an Illumina NovaSeq 6000 platform, with sequencing services provided by Macrogen Inc. (Seoul, Republic of Korea). Raw sequencing data were processed using CLC Genomics Workbench v. 21 (Qiagen, USA). Reads were initially trimmed using the Trim Reads tool and reads with a quality score ≤ 0.05 (which corresponds to a Phred score of ~13) or a length shorter than 15 bp were discarded. The trimmed reads were then filtered against the *Camellia sinensis* reference genome (GenBank accession No. GCF_004153795.1; downloaded 03-30-2025) to remove host-derived sequences. The remaining reads were subjected to *de novo* assembly using CLC Genomics Workbench with the following parameters: word size of 19, bubble size of 50, and a minimum contig length of 200 bp. To identify viral sequences, assembled contigs were screened using tBLASTx against the viral RefSeq database, followed by BLASTn searches against the NCBI online database with a cutoff E-value of 10^{-5}. To obtain the longest possible viral genome sequences, contigs identified as viral were either extended at both termini and remapped to the most closely related complete viral genome sequences using the Map Reads to Reference function (length fraction: 0.5; similarity fraction: 0.8). Finally, the consensus viral genomes were deposited in NCBI GenBank and used for further analyses. The ORFs of viral nucleotide sequence and conserved domains in protein sequences inferred from ORFs were found using the NCBI ORF (https://www.ncbi.nlm.nih.gov/orffinder) and CD-search (https://www.ncbi.nlm.nih.gov/Structure/cdd/wrpsb.cgi) servers, respectively.

Development of a diagnostic method based on nested-PCR for HTS validation and virus detection

In this study, outer and internal primers were designed on viral contigs obtained by HTS and screened for detecting the virus identified in the symptomatic camellia from leaves and petal samples (Table 1). The cDNA was synthesized both from RNAs extracted from symptomatic leaves, used for HTS, and from symptomatic petals, using the ImProm-II reverse transcriptase system (Promega, USA) according to the manufacturer's instructions. Reactions were performed at 42 °C for 60 min, followed by incubation at 70 °C for 5 min. PCR amplification was performed using the GoTaq® DNA Polymerase (Promega, USA) under the following cycling conditions, used for both first round and second round PCR: initial denaturation at 94 °C for 4 min; 35 cycles of 94 °C for 30 s, 56 °C for 30 s, and 72 °C for 1 min; and final extension step at 72 °C for 10 min. First round of PCR was performed in 50 mL of total volume, using Cam_A/Cam_Br primers (Table 1). Five mL of the first round PCR were used as target in the second round PCR performed with four different primer pairs (Table 1). PCR products were visualized in 1.2% agarose gel, stained with ethidium bromide, and directly sequenced in both senses (Eurofins Genomics, Colonia, Germany).

RESULTS

HTS analysis

The HTS generated a raw dataset of 89,011,588 reads (101 bp paired end), totalling 8,990,170,388 bp, and have been deposited in the NCBI Sequence Read Archive (SRA) under BioProject accession number PRJNA1461450. A total of 15,174,063 reads were filtered out, resulting in a final set of trimmed reads with an average length of 90.46 bp. To isolate non-host sequences, the

Table 1. Primer pair used in first round and second round nested-PCR for CRSaV-3 detection.

Primer name	5'-sequence-3'	Interval (nt)	Size
First round			
Cam_A	GAGGCTCCATCTTTGAACAGGG	3038-3864	826 bp
Cam_Br	GAACCCACCCATCTTGAAGGTG		
Second round			
Cam_F	GATTCTGTGTGTCCAGAAGGG	3210-3820	610 bp
Cam_R	GAACCATCCTTCAATTCCCTG		
Cam_F1	CTGAATCCTATCTCTGAGCCC	3161-3712	551 bp
Cam_R1	CTCTGGCTTCTCCATCAGCAC		
Cam_F	GATTCTGTGTGTCCAGAAGGG	3210-3712	502 bp
Cam_R1	CTCTGGCTTCTCCATCAGCAC		
Cam_F1	CTGAATCCTATCTCTGAGCCC	3161-3815	654 bp
Cam_R2	CCTTCAATTCCCTGAACTCTC		

trimmed reads were mapped against the host reference transcriptome. A total of 64,470,046 reads were identified as host-derived and subsequently removed. The remaining filtered reads were then subjected to de novo assembly, which yielded 688 contigs. The assembled contigs were analysed using tBLASTx and BLASTn for plant virus identification. Three contigs were specifically annotated as plant viral sequences, all of which showed high similarity to camellia ringspot-associated virus 3 (CRSaV-3; family *Betaflexiviridae*, subfamily *Trivirinae*, genus *Capillovirus*; Gaafar and Ziebell, 2021). They were contig 30, of 3.482 bp, contig 5 of 2.932 bp and contig 44 of 833 bp, respectively. These contigs were aligned to the reference genome with the highest BLASTn score (GenBank accession no. MK050795) to determine their relative genomic positions and generate a consensus sequence (Figure S1A). After that, trimmed reads were remapped to this consensus sequences (Figure S1B), resolving the gap between contig 44 and contig 5 while gap between contigs 30 and 5 remain unresolved.

To bridge the remaining gap between the contigs 30 and 5 (Figure S1), specific primers were designed for gap filling, followed by PCR and Sanger sequencing (Table 1 and Figure 2). Through this integrative approach, the complete genome sequence of CRSaV-3 was successfully determined. Finally, the trimmed reads were re-mapped to this newly established complete sequence, with 11,234 reads uniquely mapped to the viral genome.

Genome analysis

The genomic sequence was determined to be 7402 nt (GenBank accession No. PZ012665), excluding poly(A) tail at the 3' end, and showed the highest percentage of nucleotide identity (87.1%) with the isolate CJ5_676 of CRSaV-3 (GenBank accession no. MK050795), identified in USA (Montgomery County Maryland) in 2016, in the CJ5 cultivar of *C. japonica* (Liu *et al*., 2019). According to the species demarcation criterion (< 72% identity at genomic sequence) for the family *Betaflexiviridae* (Adams *et al*., 2012), the virus identified in the present study should be considered a new isolate of CRSaV-3,

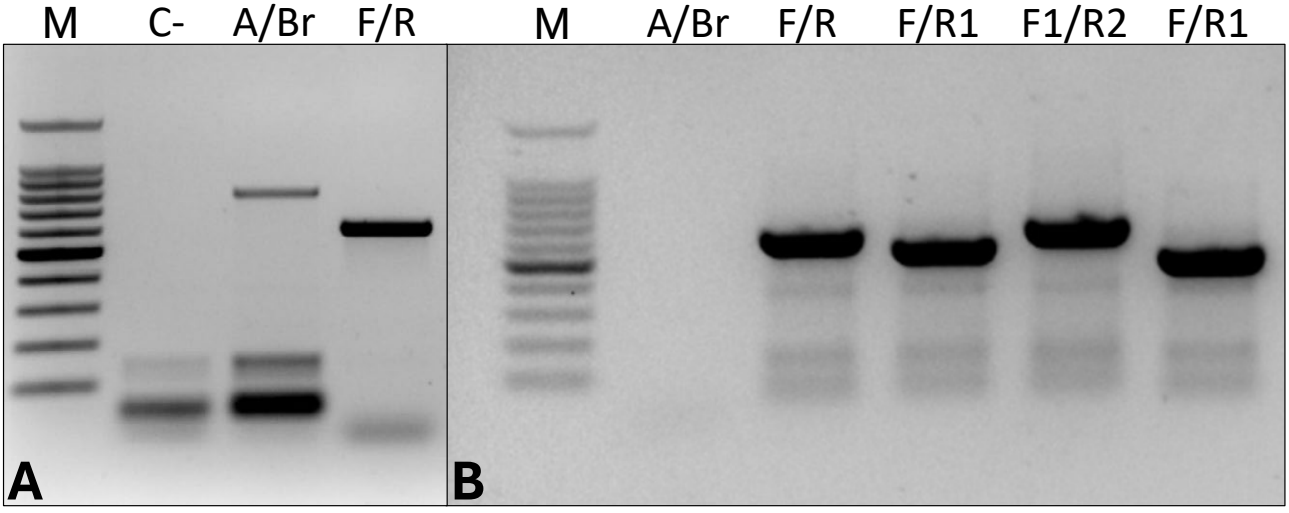

Figure 2. Results of the first round and second round nested PCR from RNA extracted from symptomatic camellia petals (A) and leaves (B), using primer pair listed in Table 1. M = 100 bp DNA ladder (Promega, USA); A/Br = first round primers Cam_A/Cam_Br; F/R = second round primers Cam_F/Cam_R; F1/R1 = second round primers Cam_F1/Cam_R1; F2/R2 = second round primers Cam_F2/Cam_R2; F/R1 = second round primers Cam_F/Cam_R1; C- = negative control.

Table 2. Percentage of identity of nucleotide (nt) and percentage of identity/similarity of amino acid (aa) sequences between the isolate 780_Campolieto and the two isolates CJ5_676 and CJ5_807 of CRSaV-3, obtained using BLASTN and BLASTP respectively (Altschul *et al*., 1997).

	Genome (nt)	Replicase (aa)	MP (aa)	CP (aa)	NBP (aa)
CJ5_676	87.1	84.4/89.0	92.9/96.0	99.4/100	91.7/94.0
CJ5_807	75.4	77.2/86.0	81.9/90.0	97.4/99.0	74.6/82.0

named 780_Campolieto, representing the first report of this virus in Europe in *C. japonica*.

The genomic organization and structure between the two CRSaV-3 isolates is similar: both genomes contain three ORFs, a large ORF 1, a nested ORF 2 and a small ORF 3 at the 3' region, with the ORF1 that encodes a polyprotein consisting of a methyltransferase, a viral RNA helicase, a RdRp domain and a Trichovirus coat protein (CP) domain; the ORF 2, nested with ORF 1, encoding a movement protein (MP); the ORF 3 that encodes a protein of 133 aa residues containing a nucleic acid binding protein (NABP) domain, as reported for some betaflexivirus (Liu *et al*., 2019, Supplementary material, Figure S2).

Genome comparison of 780_Campolieto with the two CRSaV-3 described in Liu *et al.* (2019) revealed that the 5' untranslated regions was at least of 59 nt for 780_Campolieto, 80 nt for CJ5_676 and 62 nt for CJ5_807; the 3'-UTR was at least of 7 nt for 780_Campolieto, 22 nt for CJ5_676 and 13 nt for CJ5_807. Summary results of the sequences pairwise comparison between 780_Campolieto and the two American isolates CJ5_676 and CJ5_807 of CRSaV-3 are reported in the Table 2.

Validation of HTS results and virus detection

The 780_Campolieto isolate of CRSaV-3 was easily detected in RT-PCR form RNAs extracted from symptomatic petals by using the Cam_A/Cam_Br primers. Amplicon of the expected size (826 bp) was obtained (Figure 2A) and sequence was 100% identical to the corresponding genome portion of the 780_Campolieto assembled by HTS analysis. Nevertheless, first round with these primers gave negative results when the RNAs extracted from fresh symptomatic leaves was used in RT-PCR. Thus, three nested primer pairs were designed to increase the detection sensitivity (Table 1). All of them gave expected amplicons (Figure 2B) and sequences were 100% identical among them and with 780_Campolieto. Overall, these primers were used to validate HTS results, to detect viruses in different plant tissues and to bridge gap between the two consecutive contigs 30 and 5.

DISCUSSION

As with many trees and shrubs, the multiplication of new camellia varieties is achieved through vegetative propagation from selected mother plants. This process, however, exposes the varietal germplasm to the risk of disease accumulation, especially those of viral origin. Numerous viruses have been described in *C. japonica*, often found in multiple associations, making it difficult to establish the contribution of each virus to the various symptoms observed in this plant (Liu *et al*., 2019; Peracchio *et al*., 2020; Zhang *et al*., 2020). Indeed, similar symptoms have been associated with different viral complexes, although some studies have proposed a correlation between the type of symptomatology and the prevalence of certain viral species (Zhang *et al*., 2020). Nonetheless, this approach appears to be highly empirical, failing to consider the possible multiple interactions at various levels between the plant and the viruses present. Here we report the identification of a new CRSaV-3 isolate in *C. japonica*, reported for the first time in Europe. Analysis conducted using HTS revealed that this was the only virus detected in the symptomatic plant analysed, and consequently, the symptoms observed, consisting in chlorotic spots, yellow mottling, and leaf yellowing (Figure 1), can be tentatively linked to the Italian CRSaV-3 isolate 780_Campolieto.

The complete or nearly complete genomic sequence of isolate 780_Campolieto has been produced and deposited (GenBank accession No. PZ012665). Comparison of the genomic characteristics with other CRSaV-3 isolates available in the database revealed some genetic divergence among these isolates, in the replicase, MP and NABP ORFs, unlike the CP. This would confirm previous supposition, namely that the CP plays an important role in maintaining the virion structure and plays an essential role in the virus life cycle (Liu *et al*., 2019). To validate the genomic sequence obtained by HTS, a RT-PCR was developed using primer pairs designed on the assembled sequence. This method was applied using RNA extracted from both symptomatic petals and leaves. Since camellia leaves are known to contain numerous substances that inhibit the Taq polymerase, including specific tannins such as camelliatannin D (Hatano *et al*., 1995; Uchii *et al*., 2019), and which are likely responsible for the failure of direct amplification in the first round of PCR. To increase the sensitivity of the RT-PCR on RNA extracted from leaves, due

to high content of tannins, a second round of PCR was used using internal primers (Table 1). This method was effective in amplifying CRSaV-3 (Figure 2) from leaves, which gave apparently negative results after the first round of PCR.

In conclusion, this virome analysis offers strong evidence about CRSaV-3 linked to observed symptoms, helping assess risks and manage known or new viruses of *C. japonica*.

ACKNOWLEDGEMENTS

This research was part of the Short Term Mobility (STM) 2024 programmes, financed by the National Research Council (CNR) of Italy.

LITERATURE CITED

Adams M.J., Candresse T., Hammond J., Kreuze J.F., Martelli G.P., Mamba S., ... Yoshikawa N., 2012. Family Betaflexiviridae. In: (King A.M.Q., Adams M.J., Carstens E.B., Lefkowitz E.J., ed.). *Virus taxonomy. Classification and nomenclature of viruses*. Ninth Report of the International Committee on Taxonomy of Viruses. Waltham (USA), Elsevier, pp. 920-941.

Altschul S.F., Madden T.L., Schäffer A.A., Zhang J., Zhang Z., Miller W., Lipman D.J., 1997. Gapped BLAST and PSI-BLAST: a new generation of protein database search programs. *Nucleic Acids Research* 25: 3389-3402.

Gaafar Y.Z.A., Ziebell H., 2021. Triviruses (*Betaflexiviridae*). In: (Bamford D.H., Zuckerman M., ed.) *Encyclopedia of Virology*, 4th Edition, vol. 3, pp. 805–817. Oxford, Academic Press.

Hao X., Zhang W., Zhao F., Liu Y., Qian W., ... Wang X., 2018. Discovery of plant viruses from tea plant (*Camellia sinensis* (L.) O. Kuntze) by metagenomic sequencing. *Frontiers in Microbiology* 9: 2175.

Hatano T., Han L., Taniguchi S., Okuda T., Kiso Y., Tanaka T., Yoshida T., 1995. Cammelliatannin D, a new inhibitor of bone resorption, from *Camellia japonica*. *Chemical and Pharmaceutical Bulletin* 43: 2033-2035.

Liu H., Wu L., Zheng L., Cao M., Li R., 2019. Characterization of three new viruses of the family *Betaflexiviridae* associated with camellia ringspot disease. *Virus Research* 272: 197668.

Macoboy S., Mann R., 1998. The illustrated encyclopedia of camellias. Timber press, Portland, OR 97204, USA, 304 pp.

Monda V., 2017. La camelia. https://caivaldarnosuperiore.it/la-camelia

Peracchio C., Forgia M., Chiapello M., Vallino M., Turina M., Ciuffo M., 2020. A complex virome including two distinct emaraviruses associated with virus-like symptoms in *Camellia japonica*. *Virus Research* 286: 197964.

Uchii K., Doi H., Okahashi T., Katano I., Yamanaka H., Sakata M.K., Minamoto T., 2019. Comparison of inhibition resistance among PCR reagents for detection and quantification of environmental DNA. *Environmental DNA* 1: 359-367.

Zhang S., Shen P., Li M., Tian X., Zhou C., Cao M., 2018. Discovery of a novel geminivirus associated with camellia chlorotic dwarf disease. *Archives of Virology* 163: 1709-1712.

Zhang S., Yang L., Ma L., Tian X., Li R., Zhou C., Cao M., 2020. Virome of *Camellia japonica*: discovery of and molecular characterization of new viruses of different taxa in camellias. *Frontiers in Microbiology* 11: 945.

Phytopathologia Mediterranea
The international journal of the
Mediterranean Phytopathological Union

Firenze University Press
www.fupress.com/pm

Research Papers

Phenotypic and genotypic diversity of *Fusarium proliferatum* in France; an emerging cause of dry rot of garlic

Christel LEYRONAS*, Paul CHRÉTIEN, Magali DUFFAUD, Jean-François BOURGEAY, Claire TROULET

INRAE, Pathologie Végétale, F-84140, Montfavet, France
*Corresponding author. E-mail: christel.leyronas@inrae.fr

Summary. Garlic production is affected by dry rot, which is an emerging disease caused by several *Fusarium* spp., including *Fusarium proliferatum* (the main species). There is currently no effective method to prevent garlic dry rot during storage of garlic bulbs. Increased knowledge of the characteristics of *F. proliferatum* linked to dry rot development and pathogen population genetics would increase understanding of Fusarium dry rot epidemics in garlic. The present study aimed to assess genotypic and phenotypic diversity of *F. proliferatum* isolates collected from garlic in southern France and elsewhere from other plant species. Among the 185 *Fusarium* isolates genotyped using eight microsatellite markers, 54 complete multilocus haplotypes were obtained, of which five were identified as distinct. All of 55 isolates assessed for their mycelium growth and sporulation capacities were able to grow and to produce conidia at 15, 21, 30 and 35 °C, while none grew at 4 or 40 °C. All of 20 assessed isolates were similarly pathogenic to garlic when assessed at 23 or 30 °C. All assessed isolates grew well at basic pH. No differences were detected among *F. proliferatum* isolates collected from French garlic or from other countries or other host plant species. The *F. proliferatum* isolates collected from garlic in France had low genotypic diversity and little phenotypic difference, compared with isolates obtained from garlic in other countries or from other host plants.

Keywords. *Allium sativum*, mycelium growth, conidiation, temperature, pH.

OPEN ACCESS

Citation: Leyronas, C., Chrétien, P., Duffaud, M., Bourgeay, J.-F., & Troulet, C. (2026). Phenotypic and genotypic diversity of *Fusarium proliferatum* in France; an emerging cause of dry rot of garlic. *Phytopathologia Mediterranea* 65(2): 197-208. doi: 10.36253/phyto-16681

Accepted: April 3, 2026

Published: July 12, 2026

© 2026 Author(s). This is an open access, peer-reviewed article published by Firenze University Press (https://www.fupress.com) and distributed, except where otherwise noted, under the terms of the CC BY 4.0 License for content and CC0 1.0 Universal for metadata.

Data Availability Statement: All relevant data are within the paper and its Supporting Information files.

Competing Interests: The Author(s) declare(s) no conflict of interest.

Editor: Dimitrios I. Tsitsigiannis, Agricultural University of Athens, Greece.

ORCID:
CL: 0000-0002-2693-1140
PC: 0000-0002-9176-9055
J-FB: 0009-0000-8121-0007
CT: 0009-0007-2601-4784

INTRODUCTION

Garlic (*Allium sativum* L.) is a valued vegetable because of its organoleptic and antimicrobial properties. Production of garlic has increased over the last 20 years, reaching 29 million tons in 2022 (Food & Agriculture Organization of the United Nations (FAO), 2025). In Europe, 800,000 tons are produced from 97,000 ha. In EU countries, garlic is usually grown to high quality standards (Galvez and Palmero, 2022).

Garlic produced in France (19,430 tons from 4,360 ha; FAO, 2025), mainly in the southern half of the country, benefits from high quality standards and certification, which ensure control of production including restric-

tion of production to particular regions (Chrétien *et al*., 2020). Despite intensive control and certification of seed and plants, French garlic is affected by Fusarium dry rot (FDR). Symptoms of this disease mainly manifest during garlic storage: brown discolourations and white/pink mycelia appear on cloves, and can extend until the affected plant heads collapse. Garlic heads with these symptoms can no longer be sold, and can cause severe income losses for producers (Chrétien *et al*., 2021). These causes and effects have been observed in neighbouring European countries (Galvez and Palmero, 2022).

In the past 20 years, FDR has emerged internationally. The disease has been reported in many countries in Europe (Germany, Spain, Italy, France, Serbia, Slovakia, Bulgaria), the Americas (United States of America, Argentina, Mexico), Asia (Russia, India, China, Turkey), Africa (Egypt), and more recently in Australia (Harper *et al*. 2025). Several *Fusarium* species have been isolated from garlic with FDR symptoms, but *F. proliferatum* is the most frequently identified causal agent (Dugan *et al*., 2003; Stankovic *et al*., 2007; Palmero *et al*., 2010; Sankar and Babu, 2012; Tonti *et al*., 2012; Moharam *et al*., 2013; Ochoa Fuentes *et al*., 2013; Salvalaggio and Ridao, 2013; Ignjatov *et al*., 2018; Leyronas *et al*., 2018; Mondani *et al*., 2021; Chrétien *et al*., 2021; Gálvez and Palmero, 2021; Horáková *et al*., 2021; Dedecan *et al*., 2022).

At present, there is no efficient method to prevent outbreaks of garlic dry rot. This is due to lack of knowledge about factors affecting dry rot development (e.g. nature of inoculum reservoirs, time and place of infections, conditions for symptom expression). Increased knowledge is required on epidemiology of FDR, including enhanced understanding of the biology and ecology of *F. proliferatum* as the main pathogen, and the conditions that promote its development. Since FDR is emerging internationally, comparison of the phenotypic characters that affect pathogen fitness and the genotypic profile of *F. proliferatum* isolates obtained in different countries could indicate reasons for the increasing importance of this pathogen.

Fusarium proliferatum is a polyphagous fungus, with a host range including more than 25 dicot and monocot plant species, that are herbaceous plants and trees. This fungus can cause different host symptoms including wilt, blight, rot, and dieback. The pathogen can also be endophytic in some without inducing symptoms or only causing diseases under particular conditions (Kwon *et al*., 2001; Proctor *et al*., 2010). In garlic, *F. proliferatum* can be isolated from symptomatic and asymptomatic cloves (Chrétien *et al*., 2021; Mondani *et al*., 2021), making it difficult to establish how disease develops. The conditions underlying the transition of *F. proliferatum* from the endophytic to symptomatic phases in garlic are not known.

In contrast to its diversity of hosts and the symptoms it causes, *F. proliferatum* has low genetic diversity as shown from sequencing of several genes (*tef-1α, rpb1, rpb2*, ITS, and IGS). Chretien *et al*. (2021) reported low diversity of isolates from French garlic collected from geographically separated growing regions over several years. The same low genetic diversity was observed for *F. proliferatum* isolates collected from Spanish garlic (Gálvez *et al*., 2017). Limited intraspecies divergence of the *tef-1α* sequences was also observed in isolates collected from different host species (Stępień *et al*., 2011).

The present study aimed to genotypically and phenotypically characterize *F. proliferatum* isolates to increase understanding of development of dry rot in garlic. A collection of *F. proliferatum* isolates was assessed for genetic characteristics with microsatellites markers. These neutral markers enable comparison between groups of isolates, and assessment of their possible differentiation. The study also assessed isolate phenotypic traits possibly linked to epidemic development (mycelium growth, conidiation, aggressiveness) at different temperatures and pH values.

MATERIALS AND METHODS

Fungal material

Several sets of isolates were used to assess indices of genetic diversity and effects of temperature and pH on mycelium growth, conidium production, and pathogenic aggressiveness. All the isolate sets were selected to represent the diversity present in the overall collection at the time the experiments were carried out.

One hundred and eighty-five isolates of *F. proliferatum* were genotyped (Supplementary material SI 1). Of these isolates, 178 were from the collection of the Pathologie Végétale Research Unit (Chrétien *et al*., 2021). These isolates originated from France, and their sources were distributed among garlic types (pink, white or purple), from southwestern and southeastern production areas, and among years of production (2017, 2018, or 2019). Two isolates, also collected from garlic and originating from Spain, and two from the United States of America were also provided, respectively, by the Universidad Politécnica de Madrid and the Agricultural Research Service (United States Department of Agriculture). Three *F. proliferatum* isolates were also provided by the French Agency for Food, Environmental and Occupational Health & Safety (ANSES) had been isolated from, respectively, *Triticum* sp., *Zea mays*, or *Hordeum vul-*

gare. One isolate of *F. solani* (FA574-E04) and one of *F. oxysporum* (FA112-E04), both obtained from French garlic, were also included in the isolate set that was genotyped in an assessment of the specificity of microsatellites markers.

To characterize phenotypic traits linked to epidemic development, 55 *F. proliferatum* isolates were studied for their mycelium growth on Potato Dextrose Agar (PDA; Difco). Among these, 25 isolates had been collected from French garlic. To compare life history traits of French *F. proliferatum* isolates with those of isolates of different origins, seven isolates collected in Spain and 11 isolates collected in the United States of America (USA) were included in this experiment (Supplementary material SI 1). In addition, 12 *F. proliferatum* isolates originating from plants other than garlic were also assessed; from onion (*Allium cepa*), soybean (*Glycine max*), barley (*Hordeum vulgare*), wheat (*Triticum* sp.), maize (*Zea mays*), *Populus* sp., palm tree (*Bactris gasipaes*), or banana (*Musa* sp.).

A sub sample of 25 *F. proliferatum* isolates representing the diversity of the main sample (15 from garlic, including six from France, six from the USA, three from Spain; and ten from other plants), were characterized for their conidiation capacities. Twenty *F. proliferatum* isolates collected from French garlic (13 from south eastern France and seven from the southwest) were assessed for their pathogenicity at 23 °C and at 30 °C.

Isolate genotyping

Genomic DNA was extracted in 96-well plates from 100 mg fresh weight amounts of frozen mycelium (collected from 14-d-old colonies), following the Dneasy Plant Extraction Kit protocol (Qiagen). Eight microsatellite markers designed for *F. proliferatum* by Moncrief *et al*. (2016) were amplified with forward primers conjugated with the following fluorescent dyes: 6FAM for loci SSR37 and SSR45, NED for loci SSR18 and SSR 68, VIC for loci SSR32 and SSR109, and PET for loci SSR38 and SSR92. Reverse primers did not carry any fluorescent dye. The SSR32 locus could not be amplified with the initial protocol tested on 15 isolates representing the diversity of the main sample (geographical origin, garlic type, year of isolation). Despite modifications to the protocol, no amplification product could be obtained for SSR32, so this locus was excluded from further analyses.

The seven remaining loci were amplified using 55 °C as the hybridization temperature. To determine the size of the microsatellites, the PCR products were diluted and multiplexed prior to scanning using an ABI 3730XL sequencer (Applied Biosystems). The multiplexing consisted of mixing the PCR products of several markers in each microplate well. The PCR products were separated in two mixes: one for markers SSR18, SSR37, SSR38 and SSR108, and the second for markers SSR45, SSR68 and SSR92. In each well, 500LIZ was used as a standard size marker. PCR and product scanning were carried out using Genoscreen. GeneMapper software version 4.1 (Applied Biosystems) was then used for microsatellite size analyses. Complete microsatellite size profiles (referred hereafter as "haplotypes") were obtained for 54 *F. proliferatum* isolates.

Genetic characterization and comparison of Fusarium proliferatum *isolates*

Unbiased gene diversity (Hnb) was computed separately for the isolates collected from the three garlic types (pink, purple, or white) and areas of production (southeast of southwest France), the Genetix software (Belkhir *et al*., 1996–2004).

The index of clonal richness (R) was calculated, using the following formula:

$$R = (G-1)/(N-1),$$

where G is the number of distinct haplotypes and N is the number of individuals with complete haplotypes. This index estimates the proportion of clonal haplotypes present in a population, and is equal to 1 when a population is composed exclusively of unique haplotypes (Arnaud-Haond *et al*., 2007).

The level of genetic differentiation between the *F. proliferatum* isolates from different types of garlic and different production areas was assessed by computing Weir & Cockerham's fixation indices (FST), using the software Arlequin version 3.5 (Excoffier *et al*., 2005). The monomorphic locus (SS92) was removed for these analyses.

Evaluation of mycelium growth and conidiation of Fusarium proliferatum *isolates*

To evaluate temperature effects on mycelium growth and conidiation, six temperatures were used (4, 15, 21, 30, 35 or 40 °C). In this experiment, PDA of pH 5.5 was used. Three replicate PDA plates were used for each isolate and for each temperature. To evaluate effects of pH, six values (4.5, 5.0, 6.0, 7.0, 8.0 or 9.0) were assessed. Medium pHs were adjusted with HCl and NaOH before sterilization, and were verified after sterilization. The Petri inoculated plates were stored in a climate chamber at 21 °C in the dark. Three replicate plates were used for each isolate and each pH value.

Agar plugs (4 mm diam.) were taken from the growing margins of 7-d-old colonies, and placed in the centres of PDA Petri plates (90 mm diam.). All Petri plates for every modality were then stored in the dark. Seven days after inoculation of Petri plates, the diameter of each resulting colony was measured in two directions at right angles to each other. Mycelium growth after 7 d was calculated as the average of the two diameters divided by seven, and expressed in mm d^{-1}. After 14 d, mycelium and conidia were collected from Petri plates by gently rubbing each agar surface with a cotton bud. All the collected material was then placed in 30 mL of water and homogenized. The concentration of conidia in each suspension was assessed using hemocytometer, and the total number of conidia in 30 mL was calculated. Conidium production was expressed as number of conidia produced per Petri plate.

Evaluation of Fusarium proliferatum *aggressiveness at 23 and 30 °C*

This assessment aimed to evaluate the aggressiveness of *F. proliferatum* at a temperature near 20 °C and at a higher temperature similar to those that occur in southern France in summer, when garlic is harvested, dried, and then stored. This experiment was carried out using plants growing in climate chambers set at 23 and 30 °C. Twenty isolates of *F. proliferatum* were inoculated onto garlic cloves (variety Edenrose, pink type), using the protocol of Chrétien *et al*. (2021). In brief, asymptomatic garlic cloves were surface disinfected and were then soaked in conidium spore suspensions (10^5 conidia mL^{-1}) for 24 h. Twenty-four cloves were inoculated with each isolate, and 12 cloves were then incubated in the dark at 23 °C and 12 cloves were incubated at 30 °C. The areas of resulting lesions were monitored and scored at 4, 6, 8, 11, 13, 15, and 18 d after inoculation, using the notation scale of Chrétien *et al*. (2021). These data were used to compute areas under disease progress curves (AUDPC). Isolate FA3-E01 was used as a reference for pathogen aggressiveness. For each isolate, an index of aggressiveness (IA) was calculated relative to that from isolate FA3-E01, as follows: $IA_{isolate} = 100 \times (AUDPC_{isolate}/AUDPC_{FA3\text{-}E01})$.

Statistical analyses

Statistical analyses were carried out using R software (R Core team, 2013) and Statistica (version 12, Statsoft). Mycelium growth and conidiation data were compared with analyses of variance (ANOVAs) and Tukey's HSD *post hoc* test. Dunn's tests were carried out to determine which groups were different. Statistical inferences were made at $P > 0.05$. Indices of aggressiveness were compared using Mann-Whitney tests. Kruskall-Wallis tests were used to compare mycelium growth and conidium production of the different groups of isolates for each assessed temperature or pH.

RESULTS

Genetic diversity of Fusarium proliferatum *isolates*

Locus SSR32 was removed from the genotyping since no amplifications were obtained from the 15 isolates used in the experiment, even using up to 40 amplification cycles. Locus SSR92 was monomorphic giving a single 359 bp allele, while the other loci were polymorphic with the number of alleles being 2 from isolates SSR18, SSR38, SSR68 and from SSR37 (Table 1). Some of the microsatellite markers lacked specificity: all except SSR109, were amplified for *F. oxysporum*, while none amplified for the *F. solani* isolate.

Despite successive trials to amplify the seven microsatellites loci, complete haplotypes were obtained for only 54 *F. proliferatum* isolates out of 185. Only five different multilocus haplotypes (MLH) were identified among the 54 haplotypes, leading to a low value index of clonal richness (0.07). The most frequent MLH was represented by 46 isolates, among which 24 isolates were from the southeastern region of France, 21 were from the southwestern basin, and one was from Spain (Table 2). The number of alleles per locus did not exceed 1.71 for any group of isolates.

There was no evidence of genetic differentiation between *F. proliferatum* isolates from southeast and southwest France, and the FST index statistic was not significant ($P > 0.05$). Also, there was no genetic differentiation between *F. proliferatum* isolates from pink,

Table 1. Polymorphism of the seven microsatellite markers (Moncrief *et al*., 2016) used in the present study to characterize the genetic diversity of the 185 *Fusarium proliferatum* isolates.

Microsatellite locus	Number of alleles	Size range (bp)
SSR18	2	380–382
SSR37	4	271–273–275–279
SSR38	2	380–382
SSR45	3	148–150–152
SSR68	2	116–121
SSR92	1	359
SSR109	2	401 - 404

Table 2. Number, origin and genetic diversity of *Fusarium proliferatum* isolates collected from garlic and other plant species in France, Spain or the United States of America (USA).

Origin	Number of isolates	Number of complete haplotypes	Hnb [a]	Number of alleles per locus	Number of distinct MLHs [b]	R[c]
France	178	53	0.0606 (0.07)	1.71	5	0.07
Southeast of France	91	28	0.0393 (0.05)	1.43	4	0.11
Southwest of France	87	25	0.0821 (0.11)	1.43	3	0.08
Pink garlic type	56	21	0.0252 (0.06)	1.14	2	0.05
White garlic type	61	16	0.1014 (0.08)	1.71	5	0.26
Purple garlic type	57	16	0.0668 (0.09)	1.43	3	0.13
USA	2	0	nd	nd	nd	nd
Spain	2	1	nd	nd	1	nd
Plant species other than garlic	3	0	nd	nd	nd	nd
Total	185	54	0.0595 (0.07)	1.71	5	0.07

[a] Unbiased gene diversity (standard deviation in parentheses).
[b] Multilocus haplotype.
[c] Clonal richness: (number of distinct MLH-1)/(total number of complete haplotypes-1).
nd: no data.

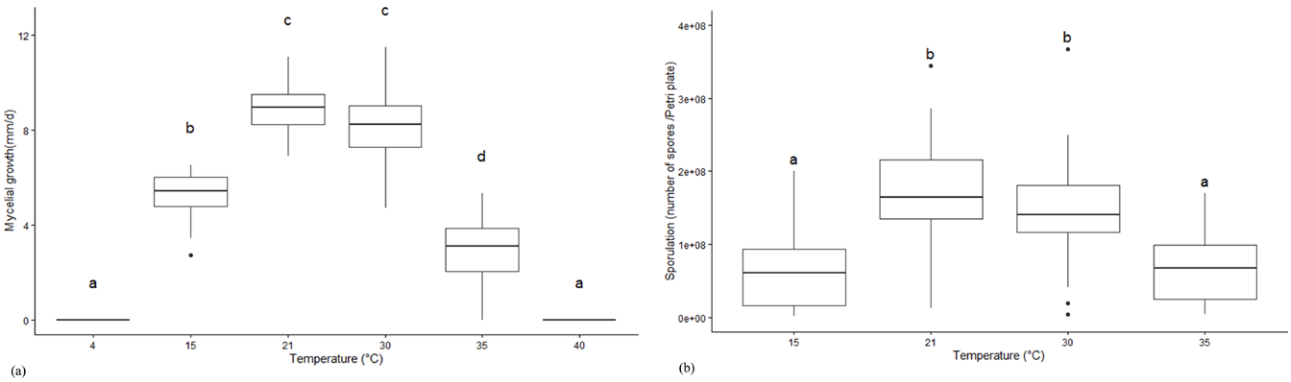

Figure 1. Mean mycelium growth rates (mm d-1; a) and numbers of conidia per Petri plate (b) for *Fusarium proliferatum* isolates collected from garlic in France, Spain or the United States of America (USA), or and from other plant hosts, grown at different temperatures. Fifty-five isolates were used in the mycelium growth assessment (a), and 25 isolates were used in the conidium production assessment. No mycelium growth or conidium production occurred at 4 or 40°C. For each temperature, the bold horizontal line inside the rectangle is the median, the horizontal borders of the rectangle are the 25 and 75% confidence intervals and the vertical lines indicate the maximum and minimum values. Outlier data are indicated by black dots. Means accompanied by the same letters are not different ($P \leq 0.05$).

purple or white garlic host types ($P > 0.05$) for pairwise combinations.

Effects of temperature on mycelium growth, conidium production and aggressiveness on Fusarium proliferatum *isolates*

None of the 55 *F. proliferatum* isolates collected from garlic in France, or from the USA or Spain, or from other plant hosts, were able to grow or produce conidia at 4 or 40 °C (Figure 1a). Mean mycelium growth rates were 5.2 mm d^{-1} at 15 °C, 8.7 mm d^{-1} at 21 °C, 7.6 mm d^{-1} at 30 °C, and 3.74 mm d^{-1} 35 °C, with significant differences ($P < 0.003$) between temperatures.

The 25 *F. proliferatum* isolates assessed for conidium production at different temperatures showed greater production at 21 °C (1.32×10^7 to 3.44×10^8 conidia per Petri plate after in 14 d), and at 30 °C (from $3.9\ 10^6$ to 3.7×10^8) than at 15 °C (1.8×10^6 to 2×10^8) or 35 °C (from 3.7×10^6 to 1.7×10^8) ($P < 0.001$) (Figure 1b).

When grouped according to their origins, the isolate mycelium growth rates for isolate from garlic in France were not different ($P > 0.05$) from isolates from other origins. No differences ($P = 0.238$) were found between

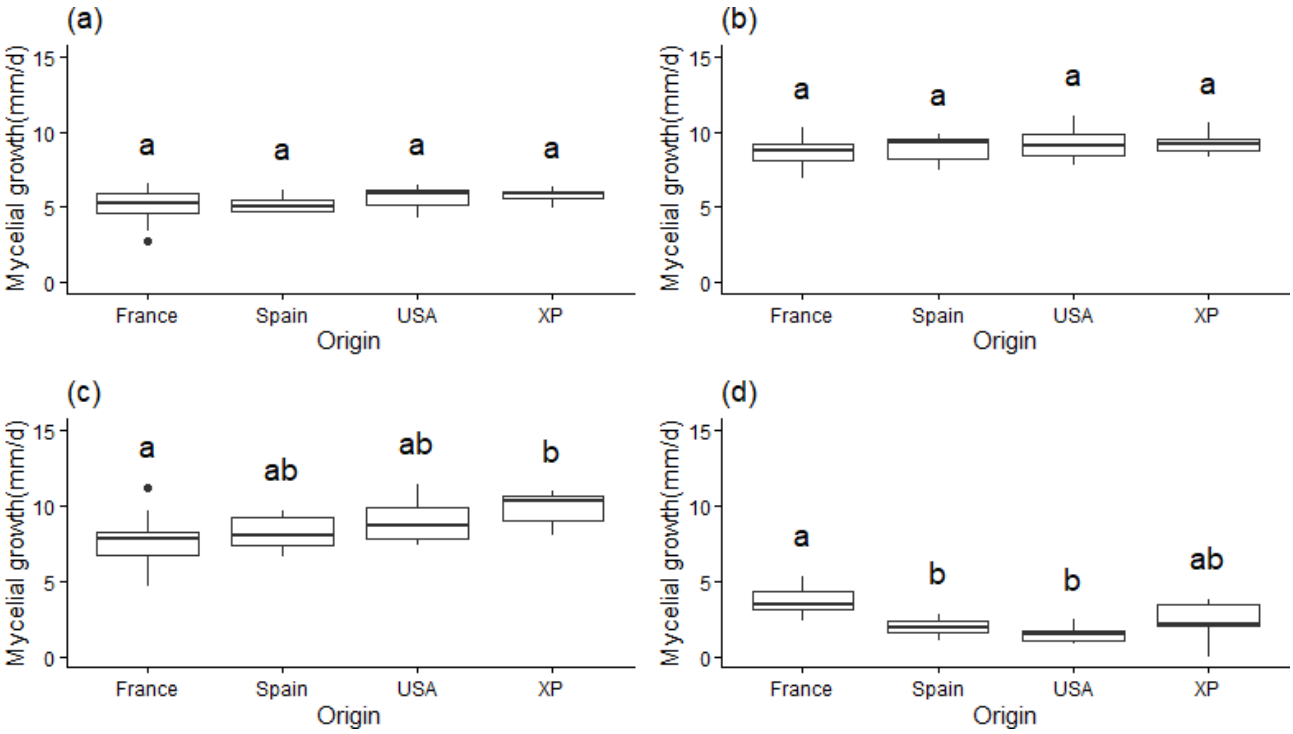

Figure 2. Mean mycelium growth rates (mm d-1) of *Fusarium proliferatum* isolates collected from garlic in France (25 isolates), Spain (seven isolates) and in the USA (11 isolates), or from other plant species (XP; 12 isolates), at 15°C (a), 21°C (b), 30°C (c) or 35°C (d). For each plot, the bold horizontal line inside the rectangle is the median, the horizontal borders of the rectangle are the 25 and 75% confidence intervals, and the vertical lines indicate the maximum and minimum values. Outlier data are indicated by black dots. Means accompanied by the same letters are not different ($P \leq 0.05$).

the isolate groups. All the isolates grew more at 21 or 30 °C than at 15 or 35 °C ($P < 0.001$ for Tukey test comparisons of means).

When comparing data from each temperature, there were significant differences between the mycelium growth of the four groups of isolates at 30 °C ($P_{Kruskall-Wallis} = 0.03$) and 35 °C ($P_{Kruskall-Wallis} < 0.001$). At 30 °C, the French isolates were the slowest-growing (Figure 2c), whereas at 35 °C they were the fastest-growing. (Figure 2d). However, there were no significant differences of conidium production between the different groups of isolates at each temperature ($0.056 < P_{Kruskall-Wallis} < 0.219$), except at 35 °C between the isolates from France and from USA (Figure 3d).

Aggressiveness at 23 and 30 °C

When inoculated onto plants of the Edenrose variety, all 20 *F. proliferatum* isolates collected from French garlic produced disease symptoms. The index of aggressiveness (IA) ranged from 67 to 142% of the reference isolate at 23 °C, and from 66 to 125% at 30 °C (Figure 4). Isolates IAs did not differ ($P_{Mann-Whitney} = 0.96$) when the garlic cloves were incubated at 23 °C, from when they were incubated at 30 °C. The IA values at 23 °C were positively correlated with the equivalent values at 30 °C ($R_{Pearson} = 0.89$, $P < 0.05$). This showed that the more aggressive a *F. proliferatum* isolate was at 23 °C, the more aggressive it was at 30 °C on garlic.

Six isolates (with IAs ranging from 72 to 142% at 23 °C) were characterized for aggressiveness and mycelium growth. There were no correlations between their mycelium growth rates and their aggressiveness at 30 °C ($R^2 = 0.01$). However, there was significant correlation between mycelium growth at 21 °C and aggressiveness at 23 °C ($R^2 = 0.7$).

Effects of pH on mycelium growth and conidium production by Fusarium proliferatum

All 55 *F. proliferatum* isolates were able to grow at pHs between 4.5 and 9.0, with mean mycelium growth rates ranging from 5.2 to 11.9 mm d^{-1}. Growth rate differences between pHs were significant ($P < 2 \times 10^{-16}$)

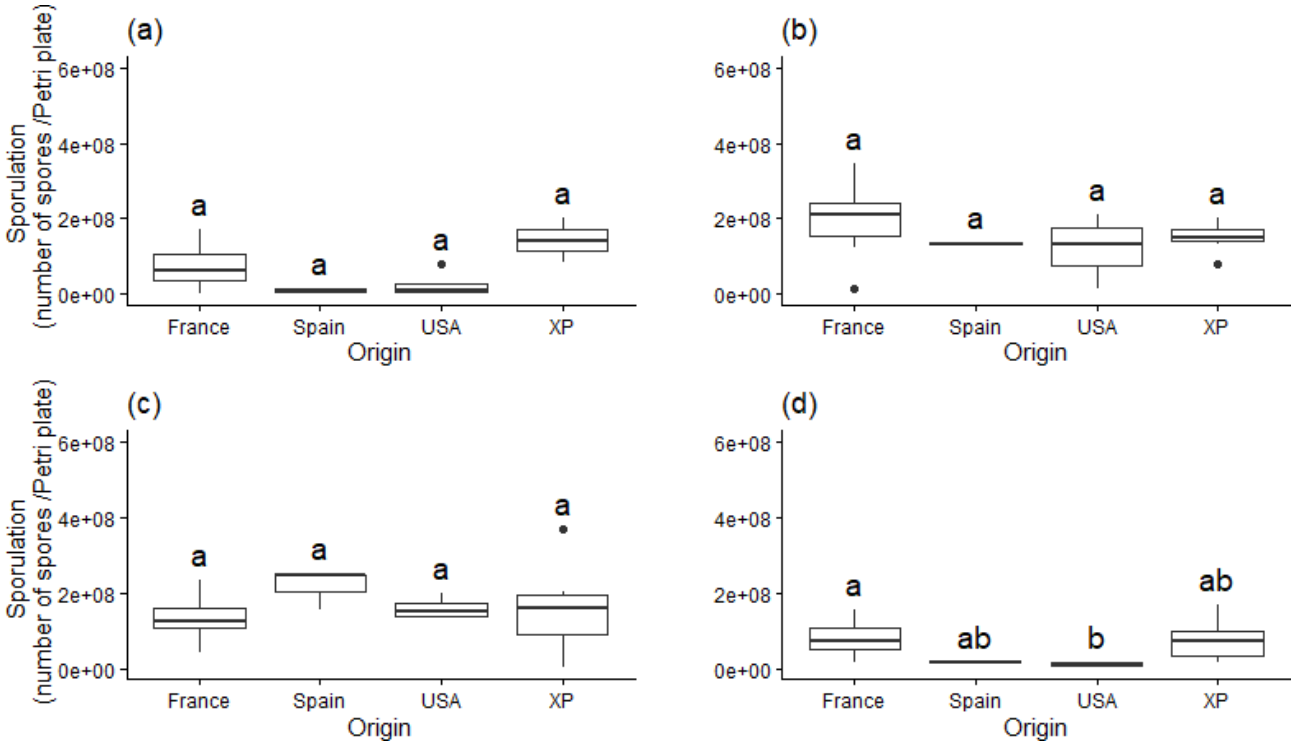

Figure 3. Mean numbers of conidia per Petri plate for cultures of *Fusarium proliferatum* isolates from garlic from France (six isolates), in Spain (three) or the USA (six), or from other plant species (XP; ten), at 15°C (a), 21°C (b), 30°C (c) or 35°C (d). For each plot, the bold horizontal line inside the rectangle is the median, the horizontal borders of the rectangle are the 25% and 75% confidence intervals, and the vertical lines indicate the maximum and minimum values. Outlier data are indicated by black dots. Means accompanied by the same letters are not different ($P \leq 0.05$).

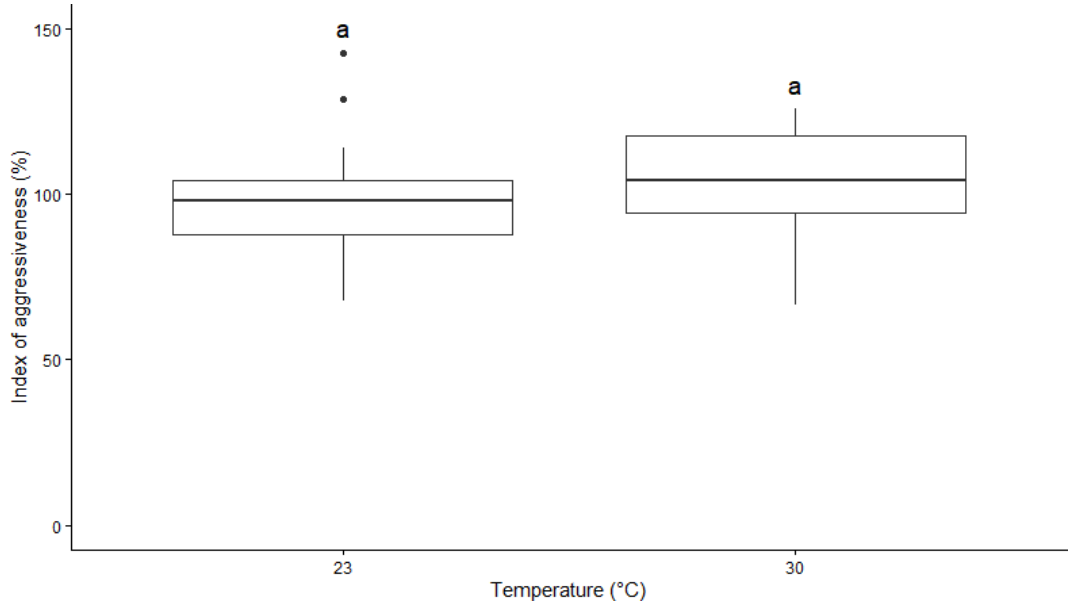

Figure 4. Mean indices of aggressiveness of 20 isolates of *Fusarium proliferatum* obtained from garlic in France, as determined at 23 or 30°C when inoculated onto bulbs of the Edenrose variety. Isolate FA3-E01 was a reference. For each plot, the bold horizontal line inside the rectangle is the median, the horizontal borders of the rectangle are the 25 and 75% confidence intervals, and the vertical lines indicate the maximum and minimum values. Outlier data are indicated by black dots. Means accompanied by the same letters are not different ($P \leq 0.05$).

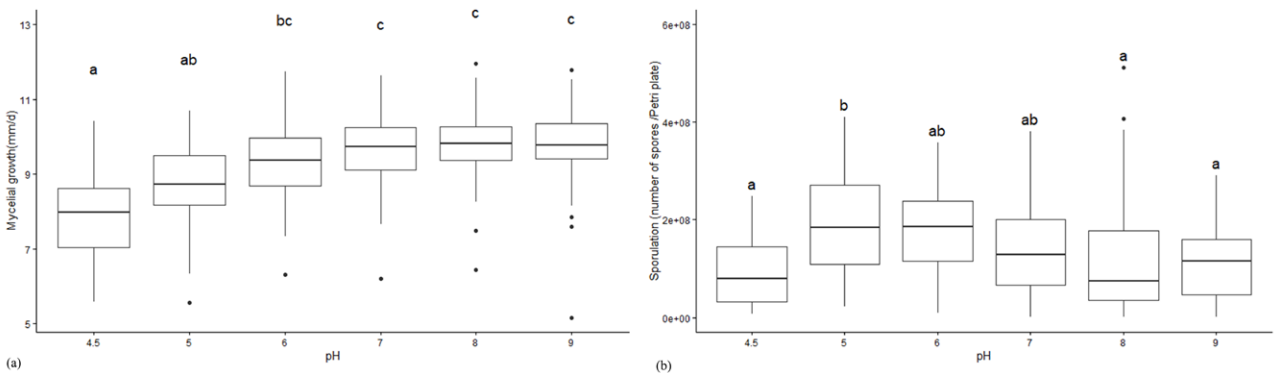

Figure 5. (a) Mean mycelium growth rates (mm d-1), and (b) mean numbers of conidia, after 7 d in Petri plates containing PDA of different pHs, for *Fusarium proliferatum* isolates obtained from garlic in France, Spain the USA, or from other plant species. Fifty-five isolates were used in the mycelium growth assessments, and 25 were used in the conidium production experiment. For each plot, the bold horizontal line inside the rectangle is the median, the horizontal borders of the rectangle are the 25 and 75% confidence intervals, and the vertical lines indicate the maximum and minimum values. Outlier data are indicated by black dots. Means accompanied by the same letters are not different ($P \leq 0.05$).

(Figure 5a). The isolates grew more slowly at pH 4.5 than at all the other pHs (all $P_{Tukey} < 0.001$). They also grew more slowly at pH 5.0 than at pH 6.0 ($P_{Tukey} = 0.049$), pH 7.0, pH 8.0, and pH 9.0 (all $P_{Tukey} < 0.001$). There were no differences ($P_{Tukey} > 0.4$) for mycelium growth at pH 9.0, pH 8.0, pH 7.0 or pH 6.0.

All the isolates of the subsample assessed for conidium production produced conidia at pHs between 4.5 and 9.0, with numbers of conidia produced per Petri plate after 14 d ranging from 4.5×10^5 at (pH 7.0, 8.0 or 9.0) to 5.11×10^8 (at pH 8.0) (Figure 5b) Conidium production was different at pH 5 compared to pH 4.5 ($P = 0.003$), pH 8.0 ($P = 0.019$) or pH 9.0 ($P = 0.002$). There were no other statistically significant differences in conidium production at the other pH values assessed.

When comparing data at a particular pH, there were no significant differences in mycelium growth between the four groups of isolates at pH 4.5 ($P_{Kruskall\text{-}Wallis} = 0.50$), pH 5.0 ($P_{Kruskall\text{-}Wallis} = 0.63$), pH 7.0 ($P_{Kruskall\text{-}Wallis} = 0.63$), pH 8.0 ($P_{Kruskall\text{-}Wallis} = 0.46$), or pH 9.0 ($P_{Kruskall\text{-}Wallis} = 0.44$) (Figure 6). There was a small difference ($P = 0.0505$) at pH 6.0. The isolates from Spain grew more slowly than the isolates from the other three regions.

When each pH value was considered separately, there were statistically significant differences among the four geographical groups of isolates at pH 5.0 ($P = 0.0019$) and pH 7.0 ($P = 0.017$) (Figure 7).

DISCUSSION

The present study aimed to characterize genetic and phenotypic characteristics of *F. proliferatum* isolates collected from different origins, to provide increased knowledge of development of dry rots in garlic bulbs.

Isolates of *F. proliferatum* were well-adapted to the cultural conditions for garlic crops, including soil pH and ambient temperatures during plant growth, harvest and storage. Garlic is cultivated in soil with basic pH (Villeneuve and Erard, 2012), and the present study results showed that isolates of *F. proliferatum* grew more rapidly at basic than at acid pHs. In Europe, garlic is harvested in early summer, and is then dried and stored. In the south of France, temperatures usually reach 30 °C and above during summer. The present study showed that *F. proliferatum* can grow and can produce conidia at these temperatures, that are generally not optimal for the development of fungi growing in temperate regions. These results are similar to those of Stępień *et al.* (2011), and Galvez *et al.* (2017). In the present study, the *F. proliferatum* isolates did not grow at low temperature but remained viable, confirming that low temperatures are suitable for garlic storage (Mondani *et al.*, 2021), to prevent or to slow appearance of FDR symptoms. As soon as garlic bulbs are back at ambient temperature, disease symptoms may develop or increase.

Internationally, there are few or no differences among *F. proliferatum* isolates collected from French garlic and those from garlic Spain or the USA, or from isolates other plants (except for mycelium growth, where the French isolates grew more slowly at 30 °C, and more rapidly at 35 °C). Phenotypic traits were investigated in the present study to reveal potential diversity among *F. proliferatum* from different regions. Although limited genetic diversity was shown, phenotypic diversity would indicate adaptation of *F. proliferatum* to different regions, and determining if there were biogeographi-

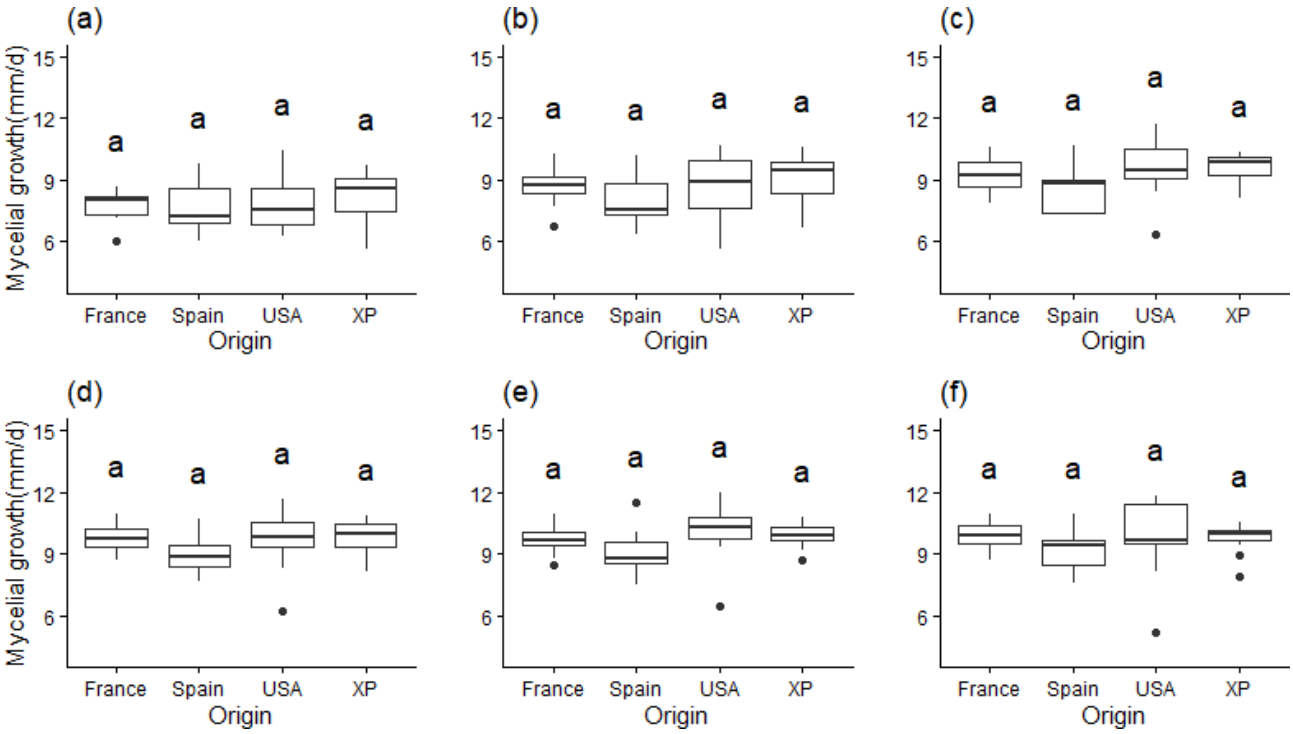

Figure 6. Mean mycelium growth rates for *Fusarium proliferatum* isolates collected from garlic in France (25 isolates), Spain (seven) or the USA (11), or from other plant species (XP; 12 isolates), at different pHs of 4.5 (a), 5.0 (b), 6.0 (c), 7.0 (d), 8.0 (e), or 9.0 (f). For each plot, the bold horizontal line inside the rectangle is the median, the horizontal borders of the rectangle are the 25 and 75% confidence intervals, and the vertical lines indicate the maximum and minimum values. Outlier data are indicated by black dots. Means accompanied by the same letters are not different ($P \leq 0.05$).

cal specializations. The regions of isolate origin in the present study were probably not sufficiently contrasting. Further research should assess isolates originating from regions where FDR is present, but with contrasting soils and climates (e.g. cold winters as in Canada or Russia, or very hot summers as in Egypt).

In the present study, microsatellite markers were used to possibly differentiate pathogen isolates. When these markers are well designed, they are suitable for genotypic characterization of fungi, enabling different groups to be compared on the basis of indices of genetic diversity (Dutech *et al.*, 2007). Despite the attempts used here, difficulty was experienced for amplifying the microsatellites designed for *F. proliferatum* by Moncrief *et al.* (2016) to the 188 *F. proliferatum* isolates. The isolates that were amplified showed low numbers of alleles. This low number, and the consequent low numbers of haplotypes, could be due to low haplotypic diversity of *F. proliferatum*, or this could be an artefact of the low polymorphism of the microsatellite markers.

Fusarium proliferatum is a polyphagous species, and the host symptoms it generates are occurring on *Allium* host species (Stankovic *et al.*, 2007; Alberti *et al.*, 2018; Haapalainen *et al.*, 2023). Therefore, study of genetic similarities or differences among groups of isolates from diverse hosts and origins would be useful. This could increase understanding of population dynamics and provide insights for possible methods for protecting garlic and other *Allium* species. If host specificities were detected, new plant rotations could be defined and utilized. In the South of France, garlic is often cultivated in rotation with wheat or maize, but these crops can harbour *F. proliferatum* (Proctor *et al.*, 2010). It would be worthwhile to determine if there is one population on the different hosts, and if *F. proliferatum* inhabiting a particular host species can produce inoculum for neighbouring or following crops, crops through crop residues. Therefore, future research should: 1) develop methods to detect endophytic forms of *F. proliferatum* in diverse hosts (we are currently developing molecular methods for detection); 2) define more microsatellites markers with high polymorphism and specificity for *F. proliferatum*; and 3) inoculate garlic with *F. proliferatum* isolates from different hosts to assess their pathogenicity.

Factors causing emergence of FDR on garlic and other alliaceous plants remain to be clarified. Emer-

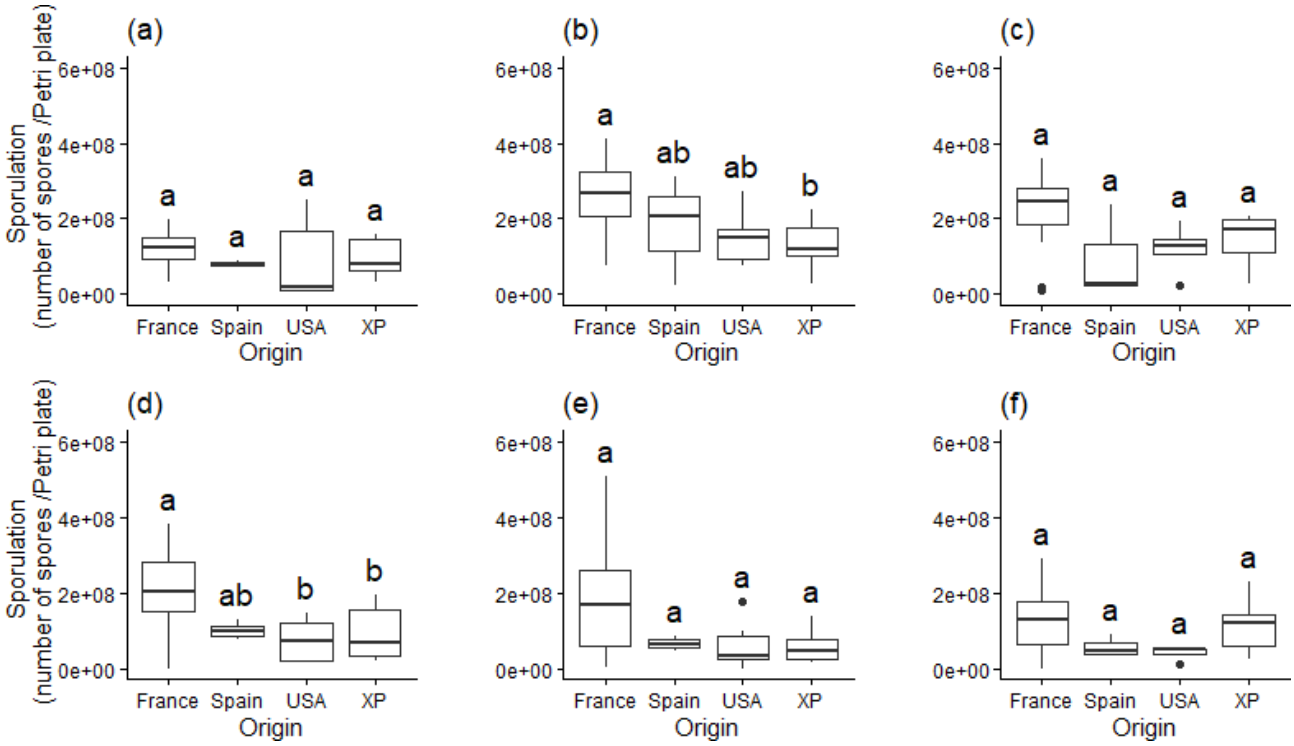

Figure 7. Mean numbers of *Fusarium proliferatum* conidia per Petri plate produced by isolates collected from garlic in France (six isolates), in Spain (three) or the USA (six), or from other plant species (XP; ten isolates), at different pHs of 4.5 (a), 5.0 (b), 6.0 (c), 7.0 (d), 8.0 (e), or 9.0 (f). For each plot, the bold horizontal line inside the rectangle is the median, the horizontal borders of the rectangle are the 25% and 75% confidence intervals, and the vertical lines indicate the maximum and minimum values. Outlier data are indicated by black dots. Means accompanied by the same letters are not different ($P \leq 0.05$).

gence of plant diseases can be driven by different factors, including introduction of new pathogens (trade in plant products, dissemination by extreme climate events), agricultural changes (intensification, globalization), evolution of host and pathogen relationships, and/or climate change (Anderson *et al*., 2004). However, most of these processes would be associated with geographic patterns, and would unlikely lead to international disease emergence. Since *F. proliferatum* is often endophytic in garlic cloves (Chrétien *et al*., 2021; Mondani *et al*., 2021), and because isolates have low genetic diversity, it is possible that this fungus has always lived in symbiosis with garlic (and other *Allium* hosts). However, the *Fusarium*/garlic association has recently been of increasing importance, probably due to climate change that is common to all areas where FDR is emerging. This situation is unlikely to improve. A recent modelling study based on different climate change scenarios has shown that increased temperatures will expand the geographic range of *F. proliferatum*, particularly in regions that are not presently suitable for this pathogen (Tagyan *et al*., 2025). Research is therefore required to determine how to maintain the *Fusarium*/garlic association as asymptomatic and without mycotoxin production.

ACKNOWLEDGMENTS

The authors thank researchers who provided fugus isolates: Dr Renaud Ioos of the French Agency for Food, Environmental and Occupational Health and Safety (ANSES), for isolates LSVM857, LSVM673, LSVM674, LSVM677, LSVM703, LSVM855, LSVM857, LSVM944, LSVM1033; Dr Daniel Palmero Llamas, of the Universidad Politecnica de Madrid, Plant Protection Laboratory, for isolates A10a, FPG20-CL, FPG56-CM, FPG83-MA, 732A17pro, 744A17pro, 746A17pro, and 780A17pro; and Shari Lupien (USDA-ARS) for isolates MR 20B Sci1, MUS1 B1 Sci1, MUS1 B2 Sci2, MUS 22 A Sci1, RG 19 A2 Sci1, RG 19 A2 Sci2, Sib 7 B Sci1, Sib 10 B Sci2, SPR 11 A Sci2, SR 3 B Sci1, SR 16 C5 Sci 1, 14-OP-FUS-025, 14-OP-FUS-026. The authors also thank the French garlic industry for providing garlic bulbs used in the study.

The authors also thank Mrs M. Eygrier, E. Amorim-Pinto, A. Alarçon, E. Borelly and J. Hamet, for the technical assistance, Mr T. Oudin for production of text figures, and Dr C.E. Morris and Dr L. Soucémarianadin for reviewing the manuscript of this paper. Staff of the INRAE Experimental facilities of the PROPHYLE platform of the Plant Pathology research unit ensured that operation was maintained of the plant growth facilities used in this study.

https://eng-pathologie-vegetale.paca.hub.inrae.fr/infrastructures/prophyle/experimental-facilities

AUTHOR CONTRIBUTIONS

The projects in which the data presented in this paper were collected were managed by Christel Leyronas. All authors contributed to conception and design of the study. Material preparation, laboratory experiments and data collection were carried out by Christel Leyronas, Paul Chrétien, Magali Duffaud, Jean-François Bourgeay and Claire Troulet. Data analyses was carried out by Christel Leyronas. The first draft of the manuscript was written by Christel Leyronas, and all authors commented on versions of the manuscript. All the authors read and approved the final manuscript.

FUNDING

This study benefited from a PhD student salary provided by ANRT (Association Nationale Recherche Technologie, CIFRE grant n°2017/1440) and by the French garlic industry (Prosemail, Coopérative Alinéa, Syndicat de l'ail rose de Lautrec). This study was supported in part by a CASDAR grant of the French Ministry of Agriculture (SYNERGIES Project n°2018 IP 5849) and coordinated by Dr Laure Soucémarianadin from ACTA (Association de Coordination Technique Agricole).

LITERATURE CITED

Alberti I., Prodi A., Montanari M., Paglia G., Asioli C., Nipoti P., 2018. First report of *Fusarium proliferatum* associated with *Allium fistulosum* L. in Italy. *Journal of Plant Diseases and Protection* 125: 231–233. https://doi.org/10.1007/s41348-017-0134-4

Anderson P.K., Cunningham A.A., Patel N.G., Morales F.J., Epstein P.R., Daszak P., 2004. Emerging infectious diseases of plants: pathogen pollution, climate change and agrotechnology drivers. *Trends in Ecology and Evolution* 19: 535–44. https://doi.org/10.1016/j.tree.2004.07.021

Arnaud-Haond S., Duarte C.M., Alberto F., Serrão E.A., 2007. Standardizing methods to address clonality in population studies. *Molecular Ecology* 16: 5115–5139. https://doi.org/10.1111/j.1365-294X.2007.03535.x

Belkhir K., Borsa P., Chikhi L., Raufaste N., Bonhomme F., 1996–2004. Genetix 4.05, logiciel sous Windows TM pour la génétique des populations. Laboratoire Génome, Populations, Interactions, CNRS UMR 5171, Université de Montpellier, Montpellier, France. [WWW document]. URL http://www.genetix.univ-montp2.fr/genetix/intro.htm

Chrétien P.L., Laurent S., Bornard I., Troulet C., El Maâtaoui M., Leyronas C., 2020. Unraveling the infection process of garlic by *Fusarium proliferatum*, the causal agent of root rot. *Phytopathologia Mediterranea* 59: 285–293. https://doi.org/10.14601/Phyto-11103

Chrétien P.L., Morris C.E., Duffaud M., Leyronas C., 2021. Aetiology of garlic rot, an emerging disease in France. *Plant Pathology* 70: 1276–1291. https://doi.org/10.1111/ppa.13394

Dedecan O., Talapov T., Demùral M., Sarpkaya K., Ceyhan D.I., Can C., 2022. Molecular and pathogenic characterization of *Fusarium oxysporum* and *Fusarium proliferatum* causing basal root rot in garlic in Turkey. *Australasian Plant Disease Notes* 17(1): 37. https://doi.org/10.1007/s13314-022-00484-w

Dugan F.M., Hellier B.C., Lupien S.L., 2003. First report of *Fusarium proliferatum* causing rot of garlic bulbs in North America. *Plant Pathology* 52: 426. https://doi.org/10.1046/j.1365-3059.2003.00852.x

Dutech C., Enjalbert J., Fournier E., Delmotte F., Barrès B., … Giraud T., 2007. Challenges of microstallite isolation in fungi. *Fungal Genetics and Biology* 44: 933–949. https://doi.org/10.1016/j.fgb.2007.05.003

Excoffier L., Laval G., Schneider S., 2005. Arlequin ver. 3.0: An integrated software package for population genetics data analysis. *Evolutionary Bioinformatics Online* 1: 47–50.

FAO 2025. Rome: Food &Agriculture Organization of the United Nations (FAO). Accessed 26 March 2025 https://www.fao.org/faostat/fr/#data/QCL/visualize

Gálvez L., Palmero D., 2021. Incidence and etiology of postharvest fungal diseases associated with bulb rot in garlic (*Allium sativum*) in Spain. *Foods* 10: 1063. https://doi.org/10.3390/foods10051063

Gálvez L, Palmero D., 2022. Fusarium dry rot of garlic bulbs caused by *Fusarium proliferatum*: a review. *Horticulturae* 8: 628. https://doi.org/10.3390/horticulturae8070628

Gálvez L., Urbaniak M., Waśkiewicz A., Stępień Ł., Palmero D., 2017. *Fusarium proliferatum* - Causal agent of garlic bulb rot in Spain: Genetic variability and

mycotoxin production. *Food Microbiology* 67: 41–48. https://doi.org/10.1016/j.fm.2017.05.006

Haapalainen M., Kuivainen E., Iivonen S., Niemi M., Latvala S., 2023. Pathogenicity of *Fusarium oxysporum* and *Fusarium proliferatum* isolates from symptomless onions (*Allium cepa*) and onions with Fusarium basal rot. *Plant Pathology* 72: 1122–1135. https://doi.org/10.1111/ppa.13718

Harper J.R., Galea V.J., Gambley C.F., 2025. First report of *Fusarium proliferatum* causing rot in garlic (*Allium sativum*) in Australia. *Australasian Plant Pathology* 54: 425–426 https://doi.org/10.1007/s13313-025-01046-1

Horáková M.K., Tancik J., Barta M., 2021. *Fusarium proliferatum* causing dry rot of stored garlic in Slovakia. *Journal of Plant Pathology* 103: 997–1002. https://doi.org/10.1007/s42161-021-00883-5

Ignjatov M., Milosević D., Ivanović Ž., Karaman M., Vlajić S., … Gvozdanović-Varga J., 2018. Morphological and pathogenic properties of *Fusarium proliferatum* isolates: the causal agent of garlic (*Allium sativum* L.) rot in Serbia. *Ratarstvo i Povrtarstvo* 55: 125–129. https://doi.org/10.5937/RatPov1803125I

Kwon S.I., von Dohlen C.D., Anderson A.J., 2001. Gene sequence analysis of an opportunistic wheat pathogen, an isolate of *Fusarium proliferatum*. *Canadian Journal of Botany* 79: 1115–1121. https://doi.org/10.1139/b01-084

Leyronas C., Chrétien P.L., Troulet C., Duffaud M., Villeneuve F., … Hunyadi H., 2018. First report of *Fusarium proliferatum* causing garlic clove rot in France. *Plant Disease* 102: 12. https://doi.org/10.1094/PDIS-06-18-0962-PDN

Moharam M.H.A., Farrag E.S.H., Mohamed M.D.A., 2013. Pathogenic fungi in garlic seed cloves and first report of *Fusarium proliferatum* causing cloves rot of stored bulbs in upper Egypt. *Archives of Phytopathology and Plant Protection* 46: 2096–2103. https://doi.org/10.1080/03235408.2013.785122

Moncrief I., Garzon C., Marek S., Stack J., Gamliel A., … Fletcher J., 2016. Development of simple sequence repeat (SSR) markers for discrimination among isolates of *Fusarium proliferatum*. *Journal of Microbiological Methods* 126, 12–17. https://doi.org/10.1016/j.mimet.2016.03.013

Mondani L., Chiusa G., Pietri A., Battilani P., 2021. Monitoring the incidence of dry rot caused by *Fusarium proliferatum* in garlic at harvest and during storage. *Postharvest Biology and Technology* 173: 111407. https://doi.org/10.1016/j.postharvbio.2020.111407

Ochoa Fuentes Y.M., Delgado-Ortiz J.C., Chàvez E.C., Hernàndez-Castillo F.D., Olivas A.F., … Rodríguez Guerra R., 2013. The first report of *Fusarium proliferatum* causing garlic bulb rots in Mexico. *African Journal of Agricultural Research* 8: 570–573. https://doi.org/10.5897/AJAR12.1726

Palmero D., De Cara M., Iglesias C., Moreno M., Gonzalez N., Tello J., 2010. First report of *Fusarium proliferatum* causing rot of garlic bulbs in Spain. *Plant Disease* 94: 277. https://doi.org/10.1094/PDIS-94-2-0277C

Proctor R.H., Desjardins A.E, Moretti A., 2010. Biological and chemical complexity of *Fusarium proliferatum*. In: *The Role of Plant Pathology in food Safety and Food Security* (N.M. Strange, M.L. Gullino, ed.) Birkberk College, UK, 97–111

R Core Team, 2013. R: A language and environment for statistical computing. R Foundation for Statistical Computing, Vienna, Austria. URL http://www.R-project.org/.

Sankar N.R., Babu G.P., 2012. First report of *Fusarium proliferatum* causing rot of garlic bulbs (*Allium sativum*) in India. *Archives of Phytopathology and Plant Protection* 1: 8. https://doi.org/10.1094/PDIS-08-11-0649

Salvalaggio A.E., Ridao A., 2013. First Report of *Fusarium proliferatum* causing rot on garlic and onion in Argentina. *Plant Disease* 97: 556. https://doi.org/10.1094/PDIS-05-12-0507-PDN

Stankovic S., Levic J., Petrovic T., Logrieco A., Moretti A., 2007. Pathogenicity and mycotoxin production by *Fusarium proliferatum* isolated from onion and garlic in Serbia. *European Journal of Plant Pathology* 118: 165–172. https://doi.org/10.1007/s10658-007-9126-8

Stępień Ł., Koczyk G., Waśkiewicz A., 2011. Genetic and phenotypic variation of *Fusarium proliferatum* isolates from different host species. *Journal of Applied Genetics* 52: 487–496. https://doi.org/10.1007/s13353-011-0059-8

Tagyan AI, AlAshaal S, Alkhalifah DHM, Abdelghany WR, Hozzein WN, 2025. Estimating the climate change-driven global distribution of *Fusarium proliferatum* and mycotoxin risk assessment under future warming scenarios. *Frontiers in Forests and Global Change* 8:1673494. https://doi.org/10.3389/ffgc.2025.1673494

Tonti S., Prà M.D., Nipoti P., Prodi A., Alberti I., 2012. First report of *Fusarium proliferatum* causing rot of stored garlic bulbs (*Allium sativum* L.) in Italy. *Journal of Phytopathology* 160: 761–763. https://doi.org/10.1094/PDIS-08-11-0649

Villeneuve F., Erard P., 2012. *L'ail*. CTIFL Hortipratic.

Phytopathologia Mediterranea
The international journal of the
Mediterranean Phytopathological Union

Firenze University Press
www.fupress.com/pm

Research Papers

Manganese affects grapevine wood degradation by *Fomitiporia mediterranea*: *in vitro* evidence

Francesco BIGAZZI[1,*], Giuseppe CARELLA[1], Laura MARTÍN[2], Laura MUGNAI[1]

[1] *Department of Agricultural, Food, Environmental and Forestry Science and Technology (DAGRI), Plant pathology and Entomology section, P. le delle Cascine 28, 50142 Firenze, Italy*
[2] *Área de Protección Vegetal. Instituto de Investigaciones Agrarias Finca La Orden (CICYTEX), Junta de Extremadura, Guadajira, 06187, Badajoz, Spain*
*Corresponding author. E-mail: francesco.bigazzi1@unifi.it

Summary. Grapevine trunk diseases (GTDs) are severe constraints affecting *Vitis vinifera* (grapevine) cultivation, causing vine decline, yield losses, and major economic impacts. Within the Esca disease complex, the white-rot basidiomycete *Fomitiporia mediterranea* is frequently associated with wood degradation. Despite its recognized involvement in disease development, the influence of abiotic factors on the wood-degrading activity of this pathogen has not been studied. Effects of manganese (Mn^{2+}) availability on *F. mediterranea* growth, biomass production, wood degradation, and manganese peroxidase (MnP) activity of this fungus were assessed under controlled laboratory conditions, using increasing manganese concentrations and young (3-year-old) and old (25-year-old) wood from *V. vinifera* 'Cabernet Sauvignon'. Manganese availability had a concentration-dependent effects on *F. mediterranea*. Intermediate Mn^{2+} concentrations, particularly 80 µM, promoted colony growth, biomass accumulation, and wood mass loss, whereas greater concentrations (320 µM) reduced growth and wood degradation. Qualitative observations showed formation of dark pigmented zones in wood, which became progressively more pronounced as Mn concentrations increased. MnP activities were greatest at intermediate Mn^{2+} levels, and declined at the greatest concentration, a trend consistent with *F. mediterranea* growth and wood degradation patterns. These results indicate that Mn^{2+} availability can modulate *F. mediterranea* degradative activity and may influence enzymatic processes involved in grapevine wood decay. Future studies should assess micronutrient bioavailability as an abiotic factor for reducing progression of the Esca complex in grapevines.

Keywords. Esca complex, wood decay, white-rot basidiomycete, micronutrients.

OPEN ACCESS

Citation: Bigazzi, F., Carella, G., Martín, L. & Mugnai, L. (2026). Manganese affects grapevine wood degradation by *Fomitiporia mediterranea*: *in vitro* evidence. *Phytopathologia Mediterranea* 65(2): 209-223. doi: 10.36253/phyto-17152

Accepted: June 16, 2026

Published: July 19, 2026

© 2026 Author(s). This is an open access, peer-reviewed article published by Firenze University Press (https://www.fupress.com) and distributed, except where otherwise noted, under the terms of the CC BY 4.0 License for content and CC0 1.0 Universal for metadata.

Data Availability Statement: All relevant data are within the paper and its Supporting Information files.

Competing Interests: The Author(s) declare(s) no conflict of interest.

Editor: Luisa Ghelardini, University of Florence, Italy.

ORCID:
FB: 0009-0003-1296-1204
GC: 0000-0002-0297-0428
LMB: 0000-0002-2576-642X
LM: 0000-0002-2508-9764

INTRODUCTION

The Esca complex of diseases (ECDs) causing grapevine trunk diseases (GTDs) is widespread and economically damaging. This complex includes different diseases in different vine life stages, including: Brown wood streaking, Petri Disease, Grapevine Leaf Stripe disease (GLSD). The term Esca

applies wood white rot of grapevines. This disease has slow progression, and is difficult to manage, and has impacts on vineyard longevity, causes substantial grape yield losses, causes death of vines, as well as major economic repercussions across wine-producing regions, especially in Europe (Gramaje *et al*., 2018; Guerin-Dubrana *et al*., 2019).

The wood diseases in ECD are associated with a range of symptoms, and with several pathogenic fungi. The most frequently cited of these include two vascular ascomycetes, *Phaeomoniella chlamydospora* and *Phaeoacremonium minimum* (Gramaje *et al*., 2015), and as the white-rot basidiomycete *Fomitiporia mediterranea* (Fischer *et al*., 2002). *Fomitiporia mediterranea* is one of the most frequently isolated pathogens associated with Esca (wood rot), and with GLSD, i.e. disease causing typical tiger stripe foliar symptoms and with unique epidemiology (Mugnai *et al*., 1999; Del Frari *et al*., 2019; Bruez *et al*., 2020). Recent studies on grapevine wood microbiome have indirectly confirmed the central role of *F. mediterranea* within wood decay and leaf stripe disease (Bruez *et al*., 2021; Pacetti *et al*., 2021).

Ecologically, *F. mediterranea* is a highly adaptable species, with a broad host range and distribution across diverse regions and climatic conditions (Moretti *et al*., 2021). Across its geographical range, *F. mediterranea* is strongly associated with *V. vinifera*. However, this association may partly reflect the economic importance of grapevine cultivation, which has led to increasingly detailed study of this pathogen compared to associations other hosts (Moretti *et al*., 2021). Presence of the pathogen is detected at host plant necrosis margins, between white-rot and non-necrotic tissues, as well as in adjacent non-necrotic but recently colonized wood (Fischer, 2002; Péros *et al*., 2008; Surico, 2009; Bruez *et al*., 2017; Elena *et al*., 2018; Bruez *et al*., 2021; Pacetti *et al*., 2021). Due to the extended periods required for wood colonization and degradation, *F. mediterranea* has been primarily detected in grapevines older than 8 to 10 years, while it is only occasionally found in vines younger than this (Sánchez-Torres *et al*., 2008; Mugnai *et al*., 2010). *In vivo* pathogenicity studies on wood-decaying basidiomycetes in grapevines remain scarce (Chiarappa, 1997; Sparapano *et al*., 2000a, 2000b).

Several studies have demonstrated that *F. mediterranea* produces high levels of manganese peroxidase (MnP). Based on a genomic study, MnPs were the only class II peroxidases present in the *F. mediterranea* secretome (Floudas *et al*., 2012). Furthermore, and compared with other white-rot fungi, including the model species *Trametes versicolor*, *F. mediterranea* produces large amounts of MnPs (Schilling *et al*., 2023). In mycelium exposed to wood substrates, increased basal expression of MnP genes has been related to laccase genes (Pacetti *et al*., 2022). Enzyme secretion is also substrate-dependent, with preference for grapevine wood, where *F. mediterranea* has increased MnP and laccase secretion, enhanced wood degradation, and increasingly efficient detoxification of grapevine extractives compared with beech extracts (Schilling *et al*., 2022; Schilling *et al*., 2023). These results highlight specific traits of *F. mediterranea* during grapevine wood colonization compared with other woody substrates and white-rot fungi.

The catalytic mechanism of MnP shares several features with other heme-containing peroxidases, including lignin peroxidase and horseradish peroxidase (Dunford, 1991; Wariishi *et al*., 1991; Kirk and Cullen, 1998). Like other class II peroxidases, MnP operates through formation of the reactive intermediates Compound I and Compound II (Wariishi *et al*., 1988; Kishi *et al*., 1994). However, MnP has a distinctive functional characteristic: it preferentially utilizes Mn^{2+} as its electron donor. Although Compound I can also be reduced by alternative substrates, Compound II shows a strong dependency on Mn^{2+}, while reduction by other electron donors occurs only at low rates (Wariishi *et al*., 1988; Brown *et al*., 1990). Consequently, manganese availability is a key factor regulating MnP functionality and catalytic efficiency.

Beyond *F. mediterranea*, numerous studies on other white-rot fungi have shown that manganese availability plays a central role in enhancing ligninolytic performance and wood substrate degradation. The supplementation of fungal cultures with manganese has been reported to increase lignin depolymerization and the enzymatic hydrolysis of lignocellulosic materials, indicating that manganese acts as a cofactor and as an inducer of MnP expression and activity (Fu *et al*., 2021). Investigations into the regulation of ligninolytic enzymes in white-rot fungi have also shown that manganese presence can upregulate MnP production, further strengthening the link between manganese availability and fungal lignin-degrading capacity (Scheel *et al*., 2000). Ecological studies have provided additional evidence supporting the influence of manganese on wood component degradation. Berg *et al*. (2007) reported a linear relationship between manganese concentration in foliar litter and annual mass loss during the late stages of decomposition, highlighting the broader role of manganese in lignocellulose decay processes. Experimental studies have also shown that manganese supplementation enhances MnP production in the white-rot fungus *Pleurotus ostreatus*, a well-known wood decay agent,

further confirming the stimulatory effect of manganese on MnP-mediated degradation pathways (Slavens *et al*., 2019). Additional evidence comes from studies on other wood-rotting fungi. Investigations of decayed wood have shown that black spots or black zones, which are closely associated with advanced wood degradation, contain high concentrations of manganese compared with adjacent decayed tissues. In contrast, surrounding healthy wood lacked significant manganese accumulation. The oxidized manganese buildup was detected exclusively in black zones within delignified wood, indicating close association between manganese accumulation and lignin degradation processes (Blanchette, 1984).

Taken together, these observations support the overarching hypothesis that manganese bioavailability modulates the wood-degrading performance of white-rot fungi. Consequently, the primary objective of this study was to determine whether a similar manganese-driven stimulatory effect occurs in the Esca-associated pathogen *F. mediterranea*. Investigating this relationship could help to clarify the involvement of other potential abiotic factors involved in the expression of the GLSD foliar symptom.

A long-standing hypothesis in Esca pathogenesis suggests that host plant foliar symptoms are triggered by toxic fungal byproducts or phytotoxic metabolites translocated from decayed trunk wood to grapevine canopies (Mugnai *et al*., 1999). Previous studies have shown that plant nutritional status influences foliar symptom expression (Calzarano *et al*., 2009; Calzarano *et al*., 2023; Dell'Acqua *et al*., 2025). Manganese is of particular interest due to its dual role in plant nutrition and fungal ligninolytic metabolism. Among the abiotic factors influencing disease expression, water availability has been consistently identified as the main key driver, with rainfall patterns positively correlated with the manifestation of foliar symptoms (Surico *et al*., 2000; Calzarano *et al*., 2018). This relationship is particularly relevant because soil manganese availability and plant uptake are strongly influenced by rainfall and soil moisture dynamics (Radaelli and Calamai, 2001; Marschner, 2011). Together, these observations suggest a potential mechanistic link between environmental conditions, nutrient availability, and fungal activity in wood tissues. Therefore, the primary hypothesis of the present study was that increased manganese bioavailability enhances the degradative and metabolic activity of *F. mediterranea*, which could contribute to processes potentially linked to foliar symptom expression.

To test this hypothesis, the present *in vitro* study aimed to determine whether manganese bioavailability levels stimulate fungal growth, ligninolytic activity, and wood degradation, and to assess whether host tissue age modulates these responses. Whether increased degradative capacity under elevated manganese conditions correlates with enhanced MnP production was also assessed. This characterization would establish the necessary baseline for future *in vivo* and field-based studies that aim to link wood-decay severity with grapevine canopy symptom manifestation.

MATERIALS AND METHODS

Fungus isolate identification and culture conditions

One isolate of *Fomitiporia mediterranea* (Fmed It 17) was used in all experiments. This isolate was obtained from symptomatic *Vitis vinifera* wood collected in the municipality of Gambassi Terme (Tuscany, Italy). The isolate was first identified based on morphological characteristics and subsequently confirmed through molecular analyses. DNA extraction, PCR amplification, and sequencing were carried out the University of Florence internal sequencing service CIBIACI (www.cibiaci.unifi.it). DNA was extracted following the 2× cetyltrimethylammonium bromide (CTAB) protocol (Doyle and Doyle, 1990), using 10–15 mg of lyophilized material. The primer pair ITS1 (5′-TCCGTAGGTGAACCTGCGG-3′) and ITS4 (5′-TCCTCCGCTTATTGATATGC-3′) was used for amplification of the ITS region (White *et al*., 1990), while the primer pair LR0R (5′-GTACCCGCTGAACTTAAGC-3′) and LR7 (5′-TACTACCACCAAGATCT-3′) was used to amplify the LSU region (Rehner and Samuels, 1994). PCRs were carried out in 25 µL reaction volumes using 0.4 µM of each primer, 1.5 mM $MgCl_2$, 1× colourless reaction buffer, 0.5 mM dNTPs, and 1 unit of GoTaq® G2 DNA Polymerase (Promega Corporation). The PCR cycling protocol was carried out on a Bio-Rad thermal cycler under the following conditions: DNA denaturation, 1 min at 94 °C, primer annealing, 1 min at 55 °C; primer extension, 2 min at 72 °C. Negative control reactions omitting DNA were included in all amplification sets to monitor potential contamination by exogenous DNA. Subsequently, the PCR products were visualized on a 1% agarose gel stained with ethidium bromide, using a Gel Doc Bio-Rad system; a 1 kb Plus DNA Ladder (Thermo Fisher Scientific) was used as the molecular weight marker for bp dimensions. Amplicons were then purified by NucleoFast 96 PCR Plate clean-up system (Macherey-Nagel), and were sequenced with forward and reverse primers on an ABI 3130XL genetic analyser (Applied Biosystems). The newly generated sequences were then read and edited using Chromas v.1.45 software, and consensus sequences were compared using the Basic Local Alignment Search Tool (BLASTn) reveal-

ing up to 99% sequence similarity with reference sequences. Sequences from isolate Fmed It 17 used in this study were deposited in the GenBank database under accession numbers PZ489312 for the LSU region and PZ493570 for the ITS region.

The fungal mycelium was stored at −80 °C until used. Before each experiment, the isolate was reactivated by subculturing on potato dextrose agar (PDA; 18 g L^{-1}) plates and incubating for 2 weeks at 26 °C in the dark. All assays were carried out using 0.5 cm^2 mycelium plugs as inoculum and incubated at 26 °C in complete darkness under constant laboratory humidity conditions.

Experimental design

The research was divided into two main experimental sections:

- *Part I* assessed the effect of manganese on *F. mediterranea* growth, biomass production, and wood degradation, comparing young (3-year-old) and old (25-year-old) vine wood from *Vitis vinifera* 'Cabernet Sauvignon'. The objective was to determine the manganese (Mn^{2+}) concentration at which the fungus exhibited growth responses, and whether wood age influenced fungal growth.
- *Part II* focused only on old grapevine wood, as this is the natural host typically infected under vineyard conditions, and also showed the most consistent degradation patterns in Part I. Wood degradation and mycelium colonization were evaluated using *Vitis vinifera* wood discs. The fungus was also grown in submerged culture to determine whether enhanced degradation correlated with increased MnP production.

All experiments were carried out using three biological replicates, each comprising three technical replicates.

Part I: Fungal growth rate, mycelium biomass production, and wood degradation assays

This first part of the study aimed to assess effects of manganese on fungal growth, biomass production, and wood degradation, comparing young (3-year-old) and old (25-year-old) vine wood from *Vitis vinifera* 'Cabernet Sauvignon'.

Preparation of wood substrates

Fungal growth assays. Different wood-based substrates were prepared. For the mycelium growth rate assays, grapevine sawdust was used in a low-nutrient substrate consisting of PDA at 3 g L^{-1}. Two types of *Vitis vinifera* 'Cabernet Sauvignon' wood were included:

- Young wood: shoots collected from 3-year-old nursery plants
- Old wood: trunk wood obtained from a 25-year-old vineyard in Bolgheri, Italy

Wood material was cut, mechanically ground to sawdust, and sieved through a 0.2 mm mesh to obtain a uniform particle size. For each plate, 0.5 g of dry sawdust was added to 20 mL of PDA (3 g L^{-1}).

Mycelium biomass assays. The same sawdust used for the growth assays (above) was used. Petri plates each contained 20 mL of water agar supplemented with 2 g of dry sawdust. A sterile cellophane film was placed on the agar surface to facilitate clean removal of the fungal mycelium at the end of the incubation period.

Wood degradation assays. Intact wood splints were prepared from the young and old grapevine material. Splints were cut to approx. 5 cm in length and 0.3 cm in diam., then dried at 105 °C for 48 h to obtain constant dry weight of 0.25 g per splint. The splints were then placed on water agar plates amended with the respective Mn^{2+} treatments.

Manganese treatments

Mn^{2+} (as $MnSO_4$) was added to the substrates according to the different experimental treatments (Figure 1). For the *F. mediterranea* growth assays, the fungus was grown on a low-nutrient sawdust agar medium (PDA 3 g L^{-1}) formulated to reduce the influence of readily available nutrients from the culture medium, to promote fungal utilization of the lignocellulosic substrate. The experimental design included a no-sawdust control, a 0 μM Mn^{2+} control, and Mn-amended treatments at 80, 160, or 320 μM.

For the mycelial biomass assays conducted on water agar supplemented with sawdust, the treatments consisted of a 0 μM Mn^{2+} control, and Mn^{2+} concentrations of 80, 160, or 320 μM, along with an additional control of water agar without sawdust supplement.

For the wood degradation assays, intact wood splints were exposed to Mn^{2+} concentrations of 0, 80, 160, or 320 μM, together with a control condition in which wood was incubated without fungal inoculation. All treatments were conducted in triplicate.

Application protocols

Fungal growth assays. A mycelium plus agar plug (6 mm diam.) from a *F. mediterranea* PDA culture was

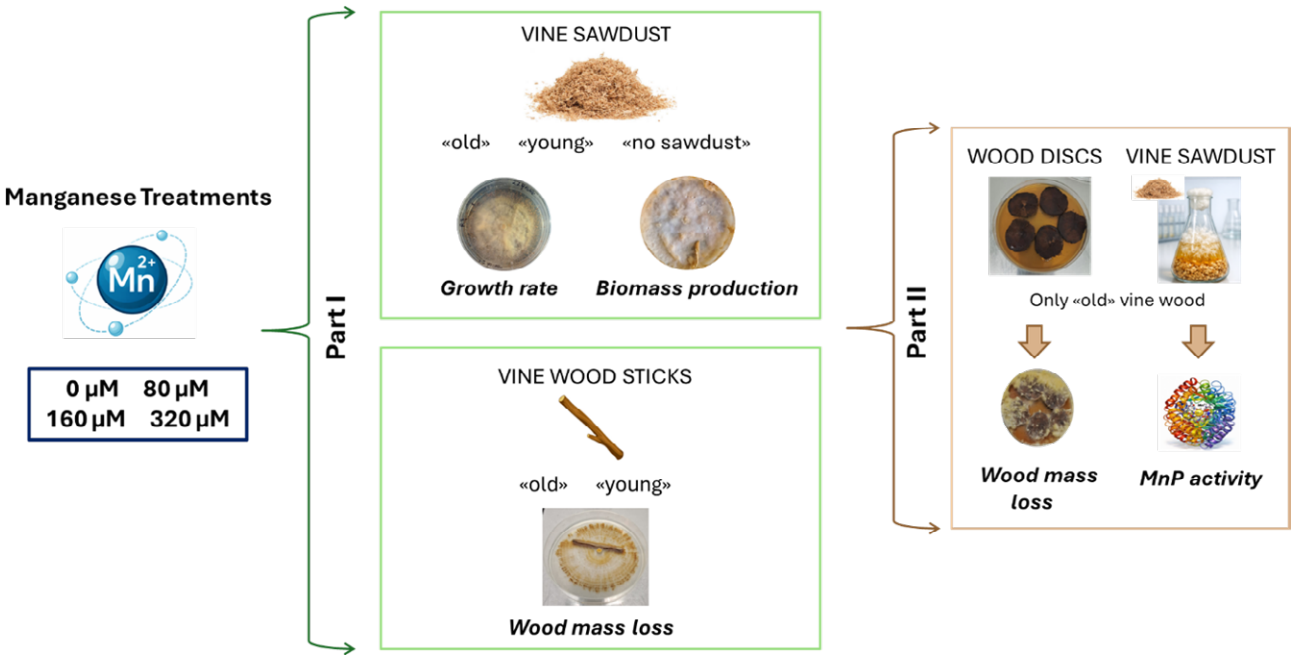

Figure 1. Experimental design.

placed at the centre of each Petri dish with sawdust prepared as described above. Plates were then incubated at 26 °C in complete darkness for 18 d. Digital images of resulting colonies were captured every 3 d, and each colony area was measured using ImageJ. Colony growth rates were expressed as the increase in colony area over time ($mm^2\ d^{-1}$).

Mycelium biomass assays. A mycelium plus agar plug (6 mm diam.) from a *F. mediterranea* PDA culture was placed at the centre of each Petri dish on the cellophane film, prepared as described above. Plates were then incubated for 1 month at 26 °C in the dark. Mycelium growing on the cellophane film was carefully scraped off, dried at 65 °C to constant weight, and weighed, to determine fungal dry biomass.

Wood degradation assays. A mycelium plug (6 mm diam.) from a *F. mediterranea* PDA culture was placed in contact with each wood splint on the agar surface. Wood splints were incubated for 1 month at 26 °C in the dark. After incubation, the splints were re-dried at 105 °C to constant weight. Wood degradation was quantified as mass loss, calculated as:

$$\text{Wood mass loss (\%)} = [(W_0 - Wt) / W_0] \times 100$$

where W_0 is the initial dry weight of the wood samples, and Wt is the dry weight after incubation.

Part II – Experiments on vine wood disks and manganese peroxidase production

This part of the study focused on old grapevine wood, as this represents the natural host typically infected under vineyard conditions, and showed the most consistent degradation patterns in Part I of this study. Wood degradation and mycelial colonization were evaluated using *Vitis vinifera* 'Cabernet Sauvignon' wood.

Wood disc degradation assay

Wood discs (approx. 3 cm diam., 0.5 mm thick) were obtained from the same 25-year-old *Vitis vinifera* stems. Five wood discs were placed in each large Petri dish (145 mm diam.), with three biological replicate plates per treatment. Total dry weight of the wood per treatment was standardized to approx. 16.5 g by selecting discs of equal total weight for each replicate. Water agar was used as the growth substrate. Mn^{2+} treatments assessed were 0, 80, 160, or 320 µM, together with a control treatment of wood incubated without fungal inoculation. The Petri dishes were incubated at 26 °C in complete darkness for 2 months. After incubation, the wood discs were dried and weighed to determine mass losses, following the procedures described above.

Enzymatic MnP assay

Liquid cultures of *F. mediterranea* were incubated for 21 d at 26 °C with orbital shaking (180 rpm) in 250-mL Erlenmeyer flasks each containing 100 mL of salt medium containing $MnSO_4$ at 0, 80,160 or 320 µM, as well as other salts (Rüttimann *et al*., 1992). The medium in each flask was supplemented with 3.5 g of *Vitis vinifera* 'Cabernet Sauvignon' sawdust, and was inoculated with three 0.5 cm diam. plugs taken from a 3-week-old PDA culture, together with a control condition in which wood was incubated without fungal inoculation. Three technical replicates of 10 mL from each of the three biological replicates were collected and processed through a four-step filtration procedure: first through a 50 µm Nilex sheet, followed by 1.0, 0.45, and 0.2 µm regenerated cellulose membrane filters. Fungal dry biomass was determined by drying the collected mycelium for at least 48 h at 103 ± 1 °C. The protein contents of the filtrates were determined spectrophotometrically, using a NanoDrop (BioSpec-nano, Shimadzu, Kyoto, Japan), assuming that absorbance of 1 OD corresponded to 1 mg mL^{-1} protein (Pacetti *et al*., 2022). The secretome was then diluted to a final protein concentration of 0.2 mg mL^{-1} for enzymatic assays.

The secretomes obtained from liquid cultures were used to assess their MnP activities, using the method of Mathieu *et al*. (2013). MnP activity was determined based on oxidative coupling between 3-methyl-2-benzothiazolinonehydrazone hydrochloride (MBTH) and p-dimethylaminobenzaldehyde (DMAB), catalyzed by peroxidases (PODs) in the presence of H_2O_2, and forming a purple indamine complex with an extinction coefficient of ε_{590} = 32,000 M^{-1} cm^{-1}. Assays were carried out at 28 °C in 96-well microplates and using a Tristar two plate reader (Berthold Technologies GmbH & Co.). Each reaction mixture (200 µL total volume) consisted of 140 µL of reagent solution, 50 µL of liquid culture secretome (0.2 mg mL^{-1}), and 10 µL of 1 mM H_2O_2 to initiate the reaction. The reagent solution contained 50 mM DMAB and 1 mM MBTH in a sodium lactate/sodium succinate buffer (100 mM; pH 4.5), supplemented with either 1 mM $MnSO_4$ (Solution A, to measure manganese-dependent activity) or 2 mM EDTA (Solution B, to measure manganese-independent activity). Specific MnP activity was calculated by subtracting the enzyme activity measured in Solution B from that measured in Solution A. Two types of controls were included using, respectively, heat-inactivated samples and H_2O_2-free mixtures. Volumetric activities (U L^{-1}) measured during the assays were converted to specific enzyme activity expressed as U mg^{-1} protein, by dividing the values by the protein concentration of the secretome, where 1 U corresponds to 1 µ mol of substrate oxidized per min.

Statistical analyses

All statistical analyses were carried out using IBM SPSS Statistics software (version 29). For the fungal growth assays and manganese peroxidase activity experiments, three biological replicates were used, each consisting of three technical replicates. Before statistical analyses, normality and homogeneity of variances were assessed, respectively, using Shapiro-Wilk tests ($P > 0.05$) and Levene's tests ($P > 0.05$). Variables meeting these assumptions were analysed using a General Linear Model (GLM) approach.

Data of fungus colony areas (mm^2), manganese peroxidase activity (U mg^{-1}), and wood discs mass loss (%), were analysed using one-way analyses of variance (one-way ANOVA) with Type III sums of squares, considering treatment as a fixed factor. Mean comparisons were made using Tukey's honestly significant difference (HSD) *post hoc* test at $P < 0.05$.

Data of wood biomass losses, fungal biomass production, and colony areas were additionally analysed using two-way factorial ANOVA within a univariate General Linear Model (Univariate GLM) framework, with Type III sums of squares. In these analyses, Mn concentrations added to culture medium (0, 80, 160, or 320 µM) and wood age (young wood, old wood) were considered as fixed factors. The interaction between Mn concentration and wood age was also included in the model to evaluate potential combined effects on the experimental variables. Mean comparisons were carried out using Tukey's HSD *post hoc* test at $P < 0.05$, and statistical significance was set at $P \leq 0.05$.

RESULTS

Part I: effect of Mn^{2+} on growth rate, biomass production, and wood degradation assays

Fungus growth rate

The no-sawdust control treatment (not shown in Figure 2), where *F. mediterranea* was inoculated onto water agar, no growth of the fungus was observed.

One-way ANOVA was first carried out to evaluate differences among individual treatments within each substrate (Figure 2). The growth area of *F. mediterranea* colonies was evaluated after 18 d of incubation. Fungal growth on PDA, without sawdust supplementation,

was consistently less than in the corresponding sawdust-amended treatments, indicating that, in addition to the limited nutrients provided by PDA, the fungus was able to utilize sawdust as a nutrient source. For the young wood substrate, the 80 µM Mn^{2+} treatment resulted in the greatest mean colony area, which differed ($P \leq 0.05$) from the other Mn^{2+} concentrations within the young wood treatments, and from all the other treatments. Similarly, in the old wood substrate, the 80 µM Mn^{2+} treatment also gave the greatest mean colony area, which differed ($P \leq 0.05$) from the corresponding 0 µM Mn^{2+} control. Therefore, in the young and old wood substrates, the 80 µM Mn^{2+} treatment gave greater fungal growth compared to the respective controls. In contrast, excessively high manganese concentrations (320 µM) inhibited fungus growth, with the 320 µM Mn^{2+} treatment giving the lowest growth values in young and old wood substrates.

Since the independent effects of substrate type (young wood, old wood, and no sawdust) and manganese concentration on the dependent variable fungal growth area were statistically significant, a two-way ANOVA was subsequently carried out to assess whether an interaction between these two factors also affected fungus growth. A two-way ANOVA showed a main effect ($P < 0.001$) on fungus growth area for substrate type and manganese concentration. A significant interaction ($P < 0.001$) between substrate type and manganese concentration was also detected, indicating that the effect of manganese on fungal growth varied depending on the substrate.

Fungus biomass production and wood degradation

Table 1 shows effects of Mn^{2+} treatments on fungus biomass production and wood degradation. The negative controls (not shown in the table), consisting of *F. mediterranea* grown on water agar without sawdust or wood sticks, and incubated without fungus inoculation, did not show detectable fungus growth or wood degradation. Two-way ANOVA showed that no statistically significant differences were detected between old and young wood at any of the manganese concentrations, either for fungus biomass production ($P = 0.822$) or wood mass loss ($P = 0.367$), showing that biomass production and wood degradation were similar for the two wood types (Table 1).

The highest amounts of fungus biomass and wood mass loss were from the 80 µM manganese treatment. Fungus biomass at 80 µM was greater than from all other treatments, regardless of wood type. Wood mass loss was also greatest at 80 µM, although no differences ($P > 0.05$) were detected between the 80 and 160 µM treatments. At 320 µM manganese, fungal biomass produc-

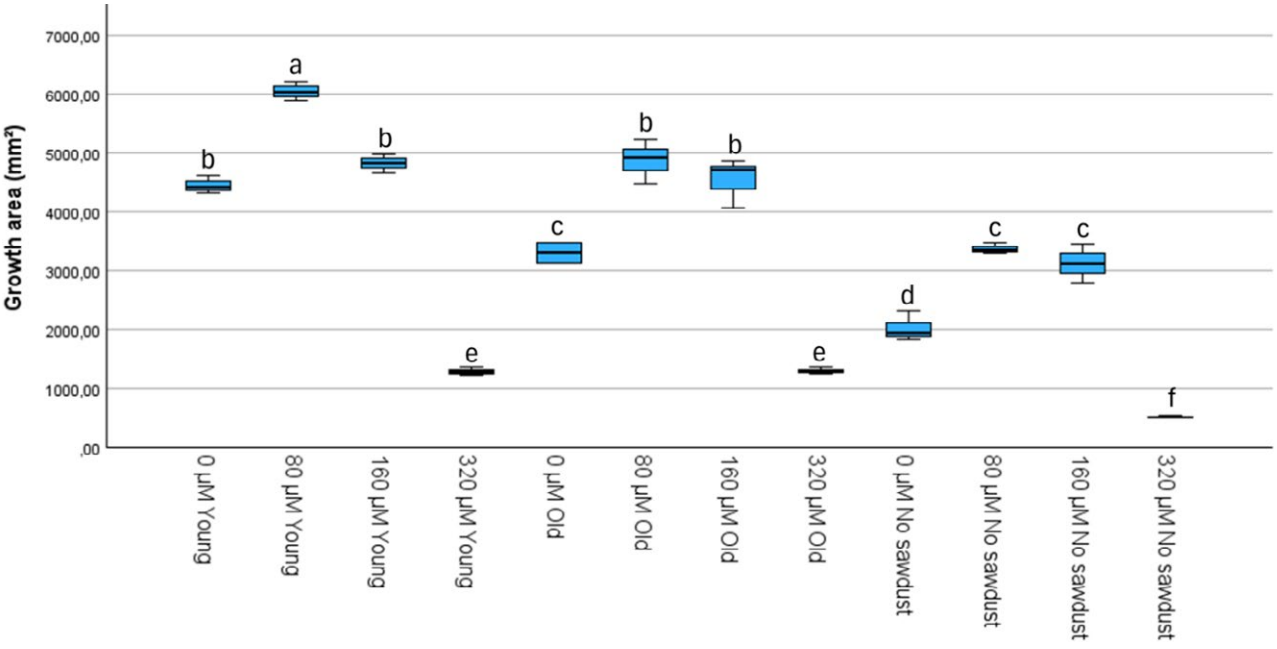

Figure 2. Mean fungal growth area (mm²) of *Fomitiporia mediterranea* after 18 d incubation on young and old *Vitis vinifera* sawdust in PDA (3 g L^{-1}) at different manganese concentrations. Box plots show median values, interquartile ranges, and minimum and maximum values. Different letters accompanying means indicate differences ($P \leq 0.05$) among treatments according to Tukey's honestly significant difference (HSD) tests.

Table 1. Mean *Fomitiporia mediterranea* biomass production (g) and wood stick dry mass loss (%) for young and old wood at different manganese concentrations. Data are means ± standard deviations. Means in each column accompanied by different letters differ ($P \leq 0.05$) among manganese concentrations, as shown by Tukey's honestly significant difference (HSD) tests.

Mn^{2+} µM	Mean fungus biomass (g)		Mean wood mass loss (%)	
	Old	Young	Old	Young
0	0.349 ± 0.034 c	0.312 ± 0.091 c	17.026 ± 3.447 b	17.173 ± 1.936 b
80	0.772 ± 0.054 a	0.758 ± 0.086 a	33.373 ± 2.341 a	29.360 ± 2.865 a
160	0.581 ± 0.060 b	0.619 ± 0.095 b	30.226 ± 2.294 a	27.772 ± 4.233 a
320	0.241 ± 0.033 c	0.228 ± 0.040 c	14.533 ± 2.610 b	16.666 ± 1.368 b

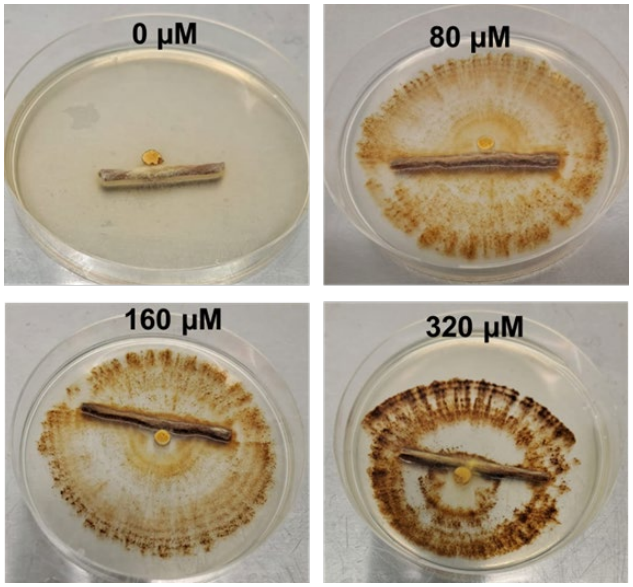

Figure 3. *Fomitiporia mediterranea* colonies on *Vitis vinifera* wood sticks, after 18 d incubation, on agar containing different manganese concentrations.

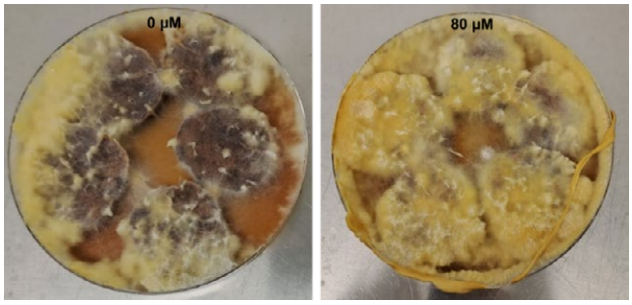

Figure 4. Growth of *Fomitiporia mediterranea* on grapevine wood discs (0 µM Mn^{2+} (left) or 80 µM (right).

tion and wood degradation were low, and were not different ($P > 0.05$) from the 0 µM treatment.

Qualitative observations of the *F. mediterranea* colonies detected visible differences among treatments (Figure 3). Compared to the experimental controls without manganese, increased release of dark brown/orange pigmentation was observed with the increasing manganese concentration treatments.

Part II: Effects of Mn^{2+} on grapevine wood discs and manganese peroxidase production

Effects of Mn^{2+} on wood disc degradation

The biomass loss experiment was repeated using old wood and cross-section discs obtained from grapevine branches (Figure 4). Old wood was selected because it is the grapevine tissue preferentially colonized by *F. mediterranea* under natural conditions. In this second experiment, the initial wood mass was increased to determine whether the differences observed in the first part of the study could be repeated under conditions of greater substrate availability.

The non-inoculated control treatment did not result in detectable changes in wood dry biomass at the end of the experiment. The results (Figure 5) showed the same overall trend observed in Part I for the old wood substrate. At 80 µM and 160 µM manganese concentrations, biomass loss was greater ($P \leq 0.05$) than in the 0 µM manganese control treatment, whereas at 320 µM manganese, biomass loss was comparable to that of the control.

Across treatments, highest degradative activity was consistently observed at 80 µM manganese, although no differences ($P > 0.05$) were detected between the 80 and 160 µM Mn^{2+} treatments, further supporting the effect of intermediate manganese concentrations in enhancing fungal degradative activity.

Effects of Mn^{2+} on production of manganese peroxidase

In the negative experimental control (not shown Figure 6, below), consisting of the liquid substrate without

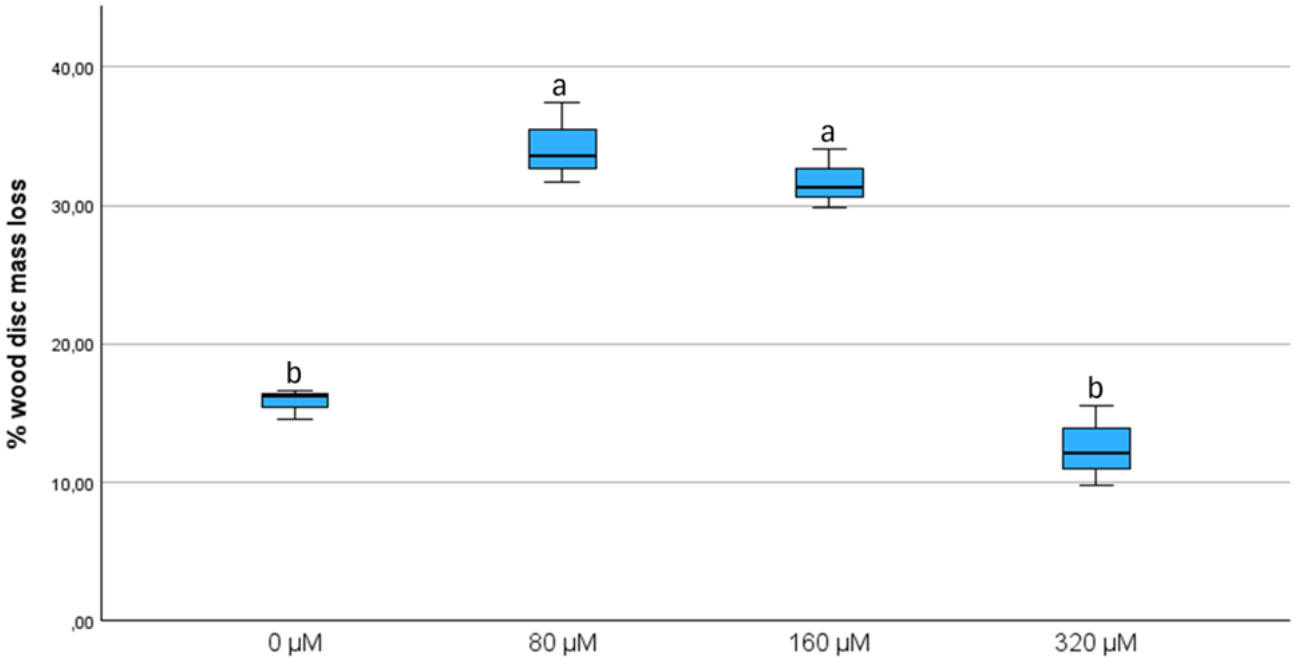

Figure 5. Mean weight losses for old *Vitis vinifera* wood discs in *Fomitiporia mediterranea* cultures at different manganese concentrations. The box plots show median values, interquartile ranges, and minimum and maximum values. Means accompanied by different letters are different ($P \leq 0.05$) according to Tukey's honestly significant difference (HSD) tests.

fungus inoculation, no manganese peroxidase activity was detected. At 80 µM and 160 µM manganese concentrations, however, peroxidase activity was greater than from the control treatment without manganese. Greatest MnP activity was detected at 80 µM Mn^{2+}, as mean specific activity of 4.19 ± 0.284 U mg^{-1} (mean ± SD), followed by the 160 µM treatment, which gave mean activity of 3.855 ± 0.289 U mg^{-1}. Both of these treatments were different from the 0 µM and 320 µM manganese treatments. The lowest MnP activities were recorded from the 0 µM control treatment (0.791 ± 0.218 U mg^{-1}), or from 320 µM Mn^{2+} (1.412 ± 1.561 U mg^{-1}).

DISCUSSION

The Part I results from this study highlight the concentration-dependent role of Mn^{2+} in modulating growth, biomass production, and wood-degrading ability of *F. mediterranea*. Manganese at intermediate concentrations was stimulatory, but inhibitory to the fungus at high concentration, confirming its dual role as an essential micronutrient and a potential toxic element for fungal metabolism, particularly in fungi causing white rot (Gadd, 1994; Baldrian, 2003). Manganese-enriched substrates have been shown to enhance manganese peroxidase production and wood-degrading activity in other white rot fungi, including *Ceriporiopsis subvermispora*, where Mn^{2+} availability directly stimulated ligninolytic enzyme systems and decay efficiency (Benavides *et al*., 2024). These results support the hypothesis that Mn^{2+} plays a key regulatory role in oxidative wood decay processes activated by the white rot pathogen *F. mediterranea*.

The Mn^{2+} concentrations used in the present study were selected to match experimentally relevant ranges previously reported in white rot pathogen systems. Mancilla *et al*. (2010) investigated a comparable gradient of Mn^{2+} concentrations, and identified an intermediate range as optimal for MnP induction, providing a methodological and biological basis for the concentrations adopted here. Among the manganese treatments applied, the 80 µM concentration promoted the greatest *F. mediterranea* growth rates and biomass production, indicating an optimal Mn^{2+} availability for metabolism and enzyme activation in this pathogen. The increased growth observed on young host wood could be related to differences in wood structure and chemical composition, including low lignin recalcitrance and high accessibility of carbohydrates (Blanchette, 1991).

Unlike mycelial radial growth, *F. mediterranea* biomass accumulation did not differ between young and old wood, indicating that manganese availability played a more dominant role than wood age, although wood age strongly influences characteristics, such as increased

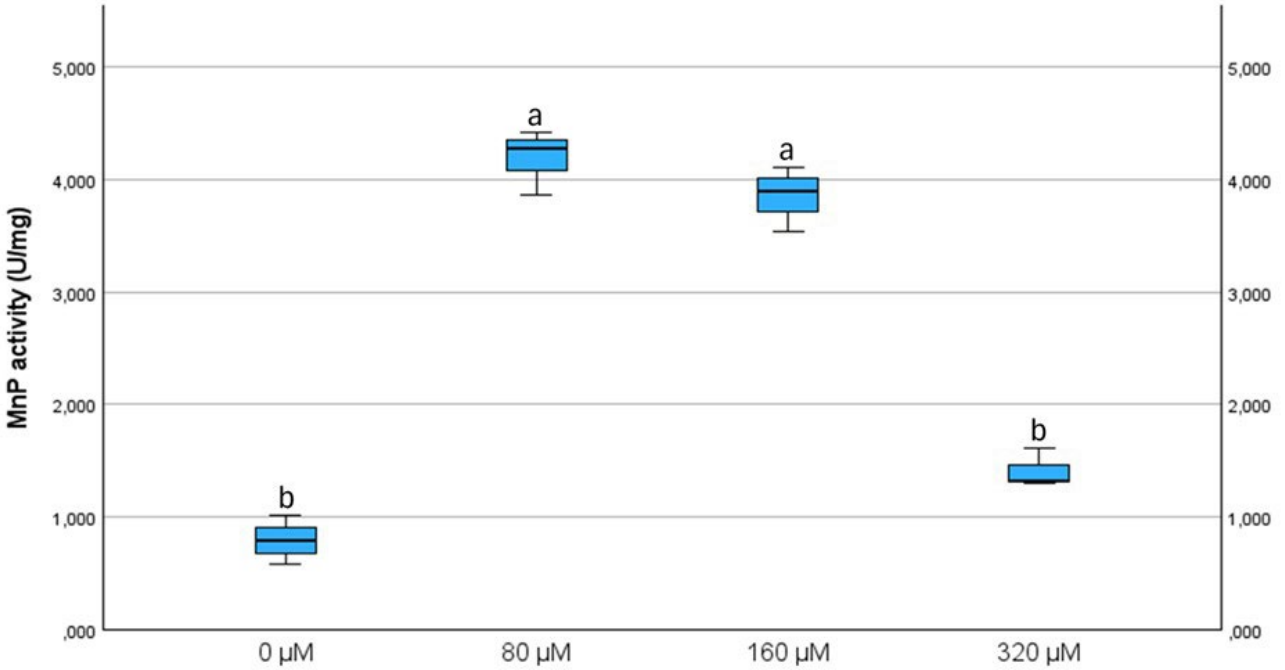

Figure 6. Mean manganese peroxidase activity in submerged *Fomitiporia mediterranea* cultures at different manganese concentrations and enriched with old *Vitis vinifera* sawdust. The box plots show median values, interquartile ranges, and minimum and maximum values. Different letters indicate differences ($P \leq 0.05$) among treatments according to Tukey's honestly significant difference (HSD) tests.

lignin content and structural complexity (Fengel and Wegener, 1984; Blanchette, 1991), and regulates mycelium production. Despite the lack of statistical significance, biomass production tended to be greater in old than in young wood. This is consistent with field observations, where grapevine trunk diseases primarily affect old grapevines. The observed stimulatory effect of manganese on fungus growth and biomass accumulation was similar to effects reported in previous research, where Mn^{2+} played a key role in support of oxidative metabolism and ligninolytic enzyme systems in white rot fungi, and promoted mycelium development (Hatakka, 1994; Hofrichter, 2002).

The wood degradation assays further indicated the stimulatory role of manganese at intermediate concentrations. At 80 µM and 160 µM Mn^{2+}, wood mass losses were greater than in the control treatment (no added manganese), confirming that manganese enhanced *F. mediterranea* degradative capacity. The absence of statistically significant differences between these two concentrations indicates a saturation effect, similar to that reported elsewhere. This indicates that manganese-dependent enzymes, such as MnP, reach maximum activity within limited Mn^{2+} concentration ranges (Hatakka, 1994).

At the greatest manganese concentration tested (320 µM), both growth rate and biomass production of *F. mediterranea* were reduced compared to the manganese-free control, indicating toxic effects. Excess Mn^{2+} has been shown to overwhelm fungal homeostatic mechanisms, causing ion imbalance, oxidative stress, and interference with essential cellular processes, as has been demonstrated in *Saccharomyces cerevisiae* and suggested for filamentous fungi (Yang *et al*., 2005; Robinson *et al*., 2021). This inhibitory threshold may also have ecological relevance for ECDs. Blanchette *et al*. (1984) reported localized Mn^{2+} accumulation within black zone lines that separate decayed from apparently healthy host wood tissues. The inhibitory effects observed at high Mn^{2+} concentrations in the present study indicate that localized Mn^{2+} accumulation could influence fungal activity within these transition zones. However, this interpretation requires direct *in planta* validation.

Qualitative observations also showed increasing release of dark brown/orange pigmentation in grapevine wood with increasing Mn^{2+} concentrations**.** Based on microscope observations and on the occurrence of Mn-rich dark zone lines previously described in decayed wood tissues (Blanchette *et al*., 1984), it is likely that this pigmentation is associated with manganese oxide compounds generated through fungal-mediated Mn^{2+} oxidation**.** Similar phenomena have been described in white rot fungi, and are often linked to manganese peroxidase

activity, which oxidizes Mn^{2+} into the highly reactive Mn^{3+} involved in ligninolytic processes (Li *et al*., 2022). However, further chemical and spectroscopic analyses are required to confirm the precise nature of these compounds.

The second part of the present study was designed to further investigate the role of Mn^{2+} in grapevine wood degradation, and to assess the possible link between biomass loss and manganese peroxidase activity, using experimental conditions that resemble those encountered by *F. mediterranea* during wood colonization in grapevine tissues. Consistent with the results obtained in Part I, manganese supplementation enhanced wood degradation at intermediate concentrations of 80 µM and 160 µM Mn^{2+}, whereas no enhancement was observed at 320 µM Mn^{2+}. These results confirm the concentration-dependent effects of Mn^{2+} observed in Part I, while extending these observations to natural grapevine wood conditions, and on an increased experimental scale. Given that *F. mediterranea* is considered a key species associated with ECDs, and that its wood degradation by-products have been suggested as contributors to foliar symptom development (Mugnai *et al*., 1999), these results further support the potential involvement of Mn^{2+}-dependent mechanisms in GLSD. Increased Mn^{2+} availability probably enhances fungus degradative activity, and consequently favours production or release of metabolites potentially associated with GLSD foliar symptom expression.

The analyses of manganese peroxidase production provided a mechanistic explanation for the observed wood degradation patterns. MnP activity increased with increasing manganese concentrations, and reached significant levels at 80 µM and 160 µM Mn^{2+}, followed by a decline at the greatest Mn^{2+}concentration assessed. This bell-shaped response mirrored the trends observed for *F. mediterranea* growth, biomass production, and wood degradation, indicating the functional link between Mn^{2+} availability, MnP expression, and fungus degradative capacity. Manganese peroxidase is a key enzyme in white rot fungi, catalyzing the oxidation of Mn^{2+} to Mn^{3+}, which acts as a low-molecular-weight diffusible oxidant capable of attacking lignin and other phenolic compounds at a distance from hyphae (Hatakka, 1994; Hofrichter, 2002). The enhanced MnP activity observed at intermediate manganese concentrations provides a direct explanation for the increased biomass loss measured in both parts of the present study. Similar manganese-dependent regulation of MnP activity has been reported in other white rot fungi, including *Ceriporiopsis subvermispora* and *Phanerochaete chrysosporium*, where Mn^{2+} availability is a limiting factor for efficient ligninolytic activity (Couto *et al*., 1998; Kannaiyan *et al*., 2015). Mn^{2+} has been shown to be an essential requirement for stimulation of extracellular MnP production in several white rot fungi, including *C. subvermispora*, *Trametes versicolor*, *P. chrysosporium*, and *Pleurotus ostreatus*, further supporting the central role of manganese in regulating ligninolytic enzyme systems (Brown *et al*., 1991; Ruttiman-Johnson *et al*., 1992; Johansson *et al*., 2002). For ECDs, MnP-mediated Mn^{2+} oxidation and the associated production of diffusible Mn^{3+} chelates may contribute to the spatial dynamics of lignin modification and wood cell wall degradation in infected grapevine tissues. These oxidative processes could influence the extent and pattern of wood decay caused by *F. mediterranea*, so factors influencing Mn^{2+} concentration could influence wood decay process and its consequences for host plant leaves. However, given the complexity of Esca aetiology, and the involvement of multiple fungal species and host responses, this interpretation should be considered as a working hypothesis rather than a direct causal link.

At 320 µM Mn^{2+}, the decline in MnP activity likely reflected interference with enzyme production and/or stability, consistent with the inhibitory effects observed on grapevine growth and biomass. As discussed for Part I (above), this may result from disruption of Mn^{2+} homeostasis, where excessive intracellular Mn^{2+} impairs oxidative metabolism (Robinson *et al*., 2021).

Some limitations of the present study should be acknowledged. Firstly, all experiments were conducted under controlled *in vitro* conditions, which, while allowing precise manipulation of Mn^{2+} availability, do not capture the full complexity of *in planta* environments, including host immune responses, competing microorganisms, and dynamic soil chemistry. Secondly, while the Mn^{2+} concentrations used were selected based on a comparable study of *Ceriporiopsis subvermispora* (Mancilla *et al*., 2010), the direct correspondence to manganese bioavailability in grapevine wood under natural conditions remains to be determined. Thirdly, the present study used one isolate of *F. mediterranea*, and intraspecific variability in Mn^{2+} sensitivity and MnP production capacity cannot be excluded. These limitations underscore the need for follow-up *in vivo* and field-based research to validate and extend the results reported here.

The results reported here provide important insights into the mechanisms underlying grapevine wood colonization and degradation by *F. mediterranea*, the white rot agent of ECDs. This pathogen preferentially colonizes old wood, where manganese availability may locally favour MnP-mediated lignin degradation,

thereby facilitating pathogen spread and the progressive development of white rot. A possible implication of these results is that soils with high manganese availability may enhance plant uptake of this element, and consequently promote manganese accumulation in woody tissues, as manganese is readily absorbed by roots and translocated through host xylem, particularly under acidic soil conditions or when Mn^{2+} bioavailability is high (Kabata-Pendias, 2000; Fageria *et al*., 2010; Marschner, 2011).

On this basis, it can be hypothesized that soil manganese availability probably influences the development of grapevine wood colonization by modulating MnP activity, and, therefore, wood degradation efficiency in Mn-dependent trunk pathogens such as *F. mediterranea*, although this remains to be confirmed by dedicated *in planta* experiments.

CONCLUSIONS

The combined results of both experimental parts of this study demonstrate that Mn^{2+} plays a key, concentration-dependent role in regulating the growth, enzymatic activity, and wood-degrading capacity of *F. mediterranea*. In addition, the use of different wood types and experimental procedures demonstrated that while substrate characteristics (e.g., young vs. old wood) can influence pathogen growth dynamics, manganese availability is a dominant factor controlling decay efficiency.

The present study was conducted using one isolate of *F. mediterranea*, which is an inherent limitation. Intraspecific variability in MnP and laccase activity has been documented in *F. mediterranea*, and associated with differential expression of peroxidase-encoding isoforms (Pacetti *et al*., 2022). Therefore, the absolute enzymatic values recorded in the present research should not be generalized for the species. Other isolates may exhibit different baseline MnP activities and different responses to manganese supplementation. Future research including multiple isolates with contrasting enzymatic profiles is required to determine whether the stimulatory effects of manganese on MnP production and wood degradative capacity observed in this study are a conserved physiological response across *F. mediterranea* strains or are an isolate-dependent trait.

Overall, these results highlight the need to investigate micronutrient bioavailability and the influencing factors of this bioavailability, as potential abiotic drivers of wood colonization in Esca complex progression, with manganese emerging as a key factor influencing pathogenesis.

LITERATURE CITED

Baldrian P., 2003. Interactions of heavy metals with white-rot fungi. *Enzyme and Microbial Technology* 32(1): 78–91. https://doi.org/10.1016/S0141-0229(02)00245-4

Benavides V., Ciudad G., Pinto-Ibieta F., Robledo T., Rubilar O., Serrano A., 2024. Enhancing laccase and manganese peroxidase activity in white-rot fungi: the role of copper, manganese, and lignocellulosic substrates. *Agronomy* 14(11): 2562. https://doi.org/10.3390/agronomy14112562

Berg B., Steffen K. T., McClaugherty C., 2007. Litter decomposition rate is dependent on litter Mn concentrations. *Biogeochemistry* 82(1): 29–39. https://doi.org/10.1007/s10533-006-9050-6

Blanchette R. A., 1984. Manganese accumulation in wood decayed by white rot fungi. *Phytopathology* 74(6): 725–730.

Blanchette R. A., 1991. Delignification by wood-decay fungi. *Annual Review of Phytopathology* 29(1): 381–403.

Brown J. A., Alic M., Gold M. H., 1991. Manganese peroxidase gene transcription in *Phanerochaete chrysosporium*: activation by manganese. *Journal of Bacteriology* 173(13): 4101–4106. https://doi.org/10.1128/jb.173.13.4101-4106.1991

Brown J. A., Glenn J. K., Gold M. H., 1990. Manganese regulates the expression of manganese peroxidase by *Phanerochaete chrysosporium*. *Journal of Bacteriology* 172(6): 3125–3130.

Bruez E., Larignon P., Bertsch C., Robert-Siegwald G., Lebrun M. H., Rey P., Fontaine F., 2021. Impacts of sodium arsenite on wood microbiota of esca-diseased grapevines. *Journal of Fungi* 7(7): 498. https://doi.org/10.3390/jof7070498

Bruez E., Larignon P., Compant S., Rey P., 2017. Investigating the durable effect of the hot water treatment used in nurseries on pathogenic fungi inhabiting grapevine wood and involved in grapevine trunk diseases. *Crop Protection* 100: 203–210. https://doi.org/10.1016/j.cropro.2017.07.001

Bruez E., Vallance J., Gautier A., Laval V., Compant S., Maurer W., Rey P., 2020. Major changes in grapevine wood microbiota are associated with the onset of esca, a devastating trunk disease. *Environmental Microbiology* 22(12): 5189–5206. https://doi.org/10.1111/1462-2920.15180

Calzarano F., Amalfitano C., Seghetti L., Cozzolino V., 2009. Nutritional status of vines affected with esca proper. *Phytopathologia Mediterranea* 48(1): 20–31.

Calzarano F., Amalfitano C., Seghetti L., Di Marco S., 2023. Effect of different foliar fertilizer applications

on esca disease of grapevine: symptom expression and nutrient content in the leaf and composition of the berry. *Agronomy* 13(5): 1355. https://doi.org/10.3390/agronomy13051355

Calzarano F., Osti F., Baránek M., Di Marco S., 2018. Rainfall and temperature influence expression of foliar symptoms of grapevine leaf stripe disease (esca complex) in vineyards. *Phytopathologia Mediterranea* 57(3): 488–505. 10.14601/Phytopathol_Mediterr-23787

Chiarappa L., 1997. Phellinus ignarius: the cause of spongy wood decay of black measles (" esca") disease of grapevines. *Phytopathologia Mediterranea* 36(2): 109–111.

Cholet C., Bruez É., Lecomte P., Barsacq A., Martignon T., Giudici M., … Gény L., 2021. Plant resilience and physiological modifications induced by curettage of esca-diseased grapevines. *OENO One* 55(1): 153–169. https://doi.org/10.20870/oeno-one.2021.55.1.4478

Couto S. R., Longo M. A., Cameselle C., Sanromán A., 1998. Influence of some inducers on activity of ligninolytic enzymes from corncob cultures of *Phanerochaete chrysosporium* in semi-solid-state conditions. *Progress in Biotechnology* 15: 703–708. Elsevier.

Del Frari G., Gobbi A., Aggerbeck M. R., Oliveira H., Hansen L. H., Ferreira R. B., 2019. Characterization of the wood mycobiome of *Vitis vinifera* in a vineyard affected by esca. Spatial distribution of fungal communities and their putative relation with leaf symptoms. *Frontiers in Plant Science* 10: 910. https://doi.org/10.3389/fpls.2019.00910

Dell'Acqua N., Gambetta G. A., Comont G., Ferrer N., Rochepeau A., Pétriacq P., Delmas C. E., 2025. Nitrogen nutrition impacts grapevine esca leaf symptom incidence, physiology, and metabolism. *Journal of Experimental Botany* 76(11): 3225–3242. https://doi.org/10.1093/jxb/eraf172

Doyle J.J. and Doyle J.L, 1987. A rapid DNA isolation procedure for small quantities of fresh leaf tissue. *Phytochemical Bulletin* 19: 11–15.

Dunford H. B., 1991. Horseradish peroxidase: Structure and kinetic properties. In: *Peroxidases in Chemistry* (Everse J., Everse K.E., Grisham M.B., ed.), 1–23.

Elena G., Bruez E., Rey P., Luque J., 2018. Microbiota of grapevine woody tissues with or without esca-foliar symptoms in northeast Spain. *Phytopathologia Mediterranea* 57(3): 425–438.

Fageria N. K., Baligar V. C., Jones C. A., 2010. *Growth and Mineral Nutrition of Field Crops*. CRC Press, Boca Raton, Florida, U.S.A., 586 pp.

Fengel D., Wegener G., 1984. *Wood: Chemistry, Ultrastructure, Reactions*. De Gruyter, Berlin, Germany, New York, NY, USA, 613 pp.

Fischer M., 2002. A new wood-decaying basidiomycete species associated with esca of grapevine: *Fomitiporia mediterranea* (Hymenochaetales). *Mycological Progress* 1: 315–324. https://doi.org/10.1007/s11557-006-0029-4

Floudas D., Binder M., Riley R., Barry K., Blanchette R. A., Henrissat B., … Hibbet D. V., 2012. The paleozoic origin of enzymatic lignin decomposition reconstructed from 31 fungal genomes. *Science*, 336, 1715–1719. 10.1126/science.1221748

Fu X., Zhang J., Gu X., Yu H., Chen S., 2021. A comprehensive study of the promoting effect of manganese on white rot fungal treatment for enzymatic hydrolysis of woody and grass lignocellulose. *Biotechnology for Biofuels*: 14(1): 176. https://doi.org/10.1186/s13068-021-02024-7

Gadd G. M., 1994. Interactions of fungi with toxic metals. In: *The Genus Aspergillus: From Taxonomy and Genetics to Industrial Application* 361–374.

Gramaje D., Mostert L., Groenewald J. Z., Crous P. W., 2015. *Phaeoacremonium*: from esca disease to phaeohyphomycosis. *Fungal Biology* 119(9): 759–783. https://doi.org/10.1016/j.funbio.2015.06.004

Gramaje D., Úrbez-Torres J. R., Sosnowski M. R., 2018. Managing grapevine trunk diseases with respect to etiology and epidemiology: current strategies and future prospects. *Plant Disease* 102(1): 12–39. https://doi.org/10.1094/PDIS-04-17-0512-FE

Guerin-Dubrana L., Fontaine F., Mugnai L., 2019. Grapevine trunk disease in European and Mediterranean vineyards: occurrence, distribution and associated disease-affecting cultural factors. *Phytopathologia Mediterranea* 58(1): 49–71.

Hatakka A., 1994. Lignin-modifying enzymes from selected white-rot fungi: production and role from in lignin degradation. *FEMS Microbiology Reviews* 13(2-3): 125–135.

Hofrichter M., 2002. Lignin conversion by manganese peroxidase (MnP). *Enzyme and Microbial Technology* 30(4): 454–466. https://doi.org/10.1016/S0141-0229(01)00528-2

Johansson T., Nyman P. O., Cullen D., 2002. Differential regulation of mnp2, a new manganese peroxidase-encoding gene from the ligninolytic fungus *Trametes versicolor* PRL 572. *Applied and Environmental Microbiology* 68(4): 2077–2080. https://doi.org/10.1128/AEM.68.4.2077-2080.2002

Kabata-Pendias A., 2000. *Trace Elements in Soils and Plants*. CRC Press. Gaithetsburg, Maryland, U.S.A.

Kannaiyan R. K., Nader Mahinpey N. M., Kostenko V., Martinuzzi R. J., 2015. Nutrient media optimization for simultaneous enhancement of the laccase and

peroxidases production by coculture of *Dichomitus squalens* and *Ceriporiopsis subvermispora*. *Biotechnology and Applied Biochemistry* 62(2): 173–185. https://doi.org/10.1002/bab.1263

Kirk T. K., Cullen D., 1998. Enzymology and molecular genetics of wood degradation by white-rot fungi. *Environmentally Friendly Technologies for the Pulp and Paper Industry* 273-307.

Kishi K., Wariishi H., Marquez L., Dunford H. B., Gold M. H., 1994. Mechanism of manganese peroxidase compound II reduction. Effect of organic acid chelators and pH. *Biochemistry* 33(29): 8694–8701.

Li T., Cui L., Song X., Cui X., Wei Y., Tang L., … Xu Z., 2022. Wood decay fungi: an analysis of worldwide research. *Journal of Soils and Sediments* 22(6): 1688–1702. https://doi.org/10.1007/s11368-022-03225-9

Mancilla R. A., Canessa P., Manubens A., Vicuña, R., 2010. Effect of manganese on the secretion of manganese-peroxidase by the basidiomycete *Ceriporiopsis subvermispora*. *Fungal Genetics and Biology* 47(7):656-661. 10.1016/j.fgb.2010.04.003

Marchi G., Peduto F., Surico G., Di Marco S., Calzarano F., Mugnai L., 2006. Some observations on the relationship of manifest and hidden esca to rainfall. *Phytopathologia Mediterranea* 45: 1000–1010.

Marschner H., 2011. *Marschner's Mineral Nutrition of Higher Plants*. Academic Press. Adelaide, Australia, 649 pp.

Mathieu Y., Gelhaye E., Dumarçay S., Gérardin P., Harvengt L., Buée M., 2013. Selection and validation of enzymatic activities as functional markers in wood biotechnology and fungal ecology. *Journal of Microbiological Methods* 92(2): 157–163. https://doi.org/10.1016/j.mimet.2012.11.017

Moretti S., Pacetti A., Pierron R., Kassemeyer H. H., Fischer M., Péros J. P., … Farine S., 2021. *Fomitiporia mediterranea* M. Fisch., the historical esca agent: a comprehensive review on the main grapevine wood rot agent in Europe. *Phytopathologia Mediterranea* 60(2): 351–379.

Mugnai L., Graniti A., Surico G., 1999. Esca (black measles) and brown wood-streaking: two old and elusive diseases of grapevines. *Plant Disease* 83(5): 404–418.

Mugnai L., Guiggiani M., Bazzo F., Marchi G., Surico G., 2010. Il mal dell'esca e la carie bianca del legno: agenti causali, sintomatologia e casi studio di esca giovane. In: *Il mal dell'esca della vite* (G. Surico, L. Mugnai, ed.), ARSIA Regione Toscana, Firenze, Italy, 65–88.

Pacetti A., Moretti S., Perrin C., Gelhaye E., Bieler E., Kassemeyer H. H., … Bertsch C., 2022. Grapevine wood-degrading activity of *Fomitiporia mediterranea* M. Fisch.: a focus on the enzymatic pathway regulation. *Frontiers in Microbiology* 13: 844264. https://doi.org/10.3389/fmicb.2022.844264

Pacetti A., Moretti S., Pinto C., Compant S., Farine S., Bertsch C., Mugnai L., 2021. Trunk surgery as a tool to reduce foliar symptoms in diseases of the esca complex and its influence on vine wood microbiota. *Journal of Fungi* 7(7): 521. https://doi.org/10.3390/jof7070521

Pèros J. P., Berger G., Jamaux-Despréaux I., 2008. Symptoms, wood lesions and fungi associated with esca in organic vineyards in Languedoc-Roussillon (France). *Journal of Phytopathology* 156: 297–303.

Radaelli L., Calamai L., 2001. *Chimica del Terreno*. Piccin, Padova, Italy, 300 pp.

Rehner S.A. and Samuels G.J., 1994. Taxonomy and phylogeny of *Gliocladium* analysed from nuclear large subunit ribosomal DNA sequences. *Mycological Research* 98(6): 625–634.

Robinson J. R., Isikhuemhen O. S., Anike F. N., 2021. Fungal–metal interactions: a review of toxicity and homeostasis. *Journal of Fungi* 7(3): 225. https://doi.org/10.3390/jof7030225

Ruttimann C., Schwember E., Salas L., Cullen D., Vicuna R., 1992. Ligninolytic enzymes of the white rot basidiomycetes *Phlebia brevispora* and *Ceriporiopsis subvermispora*. *Biotechnology and Applied Biochemistry* 16(1): 64–76.

Sánchez-Torres P., Hinarejos R., González V., Tuset J. J., 2008. Identification and characterization of fungi associated with esca in vineyards of the Comunidad Valenciana (Spain). *Spanish Journal of Agricultural Research* 6(4): 650–660. https://doi.org/10.5424/sjar/2008064-357

Scheel T., Höfer M., Ludwig S., Hölker U., 2000. Differential expression of manganese peroxidase and laccase in white-rot fungi in the presence of manganese or aromatic compounds. *Applied Microbiology and Biotechnology* 54(5): 686–691. https://doi.org/10.1007/s002530000427

Schilling M., Levasseur M., Barbier M., Oliveira-Correia L., Henry C., Touboul D., … Gelhaye E., 2023. Wood degradation by *Fomitiporia mediterranea* M. Fischer: exploring fungal adaptation using metabolomic networking. *Journal of Fungi* 9(5): 536. https://doi.org/10.3390/jof9050536

Schilling M., Maia-Grondard A., Baltenweck R., Robert E., Hugueney P., Bertsch C., … Gelhaye E., 2022. Wood degradation by *Fomitiporia mediterranea* M. Fischer: physiologic, metabolomic and proteomic approaches. *Frontiers in Plant Science* 13: 988709. https://doi.org/10.3389/fpls.2022.988709

Slavens S., Marek S. M., Wilkins M. R., 2019. Effects of copper, manganese, and glucose on the induction of ligninolytic enzymes produced by *Pleurotus ostreatus* during fungal pretreatment of switchgrass. *Transactions of the ASABE* 62(6): 1673–1681. 10.13031/trans.13446

Sparapano L., Bruno G., Ciccarone C., Graniti A., 2000a. Infection of grapevine with some esca-disease associated fungi. I. *Fomitiporia punctata* as a wood decay inducer. *Phytopathologia Mediterranea* 39: 46–52.

Sparapano L., Bruno G., Ciccarone C., Graniti A., 2000b. Infection of grapevine with some esca-disease associated fungi. II. Interaction among *Fomitiporia punctata*, *Phaeoacremonium chlamydosporum* and *P. aleophilum*. *Phytopathologia Mediterranea* 39: 53–58.

Surico G., 2009. Towards a redefinition of the diseases within the esca complex of grapevine. *Phytopathologia Mediterranea* 48(1): 5–10.

Surico G., Mugnai L., Braccini P., & Marchi G., 2000. Epidemiology of esca in some vineyards in Tuscany (Italy). *Phytopathologia Mediterranea* 1000-1016.

Wariishi H., Akileswaran L., Gold M. H., 1988. Manganese peroxidase from the basidiomycete *Phanerochaete chrysosporium*: spectral characterization of the oxidized states and the catalytic cycle. *Biochemistry* 27(14): 5365–5370.

Wariishi H., Huang J., Dunford H. B., Gold M. H., 1991. Reactions of lignin peroxidase compounds I and II with veratryl alcohol. Transient-state kinetic characterization. *Journal of Biological Chemistry* 266(31): 20694–20699.

Wariishi H., Valli K., Gold M. H., 1992. Manganese (II) oxidation by manganese peroxidase from the basidiomycete *Phanerochaete chrysosporium*. Kinetic mechanism and role of chelators. *Journal of Biological Chemistry* 267(33): 23688–23695.

White T. J., Bruns T., Lee S., Taylor J.W., 1990. *PCR Protocols: A Guide to Methods and Applications*. *Academic Press*, New York, United States.

Yang M., Jensen L. T., Gardner A. J., Culotta V. C., 2005. Manganese toxicity and *Saccharomyces cerevisiae* Mam3p, a member of the ACDP (ancient conserved domain protein) family. *Biochemical Journal* 386(3): 479–487. https://doi.org/10.1042/BJ20041582

Phytopathologia Mediterranea
The international journal of the
Mediterranean Phytopathological Union

Firenze University Press
www.fupress.com/pm

Research Papers

First detection of *Pectobacterium carotovorum* associated with potato soft rot in Georgia

Maka MURADASHVILI[1,*], Galina MEPARISHVILI[1], Zoia SIKHARULIDZE[1], Marina TEDIASHVILI[2], Tamar KOKASHVILI[2], Marjon KRIJGER[3], Jan VAN DER WOLF[3]

[1] *Institute of Phytopathology and Biodiversity, Batumi Shota Rustaveli State University, Batumi 6010, Georgia*
[2] *G. Eliava Institute of Bacteriophages, Microbiology and Virology. Tbilisi, 0160, Georgia*
[3] *Wageningen University & Research, Droevendaalsesteeg 1, 6708 PB Wageningen, the Netherlands*
*Corresponding author. E-mail: m.muradashvili@bsu.edu.ge

Summary. Potato (*Solanum tuberosum* L.) is an important food crop in Georgia; but use of poor-quality seed potatoes and presence of harmful pathogens are important contributors to low crop productivity. Potato soft rot, caused by *Pectobacterium carotovorum*, had not been previously identified in potato crops in Georgia. During field surveys, potato tubers exhibiting typical soft rot symptoms, including water-soaked lesions, tissue maceration, and discolouration, were collected from farmers' fields, storage facilities, and experimental plots. The sampled potato varieties included Marfona, Jelly, Picasso, Slovyanka, Khortytsa, and Nevsky. Research using cultural, morphological, biochemical, and molecular analyses showed that *Dickeya solani* and *Pectobacterium carotovorum* causing potato soft rot are common in the studied regions of Georgia. These results, together with the 100% sequence identity of the *gapA* gene, provide the first record *P. carotovorum* in Georgia.

Keywords. Bacterial disease, isolate, *gap*A gene, sequence.

OPEN ACCESS

Citation: Muradashvili, M., Meparishvili, G., Sikharulidze, Z., Tediashvili, M., Kokashvili, T., Krijger, M. & Van Der Wolf, J. (2026). First detection of *Pectobacterium carotovorum* associated with potato soft rot in Georgia. *Phytopathologia Mediterranea* 65(2): 225-230. doi: 10.36253/phyto-17061

Accepted: May 7, 2026

Published: July 19, 2026

© 2026 Author(s). This is an open access, peer-reviewed article published by Firenze University Press (https://www.fupress.com) and distributed, except where otherwise noted, under the terms of the CC BY 4.0 License for content and CC0 1.0 Universal for metadata.

Data Availability Statement: All relevant data are within the paper and its Supporting Information files.

Competing Interests: The Author(s) declare(s) no conflict of interest.

Editor: Gilles Cellier, Anses-Plant Health Laboratory, Saint Pierre – Reunion Island.

ORCID:
MM: 0000-0003-4577-8679
GM: 0000-0001-5212-8944
ZS: 0000-0002-9171-0109
MT: 0000-0003-4035-4746
TK: 0009-0005-1095-5702
MK: 0009-0001-8371-1814
JVDW: 0000-0002-9196-5419

INTRODUCTION

Potatoes (*Solanum tuberosum* L.) are important food crops in Georgia, where annual per capita consumption reaches approx. 55 kg. However, the total area planted with potatoes (14,000–25,000 ha) and the average yields (12.2–15.6 t ha^{-1}) during 2016–2024 were low compared with other European and neighboring countries, including Armenia, Azerbaijan, and Turkey (Geostat, 2024). "Seed degeneration", defined as yield losses in vegetatively propagated crops due to pathogen accumulation over successive propagation cycles, is among the major constraints to potato productivity (Thomas-Sharma *et al*., 2015).

In Georgia, seed potatoes are predominantly self-saved by growers or obtained from local sources. For smallholder farmers, who are the majority

of potato producers in Georgia, certified seed potatoes are often unavailable or prohibitively expensive (Kelsey *et al*., 2021). Consequently, the use of poor-quality seed potatoes and the presence of particularly harmful pathogens are among the main factors contributing to low productivity.

The major potato diseases in Georgia include late blight, caused by *Phytophthora infestans*, and early blight, caused by *Alternaria solani*. In addition, several quarantine potato diseases occur in this country, including brown rot (caused by *Ralstonia solanacearum*; Muradashvili *et al*., 2014), wart (*Synchytrium endobioticum*; Gorgiladze *et al*., 2014), and ring rot (*Clavibacter sepedonicus*; Sadunishvili *et al*., 2020). During 2010 to 2012, outbreaks of blackleg caused by *Dickeya* spp. were recorded in the main potato-producing region of Samtskhe–Javakheti (Tsror *et al.,* 2011). Subsequent molecular studies showed that the majority of soft rot cases in Georgia were caused by *Dickeya solani* (Muradashvili *et al*., 2023). However, *Pectobacterium carotovorum* had not been previously identified in Georgian potato crops.

Bacterial diseases, including soft rot caused by *Pectobacterium carotovorum*, lead to significant losses in international potato production by causing plant wilting and tuber rot under both field and storage conditions (Vand der Wolf, *el al*., 2021). The aim of the present study was to characterize bacterial isolates obtained in Georgia in 2022 to 2023 from potato tubers showing soft rot symptoms. Cultural and biochemical tests, and molecular phylogenetic analyses, were used to determine isolate identity to *Pectobacterium*, potential pathogens not previously reported in association with soft rot of potato tubers in Georgia.

MATERIALS AND METHODS

Field surveys and sample collection

Field surveys for potato soft rot were carried out during the 2022–2023 growing and harvesting seasons in major potato-producing regions of Georgia, including Marneuli (village of Maradis), Bolnisi (village of Nakhiduri), Dmanisi (villages of Sarkineti and Gomareti), Tsalka (village of Artsivani), and Ninotsminda, Adigeni, Oni, and Ambrolauri.

Potato tubers exhibiting typical soft rot symptoms, including water-soaked lesions, tissue maceration, and discolouration, were collected from farmers' fields, storage facilities, and from experimental plots of the Institute of Phytopathology and Biodiversity. Potato varieties sampled included Marfona, Jelly, Picasso, Slovyanka, Khortytsa, and Nevsky.

Isolation and culturing of bacteria

Tuber samples were washed under running tap water, surface-sterilized in 0.3% sodium hypochlorite, rinsed with sterile distilled water, and air-dried in a laminar flow cabinet. Tissue from lesion margins was aseptically excised, macerated in sterile water, and plated onto nutrient agar. After incubation at 28 °C for 24 h, single colonies were transferred to crystal violet pectate (CVP) medium (Perombelon and Van Der Wolf, 2002). The CVP plates were incubated at 28 °C for 48 h, and then examined for cavity formation.

Phenotypic and biochemical characterization of isolated bacteria

Gram reaction, fluorescence on King's B medium, growth at 37 °C, and pigmentation on yeast dextrose calcium carbonate (YDC) and nutrient glycerol manganese (NGM) media were assessed for isolates obtained. Standard biochemical tests, including oxidase, catalase, urease, indole production, carbohydrate utilization, and citrate and malonate metabolism, were carried out, according to recommended and validated protocols (EPPO, 2023).

Pathogenicity tests

Pathogenicity of bacterial isolates was assessed using whole potato tubers. Bacterial suspensions (10^8 CFU mL^{-1}) were inoculated into the tuber tissues and incubated at 27 to 30 °C in moist chambers. Symptom development was monitored for 24 to 72 h. Control samples were inoculated with sterile distilled water. Re-isolation of bacteria from symptomatic tissues was performed to determine fulfilment of Koch's postulates.

Molecular identification of bacteria

Total genomic DNA was extracted from selected isolates using the QIAamp DNA Mini Kit (QIAGEN) according to the manufacturer's instructions. The housekeeping gene *gapA* was amplified by PCR using the primer pair gapA-7-F (5′-ATGGCAGGTTGTTGGTAA-3′) and gapA-938-R (5′-TTAGCCGTTGACCTTGTTG-3′) (Cigna *et al*., 2017). PCR products were visualized on 1.5% agarose gels stained with ethidium bromide. Amplicons were purified using the QIAquick PCR Purification Kit (QIAGEN), and were sequenced by Macrogen Europe using the Sanger method with forward and reverse primers.

Raw sequence reads were assembled and edited to obtain high-quality consensus sequences using Geneious

Prime 2026.0.2 (Biomatters Ltd). Multiple sequence alignment of *gapA* gene sequences was performed using MUSCLE (Edgar, 2004).

Sequence similarity searches against the NCBI GenBank database were conducted using BLASTn (Altschul *et al*., 1990) to identify closely related taxa. BLASTn analysis showed that 11 Georgian isolates (PP060483 to PP060493) shared 100% nucleotide identity and full query coverage with *Pectobacterium carotovorum* strains MBr2 (OR651974) and ZB18121 (OP793220), indicating close genetic relationships.

Phylogenetic analysis was performed in MEGA X (Kumar *et al*., 2018). *gapA* sequences were aligned using ClustalW, and a Maximum Likelihood (ML) tree was constructed based on the best-fit nucleotide substitution model selected using the Bayesian Information Criterion (BIC). Bootstrap analysis with 1,000 replicates was used to assess tree robustness, with values ≥70% considered significant (Felsenstein, 1985).

Bacterial isolates and reference sequences

11 Georgian isolates (PP060483 to PP060493) were included in the phylogenetic analysis together with reference sequences of *Pectobacterium* species retrieved from the NCBI database, (NCBI, 2026). including *Pectobacterium carotovorum* (OP793220), *Pectobacterium atrosepticum* (NC_004547/ NZ_CP009125), *Pectobacterium basiliense* (NZ_CP020350), *Pectobacterium versatile* (NZ_CP021894), *Pectobacterium polare* (NZ_CP017482), *Pectobacterium parmentieri* (CP003415 / CP001790), *Pectobacterium punjabense* (SAMN11162174) and *Pectobacterium aroidearum* (SAMN47853470). These reference taxa were selected to represent the major phylogenetic lineages within *Pectobacterium*.

RESULTS AND DISCUSSION

The field surveys in Georgia revealed that potato tubers with typical soft rot symptoms were widespread in major potato-producing regions of Georgia. A total of 28 symptomatic samples were collected. Nineteen bacterial isolates produced characteristic cavities on CVP medium, indicating their pectolytic activity typical of soft rot bacteria (Figure 1 A). All isolates were Gram-negative, facultatively anaerobic, and non-fluorescent on King's B medium, suggesting affiliation with *Pectobacterium* spp. or *Dickeya* spp. Based on strong pectolytic activity, 11 isolates were selected for further characterization. These isolates did not produce blue pigmentation on yeast dextrose calcium carbonate (YDC) or nutrient glycerol medium (NGM), distinguishing them from five other isolates that displayed phenotypic traits consistent with *Dickeya* spp. (Figure 1 B).

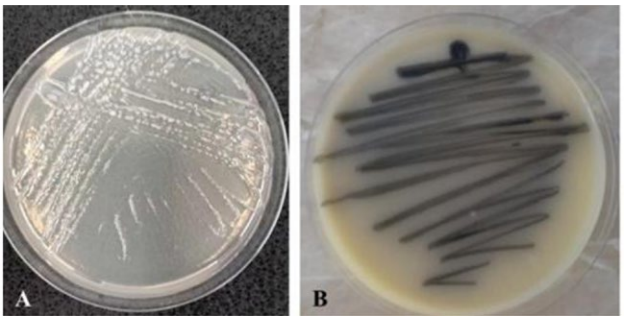

Figure 1. (A) A pure culture of *Pectobacterium carotovorum* grown on crystal violet pectate (CVP) medium. (B) Dark blue pigmentation produced by *Dickeya* spp. on yeast dextrose calcium carbonate (YDC) medium.

The 12 selected isolates were oxidase-, urease-, and indole-negative, unable to utilize citrate or malonate, and did not produce acid from dulcitol or sorbitol. All isolates were catalase-positive, fermented lactose, rhamnose, and trehalose, and were capable of growth at 37 °C.

Pathogenicity assays conducted on whole potato tubers showed that all tested isolates induced typical soft rot symptoms in the tuber tissues, including rapid maceration and decay, comparable to those observed in naturally infected samples. The bacterial isolates obtained from inoculated tubers matched the inoculation isolates, thereby fulfilling Koch's postulates for the respective bacteria.

The PCR assay resulted in amplification in all 12 Georgian isolates as well as in the reference isolate *Pectobacterium carotovorum* (43_0332), which was from National plant pathogen cultural collection of Wageningen University and Research. Agarose gel electrophoresis gave a single, distinct amplicon of approx. 932 bp in each positive reaction (Figure 2), corresponding to the expected fragment size. No amplification was detected in the negative control, confirming absence of contamination and specificity of the PCR assay. The uniformity of amplicon size among all isolates indicated conservation of the *gapA* gene region within the studied population. Minor variations in band intensity were observed, but are attributed to differences in DNA template concentrations or PCR efficiency, rather than nonspecific amplifications. The clear and consistent amplification products obtained provided high-quality templates for downstream sequencing and subsequent comparative sequence analysis.

BLASTn analysis showed that the Georgian isolates (deposited in GenBank under accession numbers: PP060483, PP060484, PP060485, PP060486, PP060487,

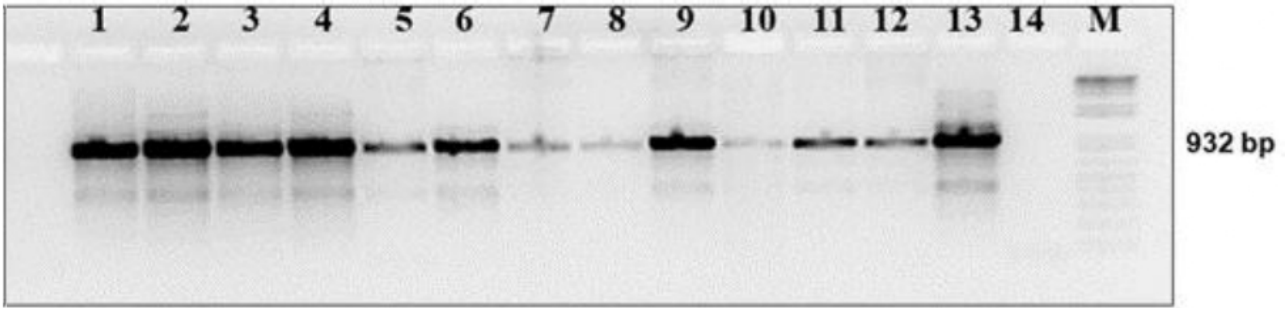

Figure 2. PCR amplification products using primer pair gapA-7-F/gapA-938-R: Lanes 1, Kob.4.22; 2, Tsk 1.22; 3, Kob 5.22; 4, Kob 3.22; 5, Tsk 3.22; 6, Mar 5.22; 7, Akh 2.22; 8, Mar 4.22; 9, Mar 1.22; 10, Mar 9.22; 11, Ats 1.22; 12, Mar 2.22; 13, Reference strain 43_0332; 14, Negative control.

PP060488, PP060489, PP060490, PP060491, PP060492, PP060493) shared 100% nucleotide identity and 100% query coverage with *Pectobacterium carotovorum* reference strains MBr2 (OR651974, Taiwan) and ZB18121 (OP793220, China), with maximum similarity scores (bit score = 1,000), confirming very close genetic relationships.

Phylogenetic analysis based on the *gapA* gene confirmed the taxonomic placement of the isolates. Both Maximum Likelihood and Neighbor-Joining analyses consistently grouped all Georgian isolates within the *Pectobacterium carotovorum* clade (Figure 3).

Phylogenetic relationships inferred from *gapA* gene sequences showed that all Georgian isolates (PP060483 to PP060493) clustered within the *Pectobacterium carotovorum* clade, together with reference strains MBr2 (OR651974) originating from Taiwan, and ZB18121 (OP793220) originating from China. This grouping was strongly supported by a high bootstrap value (98%), indicating a robust and reliable phylogenetic placement. The Georgian isolates formed a compact and well-defined subcluster characterized by short branch lengths, suggesting low intra-group genetic diversity.

In contrast, other *Pectobacterium* species, including *P. aroidearum*, *P. parmentieri*, and *P. punjabense*, were resolved in a separate lineage with moderate bootstrap support (77%). A distinct and well-supported clade (bootstrap = 96) comprised *P. atrosepticum*, *P. brasiliense*, *P. versatile*, and *P. polare*, clearly differentiated from the *P. carotovorum* cluster.

Overall, the topology of the tree (Figure 3) demonstrates a clear separation among species within *Pectobacterium*, and confirms the assignment of all the Georgian isolates to *P. carotovorum*, highlighting the close genetic relatedness and low sequence divergence within the studied population (Table 1).

The present study represents the first confirmed report of *Pectobacterium carotovorum* as a causal agent

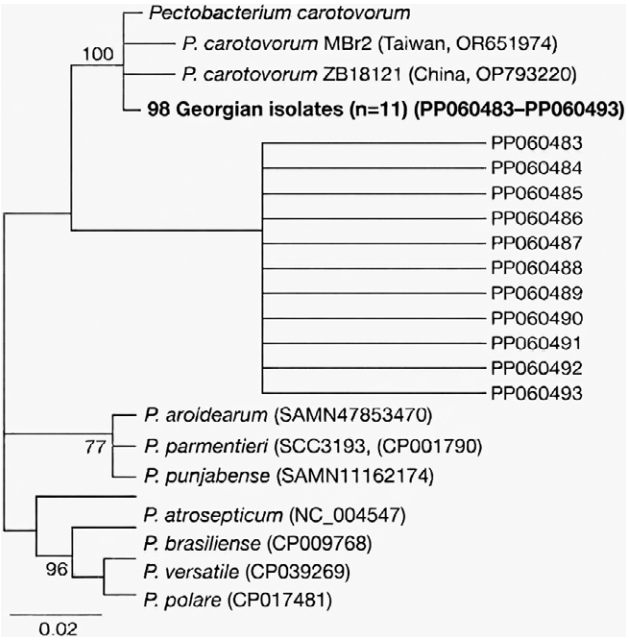

Figure 3. Phylogenetic tree based on *gapA* gene sequences, showing that Georgian isolates (PP060483 to PP060493) cluster within the *Pectobacterium carotovorum* clade with high bootstrap support (98%). Other *Pectobacterium* species form distinct, well-supported lineages. Bootstrap values (1,000 replicates) are indicated at nodes. The scale bar represents 0.02 substitutions per site.

of potato soft rot in Georgia. Previously, *Dickeya solani* had been identified as the predominant soft rot pathogen in this country, particularly in the Samtskhe–Javakheti region and adjacent areas (Muradashvili *et al*., 2023). However, *D. solani* was also detected in samples collected during the 2022–2023 field surveys. The present research demonstrates that two bacterial populations causing potato soft rot, *D. solani* and *P. carotovorum*, are predominantly circulating in the studied regions.

Table 1. List of identified *Pectobacterium carotovorum* isolates from Georgia.

No.	BioSample accession No.	Georgian isolate No.	Host potato variety	Year isolated	Sampling location
1	PP060483	Geo_Kob.4.22	Khortytsa	2023	Kobuleti
2	PP060484	Geo_Tsk.1.22	Marfona	2023	Tsalka
3	PP060485	Geo_Kob.5.22	Slovyanka	2022	Kobuleti
4	PP060486	Geo_Kob.3.22	Nevsky	2022	Kobuleti
5	PP060487	Geo_Tsk. 3.22	Picasso	2022	Tsalka
6	PP060488	Geo_Mar.5.22	Unknown	2022	Marneuli, v. Maradisi
7	PP060489	Geo_Akh.2.22	Marfona	2022	Akhalkalaki
8	PP060490	Geo_Mar.1.22	Unknown	2022	Marneuli
9	PP060491	Geo_Mar.2.22	Unknown	2023	Marneuli
10	PP060492	Geo_Mar.9.22	Unknown	2022	Marneuli
11	PP060493	Geo_Ats.1.22	Jelly	2022	Akhaltsikhe

The coexistence of *P. carotovorum* and *D. solani* within the same potato production areas may complicate disease management, as these pathogens differ in aggressiveness, environmental adaptation, and responses to control measures. The recovery of numerous isolates from seed tubers from unknown origins suggests that seed-borne dissemination is probably a major pathway for pathogen introduction, which is consistent with international reports on the epidemiology of *P. carotovorum* (Van Der Wolf *et al*., 2021). These results highlight the importance of implementing strict phytosanitary measures, including the use of certified seed potatoes and systematic monitoring of seed potato lots. Future research should focus on comprehensive epidemiological surveys, population genetic analyses, and evaluation of disease control strategies to mitigate the impact of these pathogens on potato production in Georgia.

ACKNOWLEDGEMENTS

Financial support for this research was provided by Shota Rustaveli National Science Foundation (SRNSF) of Georgia (grant No. FR-21-1778).

LITERATURE CITED

Altschul S. F., Gish W., Miller W., Myers E. W., Lipman D. J., 1990. Basic local alignment search tool. *Journal of Molecular Biology* 215(3): 403–410. https://doi.org/10.1016/S0022-2836(05)80360-2

Biomatters Ltd. 2026. *Geneious Prime 2026.0.2* [software]. Auckland, New Zealand: Biomatters Ltd.

Cigna J., Dewaegeneire P., Beury A., Gobert V., Faure D., 2017. A *gapA* PCR-sequencing assay for identifying the *Dickeya* and *Pectobacterium* potato pathogens. *Plant Disease* 101(7): 1278–1282. https://doi.org/10.1094/PDIS-12-16-1810-RE

EPPO, 2023. Diagnostic standard PM 7/155 (1): *Pectobacterium* spp. and *Dickeya* spp. *EPPO Bulletin* 53: 309–353. https://doi.org/10.1111/epp.12935

Edgar R. C., 2004. MUSCLE: multiple sequence alignment with high accuracy and high throughput. *Nucleic Acids Research* 32(5): 1792–1797.

Felsenstein J., 1985. Confidence limits on phylogenies: an approach using the bootstrap. *Evolution* 39: 783–791.

Geostat, 2024. National Statistics Office of Georgia. Agriculture of Georgia. https://www.geostat.ge/en/modules/categories/196/agriculture (accessed 26 April 2025).

Gorgiladze L., Meparishvili G., Sikharulidze Z., Natsarishvili K., Meparishvili S., 2014. First report of *Synchytrium endobioticum* causing potato wart in Georgia. *New Disease Reports* 30(4): 1. https://doi.org/10.5197/j.2044-0588.2014.030.004

Kelsey F. A., Forbes G. A., Andrade J. L., Buddenhagen C. E., Fulton J. C., … Garret K.A., 2021. An integrated seed health strategy and phytosanitary risk assessment: potato in Georgia. *Agricultural Systems* 191: 103144. https://doi.org/10.1016/j.agsy.2021.103144

Kumar S., Stecher G., Li M., Knyaz C., Tamura K., 2018. MEGA X: Molecular Evolutionary Genetics Analysis across computing platforms. *Molecular Biology and Evolution* 35: 1547–1549.

Muradashvili M., Meparishvili G., Sikharulidze Z., Meparishvili S., 2014. First report of potato brown rot caused by *Ralstonia solanacearum* in Georgia. *Journal of Plant Pathology* 96(4): S119 (abstract).

Muradashvili M., Tsror (Lahkim) L., Sikharulidze Z., Meparishvili S., Mordechai L. S., Meparishvili G., 2023. Prevalence of potato blackleg and soft rot in Georgia. *Journal of Applied Biological Sciences* 17(2): 249–256.

NCBI, 2026. National Center for Biotechnology Information (NCBI) GenBank database. https://www.ncbi.nlm.nih.gov/genbank/ (accessed 11 April 2026).

Perombelon M. C. M., Van der Wolf, J. M., 2002. Methods for the detection and quantification of *Erwinia carotovora* subsp. *atroseptica* (*Pectobacterium carotovorum* subsp. *atrosepticum*) on potatoes: a laboratory manual. *Scottish Crop Research Institute Occasional Publication* No. 10.

Sadunishvili T., Wegierek-Maciejewska A., Gaganidze D., Amashukeli N., Sturua N., ... Kvesitadze G., 2020. Molecular, morphological and pathogenic characterization of *Clavibacter michiganensis* subsp. *sepedonicus* strains of different geographical origins in Georgia. *European Journal of Plant Pathology* 158(2): 195–209.

Tsror (Lahkim) L., Erlich O., Lebiush S., Van der Wolf J. M., Mozes G., Sikharulidze, Z., 2011. First report of potato blackleg caused by a biovar 3 *Dickeya* sp. in Georgia. *New Disease Reports* 23(1): 1. https://doi.org/10.5197/j.2044-0588.2011.023.001

Thomas-Sharma S., Abdurahman A., Ali S., Andrade-Piedra J., Bao S., ... Garrett, K. A., 2015. Seed degeneration in potato: the need for an integrated seed health strategy. *Plant Pathology* 65(1): 3–16.

Van der Wolf J. M., Acuña I., Solke H., Brurberg M. B., Cahill G., ... Yedidia I., 2021. Diseases caused by *Pectobacterium* and *Dickeya* species around the world. In: *Plant Diseases Caused by Dickeya and Pectobacterium Species,* (Van Gijsegem F., van der Wolf J.M., Toth I., ed.), Springer Nature Switzerland AG 2021, 215–261. https://doi.org/10.1007/978-3-030-61459-1_7.

Phytopathologia Mediterranea
The international journal of the
Mediterranean Phytopathological Union

Firenze University Press
www.fupress.com/pm

Research Papers

Agricultural by-products from asparagus and date palm affect *Phytophthora cinnamomi*: potential for control of oak root disease

Rosa LÓPEZ GARCÍA[1], María Teresa HIDALGO FERNÁNDEZ[1], Marta GARCÍA GARCÍA[1], Rocío RODRÍGUEZ-ARCOS[2], Ana JIMÉNEZ-ARAUJO[2], María Socorro SERRANO MORAL[1,*]

[1] *Grupo de Recursos genéticos, mejora y protección del olivo y otros cultivos leñosos (UCOLIVO), Departamento de Agronomía, Universidad de Córdoba, Spain*
[2] *Grupo de Fitoquímicos y Calidad de los Alimentos, Departamento de Fitoquímica de los Alimentos, Instituto de la Grasa (IG-CSIC), Spain*
*Corresponding author. E-mail: a12semom@uco.es

Summary. As society demands healthier food production, agricultural residues could provide sustainable alternatives for plant disease control, as these residues are reservoirs of fungicidal compounds. This study aimed to identify the activity of six plant extracts and their corresponding crude residues against plant pathogen *Phytophthora cinnamomi*. Extracts enriched in bioactive compounds came from residues of asparagus spears (AS), fronds (AF) or roots (AR); olive tree fruit (OF) or leaves (OL), and seeds of date palm fruits (DS). *In vitro* experiments showed that all the asparagus extracts at 0.025 and 0.05% significantly decreased *P. cinnamomi* mycelial growth, with inhibition percentages greater than 75% for AS and AR. The AS, OL and DS extracts at 0.05% inhibited *P. cinnamomi* sporangial production by >84%. Phytotoxicity symptoms were not detected for any of the extracts assessed. *In planta* experiments were carried out to compare effects of soil application of AS and DS organic extracts with their crude residues at 0.05% against disease caused by *P. cinnamomi* on *Quercus ilex* seedlings. The AS residue was statistically more effective than the AS extracts, while DS residue and extract inhibited root rot symptoms to levels similar to the uninfested controls. Therefore, extracts and residues from seeds from date fruits, and residues from asparagus spears, are candidates for control *P. cinnamomi* root rot. Both residues are being tested in an infested field of *Q. ilex* adult trees.

Keywords. Anti-oomycete activity, extracts, phenolic compounds, residues, root rot.

OPEN ACCESS

Citation: López García, R., Hidalgo Fernández, M. T., García García, M., Rodríguez-Arcos, R., Jiménez-Araujo, A. & Serrano Moral, M. S. (2026). Agricultural by-products from asparagus and date palm affect *Phytophthora cinnamomi*: potential for control of oak root disease. *Phytopathologia Mediterranea* 65(2): 231-242. doi: 10.36253/phyto-17270

Accepted: June 10, 2026

Published: July 19, 2026

© 2026 Author(s). This is an open access, peer-reviewed article published by Firenze University Press (https://www.fupress.com) and distributed, except where otherwise noted, under the terms of the CC BY 4.0 License for content and CC0 1.0 Universal for metadata.

Data Availability Statement: All relevant data are within the paper and its Supporting Information files.

Competing Interests: The Author(s) declare(s) no conflict of interest.

Editor: Matteo Garbelotto, University of California, Berkeley CA, USA.

ORCID:
RLG: 0009-0006-6446-5773
MTHF: 0000-0001-9859-4035
MGG: 0009-0005-2964-9617
RRA: 0000-0002-0003-4345
AJA: 0000-0002-2695-4588
MSSM: 0000-0003-3896-1993

INTRODUCTION

Plants produce many secondary metabolites that have broad biological activity, including antioxidant, anticancer, antibacterial, and antifungal activities, which are related to their chemical structures (Sparg *et al.*, 2004). Previous studies have determined that wild plants are important sources of bioactive compounds, that are rich in saponins and flavonoids and have antifungal

activity against plant pathogens (Cenobio-Galindo *et al*., 2024), including *Fusarium oxysporum* (Tucuch-Pérez *et al*., 2020), and *Phytophthora capsici* (Lujan *et al*., 2021), *P. nicotianae* (Bowers and Locke, 2004), and *P. infestans* (Nagar *et al*., 2017).

Agricultural crops and their by-products are also reservoirs of phytochemicals (Jaramillo-Carmona *et al.,* 2017; Cenobio-Galindo *et al*., 2024; Mrabet *et al*., 2024). Date seeds, which are discarded organic residue, have high contents of polyphenols, and are a rich source of bioactive compounds such as carotenoids, flavonoids, and tocopherols (Mrabet *et al.,* 2024). Similarly, *in vitro* studies have shown that extracts from *Asparagus officinalis* by-products inhibited the mycelial growth of the plant pathogenic fungi *Alternaria tenuissima*, *F. oxysporum*, *Macrophomina phaseolina*, *Rhizoctonia solani* and *P. cinnamomi* (Rosado-Álvarez *et al*., 2014; Desoukey *et al.,* 2020; Romero *et al*., 2024).

Biomass from different plants varies in composition and concentration of secondary metabolites, and in antimicrobial activity (Fuentes-Alventosa *et al*., 2013; Desoukey *et al.,* 2020; Cenobio-Galindo *et al*., 2024). Del Río *et al.* (2003) noted that extracts from *Olea europaea* stems had the highest accumulation of the phytochemicals tyrosol, catechin and oleuropein in cortices, and their use resulted in a more effective inhibition of the mycelial growth of different *Phytophthora* species in comparison with extracts obtained from olive leaves. In contrast, olive leaf extract reduced host plant death caused by *P. cinnamomi* root disease more than extract from olive branches (Romero *et al*., 2024). Therefore, plant byproducts and extracts provide safe and "green" alternatives for management of plant diseases, both in agricultural and natural settings.

Perhaps, there is no better example of a pathogen that affects natural and agricultural systems than *P. cinnamomi*. This soilborne oomycete is one of the 100 worst invasive exotic species (Global Invasive Species Database 2025), and is capable of infecting close to 5000 plants species, including many of importance in agriculture, forestry, and horticulture. This pathogen has serious consequences for environments, biodiversity and substantial economic losses (Burgess *et al*., 2017; Sena *et al.,* 2018). Its impacts are in temperate and subtropical climate regions, including all Mediterranean climate regions (Burgess *et al*., 2017). In South Africa, *P. cinnamomi* severely affects eucalyptus, avocado, macadamia and autochthonous fynbos (Sena *et al*., 2018), while in Europe and California, it is associated with oak decline and chestnut ink disease (Garbelotto *et al.,* 2006; Burgess *et al*., 2017; Sena *et al*., 2018).

Phytophthora cinnamomi is the main causal agent of extensive death of *Quercus* species in the Mediterranean Basin (Brasier, 1996). The pathogen causes severe feeder root necroses with crown wilting, desiccation, and tree defoliation and death (Brasier, 1996). Several methods have been developed to control *P. cinnamomi* oak tree disease, including soil application of calcium amendments (Serrano *et al.,* 2012a), biofumigation with *Brassica* spp. with high content in sinigrin (Ríos *et al.,* 2016), and chemical control using phosphonates (González *et al*., 2020).

Society demands sustainable, healthy and environmental-friendly food production, including a significant reduction in the use of chemical products to control pests. Therefore, the development of new strategies for a sustainable and environmental-friendly biological control of *P. cinnamomi* is urgent. The objective of the present study was to assess biocidal activity against *P. cinnamomi* of six organics extracts that came from olive tree, asparagus or date palm residues. The study aimed to determine: 1) effects of organic extracts on mycelial growth and infectivity of *P. cinnamomi* in *in vitro* experiments; and 2) the comparative effects of organic extracts and their crude residues on development of *P. cinnamomi* root rot *in planta*.

MATERIALS AND METHODS

Plant extracts

Six different organic extracts were used (Table 1). Three were from asparagus crop by-products, from basal portions of spears discarded during processing, and from spears broken or deteriorated during handling (AS), fronds (AF) or roots (AR) of asparagus plants discarded after spear harvesting. Two other extracts were from olive fruit extract obtained during olive oil extractions (OF), or from leaves and twigs resulting from pruning activities (OL). The sixth extract was from discarded seeds from date fruits (DS).

Different extraction protocols were used, depending on the particular plant residues. Extracts from spears (AS), fronds (AF) or roots (AR) residues of the cultivation of *triguero* asparagus from Huetor-Tájar (Granada, Spain), were obtained using the methods of Fuentes-Alventosa *et al.* (2013). Each by-product was first autoclaved at 121 ºC for 2 h in water (1:2 w/v), to obtain an aqueous extract containing most of the soluble bioactive compounds, and the fibrous residue. The aqueous extract was then fractionated by adsorption chromatography and eluted with 40% ethanol aqueous solution as Rosado-Álvarez *et al.* (2014). The resulting extract was concentrated under vacuum and freeze-dried.

The functional organic extract from olive fruits (OF) was obtained using the method of Rodríguez *et al.*

Table 1. The bioactive compounds assessed in this study, from different agricultural by-product extracts.

Agricultural by-product sources		Code	Proportions (%) of phenolic compound	Main bioactive compounds	Reference
Asparagus	Spears	AS	6.33	Rutin (Quercetin-rutinoside)	Fuentes-Alventosa *et al.* (2008)
	Fronds	AF	24.80	Rutin (Quercetin-rutinoside)	López *et al.* (2025)
	Roots	AR	67.83	Protodioscin	Jaramillo-Carmona *et al.* (2017)
Olive	Fruits	OF	6.20	Hydroxytyrosol Tyrosol	Rodríguez *et al.* (2007)
	Leaves	OL	4.46	Oleuropein Dihydroxyphenylglycol	Romero *et al.* (2024)
Date	Seeds	DS	2.56	Pyrogallol	Mrabet *et al.* (2024)

(2007). The aqueous phase liquor generated during olive oil extraction from fruits was purified using an anion exchange chromatography column. The phenolic compounds fraction was eluted with water, and then concentrated using a rotatory vacuum evaporator. The resulting effluent was then purified using polymeric adsorption resin column and eluted with ethanol:water (30:70).

The olive leaf extract (OL) was obtained from dried leaves through aqueous extraction at 90 ºC for 40 min. Due to its high phenolic content (Romero *et al.,* 2024), no additional purification was required. The extract was then concentrated under vacuum and lyophilized (Romero *et al*., 2024).

Date seed extract (DS) was produced from a fine seed powder by extraction with 80:20 (v/v) ethanol:water. After filtration, the resulting liquor was concentrated under vacuum and freeze-dried (Mrabet *et al*., 2024).

Oomycete material

Three *P. cinnamomi* isolates were used. PE2203 was isolated from the rhizosphere of *Quercus ilex* and stored in the fungal collection of the Agronomy Department of the University of Córdoba (Romero *et al.,* 2024). Isolate PA37 was from *Quercus suber* roots, and was stored in the Universidade do Algarve (Portugal). Isolate P7S was from *Q. ilex* roots, and was obtained from the collection of the Agenzia della Regione Sardegna per la Ricerca Scientifica (Italy).

In vitro *experiments*

Effects on mycelial growth. Abilities of organic extracts of agricultural residues to inhibit mycelial growth of *P. cinnamomi* was evaluated. Corn Meal Agar medium (CMA, 17 g L^{-1}) was amended with the different organic extracts at two concentrations (0.025 and 0.05%), selected according to previous tests for AS extract (Romero *et al.,* 2022). All extracts were diluted in water, except for AR extract which was diluted in 70% ethanol before adding it to CMA to achieve a final concentration of 0.02% ethanol. To discard interferences of the solvent and AR extract on *P. cinnamomi* growth, ethanol at 0.02% was also tested (Solvent treatment). Amended CMA was poured into Petri dishes (9 cm diam.; 20 mL per dish). CMA free of extract was used as experimental controls.

Using the methods of Serrano *et al.* (2012a), agar plugs (5 mm diam.) of each *P. cinnamomi* isolate actively growing on 20% Carrot Agar (CA) were placed in the centres of Petri dishes containing the amended or control CMA. Four dishes (replicates) were prepared per isolate, organic extract, and dose, plus the untreated controls. The plates were then incubated at 25 ºC in darkness. Diameters of resulting colonies were measured daily for 5 d, when the colonies of isolates P7S and PA37 covered the entire agar surfaces in the plates, and the trial was concluded. The experiment was repeated three times. Mycelial growth throughout the experiment was expressed as the relative area under progress curve (rAUPC), as calculated using the formula (Campbell and Madden, 1990):

$$rAUPC = \frac{100}{(s_{max} \times t_e)} \times \sum_{i=1}^{n} \frac{(s_i + s_{i+1})}{2} \times \left(t_{i+1} - t_i\right)$$

where: s_i = mycelial growth for observation number *i*,
s_{max}= maximum growth value,
t_i = number of days between *i* evaluations,
t_e = total period of evaluations, and
n = number of evaluations.

Data of rAUPC did not conform to normality, even after applying transformations, so a Kruskal-Wallis One-

Way Nonparametric test was carried out for repetition, isolate, replicate, and the combination treatment-dose as three independent factors. Mean values were then compared using Dunn's test (P <0.05). In addition, percentages of mycelial growth inhibition respect to the untreated experimental controls were calculated. All statistical analysis were carried out using Statistix software 10.0 (Analytical Software).

Effects on sporangial production. The most effective dose (0.05%) of the organic extracts (AS, AF, AR, OH, OF, and DS), based on results from the mycelial growth experiments, was tested for effects on sporangial production, as described by Serrano *et al.* (2012a). Sporangial production was induced as follows: agar plugs (1 cm diam.) of the three *P. cinnamomi* isolates actively growing on Pea Agar (20%) were transferred to empty 6 cm Petri dishes, and were each covered with 7 mL of soil extract (0.1% soil:water), prepared as described in Ribeiro (1978). The dishes were then incubated under constant light at 23 ºC, and the aqueous soil extract was replaced every 24 h. Twenty-four hours before each isolate reached maximum sporangial production, which happened at 56 h for isolate PE2203, and at 72 h for isolates P7S and PA37 (previously determined), the soil extract was replaced by a soil extract amended with the six organic extracts (above, at 0.05%). The extracts were diluted in water, except for asparagus root (AR) extract, which was diluted in 70% ethanol to a concentration of 0.02%. As in the previous experiments, ethanol (0.02%) was also included to detect interference with the AR extract (Solvent treatment). Three plates (replicates) per treatment and isolate were prepared, including three more plates per isolate with unamended soil extract used as negative controls. After the last soil extract changes, all the plates were incubated for 24 h at 23 ºC under constant light, until the negative control for each isolate reached maximum sporangial production. At that time, sporangia were quantified by direct observation using an inverted microscope (Nikon, 400× magnification), and mature sporangia were counted. The experiment was carried out at four different times (repetitions).

Sporangial production values were referenced to the corresponding values of untreated controls, and were expressed as percentage inhibition of sporangial production. These data were analysed using a Kruskal-Wallis non-parametric test, and mean values were compared by Dunn's test ($P < 0.05$).

Extract phytotoxicity

A previous study demonstrated the lack of substantial phytotoxicity of AS, OH and OL extracts at 0.1 and 0.15% (Romero *et al*., 2024), so plant damage was not expected at dose rates of two or three times less. Therefore, the present study focused on determining the phytotoxic effects of AF, AR and DS organic extracts. Firstly, the extracts effects were assessed on seed germination of *Lupinus luteus*, as described by Romero *et al.* (2024) (Phytotoxicity test 1). Agar medium (1.5%) was amended with each organic extract (AR, AF or DS) at 0.05%, using unamended plates as experimental controls. Plates amended with the 70% ethanol solvent of AR in a final dose of 0.02% were included for a further comparison with AR extract. Seeds of *L. luteus* used for the germination tests were surface sterilized (Serrano *et al.,* 2012b). Six seeds were then transferred to each Petri dish with amended or non-amended (control) agar medium. Five Petri dishes (replicates) were prepared per treatment. All the plates were then incubated at 23 ºC with a 12 h photoperiod. Percentage of seed germination was determined daily for each plate over a 4 d period. Proportions of seed germination for each treatment were analysed by Kruskal-Wallis non-parametric tests, because percentages did not fit normality, and means were compared using Dunn's test ($P < 0.05$).

A second phytotoxicity test (Phytotoxicity test 2) was carried out to determine effects of the organic extracts on *L. luteus* plant growth. In this case, due to extract availability, the two different experiments were carried out separately, one using asparagus extracts (AF and AR), and the other using DS extract. For these assays, 10-d-old *L. luteus* seedlings produced as described by Serrano *et al.* (2012b) were transferred to seedbed trays containing peat amended with the three organic extracts AR, AF, or DS, each at 0.05%. Trays with peat treated with ethanol (0.02% solvent) and unamended peat were included as experimental controls. Twelve seedlings (replicates) per treatment were planted. All plants were then incubated in a growth chamber at 23 ºC with a 12 h photoperiod, and were watered as required. Phytotoxicity test 2 ended after 37 d, when the plants started to bloom. At that time, plant yields were determined by measuring total plant lengths and fresh weights. Resulting data did not fit normality after applying transformations, so they were analysed by Kruskal-Wallis non-parametric tests, and mean values were compared by Dunn's test ($P < 0.05$). Each phytotoxicity test was repeated twice.

Effects of extracts and crude residues on host plant root rot

The effects of the two organic extracts that were most effective *in vitro* and in the phytotoxicity experiments, AS and DS, were evaluated on root rot development caused by *P. cinnamomi* using *in planta* experi-

ments. Additionally, effects of both organic extracts enriched in bioactive compounds were compared with the full crude residue used to obtain them: previously dried and shredded discarded asparagus spears (AS-R) and date seeds (DS-R).

A peat: sand substrate (1:1 vol.) was infested with aqueous suspension of isolate PE2203 chlamydospores, as described by Romero *et al.* (2024). Inoculum suspension was adjusted to 250 viable chlamydospores per gram of dry soil. Four days after soil infestation, each treatment (AS or DS extracts and AS-R or DS-R residues) was separately added to the substrate at 0.05% (w/v). Substrate infested and untreated (Control 1), and uninfested and untreated (Control 0) were also prepared as experimental controls. After treatment applications, 1-year-old holm oak seedlings were planted in pots (ten replicates per treatment, each pot containing 2 L of previously prepared substrate, including controls). All pots were incubated in a shade-house. One week after the plants were potted, all pots, including the controls, were placed in plastic trays without drainage (five pots per tray), and the trays were partially filled with tap water maintaining flooding for 2 d each week until the end of the experiment (Serrano *et al.*, 2012a). The experiment was repeated twice, starting in October 2023 for repetition 1 and January 2024 for repetition 2. For both repetitions, severity of foliage symptoms was assessed each week for each plant, using a 0 to 4 scale, according to percentages of yellowing, wilting, desiccation, and defoliation: where 0 = 0%, 1 = 1–33%, 2 = 34–66%, 3 = more than 67%, and 4 = dead tissue; Romero *et al.,* 2007). The experiments ended when the mean foliar symptom severity values from Control 1 (infested and untreated) became greater than 2.5, which happened at 14 weeks after treatment for experiment repetition 1, and 27 weeks after treatment for repetition 2. At those times, plants were removed from substrate, and severity of root symptoms was evaluated using a similar 0 to 4 scale according to percentage of root necrosis (Romero *et al.*, 2007).

Evolution of foliar symptom severity during the two experiments was expressed as relative areas under disease progression curves (rAUDPC), calculated using the formula outlined above. Data of rAUDPC and severity of root symptoms did not conform normality after applying transformation, so a Kruskal-Wallis One-Way Non-parametric test was carried out considering the repetitions and treatments as independent factors. Mean values were compared using Dunn's test ($P < 0.05$). In addition, root segments from all plants, including from Control 1 and Control 0, were washed and plated onto PA-NARH medium for re-isolation of the pathogen (Romero *et al.*, 2024).

RESULTS

In vitro *experiments*

Effects on mycelial growth: Statistical analyses showed differences of rAUPCs among the three isolates ($F = 8.77$, $P = 0.0002$), so the isolate data were analysed separately. For each isolate, significant differences were observed among treatments ($F = 73.65$, $P < 0.0001$ for PE2203; $F = 62.57$, $P < 0.0001$ for PA37; $F = 56.9$, $P < 0.0001$ for P7S;), while no differences were detected among repetitions or replicates. Although no effects were recorded for olive and date palm extracts, the three organic extracts of asparagus (AF, AS and AR) at both doses tested (0.025 and 0.05%) induced less mycelial growth than the untreated control and the solvent, except for AF at 0.025% for the Italian isolate (P7S) that did not differ from the controls (Figure 1).

Since the statistical analysis of the percentage of mycelial growth inhibition did not show significant differences among repetitions ($F = 0.83$, $P = 0.4373$) and among the isolates ($F = 1.9$, $P = 0.1511$), Figure 2 shows average values for the three isolates together. The most inhibitory extracts were AS and AR at both assessed doses, reaching inhibition percentages greater than 77%.

Effects on sporangial production: Figure 3 shows mean values of the percentages of inhibition of sporangial production after treatment with each organic extract at 0.05%. Differences were found among treatments ($F = 23.1$, $P < 0.0001$), but not among isolates ($F = 1.44$, $P = 0.2395$), repetitions ($F = 1.85$, $P = 0.1385$) or replicates ($F = 0.46$, $P = 0.6338$). The aqueous extracts AS, OL and DS, inhibited *P. cinnamomi* sporangial production by greater than 84%, while AF and OF extracts gave lesser mean inhibition percentages (respectively, 27.4 and 43.1%) (Figure 3). For the ethanol extract AR, although it induced the greatest sporangial inhibition (93%), this was not different from its solvent treatment.

Extract phytotoxicity

Figure 4 shows evolution of the percentage of *L. luteus* seed germination under the influence of different organic extracts AF, AR or DS at 0.05% in Test 1. Germination percentages did not differ ($P > 0.05$) from the untreated controls at the end of the experiment. Phytotoxicity symptoms, including organ deformation, discolouration and/or necroses of plant tissues, were not observed from any treatment in Test 2. However, differences were detected among the treatments for mean plant total length ($F = 6.13$, $P = 0.0002$) and mean plant fresh weight ($F = 7.06$, $P < 0.0001$). AR and AF induced

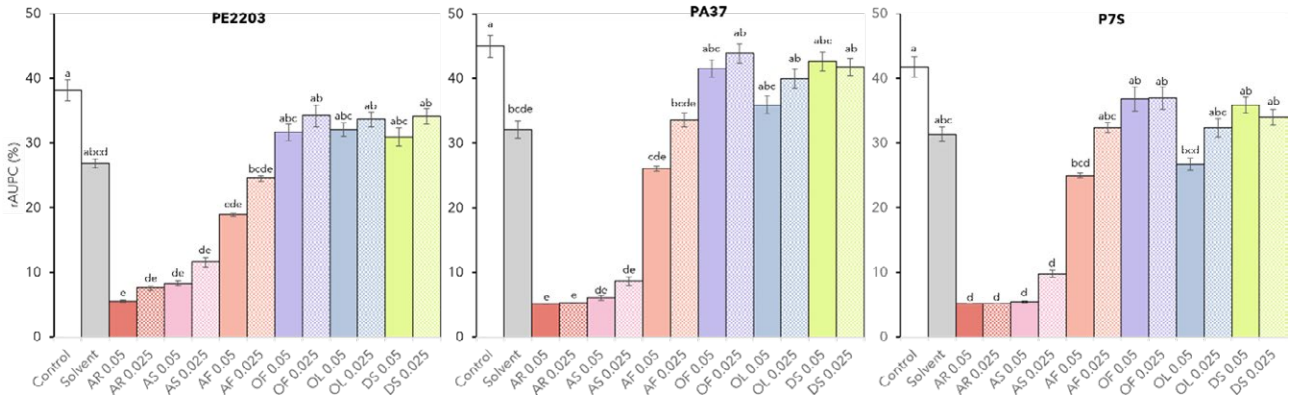

Figure 1. Means and standard errors of relative areas under progression curves (rAUPC) for mycelial growth (after 4 d) of three *Phytophthora cinnamomi* isolates (PE2203, PA37 and P7S) in medium amended with organic extracts (AR, AS, AF, OF, OL and DS) at 0.025 and 0.05%, solvent (0.02% ethanol), and in unamended media (control). Bars accompanied by different letters indicate differences according to Dunn´s tests at $P < 0.05$. AR: Asparagus Root extract, AS: Asparagus Spear extract, AF: Asparagus Frond extract, OF: Olive Fruit extracts, OL: Olive Leaf extract, DS: Date Seed extract.

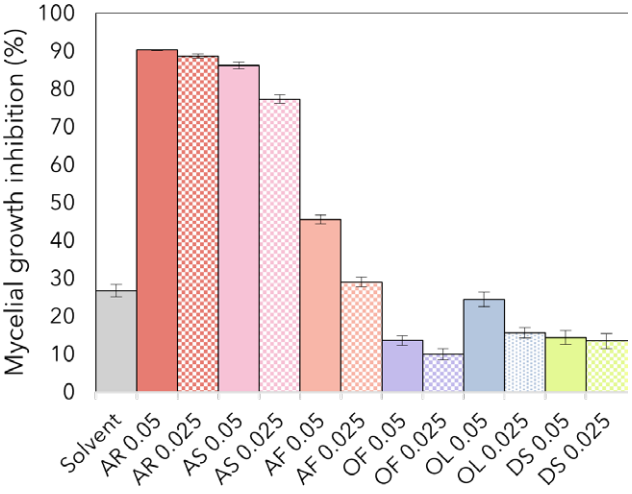

Figure 2. Mean and standard error of percentages of mycelial growth inhibition of three *Phytophthora cinnamomi* isolates (PE2203, PA37 and P7S) in media amended with the six organic extracts (AR and its Solvent, AS, AF, AL, OF and DS) at doses of 0.025 or 0.05%. AR: Asparagus Root extract, AS: Asparagus Spear extract, AF: Asparagus Frond extract, OF: Olive Fruit extract, OL: Olive Leaf extract, DS: Date Seed extract.

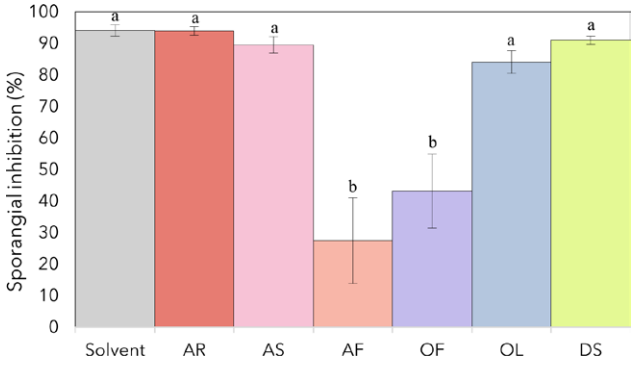

Figure 3. Mean (± standard error) of *Phytophthora cinnamomi* sporangial production inhibition induced by six organics extracts (AR, AS, AF, OF, OL and DS) at 0.05% doses, and solvent (ethanol 0.02%) for AR extract. Bars accompanied by different letters differ, according to Dunn's test ($P < 0.05$). AR: Asparagus Root extract, AS: Asparagus Spear extract, AF: Asparagus Frond extract, OF: Olive Fruits extract, OL: Olive Leaf extract, DS: Date Seed extract.

reductions in plant yields in comparison to the untreated controls (Figure 5).

Root rot development

Plants growing in infested and untreated substrate (Control 1) developed foliar symptoms (leaf yellowing and wilting) typical of *P. cinnamomi* oak tree infections in field and pot experiments (Sánchez *et al*., 2002; Romero *et al*., 2007). Statistical analyses of data of development of foliar symptoms (rAUDPC) indicated significant differences among treatments ($F = 4.96$, $P = 0.0004$), but not between repetitions ($F = 1.13$, $P = 0.2908$), so the rAUDPCs for both repetitions were combined in a single analysis. As shown in Figure 6, plants treated with residues and extracts from asparagus or date palm had reduced rAUDPCs compared to inoculated and untreated plants (Control 1), not differing among them nor with the negative controls (uninfested, untreated).

Differences in root symptoms were detected among treatments ($F = 14.1$, $P > 0.0001$), but not for repetitions ($F = 0.86$, $P = 0.3547$), so data of both repetitions were combined in a single analysis (Figure 7). Plants grow-

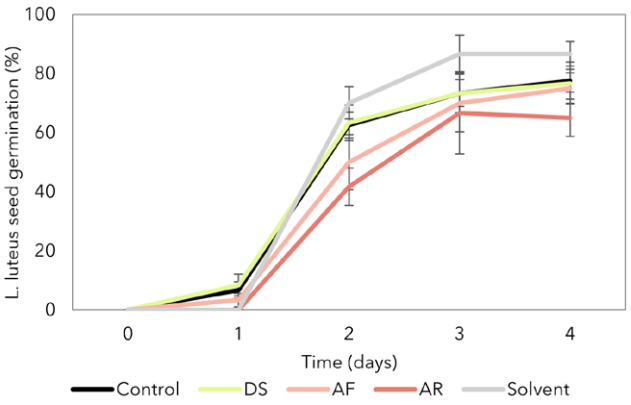

Figure 4. Mean (and standard error) of *Lupinus luteus* seed germination percentages in media amended with Asparagus Root organic extract (AR), Asparagus Frond organic extract (AF) or Date Seed organic extract (DS) at 0.05%, and in unamended media (controls).

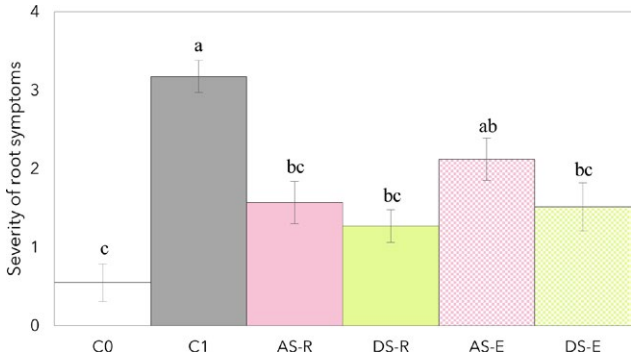

Figure 7. Mean (and standard error) root symptoms severity scores for holm oak seedlings growing in substrate infested and treated with asparagus or date palm residues (AS-R and DS-R) or organic extracts (AS-E from asparagus or DS-E from date palm), and from infested and untreated substrate (C1) and uninfested and untreated substrate (C0). Means accompanied by different letters are different according to Dunn's test ($P < 0.05$).

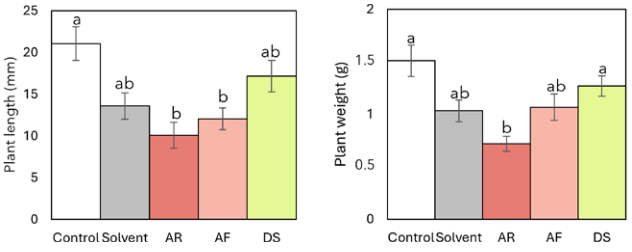

Figure 5. Mean plant lengths (and standard errors) (left), and mean plant fresh weights (right) for *Lupinus luteus* seedlings growing in peat amended with Asparagus Root organic extract (AR), Asparagus Frond extract (AF) or Date Seed extract (DS) at 0.05% concentrations, and solvent (0.02% ethanol) and unamended control. Means accompanied by different letters are different, according to Dunn's test ($P < 0.05$).

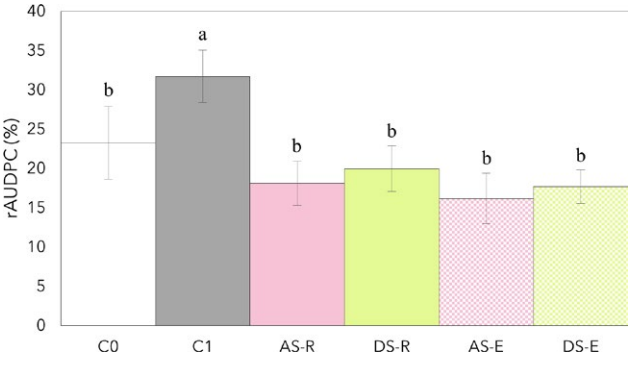

Figure 6. Mean (and standard error) areas under disease progress curves (rAUDPC) of the severity of foliar symptoms on holm oak seedlings growing in substrate infested and treated with the asparagus or date palm residues and organic extracts, or with infested and untreated substrate (C1) or uninfested and untreated substrate (C0). Means accompanied by different letters are different according to Dunn's test ($P < 0.05$).

ing in substrate treated with date seed extract or residue (DS-E or DS-R), or with asparagus spears residue (AS-R), developed significantly less severe root symptoms than the infested and untreated plants (Control 1), and were not different from untreated and uninoculated holm oaks (Control 0). AS-E plants did not differ from Control 1, and had significantly more severe root symptoms than plants in Control 0 (Figure 7). *Phytophthora cinnamomi* was re-isolated from all plants growing in infested substrate that was amended or not amended with extracts and residues (isolation proportions 36.1 to 72.2%), but never from plants growing in uninoculated substrate (Control 0).

DISCUSSION

This study assessed anti-oomycete activity of extracts obtained from by-products of *triguero* asparagus from Huétor-Tájar (Granada), olive or date palm residues in experiments across the main stages of the *P. cinnamomi* pathogenicity cycle (mycelial growth, sporangial production, and disease development). Comparisons were also made between the most effective organic extracts enriched with bioactive compounds and the residues for effects on root disease development. Although previous studies have shown that extracts from different plant species had antimicrobial activity against phytopathogenic fungi (Rosado-Álvarez *et al.*, 2014; Tucuch-Pérez *et al.*, 2020) and oomycetes (Nagar *et al.*, 2017; Lujan *et al.*, 2021; Cruz *et al.*, 2024), the studies have focused on *in vitro* experiments (Nagar *et al.*, 2017; Cruz *et al.*, 2024). The present study included *in vivo* tests to assess

the antimicrobial activity of organic plant extracts and their crude residues in a realistic setting. Additionally, the study has provided evidence of effectiveness of date palm and asparagus agricultural by-products for inhibiting *P. cinnamomi* infectivity and *in planta* disease development, indicating their potential for management of diseases caused by this pathogen.

Results from the *in vitro* experiments showed that the organic extracts most inhibitory to *P. cinnamomi* mycelial growth and sporangial production were those from asparagus spears (AS), olive leaves (OL) or date palm seed (DS). There was also a clear differential effect on pathogen inhibition depending on the origin of the residues within asparagus plants and olive trees. Extracts from asparagus spears and roots, at doses of 0.025 and 0.05%, strongly inhibited *P. cinnamomi* mycelial growth, while extract from asparagus fronds were not effective. For sporangial production, a similar response occurred for plant biomass. Inhibition percentages greater than 84% resulted from extracts from asparagus spears (AS) or olive leaves (OL) at 0.05%, while AF, AR and OF were not inhibitory. Sporangial production is directly related to zoospore release, so inhibition of these reproductive structures reduces the infectivity of *P. cinnamomi*. Other research has also reported fluctuating fungicidal activity linked to plant biomass from compounds used against the fungal pathogens *Botrytis cinerea, A. tenuissima, F. oxysporum, M. phaseolina, R. solani*, as well as *P. cinnamomi* and *P. agathicida* (Lawrence *et al*., 2019; Desoukey *et al*., 2020).

Differential behaviour associated with plant biomass could be explained by the extract phenolic profiles, since the composition and concentration of bioactive compounds in plants is related to the particular plant organ (Lawrence *et al*., 2019; Desoukey *et al*., 2020), phenological phase (Ríos *et al*., 2016), geographic location, cultivar, and/or nutritional state (Borjan *et al*., 2020), as well as extraction method (Sales *et al*., 2016). For instance, AS inhibited *P. cinnamomi*, but AF was ineffective, although flavonoid rutin (quercetin 3-O-rutinoside) was the major phytochemical, and the asparagus frond extract had a total phenolic compound concentrations that was greater than the extract from asparagus spears extract (López *et al.,* 2025). These results demonstrate the importance of correct selection plant biomass to effectively control plant pathogens. Dose should be correctly chosen, since the lower activity for reducing sporangial production of *P. cinnamomi* shown in the present study for olive fruit extract in comparison to olive leaf extract, could disappear with increasing extract dose. Romero *et al.* (2024) reported that OF and OL gave sporangium inhibition of greater than 83% at doses of 2 or 3 times greater (0.1 and 0.15%) than those used in the present study.

For asparagus root extract, although it did not affect *L. luteus* seed germination or plant yield in the phytotoxicity tests, effects on *P. cinnamomi* sporangial production from the asparagus root extract could not be differentiated from those of the solvent. Further research is required to confirm if other solvents could be used to discriminate asparagus root extract effects against sporangial production of *P. cinnamomi* without phytotoxic effects.

Limited data are available on the fungicidal activity of date palm extracts, with most of studies being focused on food-based and human pathogens (Al-Tamimi *et al*., 2021). Therefore, the present study results provide new evidence showing that ethanolic extract from date palm seed had high *in vitro* activity against *P. cinnamomi*, reducing sporangial production (91% inhibition). Conversely, no effect on mycelial growth was observed. Bokhari and Perven (2012) reported that different leaf and pit extracts from *Phoenix dactylifera* had varying degrees of mycelial growth inhibition for pathogenic *Fusarium, Aspergillus, Trichoderma* and *Alternaria* but no oomycetes were assessed in their study. In general, *in vitro* data have limited value for predicting field efficacy, while *in planta* results can provide more reliable data.

The *in planta* experiments showed that date fruit seeds effectively reduced root rot development in *Q. ilex* seedlings, both as extract and as crude residue. Conversely, while the asparagus crude residue reduced severity of root symptoms, the extract from asparagus spears was effective only *in vitro* but not *in planta*. Romero *et al.* (2024) observed reductions in *P. cinnamomi* sporangial production and chlamydospore viability when treated with extract from asparagus spears (at 0.15%), resulting in low mortality of lupin plants. The different results obtained in the present study, when testing the efficacy of asparagus spear extract *in planta*, may have been due to the low dose tested. Additionally, the differences found in the present study between *in vitro* and *in planta* experiments for asparagus spears extracts could have been due to soil factors that can modify effectiveness of compounds and host plant responses (Goufo *et al*., 2010; Serrano-Pérez *et al.,* 2021), compared with the *in vitro* experimental conditions where there are direct pathogen-extract interactions. Outcomes from this study have demonstrated the importance of confirming *in vitro* results by means of *in planta* experiments. On the other hand, the differential *in planta* behaviour found between asparagus spear extract and its crude residue could be explained by different causes. Firstly, the compositions of extract and residue are probably different. Although extract has greater total concentration of phenolic compounds, crude residue has other chemical components and fibrous biomass, that may influence on effectiveness (Desoukey *et al*.,

2020; Ahmad and Matsubara, 2020). Secondly, rapid degradation of bioactive compounds from asparagus spear extract could reduce period for inhibiting *P. cinnamomi* infectivity, compared to slow release from crude residues. *Brassica carinata* effectiveness against *P. nicotianae* was also dependent on volatile compound release and exposure time (Serrano-Pérez *et al.,* 2017; 2021).

The date seed extract assessed in the present study directly affected *P. cinnamomi* by reducing sporangial production, and (presumably) the quantity of zoospores within sporangia. This effect translated into decreased root rot symptoms on *Q. ilex* seedlings infected by the pathogen. Previous studies have also demonstrated the effectiveness of agricultural by-products extracts, including those from carob and pomegranate peel, for reducing incidence of olive anthracnose by inhibiting conidium germination in *Colletotrichum* spp. (Pangallo *et al.,* 2017; Antón-Domínguez *et al*., 2025). However, several studies have reported dual action of plant extracts against phytopathogens, with direct antimicrobial activity combined with indirect action as resistance inducers (Hassan *et al*., 2009; Saltos-Rezabala *et al*., 2022; Antón-Domínguez *et al.,* 2025). Saltos-Rezabala *et al.* (2022) observed that although thyme essential oil had direct antifungal effects against *Alternaria linariae*, it did not eradicate the pathogen, but gave effective control of the pathogen by increasing defences of tomato plants. Recent studies (Serrano, personal communication) have demonstrated preventive effects of pyrogallol against *P. cinnamomi* root rot of *Q. ilex* seedlings. Pyrogallol is the main phenolic compound in date seed extract and residue. A double action mode could be involved from treatments with date seed extracts. These results highlight the need for further research to determine possible activity of date seed residue and extract as resistance inducers during pathogen infection progression.

The present study results highlight the effectiveness of full crude residues from asparagus spears and date seeds, for control of root rot caused by *P. cinnamomi*. In addition, these treatments have advantages in comparison to extract applications, such as organic matter contribution to soil structure, the possible synergic effects with other antagonistic microorganisms (Serrano-Pérez *et al*., 2017; 2021), and the simple and low-cost treatment application, that make crude plant residues effective alternatives for control of soilborne pathogens.

CONCLUSIONS

This study provides a first approach to development of a potentially environmentally friendly approach to control *P. cinnamomi* root rot on *Quercus* species, based on soil applications of extracts and residues from agricultural crops. In particular, the promising results obtained for reducing *P. cinnamomi* infectivity and root rot development resulting from treatments of asparagus spear residue and extracts from seeds of date palm fruits, indicates that they are candidates for plant pathogen control. Their use would also promote recycling of residues and "circular economies". Effects of asparagus spears and date seed residues against *P. cinnamomi* are currently being evaluated under natural conditions in a pathogen infested field of mature *Q. ilex* trees.

ACKNOWLEDGEMENTS

The authors thank Dr AC Coelho (Universidade do Algarve, Portugal) and Dr B. Scanu and Dr S. Seddaiu (Università degli Studi di Sassari, Italy) for providing *P. cinnamomi* isolates. Authors also thank Dr ME Sánchez Hernández (University of Córdoba) provided critical review of the manuscript of this paper. The research was supported by Emergia Program (Consejería de Transformación Económica, Industria, Conocimiento y Universidades, Andalusian Government, call 2021), Grant PID2022-141864OB-I00 funded by MCIN/AEI/10.13039/501100011033 and by "ERDF A way of making Europe", and the project GreenPalm of the PRIMA European Action, Project25/Section II-2019, the grant PCI2020-112088 funded by MCIN/AEI/10.13039/501100011033, and by European Union Next Generation EU/PRTR.

LITERATURE CITED

Ahmad H., Matsubara Y.I., 2020. Antifungal effect of *Lamiaceae* herb water extracts against *Fusarium* root rot in Asparagus. *Journal of Plant Disease and Protection* 127: 229–236. https://doi.org/10.1007/s41348-019-00293-x.

Al-Tamimi A., Alfarhan A., Rajagopal R., 2021. Antimicrobial and anti-biofilm activities of polyphenols extracted from different Saudi Arabian date cultivars against human pathogens. *Journal of Infection and Public Health* 14: 1783–1787. https://doi.org/10.1016/j.jiph.2021.10.006.

Antón-Domínguez B., Sánchez-Pereira L., Lamas, S., Rodrigues N., Baptista P. Agustí-Brisach C., 2025. Carob and pomegranate extracts enhance plant defence mechanisms against olive anthracnose through antioxidant activity and phenolic com-

pounds production. *Industrial Crops & Products* 235: 121653. https://doi.org/10.1016/j.indcrop.2025.121653.

Bokhari N. A., Perveen K., 2012. *In vitro* inhibition potential of *Phoenix dactylifera* L. extracts on the growth of pathogenic fungi. *Journal of Medicinal Plants Research* 6: 1083–1088. https://doi.org/10.5897/jmpr11.1545.

Borjan D., Leitgeb M., Knez Ž., Hrnčič M. K., 2020. Microbiological and Antioxidant Activity of Phenolic Compounds in Olive Leaf Extract. *Molecules* 25: 5946. https://doi.org/10.3390/MOLECULES25245946.

Bowers J.H., Locke J. C., 2004. Effect of Formulated Plant Extracts and Oils on Population Density of *Phytophthora nicotianae* in Soil and Control of Phytophthora Blight in the Greenhouse. *Plant Disease* 88: 11–16. https://doi.org/10.1094/PDIS.2004.88.1.11.

Brasier C. M., 1996. *Phytophthora cinnamomi* and oak decline in southern Europe. Environmental constraints including climate change. *Annals of Forest Science* 53: 347–358. https://doi.org/10.1051/forest:19960217.

Burgess T. I., Scott J. K., Mcdougall K. L., Stukely M. J. C., Crane C., ..., Hardy G. E. S. J. , 2017. Current and projected global distribution of *Phytophthora cinnamomi*, one of the world's worst plant pathogens. *Global Change Biology* 23: 1661–1674. https://doi.org/10.1111/gcb.13492.

Campbell C. L., Madden L. V., 1990. *Introduction to Plant Disease Epidemiology*. John Wiley & Sons, Inc., New York, U.S.A, 532 pp.

Cenobio-Galindo A. J., Hernández-Fuentes A. D., González-Lemuè U., Zaldívar-Ortega A. K., González-Montiel L., ... Hernández-Soto I., 2024. Biofungicides Based on Plant Extracts: On the Road to Organiz Farming. *International Journal of Molecular Sciences* 25: 6879. https://doi.org/10.3390/ijms25136879.

Cruz A., Sánchez-Hernández E., Teixeira A., Martín-Ramos P., Cunha, A., Oliveira R., 2024. Antifungal and Antioomycete Activities of a *Curcuma longa* L. Hydroethanolic Extract Rich in Bisabolene Sesquiterpenoids. *Horticulturae* 10: 124. https://doi.org/10.3390/horticulturae10020124.

Del Río J. A., Báidez A. G., Botía J. M., Ortuño A., 2003. Enhancement of phenolic compounds in olive plants (*Olea europaea* L.) and their influence on resistance against *Phytophthora* sp. *Food Chemistry* 83: 75–78. https://doi.org/10.1016/S0308-8146(03)00051-7.

Desoukey S. F., El-Nahas S. E. M., Sabh A. Z., Taha Z. K., El-Shabrawi H. M., 2020. Antimicrobial effect of *Asparagus officinalis* L. extracts. *Plant Archives* 20: 9253–9264. https://www.researchgate.net/publication/348265502.

Fuentes-Alventosa J. M., Jaramillo S., Rodríguez-Gutiérrez G., Cermeño P., Espejo J. A., ... Rodríguez-Arcos R., 2008. Flavonoid profile of green asparagus genotypes. *Journal of agricultural and food chemistry* 56: 6977-6984. https://doi.org/10.1021/jf8009766.

Fuentes-Alventosa J. M., Jaramillo-Carmona S., Rodríguez-Gutiérrez G., Guillén-Bejarano R., Jiménez-Araujo A., ... Rodríguez-Arcos R., 2013. Preparation of bioactive extracts from asparagus by-product. *Food and Bioproducts Processing* 91: 74–82. https://doi.org/10.1016/j.fbp.2012.12.004.

Garbelotto M., Hüberli D., Shaw,D., 2006. First report on an infestation of *Phytophthora cinnamomi* in natural oak woodlands of California and its differential impact on two native oak species. *Plant Disease* 90: 685-685.

Global Invasive Species Database, 2025. Available at: http://www.iucngisd.org/gisd/100_worst.php. Accessed 20 October 2025

González M., Romero M. A., Serrano M. S., Sánchez M.E., 2020. Fosetyl-aluminium injection controls root rot disease affecting *Quercus suber* in southern Spain. *European Journal of Plant Pathology* 156: 101–109. https://doi.org/10.1007/s10658-019-01865-1.

Goufo P., Fontem D. A., Ngnokam D., 2010. Evaluation of plant extracts for tomato late blight control in Cameroon. *New Zealand Journal of Crop and Horticultural Science* 38: 171–176. https://doi.org/10.1080/01140671.2010.495374.

Hassan M. A. E., Bereika M. F. F., Abo-Eìnaga H. I. G., Sallam,M. A. A., 2009. Direct Antimicrobial Activity and Induction of Systemic Resistance in Potato Plants Against Bacterial Wilt Disease by Plant Extracts. *The Plant Pathology Journal* 25: 352–360. https://doi.org/10.5423/PPJ.2009.25.4.352.

Jaramillo-Carmona S., Rodríguez-Arcos R., Jiménez-Araujo A., López S., Gil J., ... Guillén-Bejarano R., 2017. Saponin profile of wild asparagus species. *Journal of Food Science* 82: 638–646. https://doi.org/10.1111/1750-3841.13628.

Lawrence S. A., Burgess E. J., Pairama C., Black A., Patric, W. M., ... Gerth M. L., 2019. Mātauranga-guided screening of New Zealand native plants reveals flavonoids from kānuka (*Kunzea robusta*) with anti-*Phytophthora* activity. *Journal of the Royal Society of New Zealand* 49: 137–154. https://doi.org/10.1080/03036758.2019.1648303.

López R., Hidalgo M. T., García M., Rodríguez R., Jiménez A., Serrano M. S., 2025. Efectividad diferencial de

extractos de espárrago frente a la podredumbre radical causada por *Phytophthora cinnamomi*. *Cuadernos de La Sociedad Española de Ciencias Forestales* 51: 173–186. https://doi.org/10.31167/csef.v0i51.20161.

Lujan P., Dura S., Guzman I., Grace M., Lila M. A., ... Sanogo S., 2021. Efficacy of Pecan Husk and Shell Phenolic Extracts Against Phytophthora Blight in Chile Pepper. *Plant Health Progress* 22: 1–6. https://doi.org/10.1094/PHP-02-21-0024-FI.

Mrabet A., Hamdi A., Rodríguez-Arcos R., Guillén-Bejarano R., Jiménez-Araujo A., 2024. Date seed by-products as source of bioactive ingredient for healthy cookies. *Food Bioscience* 61: 104543. https://doi.org/10.1016/j.fbio.2024.104543.

Nagar D., Biswas S. K., Singh M., Singh J., 2017. Evaluation of *in vitro* Efficacy of Different Plant Extracts against *Phytophthora infestans* (Mont.) de Bary. *International Journal of Current Microbiology and Applied Sciences* 6: 412–417. https://doi.org/10.20546/ijcmas.2017.606.048.

Pangallo S., Destri-Nicosia M. G., Agosteo, G. E., Abdelfattah A., Romeo F. V., ... Schena L., 2017. Evaluation of a Pomegranate Peel Extract as an Alternative Means to Control Olive Anthracnose. *Phytopathology* 107: 1462–1467. https://doi.org/10.1094/PHYTO-04-17-0133-R.

Ribeiro O. K., 1978. *A Sourcebook on the Genus Phytophthora*. Lehre, Germany, J. Cramer, 417 pp.

Ríos P., Obregón S., Haro A., Fernández-Rebollo P., Serrano M.S., Sánchez M.E., 2016. Effect of *Brassica* biofumigant amendments on different stages of the life cycle of *Phytophthora cinnamomi*. *Journal of Phytopathology* 164: 582–594. https://doi.org/10.1111/jph.12482.

Rodríguez G., Rodríguez R., Fernández-Bolaños J., Guillén R., Jiménez A., 2007. Antioxidant activity of effluents during the purification of hydroxytyrosol and 3,4-dihydroxyphenyl glycol from olive oil waste. *European Food Research and Technology* 224: 733–741. https://doi.org/10.1007/s00217-006-0366-1.

Romero M. A., Rodríguez-Arcos R., Jiménez-Araujo A., Serrano M. S., 2022. Revalorización de residuos agrícolas como herramientas de biocontrol de la podredumbre radical causada por *Phytophthora cinnamomi*. In: Proceedings of XX Meeting of the Spanish Phytopathological Society, 24-26 October, 2022, Valencia, Spain, 161 (abstract).

Romero M. A., López R., Rodríguez-Arcos R., Jiménez-Araujo A., Serrano M. S., 2024. Anti-oomycete activity of *asparagus* and olive by-products with potential to control *Phytophthora cinnamomi* root rot. *Journal of Plant Pathology* 106: 1685–1696. https://doi.org/10.1007/s42161-024-01696-y.

Romero M.A., Sánchez J.E., Jiménez J.J., Belbahri L., Trapero A., Lefort F., Sánchez M.E., 2007. New *Pythium* taxa causing root rot on Mediterranean *Quercus* species in South-West Spain and Portugal. *Journal of Phytopathology* 155: 289–295. https://doi.org/10.1111/j.1439-0434.2007.01230.x.

Rosado-Álvarez C., Molinero-Ruiz L., Rodríguez-Arcos R., Basallote-Ureba M. J., 2014. Antifungal activity of asparagus extracts against phytopathogenic *Fusarium oxysporum*. *Scientia Horticulturae* 171: 51–57. https://doi.org/10.1016/j.scienta.2014.03.037.

Sales M. D. C., Costa H. B., Fernandes P. M. B. Ventura J. A., Meira D. D., 2016. Antifungal activity of plant extracts with potential to control plant pathogens in pineapple. *Asian Pacific Journal of Tropic Biomedicine* 61: 26–31. https://doi.org/10.1016/j.apjtb.2015.09.026.

Saltos-Rezabala L. A., Ricardino Da Silveira P., Gonçalves-Talavares D., Intra-Moreira, S., Alves-Magalhães T., ... Alves E., 2022. Thyme Essential Oil Reduces Disease Severity and Induces Resistance against *Alternaria linariae* in Tomato Plants. *Horticulturae* 8(10): 919. https://doi.org/10.3390/horticulturae8100919.

Sánchez M.E., Caetano P., Ferraz J., Trapero A., 2002. *Phytophthora* disease of *Quercus ilex* in south-western Spain. *Forest Pathology* 32: 5–18. https://doi.org/10.1046/j.1439-0329.2002.00261.x.

Sena K., Crocker E., Vincelli,P., Barton C., 2018. *Phytophthora cinnamomi* as a driver of forest change: Implications for conservation and management. *Forest Ecology and Management* 409: 799–807. https://doi.org/10.1016/j.foreco.2017.12.022.

Serrano M. S., de Vita P., Fernández-Rebollo P., Sánchez-Hernández M. E., 2012a. Calcium fertilizers induce soil suppressiveness to *Phytophthora cinnamomi* root rot of *Quercus ilex*. *European Journal of Plant Pathology* 132: 271–279. https://doi.org/10.1007/s10658-011-9871-6.

Serrano M. S., Fernández-Rebollo P., De Vita P., Sánchez, M. E., 2012b. Susceptibility of common herbaceous crops to *Phytophthora cinnamomi* and its influence on *Quercus* root rot in rangelands. *European Journal of Plant Pathology* 134: 409–414. https://doi.org/10.1007/s10658-012-9999-z.

Serrano-Pérez P., Palo C., Rodríguez-Molina M. C., 2017. Efficacy of Brassica carinata pellets to inhibit mycelial growth and chlamydospore germination of *Phytophthora nicotianae* at different temperatures

regimes. *Scientia Horticulturae* 2016: 126-133. https://doi.org/10.1016/j.scienta.2017.01.002.

Serrano-Pérez P., De Santigado A., Rodríguez-Molina M. C., 2021. Biofumigation with pellets of defatted seed meal of *Brassica carinata*: factors affecting performance against *Phytophthora nicotianae* in pepper crops. *Frontiers in Sustanaible Food Systems* 5: 664531. https://doi.org/10.3389/fsufs.2021.664531.

Sparg S. G., Light M. E., van Staden J., 2004. Biological activities and distribution of plant saponins. *Journal of Ethnopharmacology* 94: 219–243. https://doi.org/10.1016/j.jep.2004.05.016.

Tucuch-Perez M. A., Arredondo-Valdes R., Hernandez-Castillo F.D., 2020. Antifungal activity of phytochemical compounds of extracts from Mexican semi-desert plants against *Fusarium oxysporum* from tomato by microdilution in plate method. *Nova Scientia* 12: 1–9.

Phytopathologia Mediterranea
The international journal of the
Mediterranean Phytopathological Union

Firenze University Press
www.fupress.com/pm

Research Papers

Susceptibility of *Citrus* germplasm to canker caused by *Neofusicoccum parvum*

Giorgio GUSELLA, Chiara CATALANO*, Bassma EL BAKKOURI, Sebastiano SEMINARA, Mario DI GUARDO, Gaetano DISTEFANO, Stefano LA MALFA, Alessandra GENTILE, Giancarlo POLIZZI

Department of Agriculture, Food and Environment (Di3A), University of Catania, via S. Sofia 100, 95123 Catania, Italy.
*Corresponding author. E-mail: chiara.catalano@unict.it

Summary. *Citrus* trees are important for fruit production, and canker pathogens can be constraints to tree productivity. In Italy, field surveys showed presence of different pathogens causing trunk and branch cankers, gummoses and shoot blight. Among these pathogens, *Neofusicoccum parvum* is aggressive and widely distributed. Susceptibility of 47 *Citrus* genotypes was assessed using detached twig assays and an *in planta* assessment. The detached twig assay identified mandarin as the most susceptible variety (mean lesion length = 3.80 cm), followed by citrumelo 'Swingle' (2.83 cm), and lemons (2.47 cm), whereas grapefruits (1.34 cm) and citrons (1.76 cm) had greatest levels of tolerance. These results were consistent with those obtained in the *in planta* assay, in which grapefruits showed greatest tolerance (mean lesion length = 1.24 cm), while the lemon cultivars 'Monachello' (7.32 cm) and 'Femminello Siracusano 2Kr' (6.48 cm) were confirmed as the most susceptible genotypes. This study provides the first overview assessment of susceptibility of different *Citrus* species to infection by *N. parvum*.

Keywords. *Botryosphaeriaceae*, citrus gummosis, phenotyping, resistance, detached twig assay, in planta assay.

OPEN ACCESS

Citation: Gusella, G., Catalano, C., El Bakkouri, B., Seminara, S., Di Guardo, M., Distefano, G., La Malfa, S., Gentile, A. & Polizzi, G. (2026). Susceptibility of *Citrus* germplasm to canker caused by *Neofusicoccum parvum*. *Phytopathologia Mediterranea* 65(2): 243-254. doi: 10.36253/phyto-17230

Accepted: July 6, 2026

Published: July 27, 2026

©2026 Author(s). This is an open access, peer-reviewed article published by Firenze University Press (https://www.fupress.com) and distributed, except where otherwise noted, under the terms of the CC BY 4.0 License for content and CC0 1.0 Universal for metadata.

Data Availability Statement: All relevant data are within the paper and its Supporting Information files.

Competing Interests: The Author(s) declare(s) no conflict of interest.

Editor: Akif Eskalen, University of California, Davis, CA, United States.

ORCID:
GC: 0000-0002-0519-1200
CC: 0000-0002-1748-3294
BEB: 0000-0002-5562-6751
SS: 0009-0000-2889-9140
MDG: 0000-0003-3339-2007
GD: 0000-0002-6080-6466
SLM: 0000-0001-5869-0348
AG: 0009-0005-1312-4808
GP: 0000-0001-8630-2760

INTRODUCTION

Citrus species are important tree crops in terms of total production and harvested areas (FAOSTAT, 2025). Among the top producing countries, China, Brazil, and India account for the greatest production of tangerines, oranges and lemons (Pereira Gonzatto and Scherer Santos, 2023). In Europe, Spain and Italy are key citrus fruit producers (Beshara *et al*., 2024). In Italy, the southern regions of Sicily, Calabria and Campania are the most suitable areas for citrus cultivation, with Sicily having the largest plantations (Ciriminna *et al*., 2024). These regions produce important local citrus products that are protected by the EU geographical indications system, including protected designation of origin (PDO) and protected geographical indication (PGI). Historically, Italian citrus orchards have been affected by severe diseases, including the "mal secco" caused by *Plenodomus tracheiphi-*

lus (homotypic synonym, *Phoma tracheiphila*), and the virus disease "Tristeza" caused by *Closterovirus tristezae* (formerly citrus tristeza virus; CTV). These pathogens shortened orchard lifetimes and severely reduced economic returns for growers (Catalano *et al*., 2021; Leonardi *et al*., 2023; Sun *et al*., 2024).

Citrus and other perennial crops, represent long-term grower investments, as productivity increases and stabilizes several years after orchard establishment, and then lasts for many years. Canker pathogens are severe threats to fruit orchard lifespans. Canker-causing pathogens usually do not completely compromise annual production, but overall yields are reduced over time (Moral *et al*., 2019).

Although canker pathogens can infect many *Citrus* species, these fungi in Italy were restricted to lemon, with only a few reports on other citrus (Scaramuzzi, 1965). However, canker caused by fungi has long been recognized in other countries (Adesemoye *et al*., 2014; Mayorquin *et al*., 2016; Vakaloumakis *et al*., 2019; Bezerra *et al*., 2021; Kayim *et al*., 2024; Gusella *et al*., 2025), but studies focused on the citrus canker etiology. *Botryosphaeriaceae*, *Diaporthaceae*, and *Diatrypaceae* have been identified as the main taxonomic groups involved on the hosts *Citrus limon*, *C. paradisi*, *C. sinensis*, *C. latifolia*, *C. unshiu*, *C. aurantifolia*, *C. medica*, *C. aurantium*, *C. reticulata*, *Microcitrus australasica*, citrumelo Swingle, and citrange Carrizo (Adesemoye *et al*., 2014; Mayorquin *et al*., 2016; Vakaloumakis *et al*., 2019; Bezerra *et al*., 2021).

In Italy, recent investigations conducted in different citrus production areas, on crops of *C. limon*, *C. bergamia*, *C. sinensis* × *C. clementina*, *C. aurantium*, or *C. paradisi*, showed a wide fungus pathogen diversity associated with branch and trunk cankers, referred to as "Bot gummosis disease". *Neofusicoccum parvum* (*Botryosphaeriaceae*) was in the most common pathogen in all the surveyed areas and was the most aggressive in the pathogenicity tests (Aloi *et al*., 2021; Gusella *et al*., 2025). Other species, in addition to the well-recognized *Botryosphaeriaceae* spp., have been characterized and were particularly aggressive, particularly *Boeremia exigua* and *Neocosmospora metavorans* (Gusella *et al*., 2025). *N. parvum* was isolated from symptomatic hybrids of *C. sinensis* × *C. reticulata* in Greece (Vakalounakis *et al*., 2019), mandarin in Turkey (Kurt *et al*., 2025), sweet orange in California (Adesemoye *et al*., 2014), and Satsuma mandarin in China (Xiao *et al*., 2021).

Phenotypic screening of plant species and/or cultivars, based on artificial inoculations, has been an important starting point for research in plant breeding and plant pathology. For *Botryosphaeriaceae* pathogens, and *N. parvum* in particular, information on host susceptibility is currently available only for a limited number of *Citrus* species. Specifically, the rootstock citrumelo Swingle (*Poncirus trifoliata x Citrus paradisi*) is considered to be tolerant to *N. parvum*, while 'Piretto' and 'Lia Kritis' citrons have intermediate tolerance, and 'Femminello Siracusano 2Kr' and 'Monachello' lemons are considered to be susceptible to Bot gummosis disease (Vakaloumakis *et al*., 2019; Aloi *et al*., 2021).

The objective of the present study was to assess the phenotypic responses of 47 *Citrus* genotypes to the infection by *N. parvum,* using detached twig assays and *in planta* inoculations. This allowed us to verify consistency between the two inoculation approaches and evaluate their respective strengths and limitations in plant pathology research, and for phenotypic screening for marker-trait association studies.

MATERIAL AND METHODS

Plant material

Responses to infection by *N. parvum* were investigated in 47 *Citrus* genotypes. Thirty-eight were used in detached twig assays and 24 were assessed in an *in planta* assay, with 15 of the genotypes used in both experiments (Table 1). Plant samples for the detached twig assays were collected from the *Citrus* germplasm collection located at the Experimental farm of the University of Catania (UniCt) (Sicily, Italy; latitude, 37°24′33″N; longitude, 15°03′20″E; altitude, 10 m asl). The UniCt germplasm collection is mainly composed of local varieties complemented with some of the most widely cultivated at national and international levels. Plants were all of similar age (~ 15-years) and were maintained in four replicates under standard agronomic practices. The plants used for the *in planta* assay were supplied by a local citrus-specialized nursery, were maintained in open-air conditions, and were of 2-years-old after grafting. They were grafted onto sour orange rootstock and grown in 5 L capacity pots containing a mixture of natural soil and peat.

Detached twig assays

Detached twig inoculations were conducted as follows: a total of eight growing twigs (each approx. 20 cm long), lignified but still green, were sampled from three plants (biological replicates) of each selected host genotype. The sterilization and inoculation procedures were conducted according to Catalano *et al.* (2025), as outlined in Figure 1.

Table 1. List of the plant genotypes used in detached twig and/or *in planta* assays.

Species	Genotype	Detached twig assays	*In planta* assay
Sweet orange (*C. sinensis*)	Valencia		x
	Ovale		x
	Navelina	x	x
	Lane Late	x	
	Tarocco Sant'Alfio	x	
	Tarocco Meli	x	
	Washington navel	x	
	Tarocco Sciré	x	x
Sour orange (*C. aurantium*)	Sour orange	x	
Mandarin and mandarin-like hybrids (*C. reticulata*)	Tardivo di Ciaculli (6022A2 clone)	x	x
	Nova	x	x
	Tacle	x	x
	Clementine	x	x
	Tardivo di Ciaculli o.l. (old line)	x	
	Clementine tardivo	x	
	Mandalate	x	
	Comune		x
Lemon (*C. limon*)	Sfusato Amalfitano		x
	Sfusato di Procida		x
	Interdonato	x	x
	Femminello Zagara Bianca	x	x
	Femminello Siracusano 2Kr	x	x
	Monachello		x
	Femminello Siracusano m296	x	
	Quattrocchi	x	
	Fino	x	
	Femminello Fior d'Arancio	x	
	Monachello Continella o.l.	x	
	Femminello Adamo	x	
Citron (*C. medica*)	Diamante		x
Citron-like (*C. limoni-medica*)	Vozza_vozza (lemon *x* pummelo hybrid)	x	
	Spatafora	x	
	Piretto	x	x
	Limone Rosso		x
Grapefruit (*C. paradisi*)	Ruby	x	x
	Star Ruby	x	
Bergamot (*C. bergamia*)	Femminello	x	x
	Castagnaro	x	
	Fantastico	x	x
Lime, limetta and their hybrids	Lime (*C. aurantifolia*)	x	x
	Eustis (limequat, *C. aurantifolia x F. japonica*)	x	
	Limetta Romana (*C. limetta*)	x	
	Palestina sweet lime (*C. limettoides*)	x	
Fortunella spp.	Kumquat (*F. japonica*)	x	x
	F. obovata	x	
Other	Citrumelo Swingle (*Poncirus trifoliata x C. paradisi*)	x	
	Meyer (*C. meyerii*)		x

Inoculum consisted of *N. parvum* mycelium/agar plugs (5 mm diam., obtained using cork borer), derived from active 7-d-old colonies *N. parvum* isolate CT84, grown on potato dextrose agar (PDA; Lickson). Isolate CT84 was previously molecularly characterized by Gusella *et al.* (2025). Eight twigs were used per host genotype. Inoculation points were not sealed to allow further manipulation of detached shoots, since the humidity inside the plastic boxes containing the twigs was sufficiently high for infection establishment. The plastic boxes (20 × 15 × 8 cm) were each filled with approx. 20 g of sterile perlite, to which 200 mL of water was added to maintain optimal humidity, and were used as humid chambers for the inoculated hos twigs. The plastic boxes were then moved into a growth chamber, set at 25 °C (± 1 °C), and a 12 h light 12 h dark cycle. r photoperiod at 25 ± 1 °C for five days. Wounded twigs inoculated with non-colonized sterile PDA plugs served as negative inoculation controls. Five days after inoculation, photographs of the inoculated stems were taken, and lesion lengths were assessed using the software ImageJ (Schneider *et al.*, 2012). Representative shoots were randomly collected from ten genotypes (three twigs per genotype) after disease assessments, and fungus re-isolations were conducted to determine if Koch's postulates were fulfilled. Re-isolations was conducted as follows: discoloured parts of twig tissue (0.5 × 0.5 cm) were excised, then surface sterilized for 1 min. in 1.5% sodium hypochlorite (NaOCl) solution, rinsed in sterile distilled water, dried on sterile absorbent paper, and then placed in Petri plates containing PDA amended with 100 mg L^{-1} of streptomycin sulfate to prevent bacterial growth. The Petri plates were then incubated in the dark at 25 (± 1 °C) for 3-5 d. until fungus colonies emerged and were ready for morphological examinations.

In planta *inoculations and disease assessments*

An *in planta* assay was carried out using a total of 24 plant genotypes (Table 1). Three plants (biological replicates) were used for each genotype, and three twigs

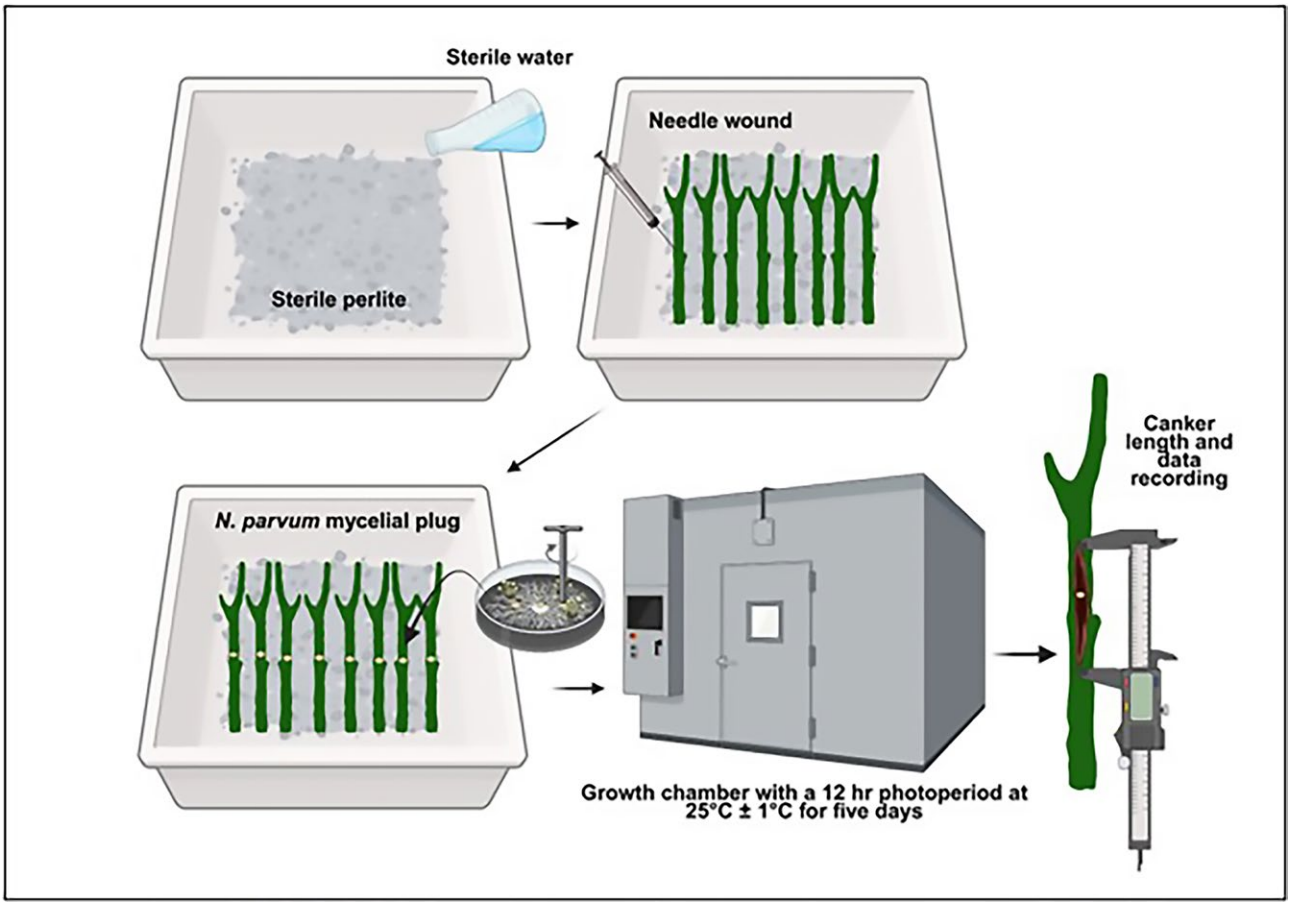

Figure 1. Scheme for detached twig assay procedure. Graphic created using BioRender.com.

were inoculated for each plant. Inoculations were conducted using the mycelium plug technique (described above) and *N. parvum* isolate CT84. The plants were maintained outside, to expose them to high humidity conditions required for infection, and the inoculation site on each plant was sealed with plastic film. Disease assessments were carried out 15 d after the inoculations. Inoculation controls consisted of plants (one for each genotype) that were wounded and inoculated with sterile PDA plugs. Plants were visually inspected, lesion lengths were measured using a caliper, and presence of gummosis, wilting, blight, and pycnidia were recorded for each plant genotype. The plants were kept outside, were regularly watered, and temperature and humidity were monitored using a datalogger. Re-isolations were carried out (as described above) for a randomly selected group of inoculated plants.

Statistical analyses of data

Descriptive statistical analyses (means, standard deviations, standard errors) were obtained using the 'stat' package, and plots using the 'ggplot2' package, both within R software (version 4.1.0, R Core Team, 2021, Wickham *et al*., 2016). Levene's test (median-centered) indicated heteroscedasticity among genotypes ($P = 0.007$). Therefore, the data were analyzed using linear mixed-effects models to account for variance heterogeneity and biological replication, using the 'lme4' package in R. Data analyses were carried out separately for each host species and genotype, to account for potential species-specific responses to *N. parvum* inoculations. A subset of 15 host genotypes, which were tested with using the detached stem and *in planta* methods, was further analyzed to evaluate agreement between the two inoculation methods, for classifying citrus genotypes as low susceptible (LS), mild susceptible (MS), high susceptible (HS), and very high susceptible (VHS). To classify genotypes into these susceptibility classes, an unsupervised k-means clustering approach was applied to the mean disease severity values obtained from the detached twig and *in planta* inoculation assays. For each dataset, k-means clustering was carried out with $k = 4$, and the resulting cluster centroids were ordered from least to greatest susceptibility. Class boundaries were then defined as the midpoints between adjacent centroids, yielding the four ordinal categories (Supplementary Table 1). Each genotype was assigned independently to one of these categories for the two inoculation methods. Agreement between the detached and the *in planta* classifications was subsequently evaluated using Cohen's Kappa coefficient, which quantified the level of concordance between the four category ratings while adjusting for chance agreement. These analyses were carried out using the *irr* and *classInt* packages in R.

RESULTS

Detached twig assays

Necroses due to *N. parvum* infections were clearly visible 5 d after inoculations, when samples were assessed (Figure 2). The calculated mean lesion lengths were varied between the host genotypes, ranging from 1.24 cm (± 0.41 cm) for the grapefruit 'Ruby' to 5.66 cm (± 0.49 cm) for the mandarin 'Clementine' (Figure 3 A). Eighteen genotypes out of the 37 assessed had mean necrosis lengths less than 2 cm, while the lemon 'Femminello Zagara Bianca' (mean = 3.07 ± 0.49 cm) and the mandarins 'Tacle' (4.1 ± 0.40 cm), 'Mandalate' (5.10 ± 0.49 cm), 'Tardivo di Ciaculli' (5.16 ± 0.42 cm), and 'Clementine' (5.66 ± 0.49 cm), developed lesions of lengths greater than 3 cm (Figure 3 A, Supplementary Table 2).

Mandarin was the most susceptible to *N. parvum* infections (mean lesion length = 3.80 ± 0.20 cm), followed by citrumelo Swingle (2.83 ± 0.46 cm), and lemons (2.47 ± 0.19 cm), while the most tolerant host were grapefruits (1.34 ± 0.34 cm) and citrons (1.76 ± 0.27 cm). Limes and citrons had medium to low susceptibility, with respective mean lesion lengths of 1.82 cm (± 0.29 cm) and 1.75 cm (± 0.27 cm) (Figure 3 B, Supplementary Table 3).

In all samples tested, re-isolations confirmed presence of the inoculated fungus *N. parvum*. Wounded control twigs inoculated with non-colonized sterile PDA plugs did not develop necroses.

In planta *assay*

In planta inoculations were carried out in open air, and a datalogger was used to monitor temperature and humidity during the assay (Supplementary Table 4). Average temperature and relative humidity when symptoms became visible were, respectively, of 19.8 °C and 62.1%. These conditions contributed to rapid onset of symptoms (Figure 2 B).

The lemons 'Monachello' (mean lesion length = 7.32 ± 1.04 cm) and 'Femminello Siracusano 2Kr' (6.48 ± 1.04 cm) developed the largest necrotic lesions (Figure 4 A). Sweet orange 'Valencia' had the smallest lesions (0.72 ± 1.04 cm) (Figure 4A; Supplementary Table 5). Most of the genotypes (18 of the 24 tested) had mean necrosis lengths greater than 2 cm.

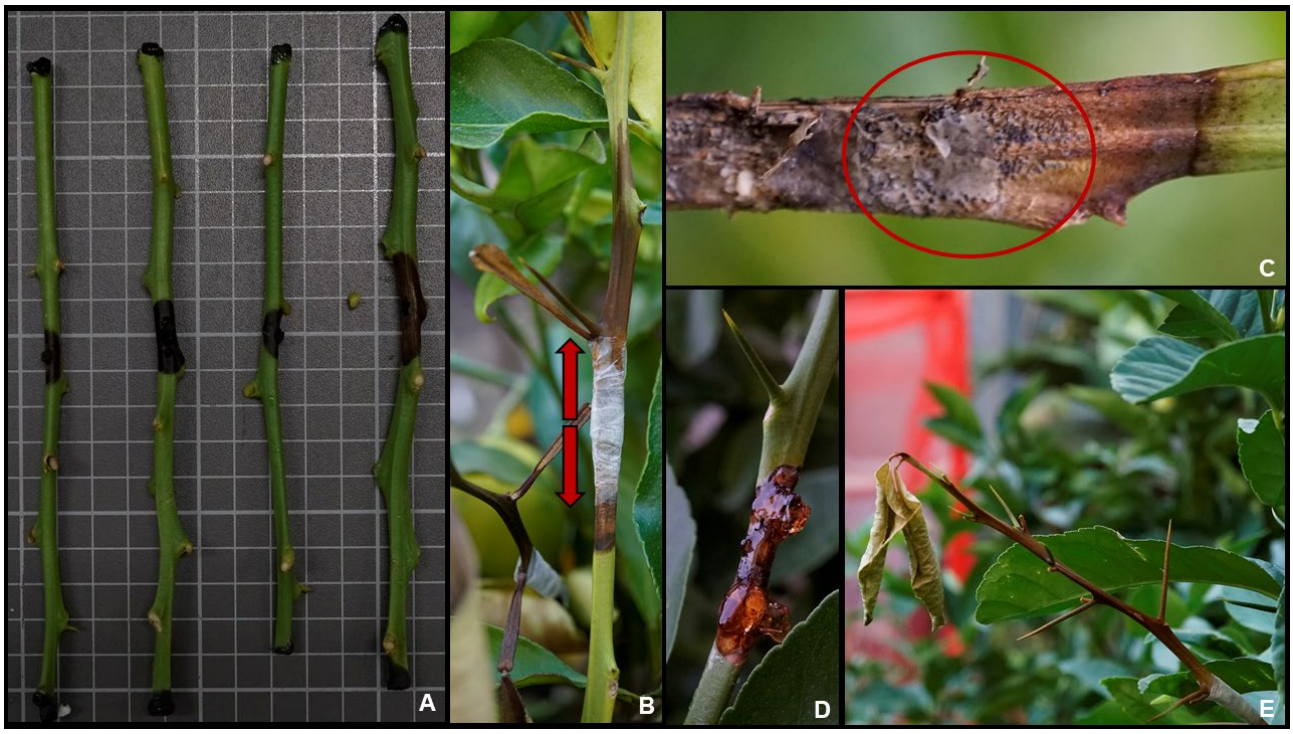

Figure 2. A) necroses developed from inoculation points on detached *Citrus* twigs (each background square is 1 cm^2). B) *In planta* assay showing necrosis upward and downward from an inoculation point sealed with Parafilm. C) Black pycnidia (red circle) developed on a necrotized area. D) Gum exudate from a canker lesion. E) Shoot blight on a plant shoot.

The *in planta* assay evaluated a total of eight host species. Grapefruits were confirmed to be the most tolerant to *N. parvum*, with a mean lesion length = 1.24 cm (± 1.30 cm), while the most susceptible were the *Fortunella* spp. Mean length = 5.14 cm; ± 1.30 cm) (Figure 4 B, Supplementary Table 3).

Re-isolations confirmed presence of *N. parvum* in all the processed samples, whereas the wounded non-inoculated control plants showed no necroses and only slight suberization at the wound sites.

Most genotypes (19 out of 24) exhibited gum production at inoculation sites in at least one replicate, whereas 'Comune' mandarin was the only genotype that produced pycnidia on the lesions without other symptoms (Supplementary Table 6, Figure 2, C to E). The mandarins 'Clementine', 'Tacle', and 'Tardivo di Ciaculli', and the sweet orange 'Tarocco Sciré', only developed blighting, with no pycnidia or gummoses. In contrast, the sweet oranges 'Navelina' and 'Ovale', and the lemons 'Femminello Siracusano 2Kr', 'Femminello Zagara Bianca', 'Interdonato', and 'Monachello', developed gummoses, pycnidia, and shoot blight.

Comparison of results from the two pathogenicity test methods gave a low positive correlation (Cohen's Kappa coefficient of 0.26). According to the Landis and Koch (1977) scale, this value corresponds to "fair agreement". The confusion matrix (Table 2) shows that seven genotypes were assigned to the same categories for the two inoculation methods, namely 'Ruby' grapefruit, 'Femminello' bergamot, lime, 'Nova' mandarin, 'Navelina' sweet orange, 'Femminello Zagara Bianca' lemon, and Clementine mandarin (Supplementary Table 7). Three genotypes were assigned into different susceptibility categories, with a difference of one category (the citron-like 'Piretto', 'Interdonato' lemon and 'Tacle' mandarin), four differed by two categories (kumquat, 'Fantastico' bergamot, 'Tarocco Sciré' sweet orange, 'Femminello Siracusano 2Kr' lemon), and one ('Tardivo di Ciaculli' mandarin) differed by three categories. Where discrepancies in susceptibility classification were observed between the two inoculation methods, susceptibility was generally greater in the *in planta* assays than in the detached twig assay. The only exception was 'Tardivo di Ciaculli' mandarin, which was classified as very high susceptibility in the detached twig assays but as low susceptible in the *in planta* assay.

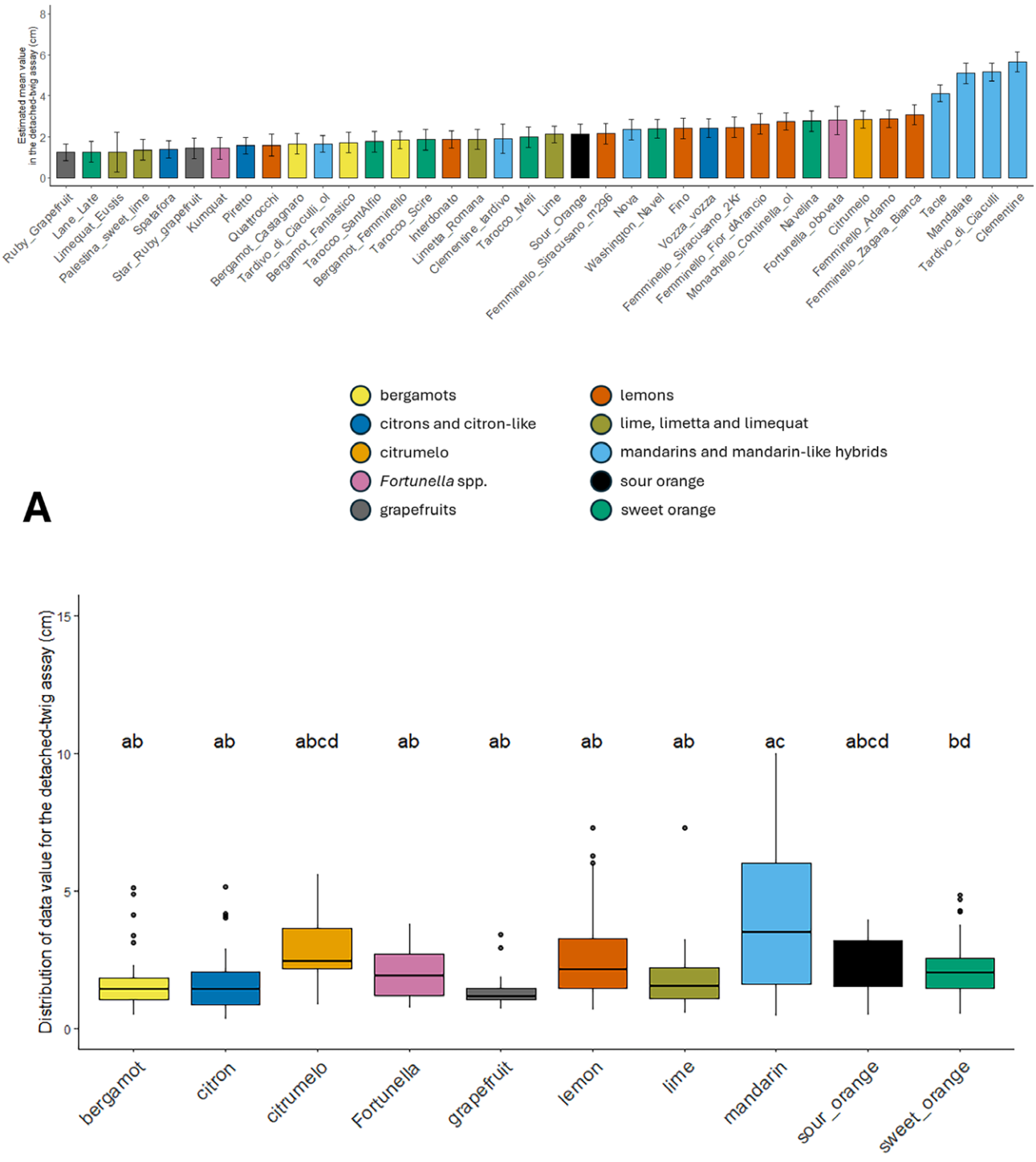

Figure 3. Barplots (A) and boxplots (B) showing results obtained in the citrus genotypes analyzed through the detached twig assay for susceptibility to *Neofusicoccum parvum*. In the boxplots (B), different letters accompanying the means indicate statistically significant differences ($P < 0.001$), according to *post hoc* Tukey HSD tests.

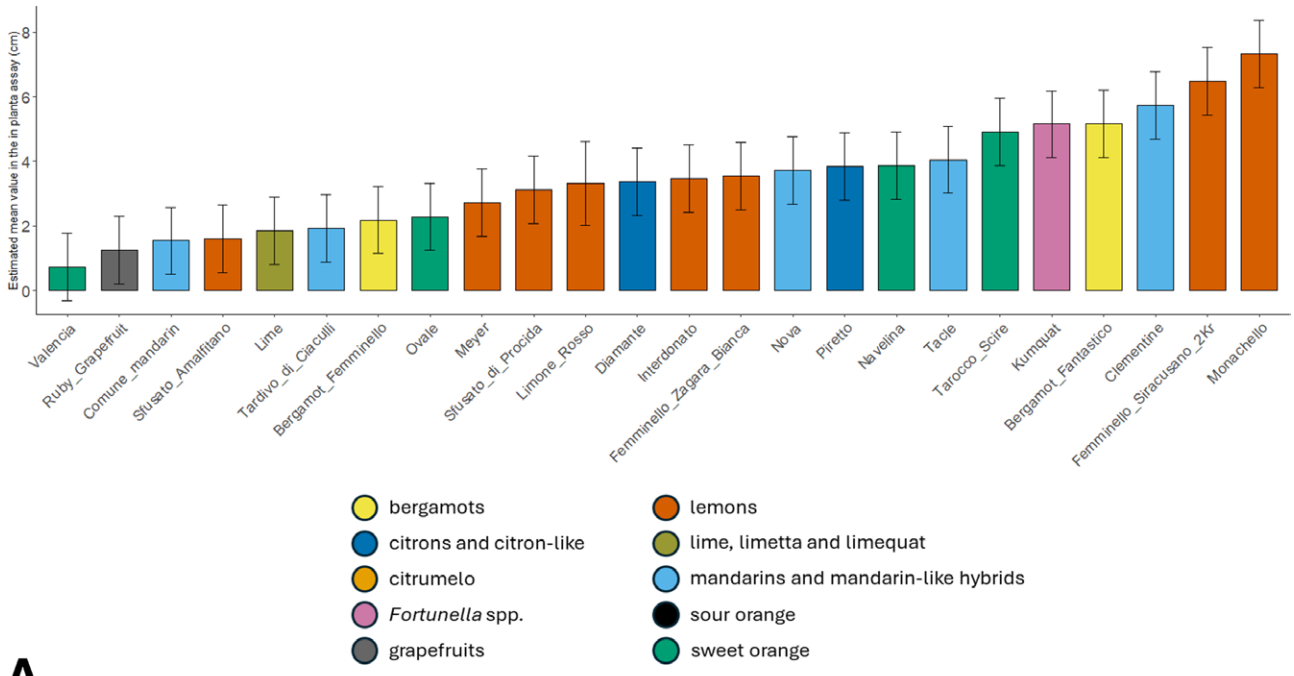

A

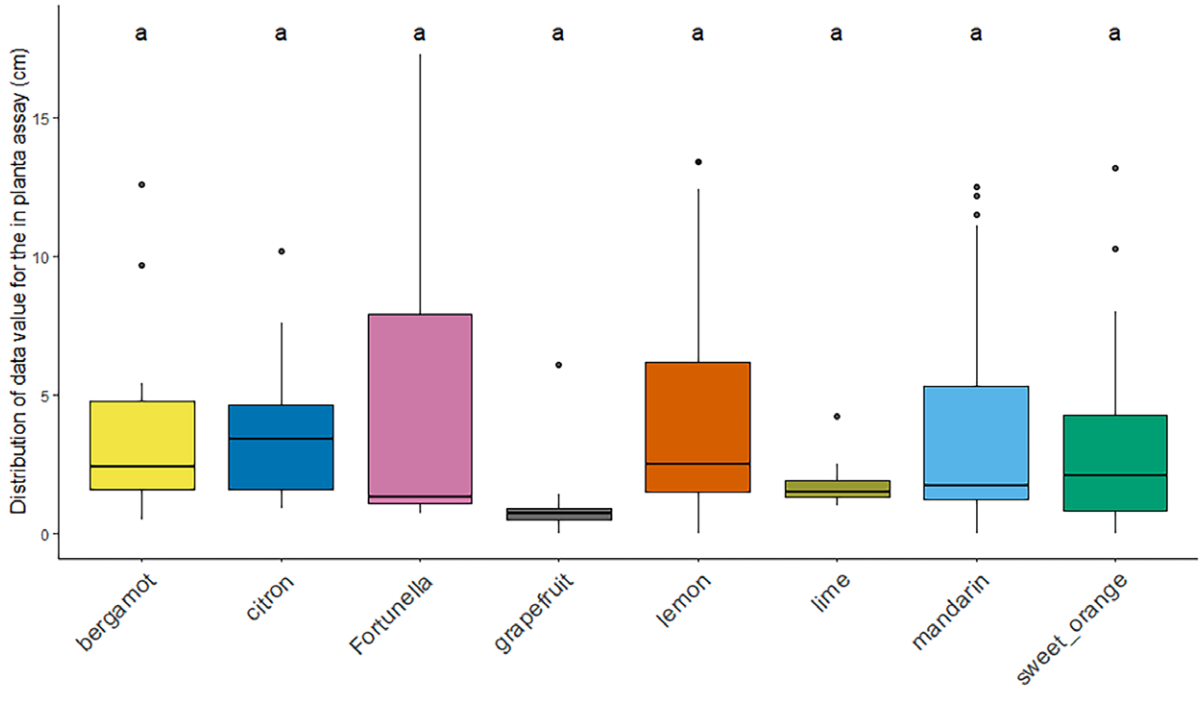

B

Figure 4. Bar plots (A) and boxplots (B) showing results obtained for *Citrus* genotypes analyzed using the *in planta* assays for susceptibility towards *Neofusicoccum parvum*. In the boxplots (B), different letters accompanying the means indicate statistically significant differences ($P < 0.001$), according to *post hoc* Tukey's HSD tests.

Table 2. Confusion matrix showing agreement between susceptibility class assignments obtained from detached twig assays and the *in planta* assay. Susceptibility classes are: low susceptible (LS), mild susceptible (MS), high susceptible (HS), and very high susceptible (VHS).

		Categorization in the *in planta* assay			
		LS	MS	HS	VHS
Categorization in the detached twig assays	LS	3	2	3	0
	MS	0	3	0	1
	HS	0	1	0	0
	VHS	1	0	0	1
Colour legend		same categorization	1 class difference in categorization	2 classes difference in categorization	3 classes difference in categorization

DISCUSSION

Previous field and laboratory studies conducted in Italy have elucidated the etiology of traditionally named "Dothiorella gummosis" of citrus plants, showing that more than one fungus is causes canker and canker-related symptoms in different *Citrus* species in Italy (Gusella *et al*., 2025). Symptoms of canker and gummoses along trunks and at branch insertion sites were attributed to *Diplodia natalensis* and *Dothiorella gregaria* (Eckert and Brown 2000; Klotz 1978; Savastano 1932). Among the fungi involved in these diseases, *N. parvum* has been the most common pathogen in all previously surveyed areas, showing also the greatest aggressiveness in pathogenicity tests (Gusella *et al*., 2025).

The present study is the first overview, using the experimental conditions described, of susceptibility of different citrus species to the *N. parvum* infections. Only sporadic and outdated observations have been reported in Italy (Aloi *et al*., 2021; Savastano 1932; Grasso and Polizzi, 1988). The present study is the first to assess *N. parvum* susceptibility of a large germplasm collection that includes many economically important species of economic interest, for their importance for fruit production and/or as ornamental plants or rootstocks. The citrus market is characterized by diverse products, geographical dynamism, and is important to the economies of many countries (Zhong and Nicolosi, 2020).

Investigations conducted on trunk and shoot canker and gummoses have mainly focused on disease etiology, but many fungi (*Botryosphaeriaceae*, *Diaporthaceae* and *Diatrypaceae*) have been isolated from symptomatic *Citrus* species and assessed for the pathogenicity (Adesemoye *et al*., 2014; Mayorquin *et al*., 2016; Vakaloumakis *et al*., 2019; Bezerra *et al*., 2021; Kayim *et al*., 2024; Gusella *et al*., 2025). Only no or limited data were available on susceptibility of different *Citrus* species. Susceptibility comparisons among different hosts have not been the immediate goal of etiology studies, which have concentrated on ascertaining the roles of the potential etiological agents isolated from samples. In the present study, the predominant role of *N. parvum* was determined in the etiology and distribution of disease (Gusella *et al*., 2025). The responses of broad and varying germplasm collection to this pathogen were evaluated.

Results from these experiments confirmed host/pathogen compatibility, and identified mandarins and mandarin-like species, and lemons, as the most susceptible to *N. parvum* under the experimental conditions used. Detached twig inoculation is a widely used technique, especially for preliminary pathogenicity tests or other similar experiments (León *et al*., 2020; Beluzán *et al*., 2022; Luo *et al*., 2022). This technique is simpler to set up than *in planta* inoculations, so was adopted for preliminary screening of large numbers of host genotypes. Only some representative host genotypes were selected for the *in planta* assay. Although the detached twig assay gave positive assay results, as also previously confirmed for almond inoculated with *Diaporthe amygdali* (Catalano *et al*., 2025), results from the *in planta* assay suggest that the detached twig inoculations need to be confirmed by *in planta* inoculations. The detached twig assays were reliable and rapid, as a starting point for large host phenotype screening, but should not be considered the only method for host screening.

Experiments conducted on walnut blight showed requirement for field testing in conjunction with detached leaf assays (Jiang *et al*., 2019). In contrast, for almond, tolerance levels assessed by detached twig and *in planta* assays were consistent (Catalano *et al*., 2025). In the present study with *Citrus* hosts, discrepancies between the two inoculation methods were detected. Seven genotypes were classified in the same susceptibility categories by the two inoculation methods, including 'Ruby' grapefruit, 'Femminello' bergamot, lime, 'Nova' mandarin, 'Navelina' sweet orange, 'Femminello Zagara Bianca' lemon and Clementine mandarin, while three genotypes were classified with one class difference (citron-like 'Piretto',

'Interdonato' lemon and 'Tacle' mandarin), four differed by two classes (kumquat, 'Fantastico' bergamot, 'Tarocco Sciré' sweet orange, 'Femminello Siracusano 2Kr' lemon), and one ('Tardivo di Ciaculli' mandarin) differed by three classes. Where these discrepancies occurred, susceptibility was generally greater in the *in planta* assay than in the detached twig assays, with the only exception being 'Tardivo di Ciaculli' mandarin, which was classified as very-high susceptible in the detached twig assay but as low susceptible in the *in planta* assay.

These discrepancies in assignment to different susceptibility classes emerged from the Cohen's Kappa coefficient calculations and the confusion matrix between the two inoculation methods, were probably a result of the small sample size that amplified differences between the class categorizations (Sim and Wright, 2005). The susceptibility classes were calculated independently for each assay, which may have further contributed to these differences. Plant susceptibility tests are generally considered more reliable when performed *in planta*, as detached assays, or assays conducted on excised plant tissues, may lead to overestimation of host plant susceptibility (Orlowska *et al*., 2013). This was not the case in the present study, where susceptibility was consistently greatest for particular host genotypes when inoculated *in planta*, highlighting high aggressiveness of *N. parvum*.

The aim of the present study was to evaluate responses of the different *Citrus* germplasms to *N. parvum*, and both the methodologies used showed that all the tested plant lines were susceptible to infection by this fungus, but with differences in susceptibility. While *in planta* inoculations provide accurate assessment of susceptibility, the detached twig method enabled evaluation of many genotypes, so was suitable for preliminary large-scale phenotyping that could be used for crop breeding. The fair agreement between the two inoculation methods (Cohen's Kappa coefficient = 0.26) further supports the suitability of the detached twig assay for this application. The importance of *in planta* inoculation is also highlighted by the appearance of symptoms that were not observed in the detached twig assays, due to specific technical time within the protocol. Typical shoot blight, gum exudation and pathogen pycnidium formation were observed from the *in planta* inoculations.

Symptomatology of some non-lemon citrus species observed after artificial inoculations, compared to field surveys, could be due to several factors. Disease development in the field is unpredictable due to variable inoculum pressure in different groves, and the different environmental/agronomic conditions within each grove (Ben-Hamo *et al*., 2020; Veresoglou *et al*., 2013). Different host susceptibility responses have been observed elsewhere between controlled and field conditions (Jiang *et al*., 2019). Grapefruit was the least susceptible to *N. parvum* in both of the present study assays. Field observations (Gusella *et al*., 2025) showed that grapefruit is highly susceptible to another *Botryosphaeriaceae* species, *Neoscytalidium dimidiatum*, as also observed in California (Dr. Themis Michailides, personal communication). These observations highlight the difficulties for disease management, especially when etiologies are complex. Results from the present study confirm that all citrus are potentially susceptible to the canker-causing pathogen *N. parvum*, but, until now, the disease seems to be particularly evident and aggressive on lemon species in the region of this research. However, the polyphagous behaviour of this pathogen, its wide distribution, the susceptibility of different *Citrus* species, and the intercropping of citrus in the local territory, as well as in many Mediterranean environments, emphasize the risks from potential inter-species infections.

CONCLUSIONS

This study has provided the first assessment, using the described experimental conditions, of susceptibility of a broad group of *Citrus* genotypes to the important pathogen *N. parvum*. Although only one isolate of this fungus was used, the results provide insights into the responses of host germplasm to *N. parvum* infection. Nevertheless, a broader picture of susceptibility could be obtained by testing multiple fungal isolates, since populations of a fungal species consist of numerous isolates that may differ in their levels of virulence. Our research also establishes practical criteria for reliable phenotyping, forming a solid basis for future screening efforts aimed at citrus genetic improvement. While the detached twig assay represents a valuable tool preliminary for large-scale phenotyping, *in planta* assay confirmed to provide a more accurate assessment of susceptibility. Our results showed that all tested genotypes are susceptible under artificial inoculation, revealing mandarins and mandarin-like species, as well as lemons, as the most susceptible. The variability in susceptibility observed suggests the possible presence of tolerance sources, which merits further investigation to elucidate the genetic determinants underlying citrus tolerance towards *N. parvum*.

FUNDING

This research was funded by: Agritech National Research Center (European Union Next-Generation EU,

PIANO NAZIONALE DI RIPRESA E RESILIENZA, PNRR – MISSIONE 4 COMPONENTE 2, INVESTIMENTO 1.4—D.D. 1032 17/06/2022, CN00000022, CUP: E63C22000960006) Spoke 2; Piano di incentivi per la ricerca di Ateneo DIME-SIECO 2024-2026, University of Catania (Italy).

LITERATURE CITED

Adesemoye A. O., Mayorquin J. S., Wang D. H., Twizeyimana M., Lynch S. C. & Eskalen A. 2014. Identification of species of *Botryosphaeriaceae* causing Bot Gummosis in Citrus in California. *Plant Disease* 98: 55–61. https://doi.org/10.1094/PDIS-05-13-0492-RE

Aloi F., Riolo M., Parlascino R., Pane A. & Cacciola S. O. 2021. Bot Gummosis of Lemon (Citrus × limon) caused by *Neofusicoccum parvum*. *Journal of Fungi* 7: 294 https://doi.org/10.3390/jof7040294

Beluzán F., Miarnau X., Torguet L., Zazurca L., Abad-Campos P... Armengol, J. 2022. Susceptibility of almond (*Prunus dulcis*) cultivars to twig canker and shoot blight caused by *Diaporthe amygdali*. *Plant Disease* 106(7): 1890–1897. https://doi.org/10.1094/PDIS-09-21-1875-RE

Ben-Hamo M., Ezra D., Krasnov H., & Blank L. 2020. Spatial and temporal dynamics of Mal Secco disease spread in lemon orchards in Israel. *Phytopathology* 110(4): 863–872. https://doi.org/10.1094/PHYTO-06-19-0195-R

Beshara S., Kassem A., Fors H. & Harraz N. 2024. A comprehensive review and mapping Citrus supply chains from a sustainability perspective across the European Union, Middle East, and Africa. *Sustainability* 16(19): 8582. https://doi.org/10.3390/su16198582

Bezerra J. D. P., Crous P. W., Aiello D., Gullino M. L., Polizzi G. & Guarnaccia V. 2021. Genetic diversity and pathogenicity of *Botryosphaeriaceae* species associated with symptomatic citrus plants in Europe. *Plants* 10: 492. https://doi.org/10.3390/plants10030492

Catalano C., Di Guardo M., Distefano G., Caruso M., Nicolosi E... La Malfa, S. G. 2021. Biotechnological approaches for genetic improvement of lemon (*Citrus limon* (L.) Burm. f.) against Mal Secco disease. *Plants* 10: 1002 https://doi.org/10.3390/plants10051002

Catalano C., Gusella G., Inzirillo I., Cannizzaro G., Di Guardo M... Distefano G. 2025. Exploring additive and non-additive genetic models to decipher the genetic regulation of almond tolerance to *Diaporthe amygdali*. *Frontiers in Plant Science* 16: 1608958. https://doi.org/10.3389/fpls.2025.1608958

Ciriminna R., Angellotti G., Luque R. & Pagliaro M. 2024. The Citrus Economy in Sicily in the early bioeconomy era: A case study for bioeconomy practitioners. *Biofuels, Bioproducts and Biorefining* 18(2): 356–364. https://doi.org/10.1002/bbb.2588

Eckert J.W. and Brown G.E. 2000. Dothiorella rot. In: *Compendium of citrus diseases* (No. Ed. 2. Timmer L. W., Garnsey S. M., Graham J. H. ed.), St. Paul, Minnesota, USA, 40.

FAOSTAT. 2025. Food and Agriculture Organization of the United Nations. Accessed on 24 January 2025 from https://www.fao.org/faostat/

Grasso S., and Polizzi G. 1988. Cryptogamic diseases of bergamot in Calabria (Italy). In: *Citriculture. Proceedings of the Sixth International Citrus Congress*, 6–11 March, 1988, Middle-East, Tel Aviv, Israel, 2: 833–837.

Gusella G., Leonardi G. R., La Quatra G., Aiello D., Voglmayr H. & Polizzi G. 2025. Re-evaluating the etiology of citrus "*Dothiorella gummosis*" in Italy. *Plant Disease* 10: 1379–1395 https://doi.org/10.1094/PDIS-02-25-0441-RE

Jiang S., Han S., He D., Cao G., Zhang F. & Wan, X. 2019. Evaluating walnut (*Juglans* spp.) for resistance to walnut blight and comparisons between artificial inoculation assays and field studies. *Australasian Plant Pathology* 48(3): 221–231. https://doi.org/10.1007/s13313-019-0621-0

Kayim M., Endes A., Alsalmo A., Yasmin S. & Nawaz H. 2024. Preliminary evaluation of citrus rootstocks and scions to four different bot canker pathogens. *Acta Horticulturae* 1399: 403–410. https://doi.org/10.17660/ActaHortic.2024.1399.50

Klotz L. J. 1978. Fungal, bacterial and non-parasitic diseases and injuries originating in the seedbed, nursery, and orchard. In: *The Citrus Industry* (Reuther W., Calavan E. C., Carman G. E., ed.), University of California Press, Berkeley, 4:1-66.

Kurt Ş., Uysal A., Guarnaccia V., Martino I., Soylu E. M., Soylu S. & Oğuz M. 2025. Molecular identification and pathogenicity of *Botryosphaeriaceae* species associated with citrus wood diseases in the eastern Mediterranean region of Türkiye. *Journal of Plant Pathology* 107(2): 1077–1089. https://doi.org/10.1007/s42161-025-01877-3

Landis J. R. & Koch G. G. 1977. The measurement of observer agreement for categorical data. *Biometrics* 33(1): 159–174. https://doi.org/10.2307/2529310

León M., Berbegal M., Rodriguez-Reina J. M., Elena G., Abad-Campos P... Armengol J. 2020. Identifica-

tion and characterization of *Diaporthe* spp. Associated with twig cankers and shoot blight of almonds in Spain. *Agronomy* 10(8): 1062. https://doi.org/10.3390/agronomy10081062

Leonardi G. R., Polizzi G., Vitale A. & Aiello D. 2023. Efficacy of biological control agents and resistance inducer for control of Mal Secco disease. *Plants* 12(9): 1735. https://doi.org/10.3390/plants12091735

Luo Y., Ma R., Barrera E., Gusella G. & Michailides T. J. 2022. Effects of temperature on development of canker-causing pathogens in almond and prune. *Plant Disease* 106(9): 2424–2432. https://doi.org/10.1094/PDIS-01-22-0048-RE

Mayorquin J. S., Wang D. H., Twizeyimana M. & Eskalen A. 2016. Identification, Distribution, and Pathogenicity of *Diatrypaceae* and *Botryosphaeriaceae* associated with citrus branch canker in the Southern California Desert. *Plant Disease* 100: 2402–2413. https://doi.org/10.1094/PDIS-03-16-0362-RE

Moral J., Morgan D., Trapero A., & Michailides T. J. 2019. Ecology and epidemiology of diseases of nut crops and olives caused by *Botryosphaeriaceae* fungi in California and Spain. *Plant Disease* 103: 1809–1827. https://doi.org/10.1094/PDIS-03-19-0622-FE

Orłowska E., Llorente B., & Cvitanich C. 2013. Plant integrity: An important factor in plant-pathogen interactions. *Plant Signaling & Behavior* 8(1): e22513. https://doi.org/10.4161/psb.22513

Pereira Gonzatto M. & Scherer Santos J. 2023. Introductory Chapter: World Citrus Production and Research. In *Citrus Research - Horticultural and Human Health Aspects. IntechOpen*. https://doi.org/10.5772/intechopen.110519

R Core Team. 2021. In R: A language and environment for statistical computing. R Foundation for Statistical Computing, Vienna, Austria. URL: http://www.R-project.org

Savastano G. 1932. A gummosis of lemon caused by Dothiorella. *Bollettino della Regia Stazione di Patologia Vegetale. Nuova Serie* 12:245-274.

Scaramuzzi G. 1965. *Le malattie degli agrumi*. Edizioni Agricole, Bologna, Italy, 167 pp.

Schneider C. A., Rasband W. S. & Eliceiri K. W. 2012. NIH Image to ImageJ: 25 years of image analysis. *Nature Methods* 9: 671–675. https://doi.org/10.1038/nmeth.2089

Sim J. & Wright C. C. 2005. The kappa statistic in reliability studies: use, interprestation, and sample size requirements. *Physical therapy* 85(3): 257–268. https://doi.org/10.1093/ptj/85.3.257

Sun Y., Yokomi R. K. & Folimonova S. Y. 2024. Citrus Tristeza Virus: A century-long challenge for the world's citrus industries. *Annals of Applied Biology* 185(3): 304–322. https://doi.org/10.1111/aab.12939

Vakalounakis D. J., Ntougias S., Kavroulakis N. & Protopapadakis E. 2019. *Neofusicoccum parvum* and *Diaporthe foeniculina* associated with twig and shoot blight and branch canker of citrus in Greece. *Journal of Phytopathology* 167(9): 527–537. https://doi.org/527-537. 10.1111/jph.12843

Veresoglou S. D., Barto E. K., Menexes G., & Rillig M. C. 2013. Fertilization affects severity of disease caused by fungal plant pathogens. *Plant Pathology* 62(5): 961–969. https://doi.org/10.1111/ppa.12014

Wickham H. 2016. ggplot2: *Elegant Graphics for Data Analysis* (2nd edition). Springer, Cham, Switzerland, 260 pp. https://doi.org/10.1007/978-3-319-24277-4

Xiao X. E., Wang W., Crous P. W., Wang H. K., Jiao C... Li H. Y. 2021. Species of *Botryosphaeriaceae* associated with citrus branch diseases in China. *Persoonia-Molecular Phylogeny and Evolution of Fungi* 47(1): 106–135. https://doi.org/10.3767/persoonia.2021.47.03

Zhong G. & Nicolosi E. 2020. Citrus origin, diffusion, and economic importance. In: *The Citrus Genome. Compendium of Plant Genomes* (Gentile A., La Malfa S., Deng Z. ed.), Springer International Publishing, Cham, Switzerland, 5–21. https://doi.org/10.1007/978-3-030-15308-3_2

Phytopathologia Mediterranea
The international journal of the
Mediterranean Phytopathological Union

Firenze University Press
www.fupress.com/pm

New or Unusual Disease Reports

Powdery mildew infection of neem in the Dominican Republic; another tropical host of *Erysiphe necator*

Miloslav KITNER[1,*], Tereza KŘIVÁNKOVÁ[1], Agáta ČURNÁ[1], Barbora MIESLEROVÁ[1], Vladan ONDŘEJ[1], David HERNANDEZ-MARTICH[2], Josef B. ŠENKYŘÍK[1], Uwe BRAUN[3], Aleš LEBEDA[1]

[1] *Department of Botany, Faculty of Sciences, Palacký University Olomouc, Šlechtitelů 27, 779 00 Olomouc, Czech Republic*
[2] *Universidad Autónoma de Santo Domingo, Av. Alma Mater 200 - Santo Domingo, DN 10105, Dominican Republic*
[3] *Martin Luther University, Institute of Biology, Department of Geobotany and Botanical Garden, Herbarium, Kirchtor 3, 06099 Halle (Saale), Germany*
*Corresponding author. E-mail: miloslav.kitner@upol.cz

Summary. This study identified the causative agent of powdery mildew on *Azadirachta indica* (*Sapindales, Meliaceae*) in the Dominican Republic, using molecular phylogenetic analysis of internal transcribed spacer (ITS) and large subunit (LSU) sequences of rDNA, and morphological examinations. The infection was caused by *Erysiphe necator*, a pathogen primarily associated with *Vitis* spp. Together with other recent reports of *E. necator* on different host plants in Brazil, the host range of this pathogen has been expanded in tropical regions of Central America and the Caribbean region.

Keywords. Erysiphales, *Azadirachta indica*, host range expansion, phylogenetic analysis.

OPEN ACCESS

Citation: Kitner, M., Křivánková, T., Čurná, A., Mieslerová, B., Ondřej, V., Hernandez-Martich, D., Šenkyřík, J. B., Braun, U. & Lebeda, A. (2026). Powdery mildew infection of neem in the Dominican Republic; another tropical host of *Erysiphe necator*. *Phytopathologia Mediterranea* 65(2): 255-266. doi: 10.36253/phyto-17075

Accepted: July 10, 2026

Published: July 27, 2026

©2026 Author(s). This is an open access, peer-reviewed article published by Firenze University Press (https://www.fupress.com) and distributed, except where otherwise noted, under the terms of the CC BY 4.0 License for content and CC0 1.0 Universal for metadata.

Data Availability Statement: All relevant data are within the paper and its Supporting Information files.

Competing Interests: The Author(s) declare(s) no conflict of interest.

Editor: Tito Caffi, Università Cattolica del Sacro Cuore, Piacenza, Italy.

ORCID:
MK: 0000-0002-3762-8067
TK: 0009-0001-8367-5569
AČ: 0009-0004-5134-0707
BM: 0000-0002-7975-5443
VO: 0000-0001-9033-5792
DHM: 0000-0002-7100-6173
JBŠ: 0000-0001-9219-5762
UB: 0000-0002-2205-9180
AL: 0000-0003-3601-583X

INTRODUCTION

Azadirachta indica A. Juss., (*Meliaceae*), commonly known as neem, margosa, nimtree, or Indian lilac, is an evergreen tree, whose native range is Assam to Indo-China, but is naturalized and grown in tropical and subtropical regions, including the Dominican Republic (POWO, 2025). Neem is valued for its ecological resilience, and for its medicinal and pesticidal properties, including antibacterial, antiviral, antifungal, anti-inflammatory, and antioxidant effects. In medicine, neem is used to treat illnesses including eye disorders, nose bleeding, loss of appetite, and liver problems. Because of its various pharmacological and therapeutic effects, neem is included in the Ayurvedic pharmacopoeia and cosmetic industry (Gupta *et al.*, 2017; Gautam and Mittal, 2021). Active substances in neem, including azadirachtin,

nimbin, nimbidin, and gedunin, have strong biological effects on range of pathogens and insect pests, making extracts from this plant important natural pesticides in sustainable agriculture (Koul *et al*., 1990; Bailey *et al*., 2010). In recent decades, interest in neem has increased in Asia, Europe, and North America, where its potential as an ecological alternative to synthetic chemicals in medicine and plant protection is being explored (Singh *et al*., 2010; Tufail *et al*., 2025).

Powdery mildews (Erysiphaceae) are an internationally widespread group of biotrophic plant pathogens with approx. 10,000 known Angiosperm host species (Braun and Cook, 2012). Powdery mildews are typically associated with their hosts, with which they are co-evolutionarily related, and they differ in the level of specificity. Species can be distinguished by their narrow host ranges – one host genus or species (monophagous), or species with host ranges covering entire plant families (oligophagous), as well as species with host ranges including numerous plant families (polyphagous) (Lebeda *et al*., 2017).

Braun and Cook (2012) showed that *Erysiphe necator* (previously *Uncinula necator*) has a narrow host range, including only some Vitaceae. These authors distinguished two varieties: var. *necator* with a host range including various species Vitaceae, mainly *Vitis* and *Cissus*, but also *Ampelopsis glandulosa* var. *heterophylla* with circumglobal distribution; and var. *ampelopsidis* with a host range confined to *Parthenocissus* (*cuspidifera, quinquefolia, tricuspidata, vitacea*, Vitaceae) occurring in North America (Canada, United States of America). The second variety differs from var. *necator* in having shorter, stiff chasmothecial appendages, that have appendages that are approx. 2 times (0.75 to 2.5) their chasmothecial diameters. Based on obvious morphological and genetic differences, distinguished using sequence analyses, Bradshaw *et al.* (2023) introduced the new combination *Erysiphe ampelopsidis*, as a species separate from *E. necator.*

Later studies confirmed occurrence of *E. necator* also on *Cissus rhombifolia* (Cho *et al*., 2012), *Caryocar brasiliense* (Caryocaraceae), and *Carica papaya* (Caricaceae) (Braun *et al*., 2017; Seress *et al.,* 2021); cashew (*Anacardium occidentale*) (Fonseca *et al*., 2019); and rubber tree (*Hevea brasiliensis*) (Pieroni *et al*., 2020). These infections have been seen mainly in Brazil, but also in Hawaii, and indicate adaptation of *E. necator* to new hosts. This supports the assumption of Braun *et al.* (2017), that the important and widespread grapevine powdery mildew can cause infections on unrelated hosts, and raises epidemiological questions.

Powdery mildew infecting *Azadirachta indica* was mentioned by Braun and Cook (2012) as *Pseudoidium azadirachtae*. This species was recorded in Africa (Niger) and Asia (India, Pakistan). Recently, Jayalakshmi *et al.* (2024) confirmed the occurrence of *Ps. azadirachtae* on *A. indica* in Pune, Maharashtra (India). In their study, however, only microscopical observation of the anamorph stage was reported. These authors also mentioned previous records of powdery mildew on neem in Bangladesh (Mridha *et al*., 2005), and in Tamil Nadu (India) (Narayanaswamy and Ramakrishnan, 1969). However, the specific identities of the powdery mildews involved cannot be verified in these cases, due to lack of sequence data.

Problems with identifying powdery mildew anamorphs on *Azadirachta* are further exacerbated by apparent occurrences of several species. Wagh *et al.* (2024) confirmed the identity of an Indian specimen as *Erysiphe aquilegiae* (*s. lat.*), using sequencing. However, the conidium length of 35 to 48 µm in the Indian collection (Wagh *et al*., 2024), did not agree with the description given for *Ps. azadirachtae* by Braun and Cook (2012), that is, conidia (22–)25–34.5 µm long. As with other groups of organisms, molecular biology methods have influenced methodological approaches in fungus identification, and in phylogenetic analyses of relationships between taxa. Standardized genomic DNA regions are available for molecular identifications of fungi. Sequence determination of the internal transcribed spacer (ITS) region of nuclear ribosomal DNA (nrDNA) has proven to be the most useful for identification of powdery mildews at the species level (e.g. Braun *et al*., 2002; 2019; Kelly *et al*., 2025; Yeh *et al*., 2025), while sequences of the 18S and 28S nrDNA regions have supported identifications and classification of genera (Marmolejo *et al*., 2018; Křivánková *et al*., 2025). Although other DNA regions have also been tested as molecular barcodes (Inuma *et al*., 2007; Pirondi *et al*., 2016; Ellingham *et al*., 2019; Qiu *et al*., 2020), the use of ITS sequences is still considered to be the standard for species-level DNA barcoding available for this fungal group (e.g., Kiss *et al*., 2020; Kelly *et al*., 2025), although ITS does not provide sufficient resolution at species level for some complexes of closely related powdery mildew species. For these, sequencing of additional loci is necessary, as in the case of the *Erysiphe alphitoides* complex (Bradshaw *et al*., 2025a), and for North America oak powdery mildews (Bradshaw *et al*., 2025b).

The aim of the present study was to carry out a precise morphological and molecular study of neem powdery mildew found in the Dominican Republic, and to increase knowledge of the host range of *E. necator* in tropical regions.

MATERIAL AND METHODS

Plant material and sampling

Leaves of *Azadirachta indica* (*Meliaceae*) exhibiting typical powdery mildew symptoms were collected on March 20, 2024, at the Dr. Rafael Ma. Moscoso National Botanical Garden, Santo Domingo, Dominican Republic (18°29.8512′ N, 69°57.3432′ W; 86 m a.s.l.; collector, Kitner, sample ID M17). A voucher specimen was deposited in the OL herbarium (Department of Botany, Palacký University, Olomouc, Czech Republic).

Microscopy and morphology

Leaf fragments (approx. 20 × 20 mm) were processed following the modified method of Shin (2000). Infected tissues were stained with lacto-fuchsin solution to visualize fungal structures, and presence of fibrosin bodies was checked using 3% KOH (Lebeda, 1983). Microscope examinations were carried out using an Olympus BX60 light microscope at 400× magnification. Only asexual morphs were developed on the leaf fragments.

Morphological traits included conidium length, width, and shape index, conidiophore length, foot cell length, number of distal cells, presence or absence of fibrosin bodies, and conidium germination pattern. Thirty conidia and 20 conidiophores were measured per sample (due to limited availability). Digital micrographs were captured using an Olympus BX60 light microscope equipped with an Olympus DP72 CCD digital camera, and measurements were carried out manually using an ocular micrometer.

Statistical analysis

Descriptive statistics (mean, standard deviation, range) were calculated for each trait using MS Excel 2010. To assess morphological similarity, the obtained values were compared with previously published data (Braun and Cook, 2012) for *Erysiphe necator* on other hosts.

Molecular identification

For molecular identification of the pathogen, the complete ITS and partial 28S regions (D1 and D2 domains) of rDNA were sequenced. For amplification of the ITS region, the powdery mildew-specific PMITS1/PMITS2 primers were used (first PCR; Cunnington *et al*., 2003), and ITS1-F/ITS4 primers (second PCR; Gardes and Bruns, 1993; White *et al*., 1990). Amplification of D1/D2 domains of the 28S rDNA was carried out according to Takamatsu *et al*. (2013), using primer sets PM3/TW14 and NL1/TW14 for the two nested PCR runs. The description of the preparation of PCR mixes and PCR conditions for both loci is described in detail elsewhere (Lebeda *et al*., 2019).

The PCR products were visualized on agarose gel, purified using an enzymatic purification protocol (Kim and Blackshaw, 2001), and were bidirectionally sequenced by Macrogen Europe (Amsterdam), and assembled in Geneious 7.1.7 (Kearse *et al*., 2012). The resulting sequences were deposited in the NCBI nucleotide database (https://www.ncbi.nlm.nih.gov/) under accession numbers PX397430 and PX397429, and their taxonomic identity was verified by BLASTn against GenBank.

For phylogenetic reconstruction, sequences from both sequenced regions of the M17 sample were concatenated. Furthermore, *Erysiphe* sequences containing both ITS and 28S regions, with *Golovinomyces bolayi* as outgroup, were downloaded from GenBank (Supplementary Table 1).

Multiple sequence alignment was generated using MAFFT v.7 (Katoh *et al*., 2019), and is provided as Supplementary data 1. Maximum Likelihood (ML) phylogenetic trees were reconstructed with RAxML (Stamatakis, 2014). The optimum substitution model was automatically selected by ModelFinder (Kalyaanamoorthy *et al*., 2017), implemented in IQ-TREE (Nguyen *et al*., 2015; Trifinopoulos *et al*., 2016) under the Bayesian Information Criterion (BIC). Branch support values were estimated using the ultrafast bootstrap approximation (Hoang *et al*., 2018), with 1000 replicates. For graphical presentation of the phylogenetic analyses, Bayesian Analysis (BA) was carried out in MrBayes 3.2.6 (Huelsenbeck and Ronquist, 2001; Ronquist and Huelsenbeck, 2003), implemented in Geneious 7.1.7. BA, and was performed under the General Time Reversible model, run for 3 M generations, sampled every 1000th generation, and 3000 trees were discarded as burn-in. All other settings were set as the default. The resulting phylogenetic tree was graphically adjusted in MS Word, where posterior probabilities (≥ 0.7) and bootstrap support values (≥ 70 %) were displayed on the main nodes.

RESULTS

Morphological characteristics

Microscope examination of the powdery mildew on the *Azadirachta indica* specimen (isolate M17) revealed hyaline, superficial mycelium with typical *Erysiphe*-like asexual structures. Conidiophores of the *Pseudoidium* type had mean length 68.5 ± 10.0 µm (range 46.4 to 80.5

Table 1. Comparative morphological characteristics of *Erysiphe necator* and *Pseudoidium azadirachtae* reported from *Azadirachta indica*, including comparison of parameters obtained in the present study (*E. necator* M17) with data from Braun and Cook (2012).

Parameter	*E. necator* M17	*E. necator*	*P. azadirachtae*
Conidiophore length (µm)	68.5 ± 10.0 (46.4–80.5)	40.0–400.0	50.0–75.0
Foot-cell length (µm)	32.2 ± 2.9 (29.3–36.6)	25.0–160.0	35.0–55.0 × 7.5–11.0
Distal cells per conidiophore	1.9 ± 0.7 (1–3)	–	1(–2)
Conidial length (µm)	28.5 ± 2.8 (24.4–34.2)	22.5–48.0	(22.0–)25.0–34.5
Conidial width (µm)	12.5 ± 1.2 (9.8–17.1)	12.2	11.0–19.0
Conidial shape index (L/W)	2.29 ± 0.31	2.29	–
Host range and distribution		cosmopolitan, mainly *Vitis* spp. (also *Carica*, *Caryocar*)	*A. indica* only; Africa (Niger), Asia (India, Pakistan)

µm), and had foot cells averaging 32.2 ± 2.9 µm (range 29.3–36.6 µm). The number of distal cells per conidiophore averaged 1.9 ± 0.7 (range 1 to 3). Conidia were cylindrical-ovoid, 28.5 ± 2.8 µm long (range 24.4 to 34.2 µm) and 12.5 ± 1.2 µm wide (range 9.8 to 17.1 µm), yielding a mean length-to-width ratio (shape index) of 2.29 ± 0.31 (Table 1).

Conidium germination occurred via single germ tubes emerging from conidium ends. Presence of fibrosin bodies was not observed, and no chasmothecia were formed even on heavily infected *A. indica* leaves (Figure 1).

Molecular identification

Sequencing of both genomic regions resulted in identical, high-quality electrophoretograms, allowing reliable molecular identification of the powdery mildew infections on *Azadirachta indica*. The ITS region sequencing results of sample M17 were subjected to BLASTn search against the GenBank nucleotide database, and this showed 100% identity with twenty published ITS powdery mildew records from various hosts and countries (Supplementary Table 2). These are: *Vitis vinifera* (Azerbaijan, Canada, France, Hungary, Israel, Mexico, New Zealand, Pakistan, Taiwan, Thailand, United States of America: Abasova *et al*., 2018; Bradshaw *et al*., 2023; Brewer and Milgroom, 2010; Cooper *et al*., 2015; Gregorio-Cipriano *et al*., 2026; Gul *et al*., 2025; Gur *et al*., 2021; Hsiao *et al*., 2022; Jaswa *et al*., 2026; LaGreca *et al*., 2025; Meeboon and Takamatsu, 2017; Péros *et al*., 2005; Pintye *et al*., 2023; Sholberg *et al*., 2005); *V. coignetiae* (Japan; Takamatsu *et al*., 2015); *V. flexuosa* (South Korea, Park *et al*., 2026); *Caryocar brasiliense* (Brazil; Braun *et al*., 2017); and *Carica papaya* (Hungary; Seress *et al*., 2021). The record from the United States of America by Brewer and Milgroom (2010) on *Vitis vinifera* (acc. no. GQ255473) represents the *E. necator* haplotype, which those authors also identified on *V. aestivalis*, *V. labrusca*, *V. riparia* and *V. rotundifolia*, From the 28S region comparison, greatest similarity (99.88%) was found in three published records of *E. necator* infections on *V. vinifera* in Mexico (Marmolejo *et al*., 2018) and *V. flexuosa* in South Korea (Park *et al*., 2026).

To verify the taxonomic status of the sample analyzed in the present study, its position relative to other representative Erysiphales, a phylogenetic tree was constructed using Genbank records containing ITS and 28S regions. From the list of identical ITS sequences listed above, only the complete acc. nos. LC777882, LC028995 and LC028996 could be used, which were derived from *Vitis vinifera* and *V. coignetiae*. As a result, samples of *E. necator* from *Carica papaya* are not present on the phylogenetic tree, contrary to records of *Carica papaya* infections caused by *E. fallax*. The phylogenetic reconstruction using Bayesian analysis showed a well-resolved tree topology representing main evolutionary lineages of Erysiphaceae (Helotiales, suborder Erysiphineae) (Figure 2).

Sequences of members of *Erysiphe* are divided into six clades. The nucleotide sequence derived from the powdery mildew infection of *Azadirachta indica* from the Dominican Republic is placed in a separate clade, together with *E. necator* sequences from *Vitis vinifera* and *V. coignetiae*. *Erysiphe necator* along with the sister clade *E. ampelopsidis* samples, are the basal clade of *Erysiphe* (Bradshaw *et al*., 2023).

DISCUSSION

Results from the present study provide the first evidence of *E. necator* occurring on *Azadirachta indica* in the Dominican Republic. The morphological characteristics of the powdery mildew isolate (M17) closely matched the diagnostic features of *E. necator* described by Braun and Cook (2012). The conidiophore and foot-cell dimensions of the examined material were near the lower limits of the wide range reported for *E. neca-*

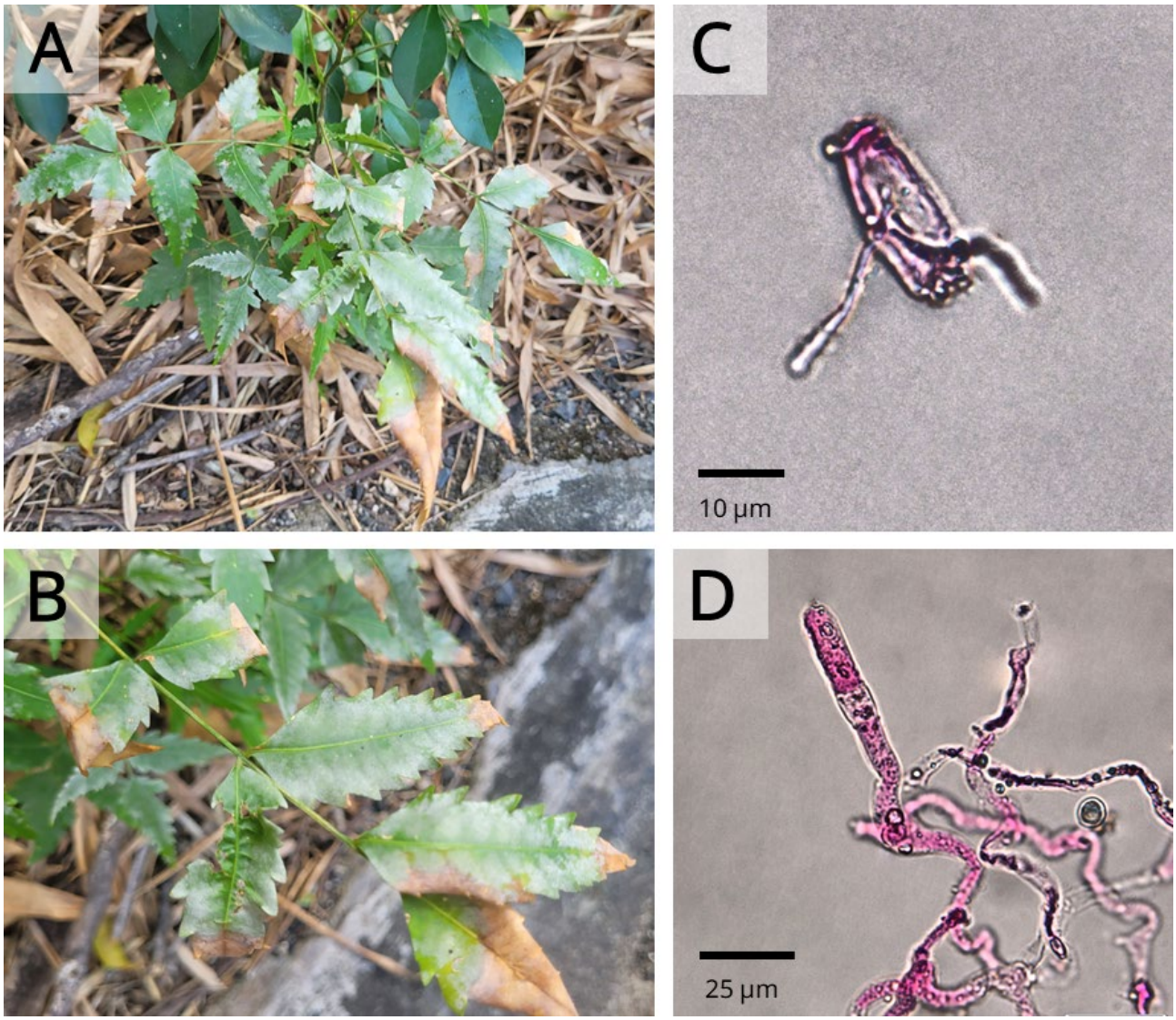

Figure 1. A and B, Symptoms of powdery mildew observed on *Azadirachta indica* in the field. C, Conidium of *Erysiphe necator*. D, Conidiophore of *Erysiphe necator* with twisted foot-cell.

tor, while conidium size and shape index fell within the mean reference values for this fungus. The molecular analyses confirmed that the powdery mildew found on *Azadirachta indica* in the Dominican Republic is *E. necator*. The collection M17 from *A. indica* nested within a strongly supported *E. necator* lineage (1.00 PP / 100 BS) containing sequences from grapevine (*Vitis* spp.).

Previous reports of powdery mildew on *A. indica* have been consistently assigned to *Pseudoidium azadirachtae* as the causative agent of infections (Braun and Cook, 2012; Jayalakshmi *et al*., 2024). A comparative analysis (Table 1) distinguished *E. necator* from *P. azadirachtae*. According to Braun and Cook (2012), *P. azadirachtae* has shorter and narrower conidia, and fewer distal cells per conidiophore, than *A. indica*. Fibrosin bodies do not occur in both species.

It is almost impossible to reliably distinguish individual powdery mildew species within *Erysiphe* anamorphs (*Pseudoidium*) only based on morphological analyses (Cook *et al*.,1997, 2009). Therefore, it is currently not possible to clarify the taxonomic affinity of *P. azadirachtae*. As type material of *Oidium azadirachtae* is not preserved, according to Art. 9.12 (Madrid Code) it would be absolutely necessary to designate the original illustration (Narayanaswamy and Ramakrishnan, 1969: Figure 25) as lectotype, and an Indian specimen morphologically

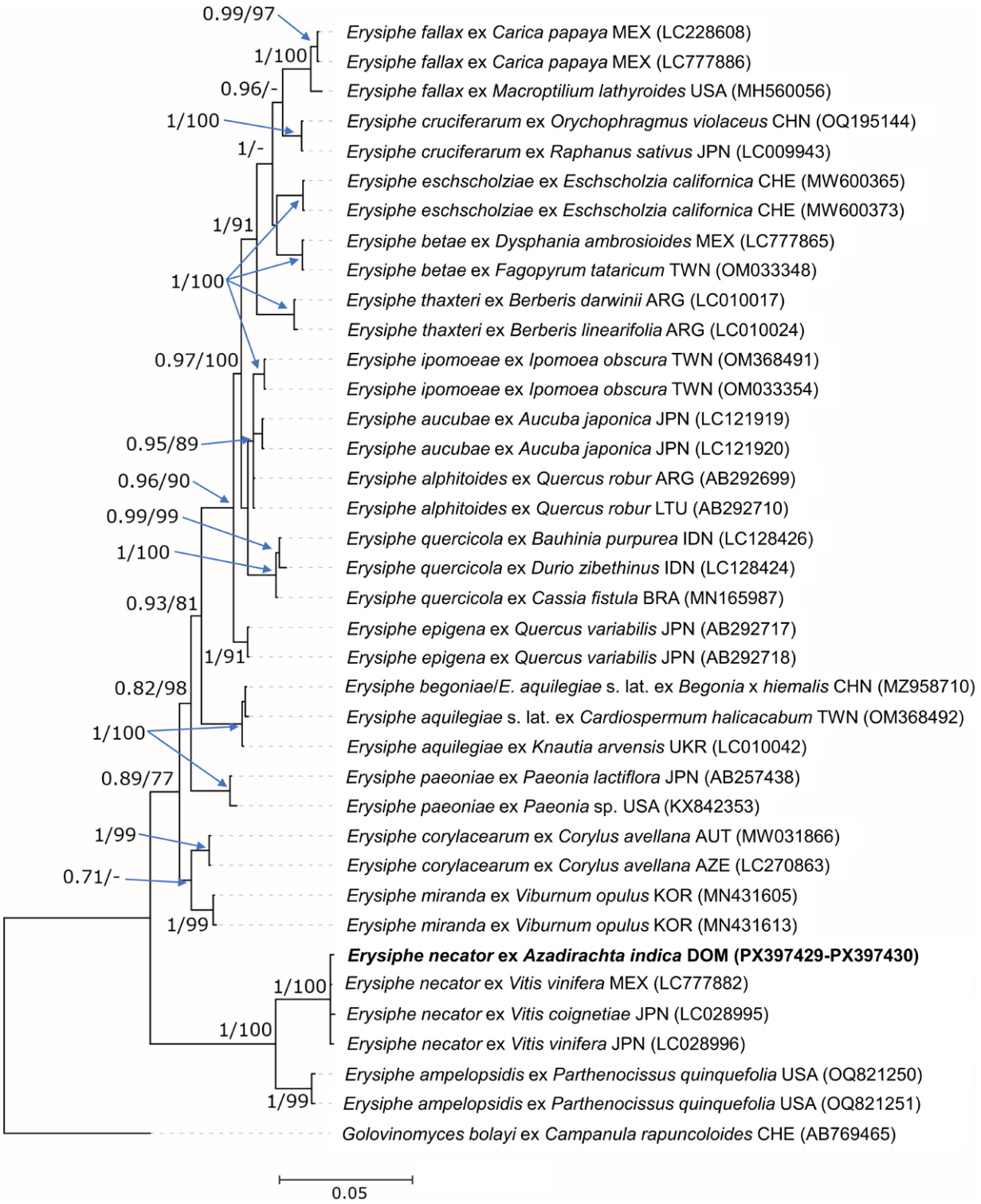

Figure 2. Phylogenetic tree based on Bayesian analysis (BA) of the ITS and 28S rDNA alignment, demonstrating the identity of *Erysiphe necator* infections from *Azadirachta indica* (in bold font) or *Vitis* spp. NCBI accession numbers and in parentheses. Bayesian posterior probabilities (≥ 0.7), and bootstrap support values for maximum likelihood (≥ 70%) are shown on main tree nodes.

in concordance with the original description should be designated as epitype with ex-epitype sequences. This would elucidate the phylogenetic-taxonomic status of this species. A morphological comparison between *P. azadirachtae* and the anamorph of the grapevine powdery mildew is difficult or impossible, mainly due to the great variability of the asexual morph of *E. necator* (Braun and Cook, 2012). In contrast to the very long conidia of *E. aquilegiae* s. lat. on neem in India (Wagh *et al*., 2024), the conidium size of the powdery mildew on this host in the Dominican Republic aligns with the original description of *O. azadirachtae* (Narayanaswamy and Ramakrishnan, 1969; Braun and Cook, 2012).

Tropical/subtropical regions host many species, with recent studies finding new species of *Erysiphe*, *Podosphaera*, and other genera, on various hosts in regions including Taiwan, Indonesia, Thailand, and Australia (Kiss *et al*., 2020; Kelly *et al*., 2025; Yeh *et al*., 2025). In Southeast Asia alone, 14 genera and 96 species have been documented. Among these, *Erysiphe* is the most species-rich genus (25 species), and several of its members are of major economic importance in tropical agriculture. Among the important pathogen species, *E. necator*, which causes grapevine powdery mildew, has been recorded throughout Southeast Asia, including from Thailand, Cambodia, Indonesia, Malaysia, Myanmar, and Vietnam, and additionally on cultivated strawberry (*Fragaria* × *ananassa*) in the Philippines (Aumentado *et al*., 2023). This is, however, a highly dubious host record (Aumentado *et al*., 2023), based solely on an entry in a checklist without morphological data or molecular confirmation.

Beyond Southeast Asia, significant powdery mildew diversity has also been documented in other tropical regions. A comprehensive survey in Puerto Rico identified 14 species on 38 host plants, with *Erysiphe* being the most frequent genus (University of Puerto Rico at Mayaguez, 2009). In Taiwan, a subtropical/tropical region with a high diversity of powdery mildews, recent surveys have documented multiple species across several genera, including *Erysiphe*, *Golovinomyces*, and *Podosphaera* (Yeh *et al*., 2025). Thirteen species (or species complexes) were confirmed on 28 host plants, many representing new island or international records. Particularly noteworthy is the detection of *E. necator* on *Ampelopsis brevipedunculata* (a new host for Taiwan), and on *Causonis japonica*, which is the first host record for this fungus.

In warm, humid environments, the asexual (anamorph) stage is often prevalent, making morphological identification difficult. DNA sequencing (mainly ITS region) is therefore crucial for species confirmations. As a consequence, many historical records from tropical plant disease surveys have identified powdery mildew pathogens only at genus levels, most frequently as *Oidium* sp. Kelly *et al.* (2025) reported that the Australian climate, and in some pathogen species, broad host ranges, allow continual survival of asexual stages of powdery mildew species on multiple hosts throughout each year. Only a few powdery mildew species have been reported to develop chasmothecia in tropical and subtropical regions (Vaghefi *et al*., 2022; Aumentado *et al*., 2023).

Powdery mildews are biotrophic parasites with highly specific linkages to their hosts, which are due to relatively long-term and complex co-evolutionary relationships (Bradshaw *et al*., 2024, 2026). Among representatives of Erysiphaceae, there are species with very narrow host ranges, and species with very wide host ranges encompassing several families (Lebeda *et al*., 2017; Mieslerová *et al.,* 2020). Beenken (2017) reported that host jumps occur regularly in powdery mildews. This process involves isolation of certain pathogen subpopulations, eventually leading to genetic differentiations and, in the long term, speciation, resulting in successful colonization of previously non-susceptible host species (Schulze-Lefert and Panstruga, 2011; Thines, 2019). Currently, sufficient information is lacking to fully elucidate the processes associated with successful transition (host jump) of a given powdery mildew species to other plants, that enable expansion of the pathogen's host spectrum. This is particularly true for host jumps to species belonging to other (and phylogenetically distant) plant families (Kusch *et al*., 2024).

In this context, limits to the present study are relevant. The herbarium material available did not allow verification of infection of the host species by the pathogen. Thus, the current study did not fulfil Koch's postulates for the pathogen, so direct causality was not confirmed, but an association is indicted between *E. necator* and the symptoms observed in *Azadirachta indica*. The *E. necator* infection on *A. indica* detected was found outside the natural range of this host (Braun and Cook, 2012; Gadoury *et al*., 2012). The present results on occurrence of *E. necator* on *A. indica* expand knowledge about the host spectrum of *E. necator.* The ability of *E. necator* to colonize unrelated hosts (*Azadirachta*, *Caryocar, Carica, Anacardium, Hevea*; Braun *et al*., 2017; Fonseca *et al*., 2019; Pieroni *et al*., 2020) indicates a broad ability for adaptation of this species than was previously recognized. Also, it supports previous hypotheses that cross-host infections may reflect incidental infections under suitable environmental conditions, or ecological overlaps between host species. This wide range across geographically and taxonomically distinct host species

indicates broad ecological plasticity of *E. necator*, and supports its role as a cosmopolitan pathogen capable of occasional host jumps.

ACKNOWLEDGEMENTS

This research was supported by the projects: Internal Grant Agency of Palacký University in Olomouc (Czech Republic) (grants PrF 2025_001 and PrF 2026_001); and National Programme of Genepool Conservation of Microorganisms and Small Animals of Economic Importance, Ministry of Agriculture of the Czech Republic. The authors thank the CoEditor-in-Chief of *Phytopathologia Mediterranea*, and the two manuscript reviewers, for their constructive improvements to the draft manuscript of this paper.

LITERATURE CITED

Abasova L.V., Aghayeva D.N., Takamatsu S., 2018. Notes on powdery mildews of the genus *Erysiphe* from Azerbaijan. *Current Research in Environmental & Applied Mycology* (*Journal of Fungal Biology*) 8: 30–53. https://doi.org/10.5943/cream/8/1/3

Aumentado H.D.R, Guerrero J.J.G., Balendres M.A.O., 2023. Powdery mildew in Southeast Asia: host range, impact, and sources of resistance. *Technology in Agronomy* 3: 9. https://doi.org/10.48130/TIA-2023-0009

Bailey A., Chandler D., Grant W.P., Greaves J., Prince G., Tatchell M., 2010. Biopesticides. Pest Management and Regulation. CAB International, Wallingford, UK.

Beenken L., 2017. First records of the powdery mildews *Erysiphe platani* and *E. alphitoides* on *Ailanthus altissima* reveal host jumps independent of host phylogeny. *Mycological Progress* 16: 135–143. https://doi.org/10.1007/s11557-016-1260-2

Bradshaw M.J., Boufford D., Braun U., Moparthi S., Jellings K., … Pfister D.H., 2024. An in-depth evaluation of powdery mildew hosts reveals one of the world's most common and widespread groups of fungal plant pathogens. *Plant Disease* 108: 576–581. https://doi.org/10.1094/PDIS-07-23-1471-RE

Bradshaw M., Braun U., Götz M., Meeboon J., Takamatsu S., 2017. Powdery mildew of *Chrysanthemum* × *morifolium*: phylogeny and taxonomy in the context of *Golovinomyces* species on Asteraceae hosts. *Mycologia* 109: 508–519. https://doi.org/10.1080/00275514.2017.1358136

Bradshaw M., Braun U., Németh M.Z., Paul A., Mitchell J.K., … Pfister D.H., 2026. Reassessment of the *Erysiphe aquilegiae* complex (Erysiphaceae)—resolution of a widespread and economically significant group of plant pathogens. *Fungal Biology* 130: 101717. https://doi.org/10.1016/j.funbio.2026.101717

Bradshaw M., Braun U., Pfister D.H., 2023. Phylogeny and taxonomy of the genera of Erysiphaceae, part 4: *Erysiphe* (the "Uncinula lineage"). *Mycologia* 115: 871–903. https://doi.org/10.1080/00275514.2023.2230853

Bradshaw M., Braun U., Takamatsu S., Németh M.Z., Seress D., Pfister D.H., 2025a. The *Erysiphe alphitoides* complex (powdery mildews) – unravelling the phylogeny and taxonomy of an intricate assemblage of species. *New Zealand Journal of Botany* 63: 28–44. https://doi.org/10.1080/0028825X.2023.2276913

Bradshaw M., Quijada L., Braun U., Smith M., Pfister D.H., 2025b. Powdery mildews on North American oaks: incredible levels of fungal diversity and pathogen-host coevolution. *Forest Pathology* 55: e70005. https://doi.org/10.1111/efp.70005

Braun U., Cook R.T.A., 2012. Taxonomic manual of the Erysiphales (powdery mildews). *CBS Biodiversity Series* 11: 1–707.

Braun U., Cook R.T.A., Inman A.J., Shin H.D., 2002. The taxonomy of the powdery mildew fungi. In: (Bélanger RR, Bushnell WR, Dik AJ, Carver TLW, ed.) The Powdery Mildews: A Comprehensive Treatise. APS Press, Saint Paul, MN, pp. 13–54.

Braun U., Meeboon J., Takamatsu S., Blomquist C., Fernández Pavía S.P., … Macedo D.M., 2017. Powdery mildew species on papaya – a story of confusion and hidden diversity. *Mycosphere* 8: 1403–1423. https://doi.org/10.5943/mycosphere/8/9/7

Braun U., Shin H.D., Takamatsu S., Meeboon J., Kiss L., … Götz M., 2019. Phylogeny and taxonomy of *Golovinomyces orontii* revisited. *Mycological Progress* 18: 335–357. https://doi.org/10.1007/s11557-018-1453-y

Brewer M.T., Milgroom M.G., 2010. Phylogeography and population structure of the grape powdery mildew fungus, *Erysiphe necator*, from diverse *Vitis* species. *BMC Evolutionary Biology* 10: 268. doi: 10.1186/1471-2148-10-268.

Cho S.E., Park J.H., Jankovsky L., Shin H.D., 2012. First report of powdery mildew on *Cissus rhombifolia* caused by *Erysiphe necator* in the Czech Republic. *Australasian Plant Disease Notes* 7: 43–45. https://doi.org/10.1007/s13314-012-0044-z

Cook R.T.A., Braun U., 2009. Conidial germination patterns in powdery mildews. *Mycological*

Research 113: 616–636. https://doi.org/10.1016/j.mycres.2009.01.010

Cook R.T.A., Inman A.J., Billings C., 1997. Identification of anamorphs of powdery mildews using morphological and host range data. *Mycological Research* 101: 975–1002. https://doi.org/10.1017/S095375629700364X

Cooper J.A., Park D., Johnston P.R., 2015. An initial genetic characterisation of the grape powdery mildew (*Erysiphe necator*) in New Zealand associated with recent reports of the sexual stage. *New Zealand Plant Protection* 68: 389-395. https://doi.org/10.30843/nzpp.2015.68.5817

Cunnington J., Takamatsu S., Lawrie A., Pascoe I., 2003. Molecular identification of anamorphic powdery mildews (Erysiphales). *Australasian Plant Pathology* 32: 421–428. https://doi.org/10.1071/AP03045

Ellingham O., David J., Culham A., 2019. Enhancing identification accuracy for powdery mildews using previously underexploited DNA loci. *Mycologia* 111: 798–812. https://doi.org/10.1080/00275514.2019.1643644

Fonseca W.L., Cardoso J.E., Ootani M.A., Brasil S.O.S., Assunçao F.S., … Martins M.V.V., 2019. Morphological, molecular phylogenetic and pathogenic analyses of *Erysiphe* spp. causing powdery mildew on cashew plants in Brazil. *Plant Pathology* 68: 1157–1164. https://doi.org/10.1111/ppa.13032

Gadoury D.M., Cadle-Davidson L., Wilcox W.F., Dry I.B., Seem R.C., Milgroom M.G., 2012. Grapevine powdery mildew (*Erysiphe necator*): a fascinating system for the study of the biology, ecology and epidemiology of an obligate biotroph. *Molecular Plant Pathology* 13: 1–16. https://doi.org/10.1111/J.1364-3703.2011.00728.X

Gardes M., Bruns T.D., 1993. ITS primers with enhanced specificity for basidiomycetes application to the identification of mycorrhizae and rusts. *Molecular Ecology* 2: 113–118. https://doi.org/10.1111/j.1365-294X.1993.tb00005.x

Gautam P., Mittal P., 2021. A review on traditional plant *Azadirachta indica*: natural source for disease curability and health promotion. *Journal of Pharmaceutical Research International* 33: 1–7. https://doi.org/10.9734/jpri/2021/v33i56A33880

Gregorio-Cipriano R., Rodríguez-Alvarado G., Takamatsu S., Braun U., Siahaan S.A.S. et al. …Fernández-Pavía S.P., 2026. New records and a new species of *Erysiphe* (Erysiphaceae, Ascomycota) from Mexico. *Mycoscience* 67: 105–116. https://doi.org/10.47371/mycosci.2026.02.002

Gul B., Naz F., Paret M.L., Iriarte F., Haider Z. …Khan A., 2025. Morpho-molecular diversity and host range dynamics of squash powdery mildew pathogens prevailing in Pothwar Plateau, Pakistan. *Journal of Plant Pathology*. https://doi.org/10.1007/s42161-025-02039-1

Gupta S.C., Prasad S., Tyagi A.K., Kunnumakkara A.B., Aggarwal B.B., 2017. Neem (*Azadirachta indica*): an Indian traditional panacea with modern molecular basis. *Phytomedicine* 34: 14–20. https://doi.org/10.1016/j.phymed.2017.07.001

Gur L., Reuveni M., Cohen Y., Cadle-Davidson L., Kisselstein B., … Frenkel O., 2021. Population structure of *Erysiphe necator* on domesticated and wild vines in the Middle East raises questions on the origin of the grapevine powdery mildew pathogen. *Environmental Microbiology* 23: 6019–6037. https://doi.org/10.1111/1462-2920.15401

Hoang D.T., Chernomor O., von Haeseler A., Minh B.Q., Vinh L.S., 2018. UFBoot2: improving the ultrafast bootstrap approximation. *Molecular Biology and Evolution* 35: 518–522. https://doi.org/10.1093/molbev/msx281

Hsiao H.Y., Ariyawansa H.A., Hsu C.C.; Wang C.J., Shen, Y.M., 2022. New records of powdery mildews from Taiwan: *Erysiphe ipomoeae* comb. nov., *E.* aff. *betae* on buckwheat, and *E. neolycopersici* comb. nov. on *Cardiospermum halicacabum*. *Diversity* 14: 204. https://doi.org/10.3390/d14030204

Huelsenbeck J.P., Ronquist F., 2001. MRBAYES: Bayesian inference of phylogenetic trees. *Bioinformatics* 17: 754–755. https://doi.org/10.1093/bioinformatics/17.8.754

Inuma T., Khodaparast S.A., Takamatsu S., 2007. Multilocus phylogenetic analyses within *Blumeria graminis*, a powdery mildew fungus of cereals. *Molecular Phylogenetics and Evolution* 44: 741–751. https://doi.org/10.1016/j.ympev.2007.01.007

Jaswa A., Vallance J., Fournier P., Martin V., Masneuf-Pomarède I., … Vacher C., 2026. Developing a culturomic approach to build a collection of grapevine foliar microorganisms with potential applications in disease biocontrol. *OENO One* 60: https://doi.org/10.20870/oeno-one.2026.60.1.9588

Jayalakshmi K., Dutta R., Gawande P.Y., Kumar V., Gurav V.S., 2024. Powdery mildew of neem caused by *Pseudoidium azadirachtae*. *Food Science Reports* 3: 1–3.

Kalyaanamoorthy S., Minh B.Q., Wong T.K.F., von Haeseler A., Jermiin L.S., 2017. ModelFinder: fast model selection for accurate phylogenetic estimates. *Nature Methods* 14: 587–589. https://doi.org/10.1038/nmeth.4285

Katoh K., Rozewicki J., Yamada K.D., 2019. MAFFT online service: multiple sequence alignment, interactive sequence choice and visualization. *Briefings Bioinformatics* 20: 1160–1166. https://doi.org/10.1093/bib/bbx108

Kearse M., Moir R., Wilson A., Stones-Havas S., Cheung M., … Drummond A., 2012. Geneious Basic: an integrated and extendable desktop software platform for the organization and analysis of sequence data. *Bioinformatics* 28: 1647–1649. https://doi.org/10.1093/bioinformatics/bts199

Kelly L.A., Dahanayaka B.A., Vaghefi N., Ahmad A., Kiss L., 2025. An unexpected diversity of powdery mildew species infecting the Fabaceae in Australia. *PLoS One* 20: e0323505. https://doi.org/10.1371/journal.pone.0323505

Kim J.B., Blackshaw S., 2001. One-step enzymatic purification of PCR products for direct sequencing. *Current Protocols in Human Genetics* 30: 11.6.1-11.6.4. https://doi.org/10.1002/0471142905.hg1106s30

Kiss L., Vaghefi N., Bransgrove K., Dearnaley J.D.W., Takamatsu S., … Braun U., 2020. Australia: a continent without native powdery mildews? The first comprehensive catalog indicates recent introductions and multiple host range expansion events, and leads to the re-discovery of *Salmonomyces* as a new lineage of the Erysiphales. *Frontiers in Microbiology* 11: 1571. https://doi.org/10.3389/fmicb.2020.01571

Koul O., Isman M.B., Ketkar C.M., 1990. Properties and uses of neem, *Azadirachta indica*. *Canadian Journal of Botany* 68:1–11. https://doi.org/10.1139/b90-001

Křivánková T., Kitner M., Mieslerová B., Hroneš M., Křístková E., … Lebeda A., 2025. Geographic distribution, species spectrum and variation of powdery mildew in the genus *Lactuca*. *Mycological Progress* 24: 62. https://doi.org/10.1007/s11557-025-02076-1

Kusch S., Qian J., Loos A., Kümmel F., Spanu P.D., Panstruga R., 2024. Long-term and rapid evolution in powdery mildew fungi. *Molecular Ecology* 33: e16909. https://doi.org/10.1111/mec.16909

LaGreca S., Crouch U., Paul A., Thomas J., Thompson J., …Bradshaw M., 2025. Hidden treasures of herbaria - even small collections contain a wealth of diversity: the powdery mildews of the North Carolina State Larry F. Grand Mycological Herbarium. *IMA Fungus* 16: e156231. https://doi.org/10.3897/imafungus.16.156231

Lebeda A., 1983. The genera and species spectrum of cucumber powdery mildew in Czechoslovakia. *Journal of Phytopathology* 108: 71–77. https://doi.org/10.1111/j.1439-0434.1983.tb00565.x

Lebeda A., Kitner M., Mieslerová B., Křístková E., Pavlíček T., 2019. The occurrence of powdery mildew *Leveillula lactucae-serriolae* on *Lactuca serriola* in Jordan. *Phytopathologia Mediterranea* 58: 359-367. https://doi.org/10.14601/Phytopathol_Mediter-10622

Lebeda A., Mieslerová B., Huszár J., Sedláková B., 2017. *Padlí kulturních a planě rostoucích rostlin* (*Powdery Mildews of Crop and Wild Plants*). Agriprint, Olomouc, Czech Republic, 368 pp.

Marmolejo J., Siahaan S.A., Takamatsu S., Braun U., 2018. Three new records of powdery mildews found in Mexico with one genus and one new species proposed. *Mycoscience* 59: 1–7. https://doi.org/10.1016/j.myc.2017.06.010

Meeboon J., Takamatsu S., 2017. New records of *Erysiphe* sect. *Uncinula* spp. (*Erysiphales*) from Thailand and *E. liquidambaris* var. *acalycinae* var. nov. *Mycoscience* 58: 236–241. https://doi.org/10.1016/j.myc.2017.01.002

Mieslerová B., Kitner M., Petřeková V., Dvořáková J., Sedlářová M., … Lebeda A., 2020. *Golovinomyces* powdery mildews on Asteraceae in the Czech Republic. *Plant Protection Science* 56: 163–179. https://doi.org/10.17221/129/2019-PPS

Mridha M.A.U., Bhuiyan M.K., Akhter M.F., Mahmud M., Dhar P.P., Jabbar F., 2005. Powdery mildew of *Azadirachta indica* A. Juss. caused by *Oidium azadirachtae* sp. recorded in Bangladesh. *Hamdard Medicus* 48: 130–132.

Narayanaswamy P., Ramakrishnan K., 1969. Powdery mildew of Coimbatore. *The Madras University Journal* 38: 84–99.

Nguyen L.T., Schmidt H.A., von Haeseler A., Minh B.Q., 2015. IQ-TREE: a fast and effective stochastic algorithm for estimating maximum-likelihood phylogenies. *Molecular Biology and Evolution* 32: 268–274. https://doi.org/10.1093/molbev/msu300

Park J.H., Abasova L., Choi, I.Y., Shin H.D., 2026. Holomorph morphology and molecular phylogeny confirm *Erysiphe necator* var. necator causing powdery mildew on *Vitis flexuosa* in Korea. *Journal of Plant Pathology* 108: 757–761. https://doi.org/10.1007/s42161-025-02031-9

Péros J.P., Troulet C., Guerriero M., Michel-Romiti C., Notteghem J.L., 2005. Genetic variation and population structure of the grape powdery mildew fungus, *Erysiphe necator*, in Southern France. *European Journal of Plant Pathology* 113: 407–416. https://doi.org/10.1007/s10658-005-4563-8

Pieroni L.P., Gorayeb E.S., Benso L.A., Kurokawa S.Y.S., Siqueira O.A.P.A., … Furtado E.L., 2020. First report of *Erysiphe necator* causing powdery mildew to rub-

ber tree (*Hevea brasiliensis*) in Brazil. *Plant Disease* 104: 3078. https://doi.org/10.1094/PDIS-04-20-0848-PDN

Pintye A., Németh M.Z., Molnár O., Horváth Á.N., Matolcsi F, ...Kovács G.H., 2023. Comprehensive analyses of the occurrence of a fungicide resistance marker and the genetic structure in *Erysiphe necator* populations. *Scientific Reports* 13: 15172. https://doi.org/10.1038/s41598-023-41454-1

Pirondi A., Kitner M., Iotti M., Sedláková B., Lebeda A., Collina M., 2016. Genetic structure and phylogeny of Italian and Czech populations of the cucurbit powdery mildew fungus *Golovinomyces orontii* inferred by multilocus sequence typing. *Plant Pathology* 65: 959–967. https://doi.org/10.1111/ppa.12480

POWO, 2025. *Plants of the World Online*. Royal Botanic Gardens, Kew.

Qiu P.L., Liu S.Y., Bradshaw M., Rooney-Latham S., Takamatsu S., ... Braun U., 2020. Multi-locus phylogeny and taxonomy of an unresolved, heterogeneous species complex within the genus *Golovinomyces* (Ascomycota, Erysiphales), including *G. ambrosiae*, *G. circumfusus* and *G. spadiceus*. *BMC Microbiology* 20: 51. https://doi.org/10.1186/s12866-020-01731-9

Ronquist F., Huelsenbeck J.P., 2003. MrBayes 3: Bayesian phylogenetic inference under mixed models. *Bioinformatics* 19: 1572–1574. https://doi.org/10.1093/bioinformatics/btg180

Seress D.,Kovács G.M., Molnár O., Németh M.Z., 2021. Infection of papaya (*Carica papaya*) by four powdery mildew fungi. *Phytopathologia Mediterranea* 60: 37–49. https://doi.org/10.36253/phyto-11976

Sholberg P.L., O'Gorman D.T., Bedford K., Levesque C.A., 2005. Development of a DNA macro-array for detection and monitoring of economically important apple diseases. *Plant Disease* 89: 1143–1150. https://doi.org/10.1094/PD-89-1143

Schulze-Lefert P., Panstruga R., 2011. A molecular evolutionary concept connecting nonhost resistance, pathogen host range, and pathogen speciation. *Trends in Plant Sciences* 16: 117–125. https://doi.org/10.1016/j.tplants.2011.01.001

Seress D., Kovács G.M., Molnár O., Németh M.Z., 2021. Infection of papaya (*Carica papaya*) by four powdery mildew fungi. *Phytopathologia Mediterranea* 60: 37–49. https://doi.org/10.36253/phyto-11976

Shin H.D., 2000. *Erysiphaceae of Korea*. National Institute of Agricultural Science and Technology, Suwon, Korea, 320 pp.

Singh U.P., Maurya S., Singh A., Gohain L., 2010. Foliar spray of aqueous extract of neem (*Azadirachta indica*) cake to control balsam (*Impatiens balsamina*) powdery mildew. *Archives of Phytopathology and Plant Protection* 43: 1056–1063. https://doi.org/10.1080/03235400802285315

Stamatakis A., 2014. RAxML version 8: a tool for phylogenetic analysis and post-analysis of large phylogenies. *Bioinformatics* 30: 1312–1313. https://doi.org/10.1093/bioinformatics/btu033

Takamatsu S., 2013. Origin and evolution of the powdery mildews (Ascomycota, Erysiphales). *Mycoscience* 54: 75–86. https://doi.org/10.1016/j.myc.2012.08.004

Takamatsu S., Ito Arakawa H., Shiroya Y., Kiss L., Heluta V., 2015. First comprehensive phylogenetic analysis of the genus *Erysiphe* (Erysiphales, Erysiphaceae) II: the Uncinula lineage. *Mycologia* 107: 903-914. https://doi.org/10.3852/15-062

Takamatsu S., Matsuda S., Grigaliunaite B., 2013. Comprehensive phylogenetic analysis of the genus *Golovinomyces* (Ascomycota: Erysiphales) reveals close evolutionary relationships with its host plants. *Mycologia* 105: 1135–1152. https://doi.org/10.3852/13-046

Takamatsu S., Niinomi S., Harada M., Havrylenko M., 2010. Molecular phylogenetic analyses reveal a close evolutionary relationship between *Podosphaera* (Erysiphales: Erysiphaceae) and its rosaceous hosts. *Persoonia* 24: 38–48. https://doi.org/10.3767/003158510X494596

Thines M., 2019. An evolutionary framework for host shifts – jumping ships for survival. *New Phytologist* 224: 605–617. https://doi.org/10.1111/nph.16092

Trifinopoulos J., Nguyen L.T., von Haeseler A., Minh B.Q., 2016. W-IQ-TREE: a fast online phylogenetic tool for maximum-likelihood analysis. *Nucleic Acids Research* 44(W1): W232–W235. https://doi.org/10.1093/nar/gkw256

Tufail T., Ul Ain H.B., Ijaz A., Nasir M.A., Ikram A., ... Abdullahi M.A., 2025. Neem (*Azadirachta indica*): A miracle herb; panacea for all ailments. *Food Science and Nutrition* 13: e70820. https://doi.org/10.1002/fsn3.70820

University of Puerto Rico at Mayaguez, 2009–2012. *Powdery mildews: Invasive and Emerging Diseases in the Tropics*. National Institute of Food and Agriculture, Special Grant No. 2009-34135-20136. Available at: https://portal.nifa.usda.gov/web/crisprojectpages/0219797-powdery-mildews-invasive-and-emerging-diseases-in-the-tropics.html

Vaghefi N., Kusch S., Németh M.Z., Seress D., Braun U., ... Kiss L., 2022. Beyond nuclear ribosomal DNA sequences: evolution, taxonomy, and closest known saprobic relatives of powdery mildew fungi (Erysiphaceae) inferred from their first comprehensive

genome-scale phylogenetic analyses. *Frontiers in Microbiology* 13: 903024. https://doi.org/10.3389/fmicb.2022.903024

Wagh S.H., Thite S., Kanade M.B., Bradshaw M., Braun U., 2024. Identification of anamorphic Indian powdery mildews (*Erysiphaceae*) based on sequence analyses. *Current Research in Environmental & Applied Mycology (Journal of Fungal Biology)*14: w371–387. https://doi.org/10.5943/cream/14/1/19

White T.J., Bruns T.D., Lee S.B., Taylor J.W., 1990. Amplification and direct sequencing of fungal ribosomal RNA Genes for phylogenetics. In: PCR Protocols. Academic Press, London, UK. https://doi.org/10.1016/B978-0-12-372180-8.50042-1

Yeh Y.W., Piepenbring M., Kirschner R., 2025. Twenty-nine new host records of powdery mildew fungi (Erysiphaceae) in Taiwan with an updated checklist. *Botanical Studies* 66: 26. https://doi.org/10.1186/s40529-025-00471-1

Phytopathologia Mediterranea
The international journal of the
Mediterranean Phytopathological Union

Firenze University Press
www.fupress.com/pm

Research Papers

Identification of antifungal essential oils for control of brown spot pathogens of 'Rocha' pear

Inês MENDONÇA[1,2], Beatriz FERNANDES[3,4], Carmo SERRANO[3,5,6], Ana C. MARQUES[4], Ricardo OLIVEIRA[1], Carina ALMEIDA[1,7], Miguel LEÃO DE SOUSA[8,9], Armando VENÂNCIO[2,10], Sónia SILVA[2,10,*]

[1] *INIAV, IP – National Institute for Agrarian and Veterinary Research, Polo de Vairão, Rua dos Lagidos, Lugar da Madalena, 4485-655, Vairão, Vila do Conde, Portugal*
[2] *CEB – Centre of Biological Engineering, University of Minho, Campus de Gualtar, 4710-057, Braga, Portugal*
[3] *INIAV, IP – National Institute for Agrarian and Veterinary Research, Avenida da República, Quinta do Marquês, 2780-157, Oeiras, Portugal*
[4] *CERENA, DEQ, Instituto Superior Técnico, University of Lisbon, Avenida Rovisco Pais, No. 1, 1049-001, Lisbon, Portugal*
[5] *LEAF – Linking Landscape, Environment, Agriculture and Food Research Unit, Associate Laboratory, Instituto Superior de Agronomia, University of Lisbon, Tapada da Ajuda 1349-017, Lisbon, Portugal*
[6] *TERRA, Instituto Superior de Agronomia, University of Lisbon, Tapada da Ajuda 1349-017, Lisbon, Portugal*
[7] *LEPABE, ALiCE, Faculty of Engineering, University of Porto, Rua Dr. Roberto Frias, 4200-465, Porto, Portugal*
[8] *INIAV, IP – National Institute for Agrarian and Veterinary Research, Polo de Alcobaça, Estrada de Leiria, 2460-059, Alcobaça, Portugal*
[9] *GREEN-IT – Bioresources for Sustainability, Avenida da República, 2780-157, Oeiras, Portugal*
[10] *LABBELS – Associate Laboratory, Braga/Guimarães, Portugal*
*Corresponding author. E-mail: soniasilva@ceb.uminho.pt

Summary. Brown spot of pear (BSP) is a major concern in 'Rocha' pear production. Essential oils were identified with *in vitro* antifungal properties against fungi isolated from BSP, and encapsulated formulations were developed via spray-drying. Four fungal isolates from symptomatic leaf and fruit tissues of 'Rocha' pears were identified as *Stemphylium vesicarium* (isolates MUM 26.01 and MUM 26.02) and *Alternaria arborescens* (isolates MUM 26.03 and MUM 26.04) through multilocus sequencing. Sensitivity of these isolates was assessed to five fungicides commonly used in Portuguese orchards. Tebuconazole and cyprodinil were the most effective across isolates, while trifloxystrobin gave limited inhibition, indicating low sensitivity of these isolates. To assess sustainable alternatives, 18 essential oils (EOs) were screened, showing that lemongrass and lemon thyme EOs were the most promising candidates, completely inhibiting mycelium growth and spore germination of the fungi at low concentrations. Encapsulation of these two EOs on HI-CAP® 100, using spray-drying, preserved their antifungal activity. Chemical characterization showed that lemongrass and lemon thyme EOs consisted primarily of oxygenated monoterpenes, which were probably responsible for the high antifungal activity observed. These results highlight the potential of lemongrass and lemon thyme EOs as promising candidates for *in vivo* validation

OPEN ACCESS

Citation: Mendonça, I., Fernandes, B., Serrano, C., Marques, A. C., Oliveira, R., Almeida, C., Leão de Sousa, M., Venâncio, A. & Silva, S. (2026). Identification of antifungal essential oils for control of brown spot pathogens of 'Rocha' pear. *Phytopathologia Mediterranea* 65(2): 267-286. doi: 10.36253/phyto-17132

Accepted: July 10, 2026

Published: September 10, 2026

© 2026 Author(s). This is an open access, peer-reviewed article published by Firenze University Press (https://www.fupress.com) and distributed, except where otherwise noted, under the terms of the CC BY 4.0 License for content and CC0 1.0 Universal for metadata.

Data Availability Statement: All relevant data are within the paper and its Supporting Information files.

Competing Interests: The Author(s) declare(s) no conflict of interest.

Editor: Tito Caffi, Università Cattolica del Sacro Cuore, Piacenza , Italy.

ORCID:
IM: 0009-0002-9963-1971
BF: 0009-0005-3536-9582
CS: 0000-0002-7632-3485
ACM: 0000-0002-2947-1186
RO: 0000-0001-9175-4278
CA: 0000-0002-0175-1119
MLdS: 0000-0002-7218-3745
AV: 0000-0002-0723-6134
SS: 0000-0003-0000-7387

as sustainable alternatives to synthetic fungicides for control of *S. vesicarium* and *A. arborescens*, and management of BSP in 'Rocha' pear production.

Keywords. *Alternaria arborescens*, *Stemphylium vesicarium*, fungicide sensitivity, *in vitro* screening.

INTRODUCTION

'Rocha' pear (*Pyrus communis* L. 'Rocha') is a Portuguese pear variety recognized with Protected Designation of Origin (PDO) status. 'Rocha' pear is an important fruit crop in Portugal, with extensive cultivation area and significant economic value (Lomba-Viana *et al*., 2022). Production is primarily concentrated in Portugal's western region, where the disease brown spot of pear (BSP) has become a major concern, resulting in substantial yield reductions and consequent economic losses (Loebler *et al*., 2020).

Stemphylium vesicarium (Wallr.) E. Simmons is a plant pathogen particularly problematic for pear production, causing BSP, and is responsible for significant losses of production in Italy (where it was first reported in the mid-1970s), Spain, France, Belgium, Poland, and the Netherlands (Głos *et al*., 2023; Cavina *et al*., 2024). Although BSP mainly affects European pear production regions, it has recently been reported in Japan and Argentina (Temperini *et al*., 2022; Tudela *et al*., 2023a).

Stemphylium vesicarium has a dual lifecycle, with a saprophytic and a pathogenic phase (Llorente and Montesinos, 2006). During the saprophytic phase, the pathogen overwinters as pseudothecia on orchard debris. These structures develop throughout autumn and winter, and reach maturity at optimal temperatures of 10-15 °C, releasing ascospores of *Pleospora allii* (Rabenh.) Ces & De Not.. These ascospores act as primary sources of the asexual conidia of *S. vesicarium* (Llorente *et al*., 2010; Cavina *et al*., 2024). In the subsequent pathogenic phase, occurring during spring and summer (the pear growing season), these conidia are the principal inoculum responsible for infections, with optimal disease development at temperatures of 20 to 25 °C (Llorente and Montesinos, 2006; Tudela *et al*., 2023a). Virulence of *S. vesicarium* is largely attributed to production of host-specific toxins, which induce leaf vein necroses and disrupt plasma membrane integrity of plant cells (Singh *et al*., 1999). BSP symptoms manifest from pear flowering to fruit harvest, with necrotic lesions on leaves, twigs, petioles, and mainly on fruits as circular brown spots, often with red haloes. These symptoms can expand due to invasion by saprophytic fungi, including *Alternaria* spp., causing fruit rots (Cavina *et al*., 2024).

Synthetic fungicides are commonly used for management of BSP, initially providing low-cost and temporary solutions (Toledo *et al*., 2023). However, due to the high disease pressures and continuous infection cycles through growing seasons, high numbers of fungicide applications at 7 to 14 d intervals may be required to achieve low disease levels in orchards with a high disease incidence (Llorente *et al*., 2012b). The dithiocarbamate, strobilurin, succinate dehydrogenase inhibitor (SDHI), dicarboximide, and triazole fungicide groups are most commonly used against *S. vesicarium* in pear orchards (Llorente *et al*., 2012b; Luz *et al*., 2018; Tudela *et al*., 2023b). In Portugal, several of these active ingredients (including tebuconazole, trifloxystrobin, kresoxim-methyl, dithianon, cyprodinil and copper) are currently authorized for pear protection against BSP, according to the technical guidelines of the Portuguese Directorate-General for Food and Veterinary (DGAV), and the official phytopharmaceutical database SIFITO (DGAV, 2024). However, their excessive and repeated use may lead to pathogen resistance (Yin *et al*., 2023). These products may also pose environmental and public health concerns, due to their toxicity, non-biodegradable nature, and long residual activity adversely affecting non-target organisms and the environment (Corkley *et al*., 2022; Dorjee *et al*., 2023; Szczygieł *et al*., 2024).

Natural compounds, including essential oils (EOs), are gaining attention as sustainable alternatives to conventional agrochemicals for control of fungal diseases. EOs are complex mixtures of hydrophobic, fragrant, and volatile compounds synthesized by plants through metabolic pathways (Parikh *et al*., 2021; Dorjee *et al*., 2023). The main biosynthetic pathways include the mevalonate (MVA), methylerythritol phosphate (MEP), and shikimic acid processes, responsible for the two major groups of EOs: terpenoids and phenylpropanoids (de Sousa *et al*., 2023). These compounds have broad antifungal spectrum (Nazzaro *et al*., 2017), inhibiting fungal growth and preventing spore germination. Their modes of action include disrupting cell membranes, damaging cell wall integrity, and interfering with mitochondrial activity (Dorjee *et al*., 2023; Fincheira *et al*., 2023), and their antifungal activity has been extensively demonstrated *in vitro* conditions (Raveau *et al*., 2020). Increasing *in vivo* evidence also demonstrates their ability to suppress disease development in treated plants (Soylu *et al*., 2010; Antonioli *et al*., 2020; Xylia *et al*., 2021; Akhtari *et al*., 2022).

Despite the potential benefits of using EOs in crop protection, the European Union (EU) currently lacks a comprehensive approval framework for these substances as plant protection products. However, some naturally occurring components found in EOs (thymol, geraniol, 1,8-cineole), have been recognized as "low-risk" substances, and are included on the list of approved active substances outlined in Commission Implementing Regulation (EU) No. 540/2011. Particular EO constituents (e.g. citral and linalyl acetate) have received authorization as flavouring agents under Commission Implementing Regulation (EU) No. 872/2012, and are deemed to be of low risk for consumers. Despite these regulatory constraints, the physicochemical properties of EOs, including their high volatility, rapid degradation, low environmental persistence, and broad-spectrum antifungal activity, make them promising candidates for new biofungicide development. These characteristics align with EU initiatives including the Sustainable Use of Pesticides Directive, which is aimed at reducing reliance on synthetic fungicides and fostering sustainable crop protection.

The same traits that benefit environmental compatibility may limit practical EO application in the field, due to challenges related to their stability and bioavailability. Nano- and micro-encapsulation techniques, including spray-drying, have been increasingly employed to enhance stability, enable controlled release, and improve bioactivity of EOs (Antonioli *et al.*, 2020; Altay *et al.*, 2024). While previous studies have documented applications of the EOs against *Alternaria* spp., particularly *A. alternata* (Minozzo *et al.*, 2023; Bajac *et al.*, 2025), their effectiveness in addressing BSP pathogens in pear orchards, specifically *S. vesicarium*, has yet to be investigated. Building on this background, the present study aimed to identify EOs with antifungal activity, and, among the most effective candidates, to validate their *in vitro* efficacy by developing encapsulated formulations through spray-drying. These formulations are intended for use in controlling pathogenic fungi isolated from 'Rocha' pears exhibiting BSP symptoms. This study hypothesized that encapsulating EOs will enhance their stability while preserving antifungal activity. Eighteen EOs were screened *in vitro* against *S. vesicarium* isolates from 'Rocha' pear, to select those with the greatest antifungal potential. The three most active EOs were then encapsulated by spray-drying with HI-CAP® 100, and these formulations were assessed for inhibition of mycelium growth and conidium germination of *S. vesicarium* and *A. arborescens* isolated from 'Rocha' pear.

MATERIALS AND METHODS

Isolation of fungi

Fungus isolates were obtained from leaf and fruit samples collected from western Portuguese pear orchards between September 2023 and November 2024. Samples of pears and leaves were surface-sterilized with 1% sodium hypochlorite for 3 min, followed by three rinses with sterile distilled water. Necrotic tissues were then plated on Potato Dextrose Agar (PDA; Liofilchem) supplemented with chloramphenicol (Sigma-Aldrich) to inhibit bacterial growth, and were incubated for 4 d at 25 °C. Three emerging isolates were isolated from fruit and one from leaf, and were transferred to PDA plates to establish pure cultures. Mycelium agar blocks (5 × 5 mm) from pure cultures were preserved at room temperature in vials containing sterile distilled water. The isolates used in this study were deposited in Micoteca da Universidade do Minho (MUM, Braga, Portugal). For inoculum preparation, isolates were each cultured in PDA at 25 °C for 10 d.

Identification of isolates

Fungi were cultured in Potato Dextrose Broth (PDB; Liofilchem) in Erlenmeyer flasks that were incubated for 7 d at room temperature at 150 rpm. Resulting biomass of each isolate was collected by filtration and stored at -20 °C until further use. Genomic DNA was extracted using MagaBio Fungal Genome DNA Purification Kits (Bioer), following the manufacturer's protocol. DNA concentration and purity were assessed using a NanoDrop One spectrophotometer (Thermo Fisher Scientific), and samples were subsequently stored at -20 °C. PCR amplification was carried out targeting the ITS region, *gpd* gene and *Alt-a1* gene, and PCR products were sent for Sanger sequencing. The PCR conditions and primer sequences used are summarized in Table S1. The quality of the resulting sequences was verified using Geneious 11.1.5 software (Biomatters Limited), and the trimmed sequences were compared against the NCBI nucleotide database (nr/nt) using the Megablast program to determine closest related taxa. The sequences of the three loci were individually aligned in MEGA 12 (Kumar *et al.*, 2024), and ambiguous regions were removed using Gblocks (Castresana, 2000; Dereeper *et al.*, 2008). The cured alignments were concatenated, and a Maximum Likelihood (ML) phylogenetic tree was constructed in MEGA 12. Reference sequences used for tree construction are listed in Tables S2 and S3.

Fungus isolation and conidium production

Isolation and production of conidia from *S. vesicarium* and *A. arborescens* were carried out using previously described methods (Puig *et al*., 2015; Loebler *et al*., 2020), with some adaptations. The isolates were grown in tomato pulp agar plates, containing 1.25% (w/v) tomato pulp (Sumol+Compal), 3 g L^{-1} calcium carbonate (Merck), and 20 g L^{-1} agar (Liofilchem). The plates were kept at room temperature for 30 d with a 16 h daily photoperiod. Conidia were then harvested by scraping the plates with 10 mL of 0.01% (v/v) Tween 80 (Merck-Schuchardt). The resulting suspensions were each filtered through glass wool and cleaned by centrifugation for 10 min at 3,600 rpm. To determine conidium concentrations, serial dilutions were prepared, and 100 µL of each dilution was spread onto PDA plates. After 3 d incubation at 25 °C, the numbers of colony-forming units (CFUs) were counted, and were then used to estimate initial conidium concentrations. The suspensions were adjusted to obtain final conidium concentrations of 1 to 3×10^3 mL^{-1}, and were stored at 4 °C until further use.

Fungicide sensitivity assessments

To assess fungus isolate sensitivity, five commercial fungicides (copper complex, tebuconazole, trifloxystrobin, fluxapyroxad, cyprodinil) were evaluated against the *S. vesicarium* and *A. arborescens* isolates, using the "poisoned food" technique (Nene and Thapliyal, 1979). Each fungicide was added to sterilized molten PDA at concentrations that corresponded to the recommended application dose for field use (Table 1). The mixed PDA was then distributed into Petri plates. After complete solidification, mycelium squares (0.5 cm × 0.5 cm) were cut from 10-d-old cultures of the fungi, and placed in the centres of the PDA plates, with mycelia facing downwards. The experimental controls assessed growth of *S. vesicarium* or *A. arborescens* isolates on PDA medium without added fungicides. Colony diameters of the fungi were measured over the following 13 d period at 25 °C, and growth inhibition factors were calculated using the following formula (1):

$$Growth\ inhibition\ factor\ (\%) = \frac{D_C - D_T}{D_C} \times 100, \quad (1)$$

where:
D_C = diameter (cm) of control colony without treatment;
D_T = diameter (cm) of colony with treatment.

The diameter of the initial colony (0.5 cm) was subtracted from all measurements.

This experiment was carried out using biological triplicates.

Antifungal effects of essential oils against pathogenic fungi isolated from 'Rocha' pear material with BSP symptoms

Essential oils

A total of 18 EOs were used in this study. For some EOs, more than one production batch from the same plant species was tested. These batches were identified as batch 1, batch 2, or batch 3 (Table 2). The EO samples were stored in sealed vials at 4 °C until used. The EOs and their respective sources are listed in Table 2.

Antifungal activity of free essential oils

Antifungal activity of 18 EOs was evaluated using the "poisoned food" technique (Nene and Thapliyal, 1979). The tested oils were each added to sterilized PDA containing 0.01% (v/v) Tween 80, at concentrations of 1, 5, 10 or 50 µL mL^{-1}. The mixed PDA was then distributed into Petri plates, and a 0.5 × 0.5 cm mycelium square of *S. vesicarium* was placed in the centre of each PDA plate. Experimental controls included *S. vesicarium* iso-

Table 1. Fungicides and concentrations tested against fungi isolated from symptomatic material from 'Rocha' pears

Type of fungicide	Active ingredient	Group name[1]	FRAC[2] group code	FRAC level of resistance risk	Concentration tested
Copper based product	Copper complex	Inorganic	M01	Low	150 mL hL^{-1}
Triazole	Tebuconazole	DMI	3	Medium	75 g hL^{-1}
Strobilurin	Trifloxystrobin	QoI	11	High	10 g hL^{-1}
Carboxamide	Fluxapyroxad	SDHI	7	Medium-high	30 mL hL^{-1}
Anilinopyrimidine	Cyprodinil	AP	9	Medium	50 g hL^{-1}

[1] DMI, demethylation inhibitions; QoI, quinone outside inhibitor; SDHI, succinate-dehydrogenase inhibitor; AP, anilinopyrimidine.
[2] FRAC, Fungicide resistance action committee (FRAC, 2025).

Table 2. Essential oils (EOs) assessed against fungi isolated from symptomatic material of 'Rocha' pears

EO common designation	Source plant species
Basil	*Ocimum basilicum*
Eucalyptus (batch 1)	*Eucalyptus globulus*
Eucalyptus (batch 2)	*Eucalyptus globulus*
Eucalyptus (batch 3)	*Eucalyptus globulus*
Laurel	*Laurus nobilis*
Lavender	*Lavanda viridis*
Lemon eucalyptus (batch 1)	*Corymbia citriodora*
Lemon eucalyptus (batch 2)	*Corymbia citriodora*
Lemongrass	*Cymbopogon citratos*
Lemon mint	*Monarda citriodora*
Lemon thyme (batch 1)	*Thymus citriodorus*
Lemon thyme (batch 2)	*Thymus citriodorus*
Mutiati	*Colophospermum mopone*
Orange essence oil	*Citrus sinensis*
Oregano	*Oregano viridans*
Rosemary (batch 1)	*Rosmarinus officialis*
Rosemary (batch 2)	*Rosmarinus officialis*
White eucalyptus	*Eucalyptus alba*

lates on PDA containing 0.01% (v/v) Tween 80, without EO. Colony diameters were measured over a 13 d period at 25 °C, and the growth inhibition factor was calculated using formula 1 (above). This experiment was carried out using biological triplicates.

Essential oil encapsulation

The three EOs exhibiting the greatest antifungal activity against the *S. vesicarium* isolates, as identified in the EO screening, were encapsulated with modified maize starch using a spray-drying technique (HI-CAP® 100) as the capsule wall material, following the methods described by Baranauskiene and Venskutonis (2009), with some modifications. The emulsions were prepared by homogenizing each EO (at concentrations of 15% or 30% w/w) in previously prepared aqueous solutions of HI-CAP® 100 (30% w/w), using an Ultra-Turrax mixer at 1,600 rpm for 5 min. Spray-drying was carried out using a Büchi B-290 Mini Spray Dryer, with an inlet air temperature of 140 °C and a feed pump rate of 8%. Detailed study of the encapsulation efficiency, formulation optimization and release profiling were described in a complementary manuscript by Fernandes *et al.* (2026). The resulting microcapsules were stored in a desiccator protected from light until further use.

Effects of three essential oils on mycelium growth

A stock solution for each of the three EOs encapsulated with HI-CAP® 100 (with 15% or 30% of EO) was prepared by diluting each atomized sample in sterile distilled water. The assessed essential oils were mixed with PDA enriched with 0.01% (v/v) Tween 80 from the prepared stock solution to obtain the following encapsulated EO concentrations: 1, 10, 20, 40, or 80 mg mL^{-1}. The mixed PDA media were transferred to Petri plates, and a 0.5 × 0.5 cm mycelium square of each *S. vesicarium* or *A. arborescens* isolate was placed into each PDA plate. Resulting colony diameters were measured over a 13 d period at 25 °C, and the growth-inhibition factors were calculated using formula 1 (above). This experiment was carried out using biological triplicates.

Effects of two essential oils on conidium germination

The two most effective encapsulated EOs against mycelium growth of the four fungi were used to evaluate their effectiveness for inhibiting germination of *S. vesicarium* or *A. arborescens* conidia.

Each atomized sample with 15 or 30% of EO was diluted in sterile distilled water and mixed with PDA containing 0.01% (v/v) Tween 80, to obtain EO concentrations of 20 or 10 mg mL^{-1}, respectively. The mixed PDA medium was transferred to Petri plates and 10 µL of previously prepared conidium suspension (1 to 3×10^3 mL^{-1}) was inoculated in the centre of each plate. Resulting colony diameters were measured over a 13 d period at 25 °C, and growth inhibition factors were calculated using formula 1 (above). This experiment was carried out using biological triplicates.

Chemical characterization of the three most active essential oils

The chemical compositions of the three EO exhibiting the greatest antifungal activity were analysed using gas chromatography–mass spectrometry (GC–MS) analysis. This was carried out using an Agilent 6890 gas chromatograph coupled to an Agilent 5973 N mass selective detector (Agilent Technologies). Samples (each of 1 µL) were injected into a fused-silica capillary column (HP-5MS; 30 m × 0.32 mm internal diameter, 0.25 µm film thickness; 5% diphenyl, 95% dimethylpolysiloxane; Agilent Technologies) via a vaporization injector maintained at 250 °C in the spitless mode (2 min). The oven temperature programme started at 45 °C (held for 1 min), then increased at 5 °C min-

^{1} to 250 °C, and this temperature was then maintained 5 min, resulting in a total run time of 47 min. Helium was used as the carrier gas, at a linear velocity of 30 cm s^{-1}. The temperature of the transfer line was set at 280 °C, the ion source at 230 °C, and the quadrupole analyser at 150 °C, and a turbo molecular pump (10-5 torr) was used. Ionization was achieved by electron impact at 70 eV, and mass spectra were acquired in full-scan mode over a mass range of 40–400 Da. A solvent delay of 3 min was applied. Data acquisition and instrument control were carried out using MSD ChemStation software (G1701CA, version C.00.00; Agilent Technologies). Compound identification was based on comparisons of calculated retention indices, relative to a standard mixture of n-alkanes, and by matching the obtained mass spectra with those available in the Wiley spectral library (G1035B, Rev D.02.00; Agilent Technologies). Semi-quantitative analyses were carried out using normalized peak area percentages without the application of correction factors.

Statistical analyses of data

The analyses were each carried out with three replicates. A two-way analysis of variance (ANOVA) was used to determine whether there were statistically significant differences between experimental group means, using Prism software packages (GraphPad Software version 9.5.0). *Post hoc* tests for assessment of statistically significant differences of factors were carried out using Tukey's and Šídák's multiple comparisons tests. The experiments were carried out with a confidence level of 95%, and statistical significance was assumed at $P < 0.05$.

RESULTS

Fungi isolated from 'Rocha' pear material with symptoms of BSP

Four fungus isolates were obtained from symptomatic 'Rocha' pear tissues, three from pear fruits, and one from a leaf. The multilocus phylogenetic analysis based on ITS and *gpd* sequences (Figure 1A) showed that isolates MUM 26.01 and MUM 26.02 clustered consistently with reference isolates of *S. vesicarium* (CBS 133914, CBS 274.31, CBS 191.86T e CBS 192.86T), forming a clade with strong bootstrap support (99%), confirming identification of both isolates as *S. vesicarium*. Figure 1B shows the phylogenetic tree for *Alternaria* based on concatenated sequence analysis of the ITS region, and *gpd* and *alt-a1* genes. Isolates MUM 26.03 and MUM 26.04 grouped together with reference isolates of *A. arborescens* (CBS 109730, CBS 102605T), forming a highly supported clade with bootstrap values of 96%. This strong support confirmed identification of MUM 26.03 and MUM 26.04 as *A. arborescens.*

Assessments of sensitivity of fungi to commercial fungicides

The inhibitory efficacy of the five tested commercial fungicides on mycelium growth depended on fungus species and isolates, as show in Figure 2A. *Alternaria arborescens* MUM 26.03 was more resistant to copper complex and tebuconazole, with mean percent inhibition of 22.6 ± 2.8% for copper complex and 49.6 ± 2.8% for tebuconazole, whereas isolate MUM 26.04 had greater tolerance to the three other fungicides assessed. For *S. vesicarium*, isolate MUM 26.02 was more sensitive to copper complex and fluxapyroxad, reaching mean percent inhibition of 39.7 ± 2.8% for copper complex and 60.9 ± 10.8% for fluxapyroxad. Cyprodinil was most effective against *S. vesicarium* MUM 26.01, achieving mean percent inhibition of 88.7 ± 1.0%.

Among the five fungicides assessed, tebuconazole and cyprodinil gave the greatest levels of inhibition for all four isolates. In contrast, trifloxystrobin and copper complex were the least effective treatments, mean percent inhibitions less than 33.1 ± 3.8%. Fluxapyroxad showed variable effectiveness. While this fungicide had moderate activity against *S. vesicarium* isolate MUM 26.02, its effect on *S. vesicarium* MUM 26.01 was minimal (mean inhibition = 12.1 ± 2.0%), and its inhibition of the *Alternaria* isolates was also comparatively low, ranging from a mean reduction of 18.6 ± 2.1% to 36.8 ± 6.6%.

The fungicides also induced visible alterations in the colony morphologies compared to the experimental controls. Representative examples are shown in Figure 2. For *S. vesicarium* MUM 26.01, exposure to copper complex, tebuconazole, or cyprodinil produced whitish colonies, in contrast to the characteristic pigmentation observed in the controls (Figure 2 B). In contrast, *S. vesicarium* MUM 26.02 showed no evident morphological alterations under the tested conditions. For A. *arborescens* MUM 26.04, the copper complex produced colonies that were dark brown, whereas cyprodinil led to noticeably lighter coloured colonies (Figure 2 C). Similarly, *A. arborescens* MUM 26.03 also had darkened colonies when exposed to copper complex.

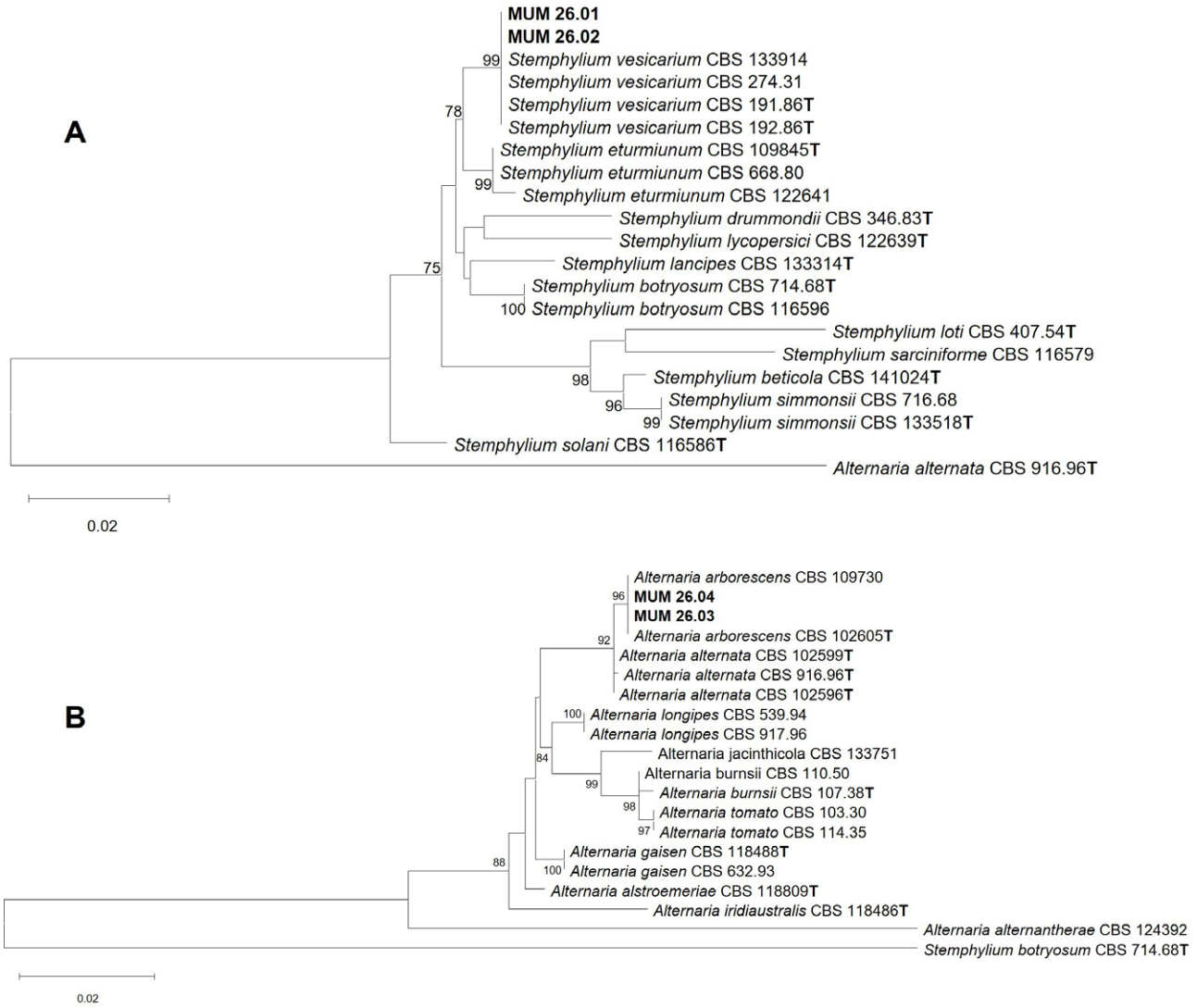

Figure 1. Identifications of the fungi isolated from 'Rocha' pear material with BSP. A, Phylogenetic tree of *Stemphylium*. B, Phylogenetic tree of *Alternaria*. Bootstrap values less than 70% were omitted from the figure.

Antifungal effects of essential oils against pathogenic fungi isolated from 'Rocha' pear with BSP symptoms

Antifungal activity of free essential oils

Eighteen EOs, at concentrations of 1, 5, 10 or 50 µL mL^{-1}, were evaluated against two *S. vesicarium* isolates. All the EOs at 50 µL mL^{-1} inhibited *S. vesicarium*, after 13 d of incubation (Table 3). However, lemon eucalyptus (batch 1), mutiati or orange EOs did not fully inhibit mycelium growth. At 10 µL mL^{-1}, most of the EOs were less inhibitory to mycelium growth of the two *S. vesicarium* isolates. Lemon eucalyptus (batch 2), lemongrass, and lemon thyme (batch 2) EOs gave complete growth inhibition at concentrations of 10 and 0.5 µL mL^{-1}. At 1 µL mL^{-1}, these three EOs had different effects, depending on the *S. vesicarium* isolate: lemongrass and lemon thyme (batch 2) prevented growth of *S. vesicarium* MUM 26.02, but were less effective against *S. vesicarium* MUM 26.01. Among these three EOs, lemon eucalyptus (batch 2) had the least antifungal activity at the lowest concentration assessed.

Based on the results of this initial screening, three EOs – lemon eucalyptus (batch 2), lemongrass, and lemon thyme (batch 2) – were selected for encapsulation assays (Fernandes *et al.*, 2026) and subsequently for the other experiments.

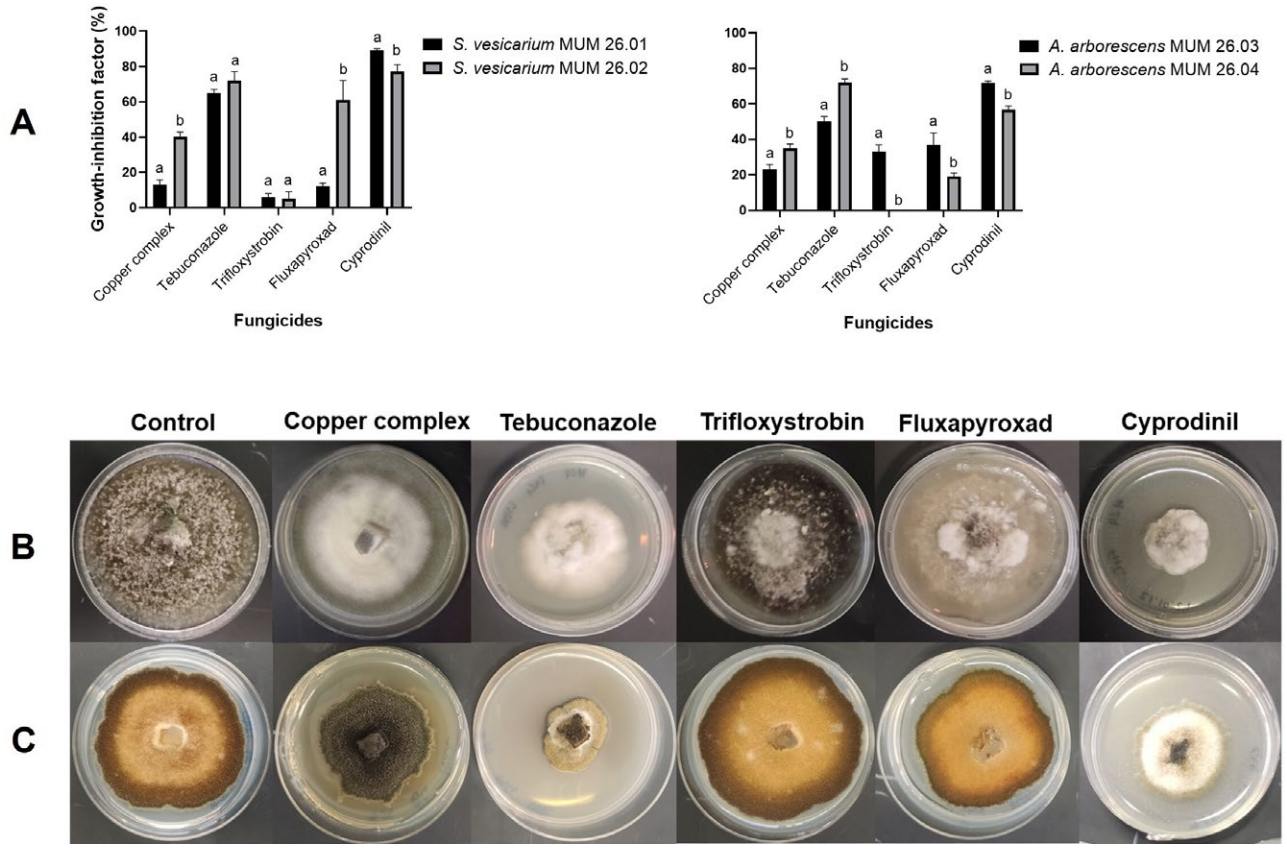

Figure 2. Effects of commercial fungicides on mycelium growth of fungi isolated from 'Rocha' pear material with BSP. A, Mean growth inhibition (%) of *Stemphylium vesicarium* or Alternaria arborescens isolates in the presence of the five assessed fungicides, after 13 d incubation at 25 °C (different letters indicates differences ($P < 0.05$) within each fungicide. B and C, Images of Petri plates containing colonies of *S. vesicarium* isolate MUM 26.01 (B) or *A. arborescens* MUM 26.04 (C) in the presence of two tested fungicides, after 13 d of incubation at 25 °C.

Effects of essential oils encapsulated with HI-CAP® 100 on mycelial growth

From the initial screening, the three most effective EOs (lemon eucalyptus, lemongrass, and lemon thyme) were encapsulated by spray-drying using HI-CAP® 100, with oil concentrations of 15 and 30%. The six EO formulations were tested against the two *S. vesicarium* isolates at different concentrations in PDA. As shown in Figure 3, all the formulations maintained their antifungal activity, inhibiting growth of the two *S. vesicarium* isolates. Lemon eucalyptus EO formulations did not fully prevent mycelium growth. The greatest observed mean inhibition from the 15% formulation was 70.4 ± 3.8% for *S. vesicarium* MUM 26.01 and 59.5 ± 1.1% for *S. vesicarium* MUM 26.02. For the 30% formulation and at the greatest concentration of 80 mg mL^{-1}, mean inhibition was 57.0 ± 2.1% for *S. vesicarium* MUM 26.01 and 71.8 ± 1.1% for *S. vesicarium* MUM 26.02. In contrast, the lemongrass and lemon thyme EO formulations gave greater isolate inhibition. Minimum mean effective inhibitory concentration for the lemongrass and lemon thyme EO formulations was observed at 20 mg mL^{-1} for both *S. vesicarium* isolates from 15% of EO encapsulated (Figure 3 A), and at 10 mg mL^{-1} for both isolates at 30% of encapsulated EO (Figure 3 B). At the 15%, both formulations completely inhibited growth of *S. vesicarium* MUM 26.02 at 10 mg mL^{1}, whereas, at the same concentration against strain MUM 26.01, lemongrass and lemon thyme EOs reduced growth by, respectively, 3.0 ± 1.0% and 37.0 ± 13.1%. The encapsulating agent HI-CAP® 100 was also tested in the absence of EOs against the two *S. vesicarium* isolates, and caused less than 3% inhibition of mycelium growth (Figure S1).

Figure 4 shows effects of encapsulated lemon eucalyptus, lemongrass, or lemon thyme EOs using HI-CAP® 100 at 15 or 30% (respectively, 20 or 10 mg mL^{-1}) on the two *A. arborescens* isolates. The inhibitory effects were similar to those observed against *S. vesicarium*. The formulations of lemongrass and lemon thyme EOs with HI-CAP® 100 completely inhibited both *A. arborescens* iso-

Table 3. Proportions (%) of mycelium growth inhibition (after 13 d in culture at 25 °C) for two *Stemphylium vesicarium* isolates (MUM 26.01 or MUM 26.02) exposed to four concentrations of different essential oils

Essential oil	Essential oil concentration (μL mL^{-1})							
	50		10		5		1	
	MUM 26.01	MUM 26.02	MUM 26.01	MUM 26.02	MUM 26.01	MUM 26.02	MUM 26.01	MUM 26.02
Basil	100%	100%	60%	50%	-	-	-	-
Eucalyptus (batch 1)	100%	100%	60%	33%	-	-	-	-
Eucalyptus (batch 2)	100%	100%	100%	88%	-	-	-	-
Eucalyptus (batch 3)	100%	100%	86%	50%	-	-	-	-
Laurel	100%	100%	86%	83%	-	-	-	-
Lavander	100%	100%	100%	40%	-	-	-	-
Lemon eucalyptus (batch 1)	83%	86%	-	-	-	-	-	-
Lemon eucalyptus (batch 2)	100%	100%	100%	100%	100%	100%	47%	34%
Lemongrass	100%	100%	100%	100%	100%	100%	61%	100%
Lemon mint	100%	100%	57%	38%	-	-	-	-
Lemon thyme (batch 1)	100%	100%	54%	30%	-	-	-	-
Lemon thyme (batch 2)	100%	100%	100%	100%	100%	100%	61%	100%
Mutiati	80%	86%	-	-	-	-	-	-
Orange essence oil	50%	40%	-	-	-	-	-	-
Oregano	100%	100%	86%	73%	-	-	-	-
Rosemary (batch 1)	100%	100%	86%	88%	-	-	-	-
Rosemary (batch 2)	100%	100%	80%	63%	-	-	-	-
White eucalyptus	100%	100%	51%	33%	-	-	-	-

lates while the lemon eucalyptus EO formulation did not fully inhibit the two isolates. For the MUM 26.03 isolate, the mean inhibition percentages were 38.7 ± 1.2% for the 15% formulation and 33.6 ± 1.2% for the 30% formulation. In contrast, for the MUM 26.04 isolate, the mean inhibition percentages were 49.6 ± 2.1% for the 15% formulation and 44.5 ± 0.0% for the 30% formulation.

Effect of EO encapsulated with HI-CAP® 100 on conidium germination

The antifungal activity of lemongrass and lemon thyme EO HI-CAP® 100 formulations encapsulated with 15 or 30% of each oil were also evaluated for effects on germination of *S. vesicarium* and *A. arborescens* conidia, at concentrations of 20 or 10 mg mL^{-1} on PDA. Figure 5 shows that all these formulations completely inhibited conidium germination and subsequent growth of each isolate of both fungi.

Chemical characterization of three active essential oils

The chemical compositions of the lemongrass, lemon thyme, and lemon eucalyptus EOs were analysed using gas chromatography (GC) and gas chromatography-mass spectrometry (GC-MS). The chemical compositions of the lemongrass, lemon thyme, and lemon eucalyptus EOs are shown in Table 4. Gas chromatography showed that lemongrass EO was mainly composed of citral isomers, with trans-citral and cis-citral together constituting greater than 88% of the total composition. Lemon thyme EO consisted predominantly (72.6%) of oxygen-containing monoterpenes, among which geraniol, 1,8-cineol, and thymol were the most abundant components. The citral isomers, geranial and neral, were also detected in the lemon thyme EO, but accounted for less than 8% of total composition. The chemical composition of lemon eucalyptus EO showed a predominance of monoterpene hydrocarbons, with α-pinene as the major constituent, accounting for 51.6% of the total composition. Eucalyptol (1,8-cineole) (12.9%) and ρ-cymene (10.7%) were the second and third most abundant compounds in this oil.

DISCUSSION

Brown spot of pear, caused by *S. vesicarium*, has become a major concern for 'Rocha' pear production in Portugal (Loebler *et al*., 2020; Cavina *et al*., 2024). In the present study, *S. vesicarium* was isolated from symptomatic 'Rocha' pear tissues, and *A. arborescens* was also

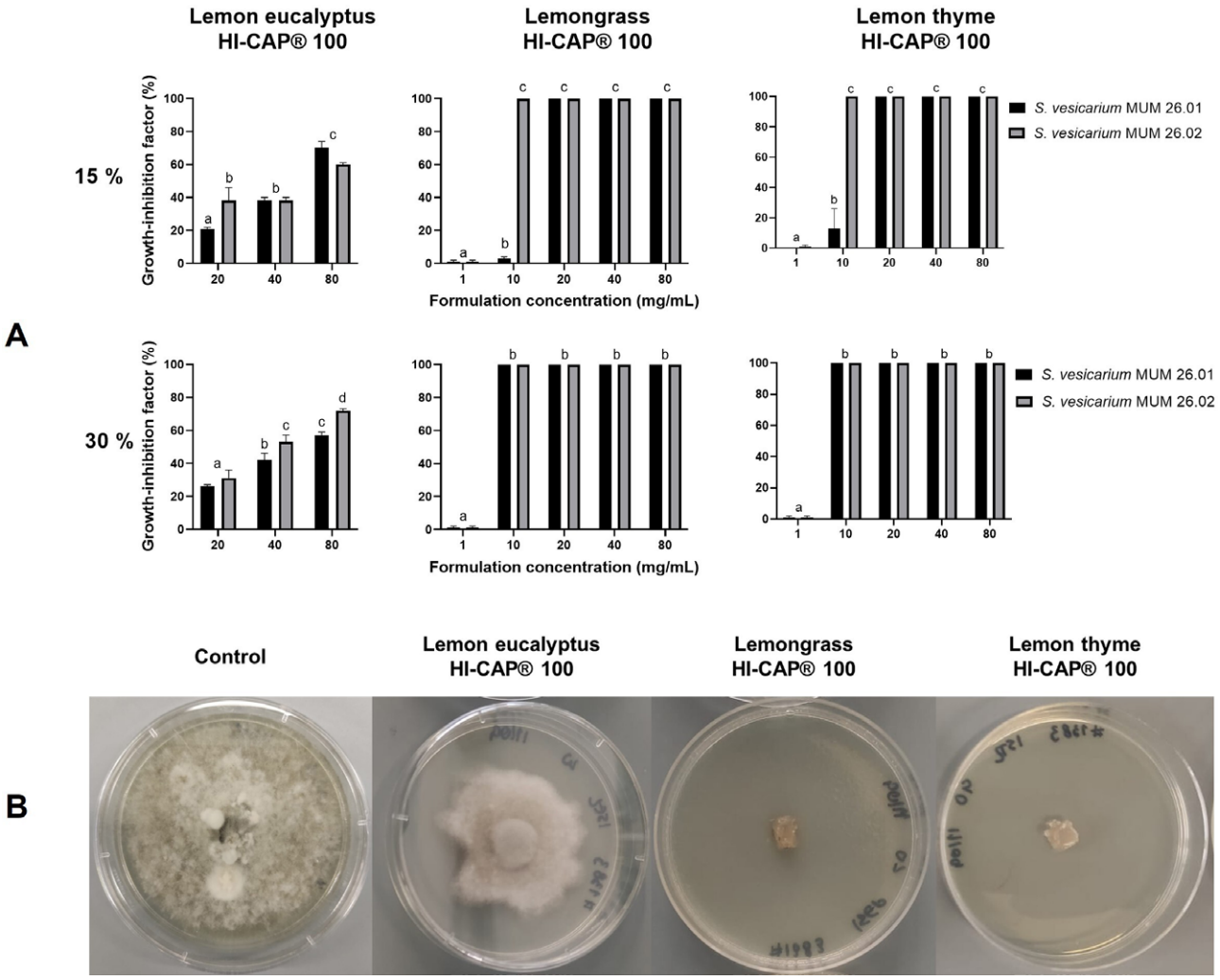

Figure 3. A) Mean percentages of growth inhibition in cultures of two *Stemphylium vesicarium* isolates (MUM 26.01 and MUM 26.02) exposed for 13 d at 25 °C to different concentrations of three essential oils encapsulated with HI-CAP® 100 at 15 or 30% of each oil. Means accompanied by different letters are different ($P < 0.05$). B) Images of cultures of *S. vesicarium* isolate MUM 26.02 with (left) no additive to the culture medium, or with lemon eucalyptus (second left), lemongrass (second right) or lemon thyme (right) EO HI-CAP® 100 formulations (20 mg mL^{-1}) after 13 d at 25 °C.

isolated, indicating that both fungi may contribute to this disease. The presence of *A. arborescens* in 'Rocha' pear had previously been reported (Sobreiro and Batalha Neto, 2024), supporting the potential involvement of this fungus in the BSP disease complex.

Since fungicides remain the primary method for managing BSP (Toledo *et al.*, 2023), the sensitivity of particular pathogen isolates was evaluated for commercial fungicides commonly applied by Portuguese 'Rocha' pear producers. The results have shown that fungicide efficacy varied depending on active ingredient, fungal species, and on the specific isolates involved. This probably shows why discussions within the technical community based on observable incidence of the disease have not yielded conclusive results.

Among the assessed fungicides, tebuconazole and cyprodinil had greatest effectiveness, achieving incidence reductions of, respectively, 70% and 88%. In contrast, trifloxystrobin had no or little inhibitory activity (0% to 33%). Fluxapyroxad showed a variable pattern among the four pathogen isolates. Inhibition percentages of the two *S. vesicarium* isolates were approx. 12% and 60%. These results indicate that sensitivity of BSP fungal pathogens to specific fungicides may be diminishing, and that continued use of these products could increase losses of pathogen sensitivity.

Efforts to reduce the number of fungicide active ingredients used, in response to standards imposed by major retail chains, have aimed to minimize the num-

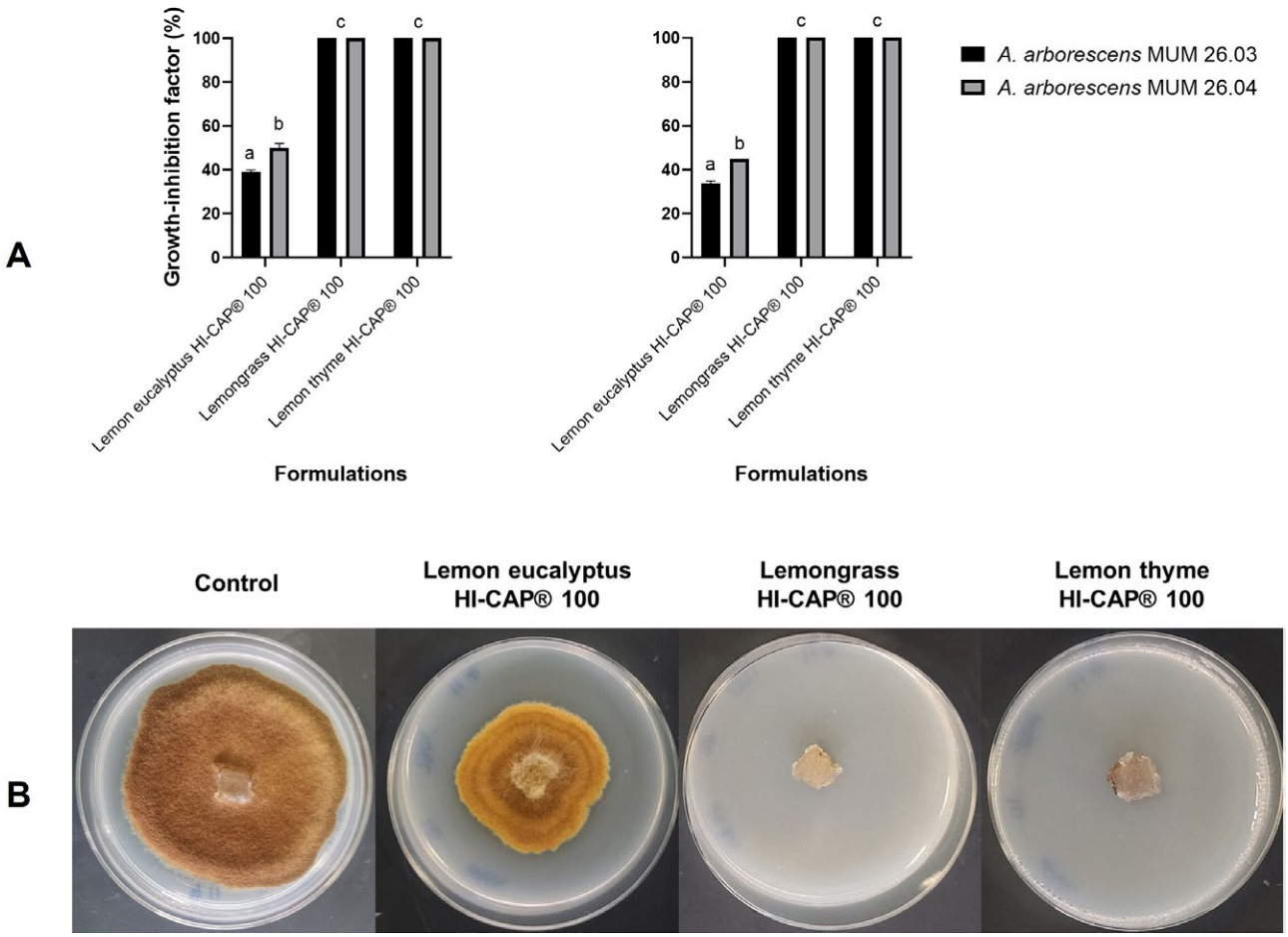

Figure 4. A) Mean percentages of growth inhibition in culture of two *Alternaria arborescens* isolates (MUM 26.03 and MUM 26.04) exposed for 13 d at 25 °C to three essential oils encapsulated with HI-CAP® 100 at 15% (20 mg mL^{-1}) and 30% (10 mg mL^{-1}) of each oil. Means accompanied by different letters are different ($P < 0.05$). B) Images of cultures of *A. arborescens* MUM 26.03 with (left) no additive to the culture medium, or with lemon eucalyptus (second left), lemongrass (second right) or lemon thyme (right) EO HI-CAP® 100 formulations (20 mg mL^{-1}) after 13 d at 25 °C.

ber of detectable pesticide substances, and this may have contributed to shifts in fungicide sensitivity, as a result of repeated applications of particular chemicals (Paušič *et al*., 2023; Olita *et al*., 2024). Previous studies have reported variable sensitivity profiles for different fungicide classes in *Stemphylium* and *Alternaria* isolates obtained from fruit crops. Strobilurin fungicides, including trifloxystrobin, have shown low efficacy against isolates of *Alternaria* (Camiletti *et al*., 2022) and *S. vesicarium* (Collina *et al*., 2007; Alberoni *et al*., 2010). In contrast, DMI fungicides, including tebuconazole, have exhibited lower risks for resistance development, and remain effective for inhibiting *Alternaria* spp. (He *et al*., 2019; Camiletti *et al*., 2022). *Alternaria* isolates have also demonstrated sensitivity to cyprodinil, although resistance to some SDHI fungicides (e.g. fluxapyroxad) has also been observed (Yang *et al*., 2015; Beg *et al*., 2025).

Copper-based products are recognized as effective contact fungicides, primarily used for preventative disease management since they reduce inoculum accumulation on plant surfaces (Lamichhane *et al*., 2018; La Torre *et al*., 2018). These products lack translaminar or systemic activity, so their curative efficacy against established fungal structures is limited compared to systemic fungicides, which can penetrate host tissues to control ongoing infections (McGrath, 2009), as shown by Donne *et al.* (2020) and Koka *et al.* (2021). This distinction was reflected in the present study, where the copper complex formulation assessed showed limited effectiveness against the *S. vesicarium* and *A. arborescens* isolates evaluated.

Beyond influencing pathogen mycelium growth, presence of fungicides also altered pigment production and colony structure of the two pathogens assessed. Exposure to copper complex fungicide consistently

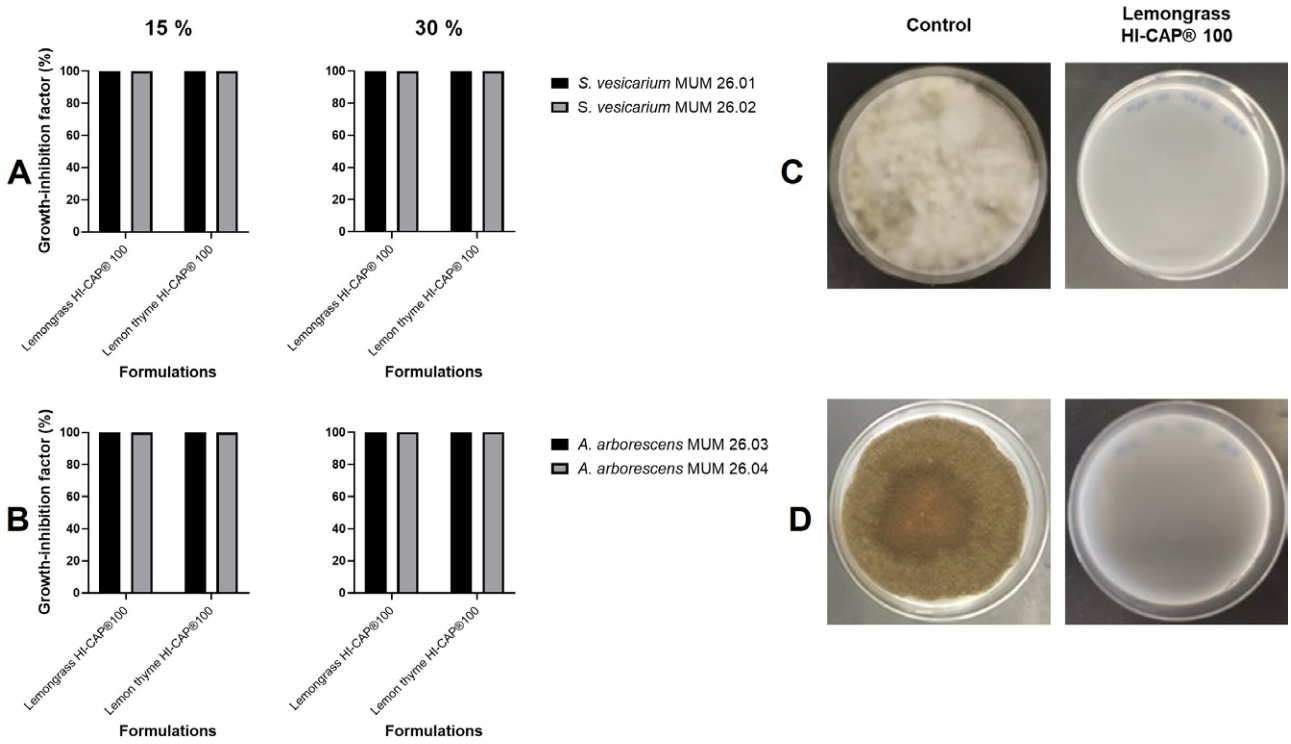

Figure 5. A) Mean percentages of growth inhibition in cultures of two *Stemphylium vesicarium* isolates (MUM 26.01 and MUM 26.02) grown from conidia and exposed for 13 d at 25 °C to two essential oils encapsulated with HI-CAP® 100 at 15% (20 mg mL^{-1}) or 30% (10 mg mL^{-1}) of each oil. No significant differences were observed ($P > 0.05$). B) Mean percentages of growth inhibition in cultures of two *Alternaria arborescens* isolates (MUM 26.03 and MUM 26.04) grown from conidia and exposed for 13 d at 25 °C to two essential oils encapsulated with HI-CAP® 100 at 15% (20 mg mL^{-1}) or 30% (10 mg mL^{-1}) of each oil. No significant differences were observed ($P > 0.05$). C) Images of cultures of *S. vesicarium* isolate MUM 26.01 with (left) no additive to the culture medium or with (right) lemongrass EO HI-CAP® 100 formulation at 15% (20 mg mL^{-1}) after 13 d at 25 °C. D) Images of cultures of *A. arborescens* isolate MUM 26.04 with (left) no additive to the culture medium or with (right) lemongrass EO HI-CAP® 100 formulation (20 mg mL^{-1}) after 13 d at 25 °C.

induced formation of dark brown colonies in both the *A. arborescens* isolates. This hyper-pigmentation may indicate an adaptative defence response to copper exposure, whereby increased melanin synthesis sequesters copper ions within the fungus cell walls and reduces oxidative stress associated with copper-induced free radicals (Fogarty and Tobin, 1996; Borkow and Gabbay, 2005). Conversely, copper, tebuconazole and cyprodinil all triggered an opposite response, resulting in whitish appearance in *S. vesicarium* MUM 26.01. This suggests that these three fungicides in contact with the *S. vesicarium* isolate probably disrupted biosynthesis of secondary metabolites, including the melanin pigments, which play important roles for cell protection (Cordero and Casadevall, 2017). *Stemphylium vesicarium* MUM 26.02 produced no visible changes in morphology, highlighting that the macroscopic shifts observed were isolate and treatment dependent.

Similar effects have been documented elsewhere. Changes in *Aspergillus flavus* pigmentation from green to white, and darkened colonies in *Cladosporium cladosporioides*, when exposed to different fungicides, have been previously reported (Llorente *et al*., 2012a; Akbari Dana *et al*., 2019). In addition, previous studies have shown that copper-based compounds can induce formation of dark pigments in fungi (Griffith *et al*., 2007), indicating that fungicides can trigger physiological stress responses manifested as morphological alterations. These results are consistent with the variable pathogen sensitivity patterns described elsewhere, and highlight the ongoing challenges for identifying fungicide efficacy against BSP pathogens.

To address this problem, focus is shifting towards exploring alternative biobased disease management strategies, which are environmentally friendly and less likely to inducing pathogen resistance. EOs are promising biocontrol agents due to their broad spectrum antifungal properties and natural origins (Nazzaro *et al*., 2017). Therefore, the present study aimed to identify plant-derived EOs able to control growth of pathogens associated with BSP. From 18 EOs assessed against the

Table 4. Chemical characterizations of lemongrass, lemon thyme, and lemon eucalyptus essential oils

Essential oil	Components	Content (%)
Lemongrass	Trans-citral (geranial)	46.8
	Cis-citral (neral)	41.6
	Nerol	4.0
	2-methyl-3-butene-2-ol	1.7
	6-methyl-5-heptene-2-one	1.4
	Cis-carveol	1.1
	Linalyl acetate	0.9
Lemon thyme	Oxygen-containing monoterpenes, including:	72.6
	Geraniol	27.5
	1,8-Cineol	16.3
	Thymol	9.2
	Geranial	4.2
	Neral	3.4
	α-Terpineol	2.2
	Sesquiterpenes hydrocarbons, including:	9.5
	E-Caryophyllene	3.3
	ρ-Cymene	3.7
	γ-Terpinene	2.1
Lemon eucalyptus	α-Pinene	51.6
	Eucalyptol (1,8-Cineol)	12.9
	ρ-Cymene	10.7
	Aromadendrene	5.6
	γ-Terpinene	4.7
	Limonene	3.4
	α-Phellandrene	1.6
	Bicyclogermacrene	1.0

S. vesicarium isolates, those from lemon eucalyptus, lemongrass, or lemon thyme had high antifungal activities, completely inhibiting *S. vesicarium* growth at 5 μL mL^{-1}. Lemongrass and lemon thyme also controlled growth of *S. vesicarium* MUM 26.02 at 1 μL mL^{-1}.

This strong antifungal activity aligned with previous reports. High inhibition rates against phytopathogenic fungi using encapsulated and non-encapsulated lemongrass EO have been reported (Antonioli *et al.*, 2020; Sattary *et al.*, 2020; Gangavarapu and Palwai, 2022). Although studies on the fungicidal effects of lemon thyme EO against plant pathogens are limited, the strong antimicrobial effects have been reported against *Cutibacterium acnes* (Oliveira *et al.*, 2022). Geraniol, the main constituent of lemon thyme EO, has also shown inhibitory activity against *Aspergillus* spp. (Tang *et al.*, 2018). Lemon eucalyptus EO has also been reported to reduce growth of *A. alternata*, *Colletotrichum gloesporioides* and *Fusarium oxysporum*, which are key pathogens associated with postharvest rot in apples (Oli *et al.*, 2019). Despite the strong antifungal activity exhibited by the EO in the present study, the treated plants were not free from disease. For instance, *Golovinomyces biocellatus* has been reported to cause powdery mildew on lemon thyme (*Thymus citriodorus*) in Italy (Garibaldi *et al.*, 2016). This highlights that, despite the antimicrobial properties associated with secondary aromatic plant metabolites, natural *in planta* concentrations may not always be sufficient to prevent pathogen establishment. However, concentrated EO extracts can still have significant antifungal activity when applied exogenously against phytopathogens.

To mitigate the common challenges of volatility and degradation of chemicals containing EOs, encapsulation techniques have been proposed for improving EO stability, potentially contributing to enhanced bioactivity (Antonioli *et al.*, 2020; Altay *et al.*, 2024). Therefore, based on their high antifungal activities in the initial screening of the present study, lemon eucalyptus, lemongrass, and lemon thyme EOs were subsequently encapsulated by spray-drying using a modified maize starch (HI-CAP® 100) and EO concentrations of 15% or 30%, to evaluate how the transition from free liquid to solid microcapsule may affect their bioactivity (Fernandes *et al.*, 2026). Both lemongrass and lemon thyme EO formulations completely inhibited *S. vesicarium* growth, at a minimum concentration of 20 mg mL^{-1} for the 15% formulations, and 10 mg mL^{-1} for the 30% formulations. This showed that spray-drying did not compromise the active constituents, and demonstrated the effectiveness of the polymer matrices.

Lemon eucalyptus EO gave decreased efficacy after encapsulation, and did not fully inhibit fungal growth at the concentrations tested, with inhibition percentages ranging between 30% and 70% among all conditions assessed. Similar results were obtained for the two *Alternaria* isolates. These results indicate that the antifungal activity of lemongrass and lemon thyme EOs was not compromised by encapsulation, validating their selection from the initial screening, and supporting their potential as encapsulated formulations for EO-based products. Previous studies have compared antifungal activities of free and encapsulated EOs. Soltanzadeh *et al.* (2021) reported lower antifungal activity of encapsulated lemongrass EO against *A. flavus*, *Penicillium notatum* and *F. solani* compared with the free oil, which completely inhibited fungal growth. Antonioli *et al.* (2020) stated that lemongrass EO containing poly(lactic acid) nanocapsules efficiently reduced *C. acutatum* and *C. gloesporioides*, but a high concentration was required compared to free EO. Formulations of *Cinnamomum cassia* EO,

both free and spray-dried encapsulated, were strongly antifungal against *A. alternata*, *A. flavus* and *P. crustosum* (Minozzo *et al*., 2023). Sattary *et al.* (2020) showed that antifungal effects of encapsulated lemongrass and clove EOs was greater than from the free EOs.

Stemphylium vesicarium and *A. arborescens* conidia are important in the crop diseases they cause, affecting pome fruit and vegetables (Fontaine *et al*., 2021; Gossen *et al*., 2021; Habib *et al*., 2021; Głos *et al*., 2023). For the BSP complex, *S. vesicarium* primarily overwinters in pear orchards as pseudothecia, releasing ascospores of *P. allii* under favourable climate conditions in the spring (Llorente *et al*., 2010). These sexual spores contribute to saprophytic colonization of plant residues, which become the principal sources of conidia as the main inoculum responsible for infections during pear growing seasons (Cavina *et al*., 2024). Given the central role of conidia in disease initiation and spread, controlling conidium germination is essential for lowering disease pressure and managing BSP. In the present study, effects of lemongrass and lemon thyme EO HI-CAP® 100 formulations were evaluated against *S. vesicarium* and *A. arborescens* conidium germination. Under the concentrations assessed (20 mg mL^{-1}, for the 15% formulations, and 10 mg mL^{-1}, for the 30% formulations), the EOs completely inhibited conidium germination. These results further confirm the antifungal potential of these selected EOs, demonstrating their effectiveness for inhibiting pathogen mycelium growth and conidium germination.

The chemical characterizations of the lemongrass, lemon thyme, and lemon eucalyptus EOs showed distinct chemical profiles. The lemongrass and lemon thyme EOs mainly contained oxygenated monoterpenes, including citral, geraniol, 1,8-cineole, and thymol. For plant protection, geraniol, the main constituent (27.5%) of lemon thyme EO, is of particular interest. This compound reduced mycelium growth of *Drechslera oryzae*, *F. oxysporum* and *Sclerotium rolfsii* (Kaur *et al*., 2019). Beyond plant protection, recent trials have demonstrated that incorporating geraniol into biodegradable composite coatings reduced incidence and lesion severity caused by *Monilinia fructicola* in plum fruit during cold storage (Asgarian *et al*., 2023). Geraniol is also listed as an approved active substance under Commission Implementing Regulation (EU) No. 540/2011, highlighting its safety and efficacy for use in plant protection products.

Citral was the main compound (88.4%) present in lemongrass EO. Citral has demonstrated protective activity in fruit systems by inhibiting mycelium growth, while also being recognized as a food flavouring agent in Commission Implementing Regulation (EU) No. 872/2012. Citral application successfully controlled mycelium growth and reduced lesion diameter caused by *A. alternata* in pitaya fruit storage (Luo *et al*., 2024), and on pears (Chen *et al*., 2025). Tao *et al.* (2014) also reported that this compound inhibited mycelium growth of *P. italicum*, an important postharvest citrus pathogen. In contrast, lemon eucalyptus EO was composed mostly of monoterpene hydrocarbons, including α-pinene (51.6%), along with lower proportion of 1,8-cineole (12.9%). Aldehydes and alcohols, including citral and geraniol, interact strongly with fungal cell membranes due to their high lipophilicity (Bakkali *et al*., 2008). Upon entering the phospholipid bilayers, they enhance membrane fluidity and permeability, potentially causing the leakage of ions and essential metabolites (Trombetta *et al*., 2005). Furthermore, aldehydes, including citral, are chemically active, and can create Schiff bases or other covalent compounds with membrane proteins. This may disrupt enzyme activities and disturb cellular equilibria (Hyldgaard *et al*., 2012). Additionally, disruption of production of ergosterol, an essential sterol for fungal membranes, can be important. Monoterpenes such as citral, geraniol, and thymol, may interfere with this process, resulting in compromised integrity of cell membranes and reduced fungal growth (Contreras Martínez *et al*., 2022). Low abundance of these oxygenated compounds in lemon eucalyptus EO may therefore account for the reduced antifungal activity against *S. vesicarium* and *A. arborescens*, compared to lemongrass and lemon thyme EOs, as was observed in the present study.

Overall antifungal efficacy cannot be solely attributed to the major EO compounds. Minor elements, while in limited amounts, can modify plant and pathogen membrane permeability or assist substance penetration, enhancing their antifungal properties (Burt, 2004). For example, 1,8-cineole has been identified as a permeabilizing agent; it improves movement of other monoterpenes across lipid bilayers (Trombetta *et al*., 2005). Synergy has been shown between citral and geraniol, which collectively improve membrane disruption and respiratory inhibition in different fungal pathogens. These connections clarify why EOs often exert stronger influences than individual compounds, as observed in previous research (Shukla *et al*., 2012; Soares *et al*., 2016).

Ongoing debate supported by an increasingly body of evidence, suggests that the antifungal activity is primarily driven by the major active compounds. Studies on *C. cassia* and *Cymbopogon martini* EOs have concluded that high-content components including trans-cinnamaldehyde and trans-geraniol accounted for the majority of inhibitory effects against toxigenic fungi (Wang *et al*., 2018). Similarly, research on EO from *Thymus vulgaris* has shown that the phenolic compound thymol outper-

formed the whole EO for control of *A. alternata* growth (Perina *et al*., 2015; Andrade-Ochoa *et al*., 2023). From a product development perspective, this duality is important, since identification of individual active compounds may facilitate product regulation. Further research is required to clarify the relative contributions of major and minor compounds to antifungal efficacy, and to determine the most suitable approaches for future development of plant protection products.

CONCLUSIONS

This study aimed to identify EOs with antifungal activity against pathogenic fungi isolated from 'Rocha' pears exhibiting BSP symptoms, and to validate their efficacy as encapsulated formulations developed through spray-drying. Of the 18 EOs assessed, low concentrations of lemongrass and lemon thyme EOs completely inhibited mycelium growth and conidium germination of *S. vesicarium* and *A. arborescens* isolates with different pesticide sensitivity profiles, which had been isolated from 'Rocha' pear material exhibiting BSP symptoms. Their antifungal activities were retained after encapsulation, indicating their potential for practical disease management applications. These results highlight that EOs are potential alternatives to conventional fungicides, with advantages in biodegradability and reduced risk of development of pathogen resistance. As existing disease management solutions have proven ineffective, and fungicide resistance is increasingly compromising crop viability and profitability, EOs may be promising tools to mitigate decline of 'Rocha' pear cropping. Nevertheless, since the present study was conducted exclusively under *in vitro* conditions, further *in vivo* and field studies are required to validate the efficacy of these EO formulations. Future research should first assess their antifungal effectiveness and potential phytotoxic effects directly on 'Rocha' pear fruit, before progressing to field-scale assessments. Subsequent studies should also evaluate formulation persistence, stability, and performance after application, considering the influence of environmental factors on antifungal activity.

CREDIT AUTHORSHIP CONTRIBUTION STATEMENT

Inês Mendonça: conceptualization, investigation, formal analyses, and writing of the original draft manuscript. Beatriz Fernandes: conceptualization, investigation, formal analyses. Carmo Serrano: Conceptualization, writing, review, and manuscript editing. Ana C. Marques: writing, review, and manuscript editing. Ricardo Oliveira: Investigation, formal analysis, writing, review and manuscript editing. Carina Almeida: writing, review and manuscript editing, funding acquisition. Miguel Leão de Sousa: writing, review, and manuscript editing. Armando Venâncio: writing, review, and manuscript editing, funding acquisition. Sónia Silva: conceptualization, writing, review and manuscript editing, funding acquisition.

ACKNOWLEDGEMENTS

The authors thank the Associação Nacional de Produtores de Pera Rocha (ANP), for their support and interaction throughout the development of this project. This study was supported by the Portuguese Foundation for Science and Technology (FCT) under scope of the strategic funding of UIDB/04469/2020 unit, with DOI 10.54499/UIDB/04469/2020, and by the Associate Laboratory in Biotechnology, Bioengineering and Microelectromechanical Systems (LABBELS), LA/P/0029/2020, and the GREEN-IT Research Centre "Biological Resources for Sustainability" Base Funding, DOI 10.54499/04551/2020. Inês Mendonça also acknowledges FCT for the fellowship 2023.04778.BDANA. Sónia Silva also thanks FCT for the CEEC Institutional (https://doi.org/10.54499/CEECINST/00018/2021/CP2806/CT0003), The authors also acknowledge FCT for supporting the project "Pacto da Bioeconomia Azul" (PRR-C644915664-00000026), and the NORTE 2030, Portugal 2030, and European Structural and Investment Funds for supporting the project BioNEXT: Integrated Platform for Sustainable Biotechnologies and Digital Transition.

LITERATURE CITED

Akbari Dana M., Hashemi S.J., Daei Ghazvini R., Khodavesi S., Modiri M., … Rezaie S., 2019. Effect of benomyl and diazinon on acquired azole resistance in *Aspergillus flavus* and expression of mdr1 and cyp51c genes. *Current Medical Mycology* 5: 27–32. https://doi.org/10.18502/cmm.5.2.1158.

Akhtari A., Davari M., Habibi-Yangjeh A., Ebadollahi A., Feizpour S., 2022. Antifungal Activities of Pure and ZnO-Encapsulated Essential Oil of *Zataria multiflora* on *Alternaria solani* as the Pathogenic Agent of Tomato Early Blight Disease. *Frontiers in Plant Science* 13: 932475. https://doi.org/10.3389/fpls.2022.932475.

Alberoni G., Cavallini D., Collina M., Brunelli A., 2010. Characterisation of the first *Stemphylium vesicarium* isolates resistant to strobilurins in Italian pear orchards. *European Journal of Plant Pathology* 126: 453–457. https://doi.org/10.1007/s10658-009-9559-3.

Altay Ö., Köprüalan Ö., İlter I., Koç M., Ertekin F.K., Jafari S.M., 2024. Spray drying encapsulation of essential oils; process efficiency, formulation strategies, and applications. *Critical Reviews in Food Science and Nutrition* 64: 1139–1157. https://doi.org/10.1080/10408398.2022.2113364.

Andrade-Ochoa S., Sánchez-Aldana D., Rodríguez-Valdez L.M., Nevárez-Moorillón G.V., 2023. In vitro and Quantitative and Structure Activity Relationship (QSAR) evaluation of the antifungal activity of terpenoid constituents of essential oils against *Alternaria alternata* and *Fusarium oxysporum*. *Biomédica* 43: 156–169. https://doi.org/10.7705/biomedica.6883.

Antonioli G., Fontanella G., Echeverrigaray S., Longaray Delamare A.P., Fernandes Pauletti G., Barcellos T., 2020. Poly(lactic acid) nanocapsules containing lemongrass essential oil for postharvest decay control: In vitro and in vivo evaluation against phytopathogenic fungi. *Food Chemistry* 326: 126997. https://doi.org/10.1016/j.foodchem.2020.126997.

Asgarian Z.S., Palou L., Souza R.F.L. de, Quintanilla P.G., Taberner V., … Pérez-Gago M.B., 2023. Hydroxypropyl Methylcellulose and Gum Arabic Composite Edible Coatings Amended with Geraniol to Control Postharvest Brown Rot and Maintain Quality of Cold-Stored Plums. *Foods* 12: 2978. https://doi.org/10.3390/foods12152978.

Bajac J., Nikolovski B., Petrović L., Nemeš T., Kostić M., … Mitrović I., 2025. Antimicrobial and insecticidal activity of spray dried juniper berry (*Juniperus communis* L.) essential oil microcapsules prepared by using gum arabic and maltodextrin. *International Journal of Biological Macromolecules* 306: 141128. https://doi.org/10.1016/j.ijbiomac.2025.141128.

Bakkali F., Averbeck S., Averbeck D., Idaomar M., 2008. Biological effects of essential oils – A review. *Food and Chemical Toxicology* 46: 446–475. https://doi.org/10.1016/j.fct.2007.09.106.

Baranauskiene R., Venskutonis P.R., 2009. Comparison of wall materials for the microencapsulation of thyme essential oil. In: *XVIIth International Conference on Bioencapsulation*, Groningen, Netherlands, 1–4.

Beg M.A., Aktaruzzaman Md., Lewis K.J., Oliver J.E., 2025. Fungicide resistance profiles of *Alternaria* spp. associated with fruit rot of blueberry in Georgia, USA. *Frontiers in Plant Science* 16: 1524586. https://doi.org/10.3389/fpls.2025.1524586.

Borkow G., Gabbay J., 2005. Copper as a Biocidal Tool. *Current Medicinal Chemistry* 12: 2163–2175. https://doi.org/10.2174/0929867054637617.

Burt S., 2004. Essential oils: their antibacterial properties and potential applications in foods – a review. *International Journal of Food Microbiology* 94: 223–253. https://doi.org/10.1016/j.ijfoodmicro.2004.03.022.

Camiletti B.X., Lichtemberg P.S.F., Paredes J.A., Carraro T.A., Velascos J., Michailides T.J., 2022. Characterization, pathogenicity, and fungicide sensitivity of *Alternaria* isolates associated with preharvest fruit drop in California citrus. *Fungal Biology* 126: 277–289. https://doi.org/10.1016/j.funbio.2022.02.003.

Castresana J., 2000. Selection of Conserved Blocks from Multiple Alignments for Their Use in Phylogenetic Analysis. *Molecular Biology and Evolution* 17: 540–552. https://doi.org/10.1093/oxfordjournals.molbev.a026334.

Cavina F., Baiocco S., Tomba L., Ravaglia F., Moretti C., … Bugiani R., 2024. A New Source of Inoculum for *Stemphylium vesicarium*: Consequences for the Management of Brown Spot of Pear. *Agronomy* 14: 2522. https://doi.org/10.3390/agronomy14112522.

Chen Y., Zeng Y., Li Y., Ye Z., Li L., Zhou Z., 2025. Antifungal effects of citral against *Alternaria alternata* in postharvest pear fruit and its potential mechanism. *Postharvest Biology and Technology* 223: 113424. https://doi.org/10.1016/j.postharvbio.2025.113424.

Collina M., Alberoni G., Brunelli A., 2007. First occurrence of strobilurin-resistant isolates of *Stemphylium vesicarium* in an Italian pear orchard. *Communications in Agricultural and Applied Biological Sciences* 72: 735–738.

Contreras Martínez O.I., Angulo Ortíz A., Santafé Patiño G., 2022. Mechanism of Antifungal Action of Monoterpene Isoespintanol against Clinical Isolates of *Candida tropicalis*. *Molecules* 27: 5808. https://doi.org/10.3390/molecules27185808.

Cordero R.J.B., Casadevall A., 2017. Functions of fungal melanin beyond virulence. *Fungal Biology Reviews* 31: 99–112. https://doi.org/10.1016/j.fbr.2016.12.003.

Corkley I., Fraaije B., Hawkins N., 2022. Fungicide resistance management: Maximizing the effective life of plant protection products. *Plant Pathology* 71: 150–169. https://doi.org/10.1111/ppa.13467.

de Sousa D.P., Damasceno R.O.S., Amorati R., Elshabrawy H.A., de Castro R.D., … Lima T.C., 2023. Essential Oils: Chemistry and Pharmacological Activities. *Biomolecules* 13: 1144. https://doi.org/10.3390/biom13071144.

Dereeper A., Guignon V., Blanc G., Audic S., Buffet S., … Gascuel O., 2008. Phylogeny.fr: robust phyloge-

netic analysis for the non-specialist. *Nucleic Acids Research* 36: W465–W469. https://doi.org/10.1093/nar/gkn180.

DGAV, 2024. *Caderno Técnico: A Estenfiliose da Pereira - Estratégia de Gestão de Resistência a Fungicidas*, Direção Geral da Alimentação e Veterinária, Lisboa, Portugal. Available at: https:/www.dgav.pt/. Accessed May 5, 2026.

Donne I., Higgins D.S., Brisco-McCann E., Hausbeck M.K., 2020. Limiting Fungal Foliar Diseases on Carrots for Organic and Conventional Markets. *Plant Health Progress* 21: 217–223. https://doi.org/10.1094/PHP-12-19-0096-RS.

Dorjee L., Gogoi R., Kamil D., Kumar R., Mondal T.K., … Gurung B., 2023. Essential oil-grafted copper nanoparticles as a potential next-generation fungicide for holistic disease management in maize. *Frontiers in Microbiology* 14: 1204512. https://doi.org/10.3389/fmicb.2023.1204512.

European Commission, 2011. *Commission Implementing Regulation (EU) No. 540/2011 of 25 May 2011 implementing Regulation (EC) No 1107/2009 of the European Parliament and of the Council as regards the list of approved active substances*. Official Journal of the European Union L153: 1–186. Available at: http://data.europa.eu/eli/reg_impl/2011/540/oj. Accessed May 26, 2026.

European Commission, 2012. *Commission Implementing Regulation (EU) No 872/2012 of 1 October 2012 adopting the list of flavouring substances provided for by Regulation (EC) No 2232/96 of the European Parliament and of the Council, introducing it in Annex I to Regulation (EC) No 1334/2008 of the European Parliament and of the Council and repealing Commission Regulation (EC) No 1565/2000 and Commission Decision 1999/217/EC*. Official Journal of the European Union L267: 1–161. Available at: http://data.europa.eu/eli/reg_impl/2012/872/oj. Accessed May 26, 2026.

Fernandes B., Mendonça I., Silva S., Sousa S., Matos C., … Serrano C., 2026. Encapsulation and Release Profiling of Antifungal Essential Oils via Spray Drying Analyzed by HS-SPME-GC-MS/MS. *Food Chemistry*.

Fincheira P., Jofré I., Espinoza J., Levío-Raimán M., Tortella G., … Rubilar O., 2023. The efficient activity of plant essential oils for inhibiting Botrytis cinerea and *Penicillium expansum*: Mechanistic insights into antifungal activity. *Microbiological Research* 277: 127486. https://doi.org/10.1016/j.micres.2023.127486.

Fogarty R. V., Tobin J.M., 1996. Fungal melanins and their interactions with metals. *Enzyme and Microbial Technology* 19: 311–317. https://doi.org/10.1016/0141-0229(96)00002-6.

Fontaine K., Fourrier-Jeandel C., Armitage A.D., Boutigny A.-L., Crépet M., … Aguayo J., 2021. Identification and pathogenicity of *Alternaria* species associated with leaf blotch disease and premature defoliation in French apple orchards. *PeerJ* 9: e12496. https://doi.org/10.7717/peerj.12496.

FRAC, 2025. *FRAC Code List 2025: Fungal control agents sorted by cross-resistance pattern and mode of action (including coding for FRAC Groups on product labels)*. Fungicide Resistance Action Committee. Available at: https://www.frac.info/. Accessed January 21, 2026.

Gangavarapu Y., Palwai S., 2022. Antifungal Activity of Lemongrass Oil Against Pathogenic Fungi. *International Journal of High School Research* 4: 34–38. https://doi.org/10.36838/v4i1.7.

Garibaldi A., Bertetti D., Franco Ortega S., Martini P., Gullino M.L., 2016. Powdery Mildew Caused by *Golovinomyces biocellatus* on Lemon Thyme (*Thymus* × *citriodorus*) 'Aureus' in Italy. *Plant Disease* 100: 2168. https://doi.org/10.1094/PDIS-04-16-0451-PDN.

Głos H., Bryk H., Michalecka M., Puławska J., 2023. First report of *Stemphylium vesicarium*, a new pathogen causing brown spot of pear in Poland. *Journal of Plant Pathology* 105: 1161–1162. https://doi.org/10.1007/s42161-023-01365-6.

Gossen B.D., Tayviah C.S., McDonald M.R., 2021. The Role of Ascospores and Conidia, in Relation to Weather Variables, in the Epidemiology of Stemphylium Leaf Blight of Onion. *Plant Disease* 105: 1912–1918. https://doi.org/10.1094/PDIS-06-20-1283-RE.

Griffith G.W., Easton G.L., Detheridge A., Roderick K., Edwards A., … Perkins W.T., 2007. Copper deficiency in potato dextrose agar causes reduced pigmentation in cultures of various fungi. *FEMS Microbiology Letters* 276: 165–171. https://doi.org/10.1111/j.1574-6968.2007.00923.x.

Habib W., Masiello M., El Ghorayeb R., Gerges E., Susca A., … Moretti A., 2021. Mycotoxin Profile and Phylogeny of Pathogenic *Alternaria* Species Isolated from Symptomatic Tomato Plants in Lebanon. *Toxins* 13: 513. https://doi.org/10.3390/toxins13080513.

He M.-H., Wang Y.-P., Wu E.-J., Shen L.-L., Yang L.-N., … Zhan J., 2019. Constraining Evolution of *Alternaria alternata* Resistance to a Demethylation Inhibitor (DMI) Fungicide Difenoconazole. *Frontiers in Microbiology* 10: 1609. https://doi.org/10.3389/fmicb.2019.01609.

Hyldgaard M., Mygind T., Meyer R.L., 2012. Essential Oils in Food Preservation: Mode of Action, Syner-

gies, and Interactions with Food Matrix Components. *Frontiers in Microbiology* 3: 12. https://doi.org/10.3389/fmicb.2012.00012.

Kaur G., Ganjewala D., Bist V., Verma P.C., 2019. Antifungal and larvicidal activities of two acyclic monoterpenes; citral and geraniol against phytopathogenic fungi and insects. *Archives of Phytopathology and Plant Protection* 52: 458–469. https://doi.org/10.1080/03235408.2019.1651579.

Koka J.A., Bhat M.Y., Wani A.H., 2021. In vitro efficacy of fungicides on mycelial growth and spore germination of *Alternaria alternata* and *Mucor plumbeus*. *Journal of Drug Delivery and Therapeutics* 11: 17–22. https://doi.org/10.22270/jddt.v11i3.4692.

Kumar S., Stecher G., Suleski M., Sanderford M., Sharma S., Tamura K., 2024. MEGA12: Molecular Evolutionary Genetic Analysis Version 12 for Adaptive and Green Computing. *Molecular Biology and Evolution* (F.U. Battistuzzi, ed.) 41(12):1–9. https://doi.org/10.1093/molbev/msae263.

La Torre A., Iovino V., Caradonia F., 2018. Copper in plant protection: Current situation and prospects. *Phytopathologia Mediterranea*, Firenze University Press 57: 201–236. https://doi.org/10.14601/Phytopathol_Mediterr-23407.

Lamichhane J.R., Osdaghi E., Behlau F., Köhl J., Jones J.B., Aubertot J.-N., 2018. Thirteen decades of antimicrobial copper compounds applied in agriculture. A review. *Agronomy for Sustainable Development* 38: 28. https://doi.org/10.1007/s13593-018-0503-9.

Llorente C., Bárcena A., Vera Bahima J., Saparrat M.C.N., Arambarri A.M., … Balatti P.A., 2012a. *Cladosporium cladosporioides* LPSC 1088 Produces the 1,8-Dihydroxynaphthalene-Melanin-Like Compound and Carries a Putative pks Gene. *Mycopathologia* 174: 397–408. https://doi.org/10.1007/s11046-012-9558-3.

Llorente I., Montesinos E., 2006. Brown Spot of Pear: An Emerging Disease of Economic Importance in Europe. *Plant Disease* 90: 1368–1375. https://doi.org/10.1094/PD-90-1368.

Llorente I., Moragrega C., Ruz L., Montesinos E., 2012b. An update on control of brown spot of pear. *Trees* 26: 239–245. https://doi.org/10.1007/s00468-011-0607-1.

Llorente I., Vilardell A., Vilardell P., Pattori E., Bugiani R., … Montesinos E., 2010. Control of brown spot of pear by reducing the overwintering inoculum through sanitation. *European Journal of Plant Pathology* 128: 127–141. https://doi.org/10.1007/s10658-010-9637-6.

Loebler M., Sánchez C., Muchagato Maurício E., Diogo E., Santos M., … Duarte M.P., 2020. Potential Application of Propolis Extracts to Control the Growth of *Stemphylium vesicarium* in "Rocha" Pear. *Applied Sciences* 10: 1990. https://doi.org/10.3390/app10061990.

Lomba-Viana X., Raymundo A., Prista C., Alegria M.J., Sousa I., 2022. Clean Label "Rocha" Pear (Pyrus communis L.) Snack Containing Juice By-Products and *Euglena gracilis* Microalgae. *Frontiers in Nutrition* 9: 825999. https://doi.org/10.3389/fnut.2022.825999.

Luo D., Ye S., Qu G., Ba L., 2024. Inhibitory effect and action mechanism of citral against black rot in pitaya fruit. *Physiological and Molecular Plant Pathology* 131: 102275. https://doi.org/10.1016/j.pmpp.2024.102275.

Luz J.P., Amaro C., Isabel R., Jambrek A., Barrios D., 2018. Efficacy of fungicides in vitro for *Stemphylium vesicarium* of pear. *Revista de Ciências Agrárias*, Especial 41: 97–101. https://doi.org/10.19084/RCA.17072.

McGrath M.T., 2009. Fungicides and other Chemical Approaches for use in Plant Disease Control. In: *Encyclopedia of Microbiology* (M. Schaechter, ed.), 3rd ed. Elsevier/Academic Press, Amsterdam, The Netherlands, 412–421. https://doi.org/10.1016/B978-012373944-5.00357-6.

Minozzo M., de Souza M.A., Bernardi J.L., Puton B.M.S., Valduga E., … Cansian R.L., 2023. Antifungal activity and aroma persistence of free and encapsulated *Cinnamomum cassia* essential oil in maize. *International Journal of Food Microbiology* 394: 110178. https://doi.org/10.1016/j.ijfoodmicro.2023.110178.

Nazzaro F., Fratianni F., Coppola R., Feo V. De, 2017. Essential Oils and Antifungal Activity. *Pharmaceuticals* 10: 86. https://doi.org/10.3390/ph10040086.

Nene Y.L., Thapliyal P.N., 1979. *Fungicides in Plant Disease Control*. Oxford & IBH Publishing Co., New Delhi, India.

Oli N., Singh U.K., Jha S.K., 2019. Antifungal Activity of Plant's Essential Oils against Post Harvest Fungal Disease of Apple Fruit. *Forestry: Journal of Institute of Forestry, Nepal* 16: 86–100. https://doi.org/10.3126/forestry.v16i0.28361.

Olita T., Stankovic M., Sung B., Jones M., Gibberd M., 2024. Growers' perceptions and attitudes towards fungicide resistance extension services. *Scientific Reports* 14: 6821. https://doi.org/10.1038/s41598-024-57530-z.

Oliveira A.S., Rolo J., Gaspar C., Cavaleiro C., Salgueiro L., … Palmeira-de-Oliveira A., 2022. Chemical characterization and bioactive potential of *Thymus* × *citriodorus* (Pers.) Schreb. preparations for anti-acne applications: Antimicrobial, anti-biofilm, anti-

inflammatory and safety profiles. *Journal of Ethnopharmacology* 287: 114935. https://doi.org/10.1016/j.jep.2021.114935.

Parikh L., Agindotan B.O., Burrows M.E., 2021. Antifungal Activity of Plant-Derived Essential Oils on Pathogens of Pulse Crops. *Plant Disease* 105: 1692–1701. https://doi.org/10.1094/PDIS-06-20-1401-RE.

Paušič A., Roškarič M., Lešnik M., 2023. Preharvest Treatments with Low-Risk Plant Protection Products Can Help Apple Growers Fulfill the Demands of Supermarket Chains Regarding Pesticide Residues and Marketing Apples under 0-Residue Brands. *Agronomy* 13: 1151. https://doi.org/10.3390/agronomy13041151.

Perina F.J., Amaral D.C., Fernandes R.S., Labory C.R., Teixeira G.A., Alves E., 2015. *Thymus vulgaris* essential oil and thymol against *Alternaria alternata* (Fr.) Keissler: effects on growth, viability, early infection and cellular mode of action. *Pest Management Science* 71: 1371–1378. https://doi.org/10.1002/ps.3933.

Puig M., Ruz L., Montesinos E., Moragrega C., Llorente I., 2015. Combined morphological and molecular approach for identification of *Stemphylium vesicarium* inoculum in pear orchards. *Fungal Biology* 119: 136–144. https://doi.org/10.1016/j.funbio.2014.11.006.

Raveau R., Fontaine J., Lounès-Hadj Sahraoui A., 2020. Essential Oils as Potential Alternative Biocontrol Products against Plant Pathogens and Weeds: A Review. *Foods* 9: 365. https://doi.org/10.3390/foods9030365.

Sattary M., Amini J., Hallaj R., 2020. Antifungal activity of the lemongrass and clove oil encapsulated in mesoporous silica nanoparticles against wheat's take-all disease. *Pesticide Biochemistry and Physiology* 170: 104696. https://doi.org/10.1016/j.pestbp.2020.104696.

Shukla R., Singh P., Prakash B., Dubey N.K., 2012. Antifungal, aflatoxin inhibition and antioxidant activity of *Callistemon lanceolatus* (Sm.) Sweet essential oil and its major component 1,8-cineole against fungal isolates from chickpea seeds. *Food Control* 25: 27–33. https://doi.org/10.1016/j.foodcont.2011.10.010.

Singh P., Bugiani R., Cavanni P., Nakajima H., Kodama M., … Kohmoto K., 1999. Purification and Biological Characterization of Host-Specific SV-Toxins from *Stemphylium vesicarium* Causing Brown Spot of European Pear. *Phytopathology* 89: 947–953. https://doi.org/10.1094/PHYTO.1999.89.10.947.

Soares C., Morales H., Faria J., Figueiredo A.C., Pedro L.G., Venâncio A., 2016. Inhibitory effect of essential oils on growth and on aflatoxins production by *Aspergillus parasiticus*. *World Mycotoxin Journal* 9: 525–534. https://doi.org/10.3920/WMJ2015.1987.

Sobreiro J., Batalha Neto C.S., 2024. Insights into brown spot disease: causal agents and host interactions in agroecosystems. In: *Estudos em Ciências Agrárias e Ambientais I* (E. Spers, ed), Editora Artemis, Curitiba, PR, Brazil, 88–100. https://doi.org/10.37572/EdArt_30072419210.

Soltanzadeh M., Peighambardoust S.H., Ghanbarzadeh B., Mohammadi M., Lorenzo J.M., 2021. Chitosan nanoparticles encapsulating lemongrass (*Cymbopogon commutatus*) essential oil: Physicochemical, structural, antimicrobial and in-vitro release properties. *International Journal of Biological Macromolecules* 192: 1084–1097. https://doi.org/10.1016/j.ijbiomac.2021.10.070.

Soylu E.M., Kurt Ş., Soylu S., 2010. In vitro and in vivo antifungal activities of the essential oils of various plants against tomato grey mould disease agent Botrytis cinerea. *International Journal of Food Microbiology* 143: 183–189. https://doi.org/10.1016/j.ijfoodmicro.2010.08.015.

Szczygieł T., Koziróg A., Otlewska A., 2024. Synthetic and Natural Antifungal Substances in Cereal Grain Protection: A Review of Bright and Dark Sides. *Molecules* 29: 3780. https://doi.org/10.3390/molecules29163780.

Tang X., Shao Y.-L., Tang Y.-J., Zhou W.-W., 2018. Antifungal Activity of Essential Oil Compounds (Geraniol and Citral) and Inhibitory Mechanisms on Grain Pathogens (*Aspergillus flavus* and *Aspergillus ochraceus*). *Molecules* 23: 2108. https://doi.org/10.3390/molecules23092108.

Tao N., OuYang Q., Jia L., 2014. Citral inhibits mycelial growth of *Penicillium italicum* by a membrane damage mechanism. *Food Control* 41: 116–121. https://doi.org/10.1016/j.foodcont.2014.01.010.

Temperini C.V., Tudela M.A.A., Gimenez G.N., Di Masi S.N., Pardo A.G., Pose G.N., 2022. Brown spot of pear, an emerging disease in Argentina: identification and pathogenicity characterization of Argentinean *Stemphylium vesicarium* isolates. *European Journal of Plant Pathology* 163: 529–544. https://doi.org/10.1007/s10658-022-02493-y.

Toledo E., Félix C., Vicente T.F.L., Augusto A., Félix R., … Lemos M.F.L., 2023. Seaweed Extracts to Control Postharvest Phytopathogenic Fungi in Rocha Pear. *Journal of Fungi* 9: 269. https://doi.org/10.3390/jof9020269.

Trombetta D., Castelli F., Sarpietro M.G., Venuti V., Cristani M., … Bisignano G., 2005. Mechanisms of Antibacterial Action of Three Monoterpenes. *Anti-*

microbial Agents and Chemotherapy 49: 2474–2478. https://doi.org/10.1128/AAC.49.6.2474-2478.2005.

Tudela M.A.A., Gimenez G.N., Di Masi S.N., Pose G.N., Basanta M., 2023a. Susceptibility of South American pear cultivars to brown spot of pear caused by *Stemphylium vesicarium*. *Journal of Plant Diseases and Protection* 130: 1347–1356. https://doi.org/10.1007/s41348-023-00783-z.

Tudela M.A.A., Lutz M.C., Giménez G.N., Del Brío D., Di Masi S.N., … Molina J.P.E., 2023b. Efficacy of fungicides against brown spot of pear in Argentina. *Crop Protection* 174: 106425. https://doi.org/10.1016/j.cropro.2023.106425.

Wang H., Yang Z., Ying G., Yang M., Nian Y., … Kong W., 2018. Antifungal evaluation of plant essential oils and their major components against toxigenic fungi. *Industrial Crops and Products* 120: 180–186. https://doi.org/10.1016/j.indcrop.2018.04.053.

Xylia P., Chrysargyris A., Ahmed Z.F.R., Tzortzakis N., 2021. Application of Rosemary and Eucalyptus Essential Oils and Their Main Component on the Preservation of Apple and Pear Fruits. *Horticulturae* 7: 479. https://doi.org/10.3390/horticulturae7110479.

Yang J.H., Brannen P.M., Schnabel G., 2015. Resistance in *Alternaria alternata* to SDHI Fungicides Causes Rare Disease Outbreak in Peach Orchards. *Plant Disease* 99: 65–70. https://doi.org/10.1094/PDIS-04-14-0387-RE.

Yin Y., Miao J., Shao W., Liu X., Zhao Y., Ma Z., 2023. Fungicide Resistance: Progress in Understanding Mechanism, Monitoring, and Management. *Phytopathology* 113: 707–718. https://doi.org/10.1094/PHYTO-10-22-0370-KD.

Phytopathologia Mediterranea
The international journal of the
Mediterranean Phytopathological Union

Firenze University Press
www.fupress.com/pm

Research Papers

Potential biocontrol of Botryosphaeria dieback pathogens using endophytic *Aspergillus*, *Penicillium* and *Trichoderma* species from grapevines

İzzet BÜLBÜL[1], Davut Soner AKGÜL[2,*]

[1] *Biological Control Research Institute, Ministry of Agriculture and Forestry, 01321, Yüreğir, Adana, Türkiye*
[2] *Department of Plant Protection, Agriculture Faculty, University of Çukurova, 01330, Balcalı, Adana, Türkiye*
*Corresponding author. E-mail:sakgul@cu.edu.tr

Summary. This research aimed to determine abilities of endophytic *Aspergillus*, *Penicillium*, and *Trichoderma* species to colonize grapevine cuttings, and to evaluate their performance for protecting pruning wounds from *Botryosphaeriaceae* fungi under greenhouse and field conditions. Colonization ability of five endophytic species (*Aspergillus allahabadi, A. flavipes, Penicillium canescens, P. fructuariae-cellae*, and *Trichoderma brevicompactum*) was assessed after introductions into cuttings using two inoculation methods: immersion in conidial suspensions or contact with dry conidia. Colonization by the inoculated fungi was subsequently confirmed through re-isolations, and species identities were verified by PCR and gene sequencing. After confirming colonization, biological activity of the endophytes was assessed against pathogens. Conidium suspensions were either sprayed onto host wounds or applied systemically to cuttings, and necrotic lengths in internal tissues were measured 4 months after inoculations. In a subsequent field experiment, conidium suspensions were applied by spraying onto pruning wounds, or placing mycelium/agar plugs, and extent of necroses was assessed 6 months after inoculations. *Penicillium* and *Trichoderma* species colonized internal tissues of grapevine plants, whereas *Aspergillus* species were not re-isolated. In greenhouse trials, the endophytes reduced lesion lengths caused by *Botryosphaeriaceae* species by 22 to 85 %. Under field conditions, and where applied to pruning wounds, these fungi gave 51 to 70% protection against *Lasiodiplodia brasiliensis* and *Neofusicoccum parvum*, with *Trichoderma brevicompactum* giving greatest efficacy. This study has shown that vineyard-derived *Penicillium* and *Trichoderma* endophytes can establish within grapevine tissues, and have potential to effectively suppress *Botryosphaeriaceae* pathogens of grapevines.

Keywords. *Botryosphaeriaceae*, Grapevine Trunk Diseases (GTDs), *Lasiodiplodia brasiliensis, Neofusicoccum parvum, Vitis vinifera*

OPEN ACCESS

Citation: Bülbül, İ. & Akgül, D. S. (2026). Potential biocontrol of Botryosphaeria dieback pathogens using endophytic *Aspergillus*, *Penicillium* and *Trichoderma* species from grapevines. *Phytopathologia Mediterranea* 65(2): 287-299. doi: 10.36253/phyto-17392

Accepted: July 25, 2026

Published: September 10, 2026

© 2026 Author(s). This is an open access, peer-reviewed article published by Firenze University Press (https://www.fupress.com) and distributed, except where otherwise noted, under the terms of the CC BY 4.0 License for content and CC0 1.0 Universal for metadata.

Data Availability Statement: All relevant data are within the paper and its Supporting Information files.

Competing Interests: The Author(s) declare(s) no conflict of interest.

Editor: José R. Úrbez Torres, Agriculture and Agri-Food Canada, Summerland, British Columbia, Canada.

ORCID:
DSA: 0000-0002-9990-4194
İB: 0000-0003-0527-8610

INTRODUCTION

Türkiye is an important grape-producing country, and grapevine nurseries are important agricultural industries. According to the Ministry of Agriculture and Forestry, approx. three million grapevine plants (registered) are produced annually in Türkiye, and these plants are sold to establish new vineyards or replace uprooted vines dying from pests or diseases in their first years (Anonymous, 2025). During vineyard establishment, some young plants die due to abiotic factors such as unfavorable soil conditions, poor cutting quality, improper planting, or biotic factors (fungal pathogens, and nematode or insect pests).

Fungal pathogens (*Botryosphaeriaceae, Diaporthe, Eutypa* species, *Cylindrocarpon*-like fungi, *Phaeomoniella*, *Phaeoacremonium, Fomitiporia* species) associated with grapevine trunk diseases (GTDs), and some soilborne fungi (species of *Phytophthora, Fusarium, Rhizoctonia, Macrophomina,* or *Verticillium*) are among the leading causes of plant death in newly established vineyards (Gramaje and Armengol, 2011). These pathogens are disseminated latently by dormant vines or propagation material, spreading over large areas and causing economic losses.

Controlling latent infections is challenging, and various management methods are followed at nursery propagation stages to ensure healthy plant production. Some disinfectants (quaternary ammonium salts, hydroxyquinoline sulfate) and fungicides added to water-soaking tanks reduce fungal contamination of propagation materials (Gramaje *et al.,* 2009). Hot water treatments can also eradicate most latent infections, and combining hot water treatments with fungicides has been found to augment these effects (Görür and Akgül, 2019). Systemic fungicides are also applied via drip irrigation systems when grafted cuttings are planted in the soil or during root formation.

These treatments may protect plant roots for short periods, but they are not effective against latent pathogen infections in grapevine stems. In recent years, research has focused on biological control of fungal pathogens associated with grapevine trunk diseases in grapevine nurseries and in field vineyards. These efforts aimed to reduce pathogen spread and promote production of healthy plants. Some microorganisms with potential biocontrol activity can minimize plant diseases by competing with pathogens for nutrients, producing antibiotics, or parasitizing pathogens. They can also contribute to plant growth by facilitating nutrient uptake and by producing beneficial substances that favour plant growth (Pieterse *et al.,* 2014).

Endophytic fungi live with most vascular plants, and do not cause disease symptoms. They are also known to suppress plant pathogens through production of various secondary metabolites, and supporting plants against environmental stress factors (Busby *et al.,* 2016). Grapevine is also a host for endophytic microorganisms, and research using advanced technologies such as Next Generation Sequencing (NGS) and metatranscriptomics analysis have shown that grapevines are rich in bacterial and fungal microbiota. Some studies have indicated that up to 60 endophytic fungal genera are present in adult grapevines, of which *Alternaria, Aspergillus, Cladosporium, Clonostachys, Epicoccum, Penicillium* and *Trichoderma* predominate. Species in these genera have been studied for biocontrol of fungal plant pathogens, due to their high proliferation, abilities to colonize organic matter rapidly, and production of antimicrobial secondary metabolites (Thambugala *et al.,* 2020). Deyett and Rolshausen (2020) showed that approx. 28% of grapevine endomycota were acquired from the soil and plant environments, gradually colonizing grapevines from the time of planting. This indicates that local and natural endophytes have coevolved with grapevine, and these have superior potential for colonization and pathogen antagonism compared to other endophytic species. *Aspergillus* and *Penicillium* are genera that are found wherever organic matter is present, and are adapted to various harsh environmental conditions, including drought and high temperatures. Some species of these genera can live with plants as endophytes, while others can cause fruit bunch rots, plant mortality, and canker diseases (Bustamente *et al.,* 2024; El-Dawy *et al.,* 2024). Endophytic species of these genera can directly or indirectly inhibit the growth of other microorganisms, and contribute to plant health by secreting various metabolites, antibiotics, or mycotoxins (Grijseels *et al.,* 2017; Hagag *et al.,* 2022). In addition to these genera, the *Trichoderma* also includes species proven to have biocontrol activities against plant diseases, including GTDs (Berbegal *et al*., 2020; Silva-Valderrama *et al.,* 2021). Most of these studies used commercially produced *Trichoderma* isolates, and some studies examined disease-reducing performance of local endophytic species.

Very few studies have assessed endophytic *Penicillium* and *Aspergillus* species for biocontrol of GTDs. Since biological fungicides produced in different countries may not perform well when used against a particular disease in another country, results obtained using local isolates can sometimes be more effective (Pollard-Flamand *et al.,* 2022).

The hypothesis examined in the present study was that antagonist isolates selected from local fungal endophytes could successfully reduce diseases caused

by *Botryosphaeriaceae*, both at young vine stages and under field conditions, through applications to pruning wounds and as inoculations of grapevine cuttings. Fungal endophytes from different locations or vineyards were assessed for abilities to suppress fungal pathogens associated with GTDs.

The objectives of this study were: (i) to determine colonization performance of the endophytic *Aspergillus, Penicillium*, and *Trichoderma* species in detached grapevine canes; and (ii) to assess their prophylactic performances for reducing lesions caused by *Botryosphaeriaceae* species through protecting wounds on grapevine plants and adult vines, using greenhouse and field experiments.

MATERIALS AND METHODS

Fungus isolates

The *Botryosphaeriaceae* pathogens and endophytic *Aspergillus, Penicillium*, or *Trichoderma* isolates used in this study were obtained from a survey conducted during 2020-21 in vineyards, from the local cultivars Hatun Parmağı, Horozkarası, Kabarcık, Mahrabaşı, or Tarsus Beyazı, grown on their own roots. These grapevines were in the Eastern Mediterranean Region of Türkiye. Pure cultures obtained were deposited in the culture collection of the Mycology Laboratory at the Faculty of Agriculture, Çukurova University. The isolates were identified using DNA analyses, and virulence of *Botryosphaeriaceae* isolates was previously shown using pathogenicity tests. In a preliminary study, endophytic *Aspergillus, Penicillium*, or *Trichoderma* isolates were subjected to dual-culture tests, and those with prominent antagonistic properties were selected for use in the pot and field trials described below (Table 1).

Assessments of colonization of grapevine cuttings by antagonistic fungi

Ability of antagonistic species to colonize grapevine cuttings was tested using two different methods. In the first, mycelial agar discs (maintained in 30% glycerol and 70% sterile distilled water) of antagonistic *Aspergillus allahabadii* (*Aab*), *A. flavipes* (*Afp*), *Penicillium canescens* (*Pcn*), *P. fructuariae-cellae* (*Pfc*), or *Trichoderma brevicompactum (Tbr)* were taken from the fungal culture collection, and transferred to Petri dishes containing potato dextrose agar (PDA). To ensure high conidium production, the isolates were incubated at 25 °C under a 12 h light, 12 h dark cycle for 15 d.

Sterile distilled water was added to the mature cultures, and conidia were dislodged into the water using a sterile spatula. The resulting conidium suspensions were then each homogenized with 50 µL of polyoxyethylene sorbitan monolaurate (Tween-20™), the conidia were counted with a haemocytometer (Thoma Slide™) under a light microscope (Olympus, model BX-51), and the concentration was adjusted to 10^8 conidia·mL^{-1}. The basal regions (5 cm) of dormant canes (*Vitis vinifera* 'Cardinal', 30 cm in length, with 2-3 buds) were dipped into the conidium suspension, and the canes were kept in this suspension at room temperature for 24 h.

The canes were then planted into the plastic pots (1 L capacity) containing rooting medium (equal volumes of peat moss and perlite). To induce root and shoot formation, the pots were kept in a climate controlled room (28 °C, relative humidity = 85%, 12 h light, 12 h dark cycle) for 4 weeks. The plants were then transferred to a lath-house to grow naturally for 4 months. During the growth period, the dormant cuttings were irrigated weekly with a liquid nutrient solution (20% nitrogen, 20% phosphorus, 20% potassium, 0.02% copper, 0.05% iron, 0.02% manganese, and 0.02% zinc), and no pesticides were applied. Twenty cuttings were used for each antagonistic species, and each cutting was planted into a separate pot.

In the second method, pure and highly sporulating PDA cultures of the antagonistic fungi were used to inoculate dormant canes. The basal ends of the canes were bluntly cut with sterilized pruning shears, and the fresh wounds were directly blotted on the surfaces of the sporulated cultures to ensure conidium adherence. The canes were then planted pots, placed in the controlled climate room, and grown as described (above) for the first method.

To assess internal colonization by antagonistic fungal species, grapevine plants were uprooted from the pots 4 months after planting, their roots were removed with pruning shears, and their basal parts were thoroughly washed under tap water. Segments (2 cm in length) were then cut from points 10 cm from the plant base, and were then surface disinfected for 3 min using a 2.5% sodium hypochlorite solution containing >5% active chlorine (Hypo: Koruma A.Ş). The segments were then rinsed twice in sterile distilled water and blotted with sterile paper towels. The bark tissues were then removed, internal tissues were cut aseptically with sterile scissors, and 3–5 mm woody tissues were plated onto PDA amended with streptomycin sulfate (250 mg·L^{-1}).

Internal stem colonization by the respective inoculated fungi was determined as the percentage of fungus re-isolated. Twenty PDA Petri plates were used for each

antagonistic fungus, with each plate containing seven internal tissues from one cane segment. Re-isolation rates were assessed as proportions of tissue pieces yielding antagonistic species.

Verifying endophytic colonization by PCR and gene sequencing

The re-isolated species were examined morphologically and microscopically, and species identifications were confirmed using PCR and gene sequencing.

Genomic DNA was extracted from *Aspergillus, Penicillium,* and *Trichoderma* colonies using the CTAB (2%) protocol described by O'Donnell *et al.* (1998). ITS1, 5.8S, and ITS2 regions of the rDNA, beta-tubulin, and partial translation elongation factor (TEF 1-α) genes were amplified with PCR reactions using ITS4/ITS5, Bt2a/Bt2b, and EF688F/EF1251R primers (White *et al.,* 1990; Glass and Donaldson, 1995; Alves *et al.,* 2008). PCR reactions were carried out in a thermal cycler (SimpliAmp A24811™, Applied Biosystems) in 50 µL mixtures for each sample. Each reaction tube contained 25 µL of Thermo Scientific Master Mix (2X)™, 23 µL of PCR grade water (Lonza™), 0.5 µL of forward and reverse primers (10 pmol·µL^{-1}), and 1 µL of genomic DNA (approx. 100 ng·µL^{-1}). PCR conditions were 95 °C for 3 min (initial denaturation), followed by 35 cycles each of denaturation at 95 °C for 1 min, annealing at 52 °C (for ITS), 55 °C (for beta-tubulin), or 53 °C (for TEF1-α), for 1 min, extension at 72 °C for 1 min, and final extension at 72 °C for 10 min. Success of PCR reactions was then confirmed using agarose gel electrophoresis (1.5% agarose, Invitrogen) and visualization of DNA bands under a UV illuminator. PCR products were sequenced by Macrogen Co. (South Korea), The sequences obtained were compared with those deposited in the NCBI GenBank database using the BLAST search (version 2.0; National Center for Biotechnology Information, United States National Institutes of Health).

Assessments of prophylactic capacity of antagonistic fungi against Botryosphaeriaece *pathogens in grapevine cuttings (pot experiments)*

The prophylactic capacities of endophytic fungi were assessed using two methods: (1) spraying conidium suspensions onto open wounds in grapevine wood tissue, or (2) systemically inoculating dormant cuttings with these suspensions.

For Method (1), dormant Cardinal grapevine cuttings, each 30 cm long with 2 to 3 buds, were washed under tap water, then superficially disinfected in a 2.5% sodium hypochlorite solution for 3 min, then rinsed twice with sterile distilled water. Endophytic fungal isolates (five species, one isolate each) were incubated on PDA at 24 °C in the dark for 10 d. Sterile distilled water plus one to two drops of polyoxyethylene sorbitan monolaurate (Tween 20™) were then added to heavily conidiating cultures, and the conidium suspensions were adjusted to 10^8 conidia mL^{-1} after counting conidia with a haemocytometer (Thoma Slide™). An internode on each cutting was wounded with a sterile 5 mm diam. cork-borer, the bark tissues were removed, and 25 µL of endophytic fungus conidium suspension was sprayed onto each wound using a fine droplet sprayer. These cuttings were then incubated at room temperature for 24 h, and mycelium/agar plugs of the *Botryosphaeriaceae* fungi (eight species, one isolate each; Table 1) were then inoculated into the wounds. For inoculation controls, no endophytic isolates were inoculated, but pathogens were inoculated into the wounds (Blundell and Eskalen, 2022). The inoculation points were each wrapped with parafilm to prevent desiccation of the inoculation agar plugs. The cuttings were then planted into plastic pots (1 L capacity) containing rooting medium (equal volumes of peat moss and perlite). The plants were grown in a controlled climate room (28 °C, 85% relative humidity, 12 h light:12-h dark cycle) for 4 weeks, to induce root and shoot formation. The pots were then transferred to the lath-house to grow naturally for 4 months.

For Method (2), endophytic isolates were inoculated into grapevine cuttings as described by Benlioğlu and Özakman (1998). Transparent sterile rubber tubing was attached to both ends of each dormant grapevine cuttings. One end of the cutting was linked, via tubing, to a Buchner funnel fitted into an Erlenmeyer flask, which was then connected to an air pump (Merck Millipore) operating under negative pressure (-0.4 bar). One mL of each endophyte conidium suspension (10^8 conidia·mL^{-1}) was then injected into the tubing at the opposite end using an automatic pipette, ensuring that the conidia entered each cutting. To facilitate endophyte colonization and prevent dehydration, the base sections of the cuttings were immersed in water in plastic containers, and were then incubated at 25 °C for 1 week. Internode sections of stems were then laterally drilled with an electric drill and 2 mm diam. bit, and mycelium agar pieces of the respective pathogens were inoculated into the holes (Pouzoulet *et al.,* 2013). The inoculation points were then wrapped with parafilm, and the cuttings were planted into the plastic pots (as described above). The cuttings were then grown in an climate controlled room (28 °C, 85% relative humidity, 12 h light:12 h dark) for 4 weeks to induce root

Table 1. Locations of source vineyards and grapevine cultivars, and details of the endophytic and pathogenic *Botryosphaeriaceae* fungi used in this study (with their respective NCBI GenBank sequence numbers).

Fungus species	Isolate code	Location (in Türkiye)	Grapevine cultivar	GenBank accession numbers*			
				ITS	BT	TEF	CAL
Endophytic species							
Aspergillus allahabadii	BMAE208IB	Tarsus, Mersin	Tarsus Beyazı	PP989656	PV864710	-	-
Aspergillus flavipes	BMAE161IB	Tarsus, Mersin	Tarsus Beyazı	PP989655	PV864709	-	-
Penicillium canescens	BMAE291IB	Tarsus, Mersin	Tarsus Beyazı	PP989657	-	-	PV864707
Penicillium fructuariae-cellae	CUZF39HIK	İslahiye, Gaziantep	Dımışkı	OM980658	-	-	PV791715
Trichoderma brevicompactum	BMAE96IB	Hassa, Hatay	Hatunparmağı	PP989654	-	PV864708	-
Botryosphaeriaceae species							
Botryosphaeria dothidea	BMAE155IB	Pazarcık, K. Maraş	Kabarcık	PP703088	-	PV795919	-
Diplodia olivarum	BMAE184IB	Toroslar, Mersin	Tarsus Beyazı	PP703095	-	PV855303	-
Diplodia seriata	BMAE68IB	Tarsus, Mersin	Tarsus Beyazı	PP703073	-	PP791972	-
Dothiorella omnivora	BMAE290IB	Saimbeyli, Adana	Mücennis	PP703108	-	PV855304	-
Lasiodiplodia brasiliensis	BMAE89IB	Hassa, Hatay	Horozkarası	PP703079	-	PV763370	-
Neofusicoccum australe	BMAE229IB	Tarsus, Mersin	Tarsus Beyazı	PP703105	-	PV855300	-
Neofusicoccum parvum	BMAE201IB	Tarsus, Mersin	Tarsus Beyazı	PP703101	-	PV795916	-
Neoscytalidium dimidiatum	BMAE103IB	Onikişubat, K. Maraş	Mahrabaşı	PP703081	-	PV832488	-

*ITS, internal transcribed spacer; BT, β-tubulin; TEF, translation elongation factor 1-α; CAL, calmodulin.

and shoot formation. The pots were then transferred to the lath-house to grow naturally for 4 months.

For both inoculation methods, six replicates per endophyte-pathogen combination (one plant per pot, each representing a replicate) were used, with completely randomized experimental design for each testing method. The inoculation experiments were each conducted twice.

To evaluate the prophylactic effects of the endophytic isolates, in Method (1) lesion lengths were measured in wood tissues by removing bark tissues. In Method (2) lesions were measured after excising the plant stems longitudinally.

Variance analyses of data obtained were carried out for lesion length data to reveal differences between means of the treatments, and the statistically similar groups were determined by Fisher's Least Significant Difference (LSD) test ($P \leq 0.05$) in all the experiments (Gomez and Gomez, 1984).

Assessments of prophylactic activity of antagonistic fungi against Lasiodiplodia brasiliensis *or* Neofusicoccum parvum *in field conditions*

Trials to assess performance of endophytic isolates under field conditions were carried out in 2023 and 2024, in a 7-year-old vineyard ('Cardinal' grapevines grafted on 1103 Paulsen rootstock) at the implementation area of Çukurova University Faculty of Agriculture.

All the endophytic fungi listed in Table 1 (five species, one isolate each) were used in field trials against the two most virulent pathogenic species (*L. brasiliensis* and *N. parvum*). To prepare inocula of the endophytic fungi, the isolates were grown on PDA at 25 °C under a 12 h light, 12 h dark cycle for 10 d. Conidium suspensions of the endophytic isolates were prepared as described above, and the suspension concentration in each suspension was adjusted to 10^8 conidia·mL^{-1}, after counting using a haemocytometer. The vines were each spur-pruned to three buds in March of 2023 or 2024. Immediately after spur pruning, the endophyte conidium suspensions were sprayed onto fresh pruning wounds. Pathogen inoculations (with either *L. brasiliensis* or *N. parvum*) were the applied 24 h later.

Two pathogen inoculation methods were used. For the first, mycelium agar plugs of *L. brasiliensis* or *N. parvum* obtained from 10-d-old PDA cultures were placed onto pruning wounds, and were sealed with parafilm. For the second method, pycniospore suspensions were used as inoculum. Because sufficient pycniospores could only be produced by *L. brasiliensis*, this method was evaluated only for that species. *Neofusicoccum parvum* was therefore tested only using mycelium agar plugs. Positive experimental control wounds received sterile distilled water instead of endophyte conidium suspensions, and were inoculated with the pathogens 24 h later. The experiment was arranged in a randomized complete block design, with four replicates. Each grapevine spur represented one replicate, and each vine car-

ried five spurs receiving different endophyte treatments. Six months after inoculation, spurs were collected, lesion lengths were measured, and pathogen re-isolations were carried out to confirm infections (Blundell and Eskalen, 2022; Akgül *et al.,* 2023). A total of 192 grapevines were used in the field experiments. The experiments were set up in separate vineyard blocks, with four replicates per block, and with randomized block designs. There were five spurs on each vine, and each spur formed one replicate. On each vine, separate endophyte fungal isolates were inoculated onto each spur (five endophyte species plus one pathogen species on five spurs).

Six months after inoculations (in September 2023 and September 2024), the spurs were cut to length 10–12 cm, and lesion lengths were measured from the treated and non-treated spurs. The re-isolation procedure was used to confirm that the lesions were caused by the particular inoculated pathogens. Efficacy of treatments was calculated according to the Abbott formula [(lesion length in non-treated control - lesion length in treated spur) / lesion length in non-treated control) ×100]. Variance analyses were carried out on these data to determine differences between means of lesion lengths, and statistically similar groups were determined by Fisher's Least Significant Difference (LSD) test ($P \leq 0.05$) in all experiments (Gomez and Gomez, 1984).

RESULTS

Abilities of antagonistic species to colonize grapevine cuttings

The re-isolation rates of endophytic fungal species inoculated into grapevine cuttings using two different methods, 10 cm from the basal ends of the cuttings, after 4 months, are shown in Table 2. *Penicillium* and *Trichoderma* species were re-isolated from inoculated tissues 10 cm from the inoculation point, whereas *Aspergillus* species were not detected. In general, the re-isolation percentages of endophytic species from internal tissues using the basal ends of the cuttings blotting-in-conidial-mass method have been greater than from the conidium suspension immersion method. The *Penicillium* and *Trichoderma* species were re-isolated from woody tissues located 10 cm above the inoculation points, whereas *Aspergillus* species were not detected. Among the assessed endophytes, *Trichoderma brevicompactum* gave the greatest re-isolation frequencies, from both of the inoculation methods and in both years, ranging from 22.8 to 34.2%. *Penicillium canescens* and *P. fructuariae-cellae* were recovered at lower frequencies, ranging from 4.2 to 12.8% for *P. canescens*, and from 5.7 to 11.4% for *P. fructuariae-cellae.* No re-isolations were obtained of *Aspergillus allahabadii* or *A. flavipes* from internal tissues sampled 10 cm from the basal ends of the cuttings. PCR amplification and gene sequencing confirmed that the re-isolated *Penicillium* or *Trichoderma* colonies corresponded to the species originally inoculated into the cuttings, showing 99% similarity in the respective BLAST analyses.

Prophylactic activity of antagonistic species against Botryosphaeriaceae *fungi in grapevine plants*

The effects of endophytic *Aspergillus, Penicillium*, or *Trichoderma* species on internal lesions caused by the eight *Botryosphaeriaceae* species were examined, focusing on their protective effects on external plant wounds. As well, the question of how much endophytes could reduce lesions caused by pathogens, if they had systemically colonized the cuttings earlier, was also assessed, four months after inoculations, in grapevine plantlets not treated with endophytes (experimental controls), *L. brasiliensis* and *N. parvum* caused the longest lesions, whereas *Diplodia olivarum* and *Neofusicoccum australe* produced shorter lesions. In comparison, *Botryosphaeria dothidea, Diplodia seriata, Dothiorella omnivora*, and *Neoscytalidium dimidiatum* caused shorter lesions than the previously fungi. All the endophytes applied to grapevine canes reduced ($P \geq 0.05$) mean internal lesion lengths compared to the experimental controls.

All the endophyte treatments reduced mean lesion lengths ($P \geq 0.05$) caused by the eight *Botryosphaeriaceae* species, compared with the pathogen-inoculated controls in both years (Figures 1 and 2). *Lasiodiplodia brasiliensis* and *Neofusicoccum parvum* produced the longest lesions in the control plants, whereas *Botryosphaeria dothidea*, *Diplodia seriata*, *Dothiorella omnivora*, and

Table 2. Mean re-isolation proportions for endophytic fungi from internal grapevine tissues sampled at 10 cm from the basal ends of grapevine rootstock cuttings.

Endophytic fungus species	Re-isolation proportions (%)			
	Dipping in conidial suspension		Blotting in conidial mass	
	2023	2024	2023	2024
Aspergillus allahabadii	-	-	-	-
A. flavipes	-	-	-	-
Penicillium canescens	11.4	4.2	12.8	7.1
P. fructuariae-cellae	8.5	5.7	11.4	8.5
Trichoderma brevicompactum	28.5	22.8	34.2	28.5

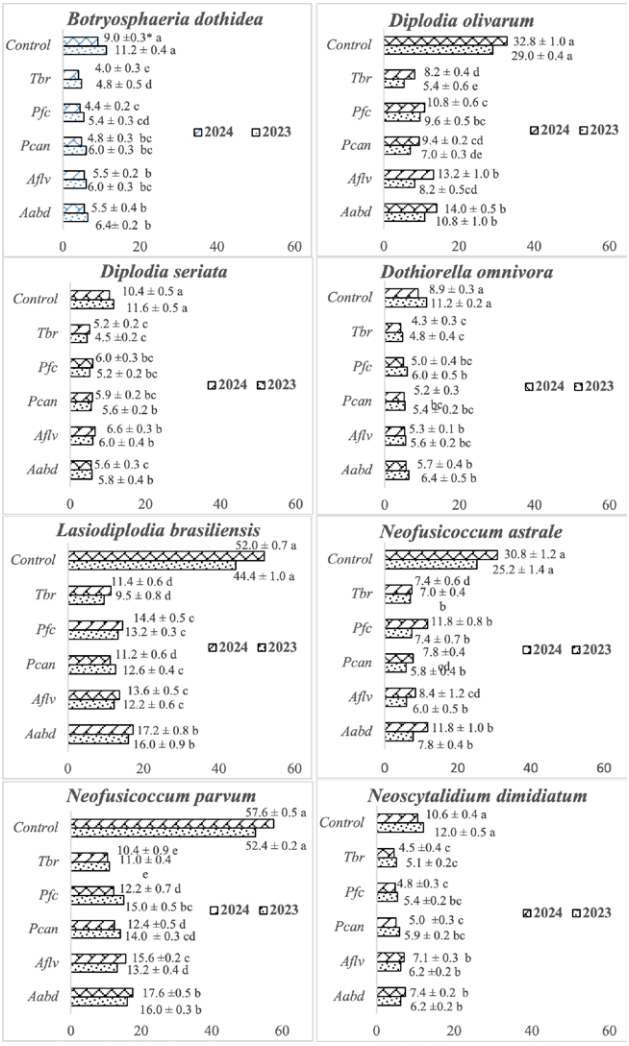

Figure 1. Mean lesion lengths (mm) caused by six *Botryosphaeriaceae* fungi in grapevine plants under greenhouse conditions, following applications of five endophytic fungi (by wound spraying). *Means (± standard errors) accompanied by different letters are different ($P \leq 0.05$), as indicated by Fisher's Least Significant Difference tests. *Aabd*, *Aspergillus allahabadi*; *Aflv*, *A. flavipes*); *Pcan*, *Penicillium canescens*; *Pfc*, *P. fructuariae-cellae*; *Tbr*, *Trichoderma brevicompactum*.

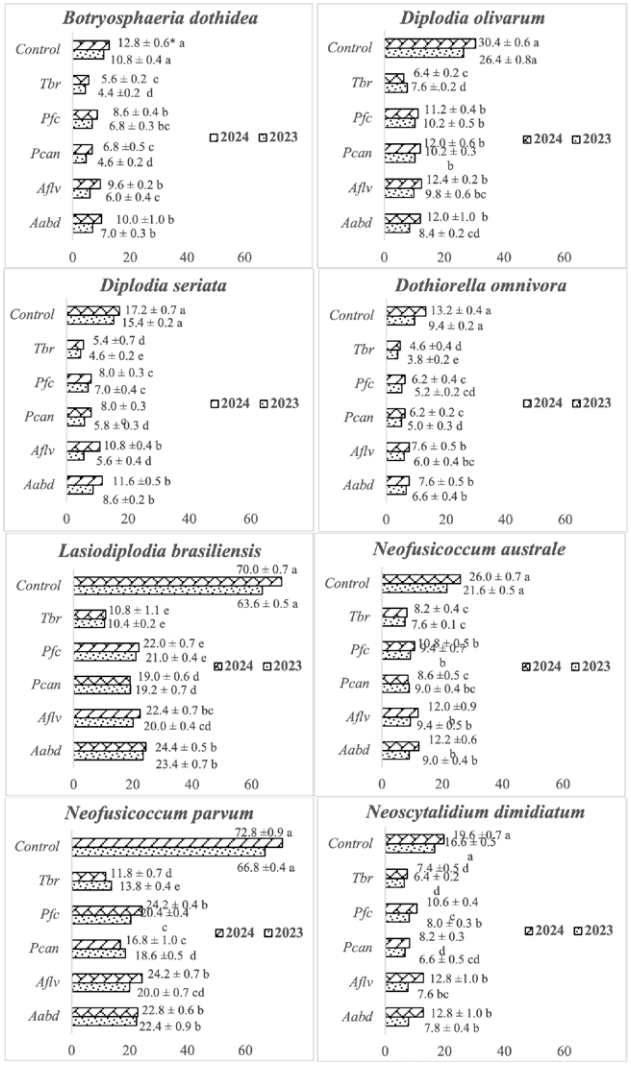

Figure 2. Mean lesion lengths (mm) caused by six *Botryosphaeriaceae* fungi in grapevine plants under greenhouse conditions, following applications of five endophytic fungi (by systemic inoculation). *Means (± standard errors) accompanied by different letters are different ($P \leq 0.05$), as indicated by Fisher's Least Significant Difference tests. *Aabd*, *Aspergillus allahabadi*; *Aflv*, *A. flavipes*); *Pcan*, *Penicillium canescens*; *Pfc*, *P. fructuariae-cellae*; *Tbr*, *Trichoderma brevicompactum*.

Neoscytalidium dimidiatum caused comparatively shorter lesions. Similar trends were observed in the wound-protection and the systemic-inoculation experiments. Depending on the pathogen, endophyte species, or inoculation method, lesion reduction ranged from means of 21.9% to 84.6%. The greatest reductions were obtained from *Trichoderma brevicompactum* against *L. brasiliensis* or *N. parvum* in the systemic inoculation experiments, whereas the lowest efficacy was observed for *Aspergillus allahabadii* against *B. dothidea*. Overall, *Trichoderma* treatments provided the greatest levels of protection, followed by *Penicillium* species, while *Aspergillus* species generally gave lower efficacy.

Effects of antagonists on lesion development caused by Lasiodiplodia brasiliensis *or* Neofusicoccum parvum *under field conditions*

The effects of endophytic fungi on lesion development caused by *L. brasiliensis* and *N. parvum* were evalu-

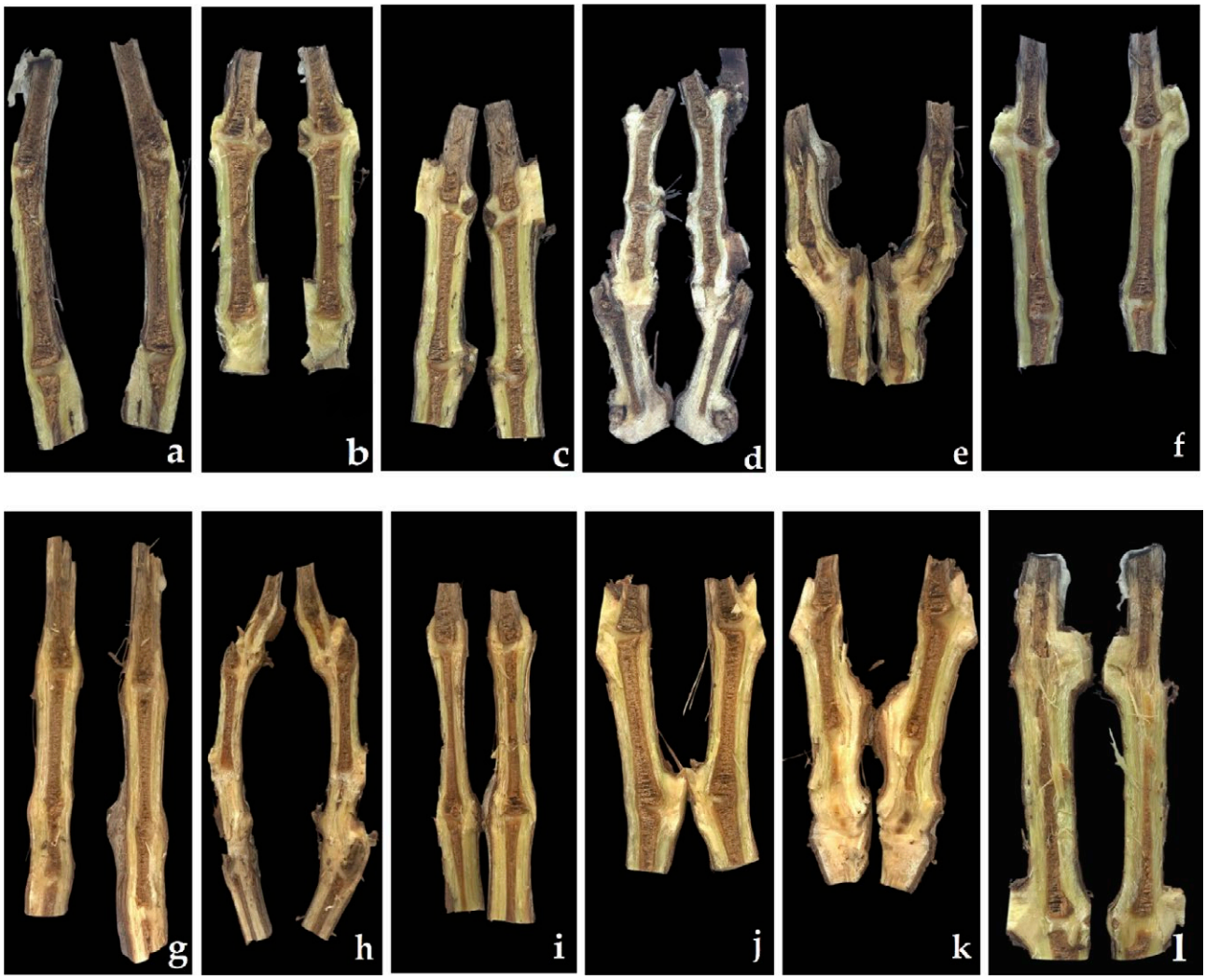

Figure 3. Internal lesions in 1-year-old woody shoots of grapevine ('Cardinal'), caused by *Botryosphaeriaceae* pathogens under field conditions, following prior applications of endophytic fungi. a to f; Inoculation with *L. brasiliensis*: a, control (water); b, *A. allahabadi*; c, *A. flavipes*; d, *P. canescens*; e, *P. fructuariae-cellae*; f) *T. brevicompactum.* g to l; Inoculation with *N. parvum*: g, control (water); h, *A. allahabadi*; i, *A. flavipes*; j, *P. canescens*; k, *P. fructuariae-cellae*; l, *T. brevicompactum.*

ated under field conditions in 2023 and 2024. Six months after inoculations, all *Aspergillus, Penicillium*, and *Trichoderma* treatments reduced internal lesion lengths ($P \geq 0.05$) compared with the pathogen-inoculated controls (Figure 3; Table 3). All treatments reduced lesion lengths compared with the pathogen-inoculated controls. Overall, biological efficacy ranged from 42.8% to 71.8% against *L. brasiliensis* and from 51.0% to 69.6% against *N. parvum*. Among the tested endophytes, *T. brevicompactum* consistently provided the greatest reductions in lesion development, whereas Aspergillus species generally showed lower efficacy. *Penicillium canescens* and *P. fructuariae-cellae* exhibited intermediate but consistent performance in both years. Similar trends were observed regardless of the inoculation method used.

DISCUSSION

This is the first study to evaluate local endophytic isolates against *Botryosphaeriaceae* pathogens in grapevines in Türkiye. To date, research has focused on species such as *T. asperellum, T. atroviride, T. harzianum*, and *T. viride*, or antagonistic *Bacillus* bacteria, for effects on grapevine trunk pathogens (Billar de Almeida *et al.,* 2020; Langa-Lomba *et al.,* 2023; Zanfano *et al.,* 2025). Little data on bioactivity of *T. brevicompactum* against these pathogens has been reported.

Aspergillus species can exist as pathogens or endophytes in agricultural plants, and they are most prevalent in hot, arid regions (Sibakwe *et al.,* 2017). Some endophytic *Aspergillus* species can protect plants to some

Table 3. Mean lesion lengths (± standard errors) and bio-control efficacy (%) from treatments with endophytic fungi against *L. brasiliensis (Lbra)* or *Neofusicoccum parvum (Np)* infections in field conditions

Endophyte	Pycniospore inoculations				Mycelium disc inoculations			
Treatment	Lesion length (mm)		Efficacy (%)		Lesion length (mm)		Efficacy (%)	
	2023	2024	2023	2024	2023	2024	2023	2024
Aab + Lbra	17.8 ± 0.9 b*	19.8 ± 1.4 b	47.0	42.8	15.5 ± 0.9 b	15.8 ± 0.6 b	51.6	53.0
Afp + Lbra	14.8 ± 0.3 c	17.3 ± 0.8 c	56.0	50.0	15.3 ± 0.9 b	15.0 ± 0.6 b	52.3	54.9
Pcn + Lbra	12.8 ± 0.5 d	12.5 ± 0.6 d	62.0	63.8	12.5 ± 0.3c	11.3 ± 1.0 c	60.9	66.1
Pfc + Lbra	12.0 ±0.4 de	12.8 ± 0.5 d	64.1	63.0	12.3 ± 0.9 c	11.5 ± 0.6 c	61.7	65.4
Tbr + Lbra	10.5 ± 0.5 e	11.3 ± 0.3 d	68.7	67.4	9.0 ± 0.7 d	10.0 ± 0.4 c	71.8	69.9
Control (*Lbra*)	33.5 ± 0.5 a	34.5 ± 0.6 a	-	-	32.0 ± 0.8 a	33.3 ± 1.3 a	-	-
Aab + Np	-	-	-	-	13.3 ± 0.3 b	14.3 ± 0.6 b	51.4	51.7
Afp + Np	-	-	-	-	12.0 ± 0.8 bc	11.3 ± 0.8 c	56.0	61.9
Pcn + Np	-	-	-	-	10.5 ± 0.6 cd	11.0 ± 0.4 c	61.5	67.8
Pfc + Np	-	-	-	-	11.3 ± 0.6 c	9.5 ± 0.6 cd	58.7	62.8
Tbr + Np	-	-	-	-	9.3 ± 0.5 d	9.0 ± 0.7 d	66.1	69.6
Control (*Np*)	-	-	-	-	27.3 ± 0.9 a	29.5 ± 0.5 a	-	-

*Means within columns are different ($P \leq 0.05$), based on Fisher's Least Significant Difference tests. *Aab*, *Aspergillus allahabadi*: *Aflv*, *A. flavipes*; *Pcn*, *Penicillium canescens*; *Pfc*, *P. fructuariae-cellae*; *Tbr*, *Trichoderma brevicompactum*.

extent against adverse environmental stresses, including high temperatures and drought, through the secondary metabolites they produce, and may these fungi can enhance plant growth (Ngo *et al.,* 2021; Niaz *et al.,* 2024). As endophytes, *Penicillium* species can produce a variety of metabolites that protect plants from stresses, encourage plant growth, and inhibit the development of plant diseases. Poveda *et al.* (2025) reported that *Trichoderma* species have antagonistic activity against plant diseases, and have beneficial effects comparable to endophytes. These results are supported by the fact that the *Aspergillus, Penicillium*, and *Trichoderma* isolates employed by Poveda *et al.* (2025) were from old vineyards (>40-years-old) growing in the hot, arid regions of southern Türkiye. Their prevalence under these challenging conditions, and their stability, demonstrate their potential as biological control agents, and indicate that they have adapted to the local environment. According to Baron and Rigobelo (2022), soil-borne fungi in plant rhizospheres disrupt root hair apical dominance, infect root cortices with hyphae, and then spread to endoderm cells, pericycles, and xylem and phloem tissues. This lends credence to the theory that the grapevines may have been infected over time by soil-inhabiting *Aspergillus, Penicillium*, and *Trichoderma*.

Although the re-isolation frequencies of *Penicillium* and *Trichoderma* species were moderate (4.2–34.2%), their recovery from woody tissues located 10 cm above the inoculation points demonstrated that these endophytes were could establish within grapevine tissues following inoculations. The present study was designed to assess the ability of selected local endophytes to colonize grapevine cuttings, rather than to optimize colonization under nursery production conditions. Colonization efficiency is likely to be influenced by factors such as inoculum formulation, application method, frequency of exposure, and environmental conditions during propagation. Previous studies have shown that *Trichoderma*-based biological control agents can establish in grapevine tissues, and provide long-term protection when applied during nursery propagation processes (Berbegal *et al*., 2020). Therefore, further research focusing on formulation development and nursery-scale applications may provide knowledge to help improve establishment of these local endophytic isolates. The present study results further highlight the potential of *Penicillium* and *Trichoderma* as biological control agents, demonstrating that they can successfully colonize grapevine cuttings when adequately formulated.

Aspergillus allahabadi has previously been detected in the rhizospheres of tomatoes and cabbage in northern Benin, as well as in internal tissues of these plants (Affokpon *et al.,* 2010). This fungus has also been found in root endodermis tissues of cinnamon plants in Thailand (Sadorn *et al.,* 2016), and in agricultural soils in India and South Korea (Mehrotra and Agnihotri, 1962; Tagele *et al.,* 2018). On the other hand, neither its rhizospheric nor endophytic forms have been documented in grapevines. Thus, the present study observation in Türkiye constitutes the first known detection of *A. allahabadi* in

grapevines. This species was isolated from a vine that was more than 40 years old, indicating, as with other plants, that it infects roots of grapevine plants before progressively colonizing internal tissues. *Aspergillus allahabadi* and *A. flavipes*, on the other hand, have slower infection and colonization processes than *Penicillium* and *Trichoderma* species, which can be occur more rapidly in these tissues. This was shown by their inabilities to be isolated from woody tissues 10 cm from the stem bases, even at 4 months after two separate inoculations. *Trichoderma brevicompactum* had a greater re-isolation rate than *Penicillium*, suggesting a greater ability to persist or grow in grapevine cuttings in the internal tissues within 4 months.

This study has also shown that these endophytes prevented internal lesions caused by *Botryosphaeriaceae* pathogens in grapevine stems, at rates of up to 84.6% when applied as sprays over open trunk wounds or systemically infiltrated into dormant grapevine cuttings. These results indicate that the endophytic isolates used in this study may have exerted their effects through competition for nutrients and for habitat, as well as through the secondary metabolites they produce. Sadorn *et al.* (2016) reported that *A. allahabadi* produced twelve different antimicrobial compounds, including allahabadolactones A and B. Ten of these compounds were found to inhibit growth of *Bacillus cereus*. Additionally, Nashat *et al. (*2024) investigated ability of *A. flavipes* isolated from grapevine trunks to prevent the *in vitro* mycelium growth of several grapevine trunk disease pathogens. Culture filtrates of *A. allahabadi* inhibited the mycelium growth of *Ilyonectria liriodendri* by 100%, of *Botrytis cinerea* by 49%, of *Macrophomina phaseolina* by 28%, and of *Neoscytalidium dimidiatum* by 3%.

Penicillium fructuariae-cellae was first discovered as a unique species on withered grape berries in the two Italian wine-producing regions of Soave and Valpolicella, and was classified as a weak pathogen (Lorenzini *et al.,* 2019). Its presence on grapevine trunks in Türkiye was later reported by Akgül and Kara (2022), who discovered that it had antagonistic properties that prevent growth of other fungi associated with GTDs. Building on these results, the present study has shown that *P. fructuariae-cellae* has potential to be an antagonistic fungus for use in grapevine wound protection, producing systemic infections and protecting grapevine wounds by 42 to 78.8%. Beyond grapevines, the study of Ren *et al.,* (2024) in China showed that applying culture filtrates of endophytic *P. fructuariae-cellae* isolates as sprays to seedling shoots decreased (by approx. 50-60%) internal lesions caused by *Diplodia sapinea*, a pathogen linked to shoot dieback of Mongolian pine. Through processes including nutrient and space competition, the treatment also had positive impact on Mongolian pine microbiota. Similarly, *P. canescens* isolated from grapevine roots reduced *in vitro* mycelium growth of pathogenic *Cytospora chrysosperma*, associated with GTDs, by 39% (using a dual culture assay) (Pazooki *et al*. (2026) in Iran. *Penicillium canescens* has been proposed as a possible biocontrol agent based on this effect, which is due to the synthesis of secondary metabolites (Toghueo and Boyom, 2020).

Biocontrol studies on grapevine plants and mature vines under field conditions using *Trichoderma* species have shown that fungi are consistently preferred over others, due to their significant activities. For example, in southern Italy (Urbez-Torres *et al.,* 2020), protective and tissue-colonizing properties of eight *Trichoderma* species isolated from grapevines against infections by *Diplodia seriata, N. parvum*, and *Eutypa lata* were examined. Of these, *T. atroviride, T. koningiopsis, and T. paratroviride* provided the strongest protection and host colonization abilities, while the other species showed comparatively lower performance. Contrary to present study results, *T. brevicompactum* was not detected in the southern Italian vineyards where isolations were carried out. These results indicate regional variability in presence and biocontrol effectiveness of different fungal species. In similar in Chile (Silva-Valderrama *et al.,* 2021), endophytic *Clonostachys rosea* and *Trichoderma* sp. obtained from grapevine rhizospheres and internal tissues inhibited *D. seriata, N. parvum*, and *Phaeomoniella chlamydospora* in grapevine cuttings. *Clonostachys rosea* gave stronger inhibitory effects than *Trichoderma* sp., likely due to a dual mechanism involving both hyperparasitism and antibiosis. These results show that performance of endophytic isolates can vary with regional and experimental conditions. Pollard-Flamand *et al. (*2023) conducted studies in Canada in greenhouse and field conditions, comparing how local isolates of *T. asperelloides*, *T. atroviride*, and *T. canadense* protected grapevine wounds after pruning, alongside a commercial product (*T. atroviride* 77-b) and a fungicide (tebuconazole + boric acid). The local *T. atroviride* and *T. asperelloides* together reduced lesions of *D. seriata* and *N. parvum* by 93 to 100%, and this combination gave better pathogen control than commercial treatments in glasshouse and field conditions.

A limitation of the present study was that pycniospore inoculations could not be assessed for *N. parvum* under field conditions. Despite repeated attempts using the methods of Amponsah *et al*. (2008), pycniospore production by the isolate used in the present study remained insufficient for inoculation experiments. Consequently, mycelium agar plugs were used as inoculum for *N. parvum*. Since *Botryosphaeriaceae* species naturally infect pruning wounds primarily through airborne

conidia, results obtained with mycelium inoculations should be interpreted with caution, although use of mycelium plugs is a common experimental approach for evaluating susceptibility of grapevine tissues and efficacy of pruning wound protectants under controlled conditions (e.g. Blundell and Eskalen, 2022). Future research should evaluate endophytic fungi for effects on naturally produced pathogen conidia under field conditions.

CONCLUSIONS

This study has demonstrated the biocontrol potential of vineyard-origin endophytic *Penicillium* and *Trichoderma* species from the Eastern Mediterranean Region (Türkiye) against *Botryosphaeriaceae* pathogens, in laboratory and field conditions. This is also the first report of *P. fructuariae-cellae* and *T. brevicompactum* applications against GTDs. While *Aspergillus* species showed lower performance than other candidate fungi, they still protected grapevine pruning wounds. Effective colonization and systemic establishment of *Penicillium* and *T. brevicompactum*, together with substantial wound protection, indicates that these local isolates merit further evaluation for nursery and field uses. Nevertheless, practical applications in vineyards require formulation development and further field performance assessments across different locations.

ACKNOWLEDGEMENTS

The authors thank the Rectorate of Çukurova University, the Turkish Ministry of Agriculture and Forestry, General Directorate of Agricultural Research and Policies, and the Directorate of the Biological Control Research Institute. Additionally, T. Tarık Erper, Suat Erdem, Utkucan Özbilen, and Mert Sönmez are acknowledge for their assistance in the laboratory and field. This study was financially supported by the Turkish Ministry of Agriculture and Forestry, in project TAGEM/BSAD/A/22/A2/P1/5333, and The Çukurova University Scientific Research Projects Department, in project FDK-2021-14133.

LITERATURE CITED

Affokpon D., Coyne L., Tossou C., Coosemans J., 2010. First report of *Aspergillus allahabadii* Mehrotra and Agnihotri in vegetable fields in Northern Benin (West-Africa). *Bulletin de la Recherche Agronomique du Bénin* 67: 20–25.

Akgül D.S., Kara H.İ., 2022. Gaziantep bağ alanlarındaki endofitik funguslar ve bunların fungal gövde patojenleriyle antagonistik ilişkileri. *Türkiye Biyolojik Mücadele Dergisi* 13: 48–66 (in Turkish). https://doi.org/10.31019/tbmd.1095497

Akgül D.S., Savaş N.G., Yildiz M., Bülbül I., Özarslandan M., 2023. Current status of grapevine trunk disease pathogens on asymptomatic nursery-produced grapevines in Türkiye. *Phytopathologia Mediterranea* 62:151–163. https://doi.org/10.36253/phyto-14148

Alves A., Crous P.W., Correia A., Phillips A.J.L., 2008. Morphological and molecular data reveal cryptic speciation in *Lasiodiplodia theobromae*. *Fungal Diversity* 28:1–13.

Amponsah N., Jones E., Ridgway H., Jaspers M., 2008. Production of Botryosphaeria species conidia using grapevine green shoots. *New Zealand Plant Protection*, 61: 301–305. https://doi.org/10.30843/nzpp.2008.61.6840

Anonymous, 2025. General Directorate of Plant Production at Turkish Ministry of Agriculture and Forestry. https://www.tarimorman.gov.tr/BUGEM. Accessed 14.04.2026

Baron N.C., Rigobelo E.C., 2022. Endophytic fungi: a tool for plant growth promotion and sustainable agriculture. *Mycology* 13:39–55. https://doi.org/10.1080/21501203.2021.1945699

Benlioğlu K., Özakman M., 1998. Bağ üretim materyalinde kök uru etmeni *Agrobacterium tumefaciens*'in saptanması (in Turkish). *Turkish Journal of Agriculture and Forestry* 22: 167–174.

Berbegal M., Ramón-Albalat A., León M., Armengol J. 2020. Evaluation of long-term protection from nursery to vineyard provided by *Trichoderma atroviride* SC1 against fungal grapevine trunk pathogens. *Pest Management Science* 76: 967–977. https://doi.org/10.1002/ps.5605

Billar de Almeida A., Concas J., Campos M.D., Materatski P., Varanda C., Patanita M., Felix M.D.R., 2020. Endophytic fungi as potential biological control agents against grapevine trunk diseases in Alentejo region. *Biology* 9: 420. https://doi.org/10.3390/biology9120420

Blundell R., Eskalen A., 2022. Evaluation of biological and chemical pruning wound protectants to control grapevine trunk disease pathogens. *Eutypa lata* and *Neofusicoccum parvum*. *Plant Health Progress* 23: 197–205. https://doi.org/10.1094/PHP-08-21-0113-RS

Busby P.E., Ridout M., Newcombe G., 2016. Fungal endophytes: modifiers of plant disease. *Plant Molecular Biology* 90: 645–655. https://doi.org/10.1007/s11103-015-0412-0

Bustamante M.I., Elfar K., Kuzmenko J., Zaninovich T., Arreguin M., Carachure C., Eskalen A., 2024. Reassessing the etiology of Aspergillus vine canker and summer bunch rot of table grapes in California. *Plant Disease* 108:941–950. https://doi.org/10.1094/PDIS-06-23-1137-RE

Deyett E., Rolshausen P.E., 2020. Endophytic microbial assemblage in grapevine. *FEMS Microbiology Ecology* 96: fiaal053. https://doi.org/10.1093/femsec/fiaa053

El-Dawy E.G., Hussein M.A., El-Nahas S., 2024. Description and management of *Aspergillus* section Nigri causing post-harvest bulbs rot of onion. *Scientific Reports* 14: 6076. https://doi.org/10.1038/s41598-024-53849-9

Glass N.L., Donaldson G.C., 1995. Development of primer sets designed for use with PCR to amplify conserved genes from filamentous ascomycetes. *Applied Environmental Microbiology* 61: 1323–1330. https://doi.org/10.1128/aem.61.4.1323-1330.1995

Gomez K.A., Gomez A.A., 1984. *Statistical Procedures for Agricultural Research* (2nd ed.). Wiley, London, 680 pp.

Görür V., Akgül D.S., 2019. Fungicide suspensions combined with hot-water treatments affect endogenous *Neofusicoccum parvum* infections and endophytic fungi in dormant grapevine canes. *Phytopathologia Mediterranea* 58: 559–571. https://doi.org/10.14601/Phyto-10822.

Gramaje D., Aroca A., Raposo R., García-Jiménez J., Armengol J., 2009. Evaluation of fungicides to control Petri disease pathogens in the grapevine propagation process. *Crop Protection* 28: 1091–1097. https://doi.org/10.1016/j.cropro.2009.05.010

Gramaje D., Armengol J., 2011. Fungal trunk pathogens in the grapevine propagation process: potential inoculum sources, detection, identification, and management strategies. *Plant Disease* 95: 1040–1055. https://doi.org/10.1094/PDIS-01-11-0025

Grijseels S., Nielsen J.C., Nielsen J., Larsen T.O., Frisvad J.C., Nielsen K.F., Workman M., 2017. Physiological characterization of secondary metabolite producing *Penicillium* cell factories. *Fungal Biology and Biotechnology* 4: 8. https://doi.org/10.1186/s40694-017-0036-z

Hagag A., Abdelwahab M.F., Abd El-Kader A.M., Fouad M.A., 2022. The endophytic *Aspergillus* strains: a bountiful source of natural products. *Journal of Applied Microbiology* 132: 4150–4169. https://doi.org/10.1111/jam.15489

Langa-Lomba N., González-García V., Venturini-Crespo M.E., Casanova-Gascón J., Barriuso-Vargas J.J., Martín-Ramos P., 2023. Comparison of the efficacy of *Trichoderma* and *Bacillus* strains and commercial biocontrol products against grapevine Botryosphaeria dieback pathogens. *Agronomy* 13: 533. https://doi.org/10.3390/agronomy13020533

Lorenzini M., Cappello M.S., Perrone G., Logrieco A., Zapparoli G., 2019. New records of *Penicillium* and *Aspergillus* from withered grapes in Italy, and description of *Penicillium fructuariae-cellae* sp nov. *Phytopathologia Mediterranea* 58: 323–340. https://doi.org/10.14601/Phytopathol_Mediter-10619

Mehrotra B.S., Agnihotri V.P., 1962. Two new species of *Aspergillus* from India. *Mycologia* 54: 400–406.

Nashat L.H., Haleem R.A., Ali S.H., 2024. Molecular identification and antimicrobial potential of endophytic fungi against some grapevine pathogens. *PLoS One* 19: e0309041. https://doi.org/10.1371/journal.pone.0309041

Ngo M.T., Van Nguyen M., Han J.W., Kim B., Kim Y.K., Park M.S., Choi G.J., 2021. Biocontrol potential of *Aspergillus* species producing antimicrobial metabolites. *Frontiers in Microbiology* 12: 804333. https://doi.org/10.3389/fmicb.2021.804333

Niaz K., Rauf M., Arif M., Hamayun M., Gul H., Hashem A., Abd_Allah E.F., Wu Q.S., 2024. Drought-tolerant fungal microbes *Aspergillus oryzae* and *Aspergillus fumigatus* elevate physiohormonal and antioxidant responses of maize under drought stress. *Frontiers in Microbiology* 15: 1488639. https://doi.org/10.3389/fmicb.2024.1488639

O'Donnell K., Cigelnik E., Nirenberg H.I., 1998. Molecular systematics and phylogeography of the *Gibberella fujikuroi* species complex. *Mycologia* 90 (3): 465–493. https://doi.org/10.1080/00275514.1998.12026933

Pazooki S., Shekariesfahlan A., Maleki M., Naeimi S., 2024. Isolation and identification of endophytic and grapevine trunk diseases associated fungi with antagonistic potential against *Cytospora chrysosperma*. *Journal of Plant Pathology* 108: 99–110. https://doi.org/10.1007/s42161-024-01731-y

Pieterse C.M.J., Zamioudis C., Berendsen R.L., Weller D.M., Van Wees S.C.M., Bakker P. 2014. Induced systemic resistance by beneficial microbes. *Annual Review of Phytopathology* 52: 347–375. https://doi.org/10.1146/annurev-phyto-082712-102340

Pollard-Flamand J., Boulé J., Hart M., Úrbez-Torres J.R., 2022. Biocontrol activity of *Trichoderma* species isolated from grapevines in British Columbia against Botryosphaeria dieback fungal pathogens. *Journal of Fungi* 8: 409. https://doi.org/10.3390/jof8040409

Pollard-Flamand J., Boulé J., Hart M., Úrbez-Torres J.R., 2023. Biological control of Botryosphaeria dieback of grapevines in British Columbia, Canada. *Ameri-*

can Journal of Enology and Viticulture 74. https://doi.org/10.5344/ajev.2023.23052

Pouzoulet J., Mailhac N., Couderc C., Besson X., Dayde J., Jacques A., 2013. A method to detect and quantify *Phaeomoniella chlamydospora* and *Phaeoacremonium aleophilum* DNA in grapevine wood samples. *Applied Microbiology and Biotechnology* 97: 10163–10175. https://doi.org/10.1007/s00253-013-5299-6

Poveda J., Santamaria O., Martin-Garcia J., 2025. Fungal metabolites in plant protection. In: *Fungal Metabolites for Agricultural Applications: Biostimulation fnd Crop Protection by Fungal Biotechnology*. (Poveda J, Santamaría Ó, Martín-García J,. ed.) Springer, Cham. https://doi.org/10.1007/978-3-031-76587-2

Ren N., Wang L., You C., 2024. Diversity, community structure, and antagonism of endophytic fungi from Mongolian pine trees. *Journal of Fungi* 10: 212. https://doi.org/10.3390/jof10030212

Sadorn K., Saepua S., Boonyuen N., Laksanacharoen P., Rachtawee P., Prabpai S., 2016. Allahabadolactones A and B from the endophytic fungus *Aspergillus allahabadii*. *Tetrahedron* 72: 489–495. https://doi.org/10.1016/j.tet.2015.11.056

Sibakwe C.B., Kasambara-Donga T., Njoroge S.M.C., Msuku W.A.B., Mhango W.G., Brandenburg R.L., Jordan D.L., 2017. The role of drought stress on aflatoxin contamination in groundnuts (*Arachis hypogea* L.) and *Aspergillus flavus* population in the soil. *Modern Agricultural Science and Technology* 3(5-6): 22–29. https://doi.org/10.15341/mast(2375-9402)/03.03.2017/005

Silva-Valderrama I., Toapanta D., Miccono M.L.A., Lolas M., Díaz G.A., Cantu D., Castro A., 2021. Biocontrol potential of grapevine endophytic and rhizospheric fungi against trunk pathogens. *Frontiers in Microbiology* 11: 614620. https://doi.org/10.3389/fmicb.2020.614620

Tagele S.B., Adhikari M., Gurung S.K., Lee H.G., Kim S.W., Kim H.S., Lee Y.S., 2018. New records of *Aspergillus allahabadii* and *Penicillium sizovae* from crop field soil in Korea. *Mycobiology* 46: 297–304. https://doi.org/10.1080/12298093.2018.1538069

Thambugala K.M., Daranagama D.A., Phillips A.J.L., Kannangara S.D., Promputtha I., 2020. Fungi vs fungi in biocontrol: an overview of fungal antagonists applied against fungal plant pathogens. *Frontiers in Cellular and Infection Microbiology* 10: 604923. https://doi.org/10.3389/fcimb.2020.604923

Toghueo R.M.K., Boyom F.F., 2020. Endophytic *Penicillium* species and their agricultural, biotechnological, and pharmaceutical applications. 3 *Biotech* 10: 107. https://doi.org/10.1007/s13205-020-2081-1

Urbez-Torres J.R., Tomaselli E., Pollard-Flamand J., Boule J., Gerin D., Pollastro S., 2020. Characterization of *Trichoderma* isolates from southern Italy and their potential biocontrol activity against grapevine trunk disease fungi. *Phytopathologia. Mediterranea* 59: 425–440. https://doi.org/10.14601/Phyto-11273

White T.J., Bruns T., Lee S., Taylor J., 1990. Amplification and direct sequencing of fungal ribosomal RNA genes for phylogenetics. In: (Innis M.A. *et al*., ed.), *PCR protocols*. Academic Press, pp 315–322.

Zanfaño L., Carro-Huerga G., Rodríguez-González Á., Ramírez-Lozano D., Mayo-Prieto S., Gutiérrez S., Casquero P.A., 2025. Biosolutions from native *Trichoderma* strains against grapevine trunk diseases. *Agronomy* 15:1901. https://doi.org/10.3390/agronomy15081901

Phytopathologia Mediterranea
The international journal of the
Mediterranean Phytopathological Union

Firenze University Press
www.fupress.com/pm

Research Papers

Identification and characterization of two isolates of Bougainvillea chlorotic vein banding virus (*Badnavirus venabougainvilleae*) in bougainvillea plants from Italy

Amani BEN SLIMEN, Reem YAZBECK, Toufic ELBEAINO, Michele DIGIARO*

International Centre for Advanced Mediterranean Agronomic Studies (CIHEAM of Bari), Valenzano, Italy
*Corresponding author. E-mail: digiaro@iamb.it

Summary. Ornamental plants can be reservoirs of plant viruses, facilitating virus dissemination through international trade. In this bougainvillea study, 58 samples collected from six ornamental nurseries in Apulia (southern Italy) were screened for the presence of known bougainvillea-infecting viruses, using PCR assays. Among the viruses tested, only Bougainvillea chlorotic vein banding virus (BCVBV) was detected, occurring in five (8.6%) of the samples, whereas Impatiens necrotic spot virus (INSV), Clerodendron yellow mosaic virus (ClYMV), tomato yellow ring virus (TYRV), and cucumber mosaic virus (CMV) were not detected. High-throughput sequencing (HTS) of one BCVBV-positive sample (O54) enabled reconstruction of a complete viral genome, designated BCVBV Mini-Thai (GenBank accession no. PQ682517). A second HTS analysis of a pooled set of PCR-negative samples revealed a genetically distinct BCVBV isolate that was not detected by PCR using previously published primers. The complete genome of this isolate was reconstructed through contig assembly and gap-filling PCR using newly designed primers, and was named BCVBV Apulia 1 (PQ682518). The genome of Mini-Thai was 8,822 nucleotides long, and had high nucleotide (98.5%) and amino acid (98.7%) similarities with the Malaysian isolate BCVBV-UKM. In contrast, BCVBV Apulia 1 (PQ682518) was 8,694 nucleotides long and had greatest nucleotide similarity (81.6%) with the Brazilian isolate BCVBV UNB-01, with 84.0% amino acid similarity in the polyprotein. Both isolates had typical *Badnavirus* genome organization, with four open reading frames, and clustered in distinct phylogenetic clades. Further screening of the 58 collected samples using primers designed on the Apulia 1 isolate detected seven (12.1%) additional infected samples. A primer set targeting conserved genomic regions was also developed, enabling detection of both isolates. This report is the first detection of BCVBV in Italy and Europe, and also reveals the presence of a genetically divergent isolate of this virus.

Keywords. BCVBV, HTS, *Badnavirus*, genetic diversity, Apulia.

OPEN ACCESS

Citation: Ben Slimen, A., Yazbeck, R., Elbeaino, T. & Digiaro, M. (2026). Identification and characterization of two isolates of Bougainvillea chlorotic vein banding virus (*Badnavirus venabougainvilleae*) in bougainvillea plants from Italy. *Phytopathologia Mediterranea* 65(2): 301-308. doi: 10.36253/phyto-17358

Accepted: July 22, 2026

Published: September 10, 2026

© 2026 Author(s). This is an open access, peer-reviewed article published by Firenze University Press (https://www.fupress.com) and distributed, except where otherwise noted, under the terms of the CC BY 4.0 License for content and CC0 1.0 Universal for metadata.

Data Availability Statement: All relevant data are within the paper and its Supporting Information files.

Competing Interests: The Author(s) declare(s) no conflict of interest.

Editor: Arnaud G Blouin, Institut des sciences en production végétale IPV, DEFR, Agroscope, Nyon, Switzerland.

ORCID:
ABS: 0000-0001-8070-5120
TE: 0000-0003-2211-7907
MD: 0009-0006-3089-3606

INTRODUCTION

Bougainvillea is a perennial ornamental plant genus that is widely cultivated and traded. *Bougainvillea* (*Nyctaginaceae*) includes 18 species, of which three are of major commercial importance: *Bougainvillea spectabilis* Willd., *B. glabra* Choisy, and *B. peruviana* Bonpl. (Abarca-Vargas and Petricevich, 2018). Numerous hybrids and cultivars have arisen from interspecific crosses or spontaneous hybridizations where these species are co-cultivated, such as in East Africa, India, the Canary Islands, Australia, North America, and the Philippines (Datta *et al*., 2021).

Despite its global distribution, relatively few viral diseases have been reported in *Bougainvillea*, likely reflecting limited research attention rather than true resistance. The most studied virus is Bougainvillea chlorotic vein banding virus (BCVBV; *Badnavirus venabougainvilleae*), a putative *Badnavirus* first described in Brazil on *B. spectabilis* (Chagas *et al*., 2001) and subsequently confirmed at the molecular level by Rivas *et al.* (2005). A related *Badnavirus* infecting *B. glabra*, associated with chlorotic spot and mild mosaic symptoms, was also reported in Brazil (Yamashita *et al*., 2004). A complete genome sequence of this virus, initially named Bougainvillea spectabilis chlorotic vein-banding virus, was characterized in Taiwan by Wang and coworkers in 2007 (NC_011592). Similar pathogens were later described in Taiwan, India, and Malaysia (Tsai *et al*., 2008; Baranwal *et al*., 2010; Yusop *et al*., 2019), and were subsequently assigned to BCVBV by the International Committee on Taxonomy of Viruses (2026). Another *Badnavirus*, showing 75% similarity to BCVBV and named Bougainvillea glabra chlorotic spot virus-Egypt (BgCSV-E), was reported in Egypt (Abdel-Salam, 2020).

The BCVBV genome consists of a circular dsDNA molecule of 8,759 bp containing four ORFs. Molecular analyses of Brazilian and Asian isolates have indicated the presence of at least three novel *Badnavirus* species or strains infecting *Bougainvillea* (Alexandre *et al.,* 2016). Typical symptoms caused by these viruses include leaf mottling, vein banding, chlorosis, and distortion, and plant stunting (Bhat *et al*., 2016).

Other viruses reported in *Bougainvillea* include: Clerodendron yellow mosaic virus (ClYMV, *Begomovirus clerodendronflavi*) infecting *B. peruviana* in India (Nehra *et al.,* 2014); Impatiens necrotic spot virus (INSV, *Orthotospovirus impatiensnecromaculae*) in Iran (Shahraeen *et al*., 2002); tomato yellow ring virus (TYRV, *Orthotospovirus tomatanuli*) (Ghotbi *et al*., 2005); and cucumber mosaic virus (CMV, *Cucumovirus CMV*) on *B. spectabilis* (Shahmohammadi *et al*., 2015).

The present study investigated occurrence of viruses in *Bougainvillea* spp. in ornamental nurseries in Apulia (Southern Italy) and outlines the first detection of Bougainvillea chlorotic vein-banding virus in *Bougainvillea* spp. in Italy.

MATERIALS AND METHODS

Plant material

From April to June 2022, 58 leaf samples were collected from symptomatic (chlorotic leaf spots and mottling) and asymptomatic bougainvillea plants, in six ornamental nurseries in Apulia (Southern Italy), located in Terlizzi (n = 16), Valenzano (n = 8), Sammichele di Bari (n = 6), Monopoli (n = 25), and Muro Leccese (n = 3) (Supplementary Table S1).

DNA and RNA extractions

DNA was extracted using a CTAB-based protocol (Doyle, 1991). Approximately 50 to 80 mg of midribs and petioles from each leaf sample were homogenized in CTAB buffer (1M Tris-HCl, NaCl, 0.5M EDTA, 2% CTAB, 2.5% PVP40), then incubated at 65 °C, purified with chloroform: isoamyl alcohol (24:1), precipitated with isopropanol, and then resuspended in sterile water for storage at –20 °C. Total RNA was extracted according to Foissac *et al*. (2001), using a guanidine thiocyanate-based buffer and silica particle purification. Nucleic acid quality and concentrations were assessed using a Qubit™ Fluorometer (ThermoFisher Scientific) and agarose gel electrophoresis (1.2% TBE). Purified DNAs were stored at –20 °C until further analysis.

Complementary DNA synthesis and PCR assays

cDNA was synthesized from 500 ng of total RNA, using 1 µL random hexamer primers (0.5 mg mL^{-1}) and M-MLV reverse transcriptase (200 U μL^{-1}), according to the manufacturer's instructions (Thermo Fisher Scientific).

PCR reactions were carried out using DreamTaq DNA Polymerase (5 U μL^{-1}), each in a final volume reaction of 25 µL, with 2.5 µL of cDNA as template. Different primer sets were used for each virus (Table 1). Cycling conditions each consisted of an initial denaturation at 94°C for 4 min, followed by 40 cycles each of 94°C for 30 s, annealing at 50–55°C for 35 s, and 72°C for 45–50 s, with a final extension at 72°C for 7 min. All

Table 1. List of primers used for RT-PCR detection of viruses in bougainvillea plants.

Virus	Primers	Sequence 5′- 3′	Amplicon size (bp)	References
Bougainvillea chlorotic vein banding virus (BCVBV)	BCVBV-1 BCVBV-2	ACAGCGATTTCATTGCTGTG GACTAGTTCTCGATCAGAAGG	413	Tsai *et al.,* 2008
Clerodendron yellow mosaic virus (ClYMV)	ClYMV-FP ClYMV-RP	GTGTGAATATTGGTTGCATCATGTGGG ACCCAGGCCTGTCTTCTTGTGACG	313	Akram *et al*., 2020
cucumber mosaic virus (CMV)	CMV-F4 CMV-F3	TGAGTCGAGTCATGGACAAA CTCCCAGTCTGATTCCGTGT	657	Lin *et al*., 2003
Impatiens necrotic spot virus (INSV)	INSV-F3 INSV-R2	GCAAAGATTACCAAGGAG TCCCAAAATCAATAGTAGC	763	Elliott *et al.,* 2009
tomato yellow ring virus (TYRV)	TYRV-F TYRV-R	ACTCATTAAAATGCATCGTTCT CTAAGTAAACACCATGGCTACC	912	Birithia *et al.,* 2012

amplifications were carried out in a Bio-Rad T100 thermal cycler. Amplified products were analysed on 1.2% agarose gels and were sequenced using Sanger sequencing by Eurofins Genomics, Germany.

High-Throughput Sequencing (HTS) using Illumina

Based on the results of the previous molecular analyses, one virus-infected sample was selected for high-throughput sequencing (HTS). In addition, HTS was used for a pooled set of 20 randomly selected and apparently negative samples, to investigate the possible presence of other, potentially unknown viruses, or of highly divergent isolates of known viruses that may not have been detected by the primers used in the initial molecular assays. A total of 500 ng of RNA was used for ribosomal RNA (rRNA) depletion, carried out by Eurofins Genomics, Ebersberg, Germany. Library preparation was subsequently carried out, followed by fragment amplification and purification. Illumina sequencing was then used on the reverse-transcribed templates, with a 2 × 150 bp paired-end sequencing run to obtain approx. 5 million sequence pairs (10 million reads per sample per pool) (Eurofins Genomics).

Sequence and library analysis

Raw reads were processed using Geneious Prime 2024.0. Quality assessment and trimming were carried out using the BBDuk package (k-mer length = 21, allowing one mismatch). Filtered reads were then error-corrected and normalized using BBNorm, targeting 40× coverage, while retaining regions with minimum depths of 6×. *De novo* assembly was carried out using SPAdes v3.15.5 (Bankevich *et al*., 2012). The resulting contigs were screened for sequence homology using BLASTx (e-value cut-off 10^{-6} to 10^{-2}) and BLASTn against the NCBI viral RefSeq database (accessed 6 May 2025). Complete virus genomes were reconstructed by reference mapping using the Geneious mapper, with the medium sensitivity / fast setting and associated default parameters, and remaining gaps were filled by designing additional primers. Preliminary phylogenetic relationships were inferred in Geneious, using the Maximum Likelihood method with 1,000 bootstrap replicates.

RESULTS

PCR detection of Bougainvillea viruses

The PCR assays carried out on the 58 bougainvillea samples detected presence of one virus, BCVBV, of the five viruses assessed. Five plants (P53, P54, P55, O54, O58), all of Mini Thai cultivar, were found to be infected (8.6% of the samples): two were from Terlizzi and three from Monopoli. None of the infected plants exhibited symptoms at the time of sampling. Contrary to the 413-bp amplicon size reported by Tsai *et al*. (2008), the same primers in this study amplified a 390-bp fragment, due to sequence differences between the virus isolates. Sequence analysis of 390 bp amplicons revealed 99.6 to 100% nucleotide similarities among them, and 97.2 to 99.6% similarities with the BCVBV UKM isolate from Malaysia (GenBank accession no. MK501794).

High-Throughput Sequencing (HTS) and subsequent PCR assays

The Illumina sequencing run carried out on RNA extracted from a single BCVBV-positive sample (O54) yielded 6.4 million paired-end reads, and 10.6 million paired-end reads from the pooled PCR-negative samples.

After quality filtering, these were each reduced to approx. 2.7 and 4.8 million high-quality reads. *De novo* assembly produced 13,454 contigs from sample O54 with contig lengths of 200 to 2,082 bp, and 32,126 contigs from the pooled samples with contig lengths of 160 to 1,452 bp.

BLASTn and BLASTx analyses revealed presence of BCVBV in both datasets. Using three contigs of varying lengths obtained from the BCVBV-infected sample (O54), the complete virus genome was successfully reconstructed. This isolate was tentatively designated as BCVBV isolate Mini Thai (PQ682517), as it was detected exclusively in the Mini-Thai cultivar. The assembled genome was 8,822 bp in length and had 98.5% nucleotide similarity with the BCVBV UKM isolate.

In the pooled sample, which had initially tested negative by PCR, several contigs were assembled. These were used for preliminary identification of virus sequences and showed greatest nucleotide similarities (from 70 to 90%) with the Brazilian isolate BCVBV UNB-01 (GenBank accession number MK473389). However, mapping against this reference genome revealed several gaps, indicating incomplete genome coverage.

To investigate the prevalence of this putative divergent variant, the specific primer pair BVs-ACAAGAAGAATCAGGAAGCT / BVas-CAATGGTGCAGAGGGTTT was designed to amplify a 197 bp fragment within the most divergent genomic region identified during mapping against the BCVBV Mini-Thai isolate. Of the 58 samples tested, seven (12.1%) were positive, including O109, O110, P47, P48, C4, O77, and O81, (Supplementary Table S1). None of the five plants infected with the Mini-Thai isolate tested positive with these primers.

To complete the virus genome, ten additional primer pairs were designed based on the newly assembled contigs and their alignments with the BCVBV UNB-01 reference genome, allowing all the remaining gaps to be bridged (Supplementary Table S2). PCR assays using these primers were carried out on a single positive sample (P47), and all target regions were successfully amplified. The resulting sequences were assembled to reconstruct the complete genome of the virus isolate, which was designated as BCVBV Apulia 1 (GenBank accession no. PQ682518).

A universal primer set was developed by aligning all available BCVBV sequences in GenBank together with those obtained in the present study. Primers (7bs- GACCTCACCACATGGAGATA and 7ba-AGGRTKATCTCYTCTTTGTCAA), targeting a highly conserved region, reliably amplified a 330 bp fragment within the polyprotein of the Mini-Thai and Apulia 1 isolates (Figure 1).

Characterization of BCVBV isolate genomes

Both BCVBV isolates identified in the present study retained the typical genome organization of badnaviruses. BCVBV Apulia 1 possessed a double-stranded DNA genome of 8,694 nt, in which four open reading frames (ORFs) were identified. The functions of ORF1, ORF2, and ORF4 remain unknown; these ORFs encode proteins of, respectively, 151, 145, and 197 amino acids (Figure 2 A). ORF3, the largest coding region, encodes a polyprotein of 2,214 amino acids, containing, in sequential order, motifs corresponding to a zinc-finger domain, a pepsin-like aspartic protease domain, a reverse transcriptase domain, and an RNase H-like domain. The genome is flanked by two non-coding regions (NCRs), measuring 537 nt at the 5′ end and 349 nt at the 3′ end.

The BCVBV Mini-Thai genome shared high nucleotide similarity (98.5%) with the Malaysian BCVBV

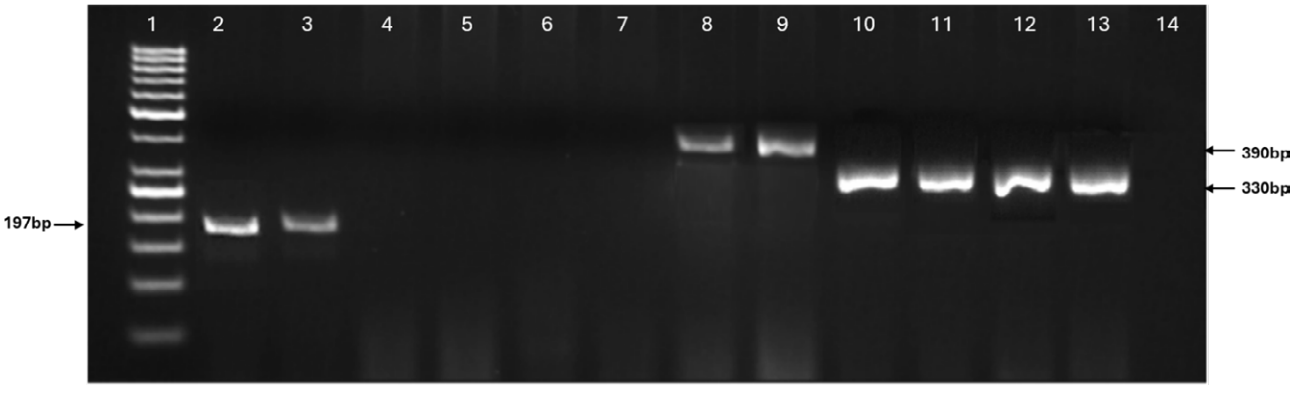

Figure 1. PCR amplifications of BCVBV isolates Apulia 1 and Mini-Thai, using isolate-specific and universal primers. Lane 1: 50 bp DNA ladder. Lanes 2 to 5: amplifications with primers BVs/BVa; lanes 6 to 9: amplifications with primers BCVBV-1/BCVBV-2; lanes 10 to 13: amplifications with universal primers 7bs/7ba. For each primer set, lanes 2 and 3, 6 and 7, and 10 and 11 correspond to isolate Apulia 1, while lanes 4 and 5, 8 and 9, and 12 and 13 correspond to isolate Mini-Thai. Lane 14 is the negative control.

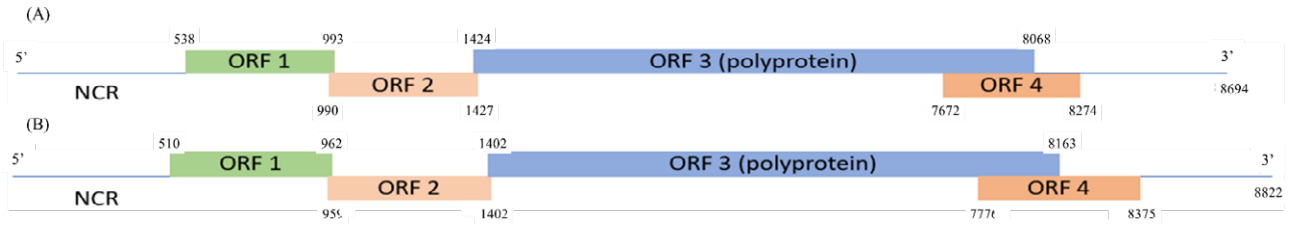

Figure 2. Genome organization of the two BCVBV isolates, showing the relative positions of the ORFs: (A) isolate Apulia 1; (B) isolate Mini-Thai.

UKM isolate. Its genome consisted of 8,822 nt and contained four ORFs: ORF1 encoding a protein of 150 amino acids, ORF2 of 147 amino acids, ORF3 (polyprotein) of 2,254 amino acids, and ORF4 encoding a protein of 199 amino acids (Figure 2B). The 5′ and 3′ non-coding regions (NCRs) were, respectively, of lengths 509 nt and 447 nt.

BLASTn analysis of the complete BCVBV Apulia 1 genome revealed greatest nucleotide similarity (81.6%) with the BCVBV UNB-01 isolate, whereas the least similarity (73.7%) was with the Taiwanese BCVBV isolate (NC_011592).

Detailed pairwise comparison of the polyprotein sequences between the two isolates identified in this study (Apulia 1 and Mini-Thai), previously reported as BCVBV isolates, and with other members of *Badnavirus*, confirmed the high divergence of Apulia 1 (Table 2). Sequence divergence ranged from 19.5% to 23.4% at nucleotide level, and from 15.4% to 19.0% at amino acid level. This comparison is particularly relevant, as this genomic region forms the basis for species demarcation criteria within *Badnavirus*, which is currently set at 20% nucleotide divergence.

Phylogenetic analyses based on the amino acid sequences of the polyprotein were carried out for the same viruses and isolates. Consistent with the results of the pairwise sequence comparison, two major clades were identified. Clade 1 comprised exclusively BCVBV isolates, with the Apulia1 isolate clustering in a subclade with the UNB-01 isolate, whereas the Mini-Thai isolate formed a separate subgroup with the Taiwanese and Malaysian (UKM) isolates. The remaining *Badnavirus* members included in the analysis clustered in a distinct, separate clade (Figure 3).

DISCUSSION AND CONCLUSIONS

Ornamental plants may serve as reservoirs of plant viruses, facilitating virus spread through international trade. Movements of infected plant material have repeatedly been associated with introductions of emerging pathogens into new areas, often with significant economic and environmental impacts. A notable example was introduction of *Xylella fastidiosa* into Italy via infected ornamental coffee plants, which resulted in severe out-

Table 2. Pairwise comparison matrix of polyprotein sequences from different BCVBV isolates and other *Badnavirus* members, based on nucleotide and amino acid sequences.

		% similarity of polyprotein sequences (nt)										
		Mini-Thai	UKM	TWN	Apulia 1	UNB-01	BVF	DBALV2	MBV1	RYNV	GVBaV	PVCV
% similarity of polyprotein sequences (aa)	Mini-Thai		**98.6**	99.3	**76.6**	**75.3**	43.8	42.0	38.7	41.4	39.3	37.3
	UKM	**98.7**		98.6	76.8	75.7	43.8	41.8	38.7	41.4	39.4	37.3
	TWN	98.5	98.7		76.7	75.5	43.9	42.0	38.8	41.5	39.4	37.3
	Apulia 1	**82.5**	83.3	82.7		80.5	43.0	42.1	38.9	41.3	39.1	35.7
	UNB-01	**81.0**	81.8	81.5	**84.6**		43.5	41.8	39.1	40.8	39.3	35.9
	BVF	35.8	36.0	36.1	36.2	36.0		40.6	39.1	38.9	38.9	25.3
	DBALV2	33.8	34.2	34.1	34.7	34.5	38.6		46.9	36.7	38.1	24.5
	MBV1	32.2	32.6	32.5	32.6	32.5	35.1	40.8		35.8	36.3	23.6
	RYNV	31.6	31.8	31.8	32.3	32.2	35.3	32.4	32.3		54.6	24.9
	GVBaV	33.8	34.1	33.9	33.7	34.3	36.9	34.1	34.3	50.4		23.3
	PVCV	16.3	16.4	16.3	15.9	16.2	15.2	14.2	13.6	12.7	13.8	

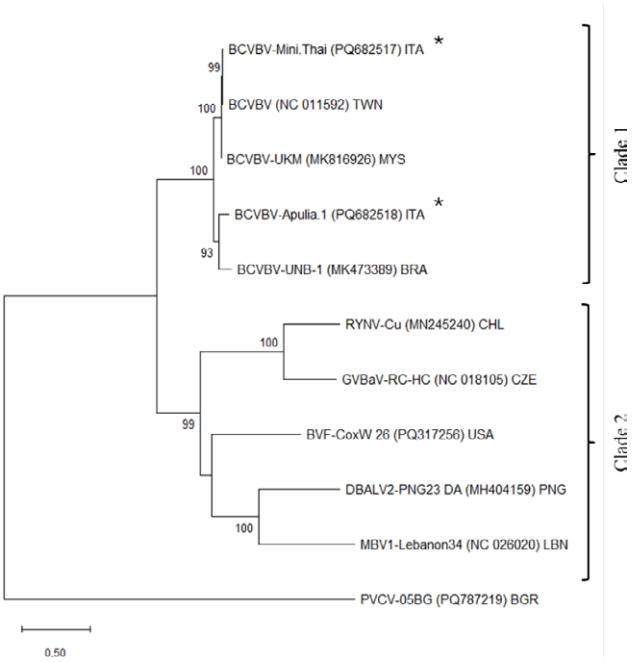

Figure 3. Maximum likelihood (ML) phylogenetic tree based on polyprotein amino acid sequences of BCVBV isolates found in this study (*), compared with homologous sequences from representative *Badnavirus* species. BCVBV, Bougainvillea chlorotic vein banding virus; RYNV, Rubus yellow net virus; GVBaV, Gooseberry vein banding virus; DBALV2, Dioscorea bacilliform AL virus 2; MBV1, Mulberry badnavirus 1; BVF, Blueberry virus F. Petunia vein clearing virus (PVCV) was used as an outgroup. GenBank accession numbers and countries of origin are indicated at the branch tips. The scale bar represents number of substitutions per site.

breaks of the bacterium infections in olive orchards in southern Italy (Saponari *et al*., 2013). These cases highlight the importance of effective phytosanitary measures and early pathogen detection systems.

In the present study, BCVBV was detected for the first time in Italy and in Europe. Initial RT-PCR screening associated the virus exclusively with the Mini Thai cultivar, with all infected plants (8.6% of those assessed) remaining asymptomatic at the time of sampling. Within the limits of this survey, no evidence of virus spread to other cultivars grown in close proximities was observed. Symptoms recorded during the surveys were not associated with any of the detected virus agents, suggesting that the symptoms may have been caused by physiological disorders or other biotic factors.

HTS analyses were essential for the detection of a previously undetected and genetically divergent isolate, designated BCVBV Apulia 1. This isolate had polyprotein nucleotide divergence ranging from 23.2 to 23.4% compared to other known BCVBV isolates, with the exception of isolate UNB-01, from which it differed by 19.5%. UNB-01, similarly to Apulia 1, also had divergence values exceeding 20% relative to other BCVBV isolates (Table 2). Current guidelines establish a 20% polyprotein nucleotide divergence as the species demarcation threshold within *Badnavirus* (Fauquet *et al*., 2005; International Committee on Taxonomy of Viruses, 2026). Therefore, Apulia 1, together with UNB-01, should be considered as a new species within *Badnavirus*, rather than BCVBV isolates, unless this demarcation threshold is increased. Subsequent targeted assays showed presence of BCVBV Apulia 1 in additional samples (12.1%) across different host cultivars, increasing the overall BCVBV infection rate to 20.7% when both isolates were considered. These results highlight the limitations of conventional PCR assays for genetically variable viruses, and the requirement for continuous refinement of virus diagnostic tools (Adams *et al*., 2013; Massart *et al*., 2014).

Development of a primer set capable of detecting both the Mini-Thai and Apulia 1 isolates is a diagnostic improvement, although further validation is required across a greater range of isolates than assessed in the present study. The absence or mildness of symptoms in infected plants indicates possible latent infections, possibly influenced by host age or environmental conditions. Latent infections would increase risks of spread of unnoticed viruses in ornamental production systems. Previous reports describing severe symptoms (Yamashita *et al*., 2004; Tsai *et al*., 2008; Bhat *et al*., 2016) indicate that pathogenicity of the isolates requires further assessment.

The present study has expanded knowledge of the distribution and genetic diversity of BCVBV, reporting its presence in Europe, and identifying a highly divergent BCVBV isolate. These results demonstrate the added value of integrating HTS with conventional diagnostic approaches to improve the detection and management of plant viruses in ornamental crops, thereby supporting effective phytosanitary strategies for virus disease management.

FUNDING

This research was financially supported by the Regional Project “Pro.Di.Qua.Vi.” (Trasferimento di Protocolli per organismi da quarantena e nocivi e per la selezione di materiali sanitariamente migliorati per il vivaismo pugliese). Misura 16 Cooperazione – Sottomisura 16.2

LITERATURE CITED

Abarca-Vargas R., Petricevich V.L., 2018. Bougainvillea genus: A review on phytochemistry, pharmacol-

ogy, and toxicology. *Evidence-Based Complementary and Alternative Medicine* 1-17. https://doi.org/10.1155/2018/9070927

Abdel-Salam A.M., 2020. Research Article Serological and Molecular Characterization of a New *Badnavirus* Species in *Bougainvillea glabra* Plants in Egypt. *International Journal of Virology* 16: 8–15. https://doi.org/10.3923/ijv.2020.8-15

Adams I.P., Miano D.W., Kinyua Z.M., Wangai A., Kimani E., Phiri N., ... Boonham N., 2013. Use of next-generation sequencing for the identification and characterization of Maize chlorotic mottle virus and Sugarcane mosaic virus causing maize lethal necrosis in Kenya. *Plant Pathology* 62(4): 741–749. https://doi.org/10.1111/j.1365-3059.2012.02690.x

Akram A., Khan A.H., Mansoor S., Moffett P., Briddon R.W., Saeed M., 2020. Detection and molecular characterization of *Clerodendron yellow mosaic virus* infecting *Volkameria inermis* in Pakistan. *Journal of Plant Pathology* 102(3): 957–957. https://doi.org/10.1007/s42161-020-00529-y

Alexandre M. A.V., Duarte L.M.L., Harakava R., 2016. Genetic diversity of Badnaviruses associated with *Bougainvillea* in Brazil. *Journal of Phytopathology* 164(2): 125–130. https://doi.org/10.1111/jph.12394

Bankevich A., Nurk S., Antipov D., Gurevich A.A., Dvorkin M., Kulikov A.S., Lesin V.M., Nikolenko S.I., Pham S., Prjibelski A.D., 2012. SPAdes: a new genome assembly algorithm and its applications to single-cell sequencing. *Journal of Computational Biology* 19(5):455–477. https://doi.org/10.1089/cmb.2012.0021

Baranwal V.K., Arya M., Singh J., 2010. First report of two distinct badnaviruses associated with *Bougainvillea spectabilis* in India. *Journal of General Plant Pathology* 76(3): 236–239. https://doi.org/10.1007/s10327-010-0234-5

Bhat A. I., Hohn T., Selvarajan R., 2016. Badnaviruses: the current global scenario. *Viruses* 8(6): 177. https://doi.org/10.3390/v8060177

Birithia R., Subramanian S., Villinger J., Muthomi J.W., Narla R.D., Pappu H.R., 2012. First report of *Tomato yellow ring virus* (*Tospovirus, Bunyaviridae*) infecting tomato in Kenya. *Plant Disease* 96(9): 1384–1384. https://doi.org/10.1094/PDIS-05-12-0462-PDN

Chagas C.M., Alexandre M.A.V., Duarte L.M.L., Rivas E.B., Tombolato A.F.C. 2001. Badnavirus-like particles associated with chlorotic vein-banding symptoms in *Bougainvillea spectabilis*. *Virus Reviews Research* 6: 153.

Datta S. K., Jayanthi R., Janakiram T., 2021. Bougainvillea. In: (Datta S. K., Gupta Y. C. ed.). *Floriculture and Ornamental Plants*. Singapore, Springer Nature 1-34. https://doi.org/10.1007/978-981-15-1554-5_2-1

Doyle J., 1991. DNA protocols for plants. In: *Molecular Techniques in Taxonomy*. Springer, Berlin Heidelberg, D., 283–293.

Elliott D.R., Lebas B.S.M., Ochoa-Corona F.M., Tang J., Alexander B.J.R., 2009. Investigation of *Impatiens necrotic spot virus* outbreaks in New Zealand. *Australasian Plant Pathology* 38(5): 490–495. https://doi.org/10.1071/AP09031

Fauquet C.M., Mayo M.A., Maniloff J., Desselberger U., Ball L.A. (ed.), 2005. *Virus taxonomy. 8th Report of the International Committee on Taxonomy of Viruses*. San Diego, Elsevier Academic Press.

Foissac X., Svanella-Dumas L., Dulucq M.J., Gentit P., Candresse T., 2001. Polyvalent detection of fruit tree tricho, capillo and foveaviruses by nested RT-PCR using degenerated and inosine containing primers (PDO RT-PCR). *Acta Horticulturae* 550: 37–43.

Ghotbi T., Shahraeen N., Winter S., 2005. Occurrence of *tospoviruses* in ornamental and weed species in Markazi and Tehran provinces in Iran. *Plant Disease* 89(4): 425–429. https://doi.org/10.1094/PD-89-0425

International Committee on Taxonomy of Viruses (ICTV), 2026. *Virus Taxonomy: 2026 Report*. Available online: https://ictv.global/report/chapter/caulimoviridae/caulimoviridae/badnavirus. Family *Caulimoviridae*, Genus *Badnavirus* (accessed in May 2026).

Lin H.X., Rubio L., Smythe A., Jiminez M., Falk B.W., 2003. Genetic diversity and biological variation among California isolates of *Cucumber mosaic virus*. *Journal of General Virology* 84(1): 249–258. https://doi.org/10.1099/vir.0.18673-0

Massart S., Olmos A., Jijakli M.H., Candresse T., 2014. Current impact and future directions of high throughput sequencing in plant virus diagnostics. *Virus Research* 188: 90–96. https://doi.org/10.1016/j.virusres.2014.03.029

Nehra C., Sahu A.K., Marwal A., Gaur R.K., 2014. Natural occurrence of *Clerodendron yellow mosaic virus* on *Bougainvillea* in India. *New Disease Reports* 30(19): 2044–0588.

Rivas E.B., Duarte L.M., Alexandre M.A.V., Fernandes F., Harakava R., Chagas C.M., 2005. A new Badnavirus species detected in *Bougainvillea* in Brazil. *Journal of General Plant Pathology* 71(6): 438–440. https://doi.org/10.1007/s10327-005-0227-y

Saponari M., Boscia D., Nigro F., Martelli G., 2013. Identification of DNA Sequences Related to *Xylella fastidiosa* in Oleander, Almond and Olive Trees Exhibit-

ing Leaf Scorch Symptoms in Apulia (southern Italy). *Journal of Plant Pathology* 95: 668.

Shahmohammadi N., Dizadji A., Habibi M.K., Nateqi M., 2015. First report of *Cucumber mosaic virus* infecting *Bougainvillea spectabilis*, *Coleus blumei*, *Kalanchoe blossfeldiana* and *Zinnia elegans* in Iran. *Journal of Plant Pathology* 97(2): 394–394.

Shahraeen N., Ghotbi T., Mehraban A.H., 2002. Occurrence of *Impatiens necrotic spot virus* in ornamentals in Mahallat and Tehran provinces in Iran. *Plant Disease* 86(6): 694–694. https://doi.org/10.1094/PDIS.2002.86.6.694A

Tsai C.H., Su H.J., Wu M.L., Feng Y.C., Hung T. H., 2008. Identification and detection of Bougainvillea spectabilis chlorotic vein-banding virus in different bougainvillea cultivars in Taiwan. *Annals of Applied Biology* 153(2), 187–193. https://doi.org/10.1111/j.1744-7348.2008.00251.x

Yamashita S., Ferreira P.T.O., Figueiredo D.V., Brioso P.S.T., Kitajima E.W., 2004. Occurrence of badnavirus in *Bougainvillea* in Brazil. *Summa Phytopathology* 30: 68.

Yusop M.S.M., Ersoy R., Akbar M.A., Saad M.F.M., Goh H.H., Baharum S.N., Bunawan H., 2019. First report of *Bougainvillea chlorotic vein-banding virus* causing chlorosis and vein banding of *Bougainvillea spectabilis* in Malaysia. *Plant Disease* 103(11): 2974. https://doi.org/10.1094/PDIS-02-19-0292-PDN

Phytopathologia Mediterranea
The international journal of the
Mediterranean Phytopathological Union

Firenze University Press
www.fupress.com/pm

Research Papers

Integrated management of citrus gummosis (*Phytophthora* spp.) in semi-arid Iran: combined effects of chemical, cultural, and nutritional strategies

Seyed Ali Akbar BAGHERIAN[1], Behzad HAJIEGHRARI[2]

[1] *Department of Horticultural Science, College of Agriculture, Jahrom University, Jahrom, Iran*
[2] *Department of Agricultural Biotechnology, College of Agriculture, Jahrom University, Jahrom, Iran*
*Corresponding author. E-mail: sabagherian@gmail.com

Summary. Citrus gummosis (citrus foot rot), commonly associated with *Phytophthora* spp. in citrus orchards, significantly limits citrus production in semi-arid regions, causing trunk cankers, gum exudation, and substantial yield losses. Field efficacy of an integrated disease management (IDM) programme combining chemical, cultural, and nutritional strategies was evaluated for reducing disease incidence and enhancing tree vigour and fruit yield. Over two years, trials were carried out across 12 commercial orchards. Cultural measures included soil aeration by collar excavation, conversion to dual-line drip irrigation, and application of well-decomposed organic manure as a surface mulch within the drip line. Assessments included disease incidence, severity of gum exudation, host plant vegetative growth, and fruit yields. Six months after implementation, disease incidence decreased from 65% at baseline to 20 ± 3% in the surviving IDM-treated trees, compared with 65 ± 5% in the untreated controls (GLMM treatment effect: $\chi^2(1) = 48.3$, $P < 0.001$). IDM-treated trees exhibited a 40% increase in shoot length and a 38% increase in trunk-diameter increment, while mean fruit yield increased from 15 ± 2 to 25 ± 3 kg tree^{-1}, corresponding to a 66.7% increase ($P < 0.001$). The IDM programme also improved tree recovery relative to the untreated controls in the semi-arid orchards evaluated. Although this IDM package gave short-term efficacy under the semi-arid conditions evaluated, its regional transferability should be validated through multi-location trials before broad implementation. Because *Phytophthora* pathogens were not isolated and identified, these results came from management of a macroscopic gummosis symptom complex, so long-term economic analyses and robust epidemiological monitoring are required to substantiate robust field recommendations.

Keywords. Soil waterlogging, orchard sanitation, fungicide management, tree recovery, soil aeration.

OPEN ACCESS

Citation: Bagherian, S. A. A. & Hajieghrari, B. (2026). Integrated management of citrus gummosis (*Phytophthora* spp.) in semi-arid Iran: combined effects of chemical, cultural, and nutritional strategies. *Phytopathologia Mediterranea* 65(2):309-317.doi:10.36253/phyto-17259

Accepted: July 31, 2026

Published: September 10, 2026

© 2026 Author(s). This is an open access, peer-reviewed article published by Firenze University Press (https://www.fupress.com) and distributed, except where otherwise noted, under the terms of the CC BY 4.0 License for content and CC0 1.0 Universal for metadata.

Data Availability Statement: All relevant data are within the paper and its Supporting Information files.

Competing Interests: The Author(s) declare(s) no conflict of interest.

Editor: Epaminondas Paplomatas, Agricultural University of Athens, Greece.

ORCID:
SAAB: 0000-0003-4330-2335

INTRODUCTION

Citrus gummosis, caused primarily by the oomycete pathogens *Phytophthora nicotianae, P. citrophthora,* and *P. palmivora*, is among the most destructive diseases affecting citrus production, with particularly severe impacts in semi-arid regions (Hamdan *et al.,* 1995; Ippolito *et al.,* 2004; Hussain *et al*., 2025). The disease causes gum exudation from distinct citrus tree cortical lesions and trunk cankers, accompanied by longitudinal cracking and bark necroses, which gradually reduces tree vigour and fruit yields (Cacciola and Magnano di San Lio, 2008). Infected trees typically show initial symptoms at crown or collar regions, with necrotic lesions progressing upward to form extensive cankers that can lead to tree death if left unmanaged. The pathogens thrive under conditions of excessive soil moisture and poor aeration, where motile zoospores readily infect roots and the host collar regions. Irrigation management and soil drainage are therefore important determinants of disease incidence and severity. Yield losses attributed to citrus gummosis range from 10 to 30% in areas with environmental conditions favourable for pathogen survival and spread (Chaudhary *et al.,* 2016; Chaudhary *et al.,* 2020).

Growers have traditionally managed citrus gummosis by using resistant rootstocks, pruning infected bark tissues, improving soil drainage, and avoiding excessive irrigation, in addition to applying systemic fungicides such as metalaxyl and fosetyl-Al (Leoni and Ghini, 2006; Cacciola and Magnano di San Lio, 2008; Mekonen *et al.,* 2015). However, single-component disease management methods often fail because *Phytophthora* populations can rapidly develop fungicide resistance and maintain persistent soilborne inoculum (Bittner *et al.,* 2017; Massi *et al.,* 2021; Moreira *et al.,* 2023; Islam *et al.,* 2024). Integrated disease management (IDM), which combines chemical treatments with cultural and nutritional interventions, offers potential to reduce pathogen pressure and accelerate tree recovery (Razdan and Sabitha, 2009; Gilardi *et al.,* 2013; Lahlali *et al.,* 2024). For example, adding organic manure to soil enhances its structure and aeration, which reduces the survival of *Phytophthora* propagules (Kim *et al.,* 1997; Núñez-Zofío *et al.,* 2011; Farooq *et al.,* 2024). Likewise, foliar sprays of humic acid and calcium chelates can enhance tree vigour and increase resistance to stress conditions (Ramírez-Gil and Morales-Osorio, 2020; Ennab *et al.,* 2023; Amerian *et al.,* 2024).

Despite these advancements, few studies have evaluated integrated management programmes under the specific environmental conditions of semi-arid citrus production regions such as Jahrom and Qir in southern Iran, where high temperatures and irregular rainfall intensify disease impacts. Combined effects of fungicide applications, irrigation system modifications, trunk sanitation, and nutritional supplements also remain poorly documented for these agro-ecological zones (Rovetto *et al.,* 2024).

The present study was designed to test effectiveness of an integrated management strategy for citrus gummosis in commercial orchards of Jahrom and Qir. The programme combined systemic fungicides (metalaxyl and fosetyl-Al), soil and trunk sanitation, conversion from flood to drip irrigation, and foliar nutrition with humic acid–calcium chelate and amino acids. The study aimed to evaluate short-term efficacy of these control methods for reducing incidence and severity of gummosis, effects on plant growth and fruit yields, and as potentially sustainable disease management recommendations for semi-arid regions.

MATERIALS AND METHODS

Study area and experimental layout

This study was conducted during two consecutive citrus growing seasons (in 2023 and 2024), in twelve commercial orchards located in the Jahrom and Qir regions of southern Iran. The selected orchards had documented histories of high gummosis incidence (>60% of trees showing visible gum exudation on trunks). All trees were mature orchard trees, 15 to 20 years old, and were grafted on sour orange (*Citrus aurantium*) rootstock. Tree age within each orchard was uniform (±2 years), and no rooted cuttings were used. Although sour orange is historically classified as moderately tolerant of *Phytophthora* gummosis, this natural tolerance can be overwhelmed under sustained high disease pressure. The high gummosis incidence in the selected orchards occurred in the context of long-term flood irrigation and prolonged waterlogging at the plant collar regions, together with the absence of a previous specific disease-management programme.

Within each of the 12 orchards, four randomized replicate blocks were established; each block contained both an IDM-treated plot and an untreated control plot, consistent with the random-effects structure (orchard and block nested within orchard) used in the mixed models described below. Each treatment arm comprised five monitored trees per replicate block (five trees × four blocks = 20 trees per orchard per treatment), giving totals of 240 trees per treatment (control and IDM) across the 12 orchards (total = 480 trees). All trees were

monitored for disease incidence, severity, vegetative growth, chlorophyll content, and yield.

Treatment description

An integrated disease management strategy was assessed, combining chemical, cultural, and nutritional interventions.

Chemical treatments. Two targeted interventions were assessed: a soil-applied drench of mefenoxam (metalaxyl-M; Ridomil Gold SL®, 480 g a.i. L^{-1}; ≈1.75 g a.i. L^{-1}, as prepared), delivered through the dual-line drip irrigation system to ensure uniform distribution throughout the active root profile without mechanical root disturbance; or scheduled foliar applications of fosetyl-Al (Aliette® 80 WP; 2.0–2.5 g a.i. L^{-1}), applied to the tree canopies until runoff at 45 d intervals during peak infection periods. The two fungicides were not tank-mixed or applied simultaneously to individual trees. Surgical trunk wounds were protected only with a copper sulfate–lime (Bordeaux) paste (100 g L^{-1}), applied to collar regions and surrounding soil to suppress *Phytophthora* spp. infections.

Cultural practices. Cultural measures included tree collar excavation to keep trunk bases dry, carried out during the dry season (June to August), only for the IDM treatment. Experimental control trees remained undisturbed, representing standard local practice. Irrigation was converted from traditional flood irrigation to a dual-line drip system, with emitters displaced 75 cm from the trunk of each treated tree to prevent water from pooling in the excavated collar basin. Irrigation volumes and frequency were obtained from orchard records for both systems. Well-decomposed manure (20 kg per tree) was applied as surface mulch within the each irrigation drip line (i.e. not incorporated into the soil) to stimulate biological activity and improve soil structure without injuring shallow roots.

Nutritional management. Monthly foliar applications of a humic acid–calcium chelate solution (100 mL per tree) and amino acids (100 g per 100 L of water) were applied to improve plant vigour, nutrient uptake, and stress tolerance. For 2 years following these treatments, nitrogenous fertilizers were not applied to the soil, but nitrogen was applied only through foliar feeding, to minimize excessive vegetative growth and reduce susceptibility to gummoses.

Sanitation measures. Diseased bark tissues were carefully scraped away from trees with less than 30% collar circumference affected by gum exudation, using sterilized tools. To prevent the potential pathogen spread, all infected material was removed from the orchards. For trees with more than 30% of collar circumference infected, the trees were uprooted and removed from the orchard, to eliminate primary inoculum sources. To suppress residual soilborne propagules within canopy drip lines, the empty planting sites were drenched with a mefenoxam (metalaxyl-M) solution to a depth of 20 cm, with mefenoxam and fosetyl-Al never tank-mixed, and reflecting that fosetyl-Al requires systemic uptake through living plant tissue to be effective so is unsuitable for soil application to an unplanted site, in accordance with optimized application guidelines. Pruning tools were disinfected with 10% bleach. Wounds were immediately protected with a Bordeaux paste (copper sulfate–lime) or a copper-based dressing following label recommendations. Bleach was not applied directly to living bark.

All selected trees within each orchard were of uniform age (± 2 years) and of similar trunk diameters, to minimize host plant variability.

Data collection

Disease evaluations. Disease incidence was recorded monthly as percentage of infected trees per replicate, and gum exudation severity classified using 0 to 5 scale, where 0 indicated no symptoms, and 5 indicated that >75% of the tree collar circumference was affected.

Vegetative tree growth, leaf chlorophyll contents, and fruit yields. Vegetative growth (annual shoot extension, trunk diameter increments), and leaf chlorophyll contents (SPAD index), were measured on five randomly selected trees per replicate (i.e., five trees × four replicates = 20 trees per orchard per treatment) across the 12 orchards). This gave 240 trees per treatment. Following removal of 47 infected IDM trees (see below), post-treatment vegetative-growth and yield values for the IDM group were based on the 193 surviving trees, while experimental control values remain based on all 240 control trees. These tree-level observations were used in the tree-level mixed-model analyses described below. Leaf chlorophyll content was measured using a portable SPAD-502 Plus chlorophyll meter (Konica Minolta Inc., Osaka, Japan), following the calibration framework of Markwell *et al.* (1995). Measurements were taken between 9:00 and 11:00 am each measurement day to minimize diurnal variations. For each tree, five mature, fully expanded, sun-exposed leaves were selected from current season growth, and three readings were taken per leaf (avoiding midribs). The arithmetic mean of all 15 readings (five leaves × three readings) was recorded as the SPAD value for each tree. Fruit yield was measured by counting fruits per tree, and recording total fruit weight (kg $tree^{-1}$) at harvest.

Soil parameters. Soil parameters were assessed monthly in a subset of experimental plots. These parameters included soil moisture content, duration of surface soil saturation (waterlogging) at tree collars, soil porosity measured using the core method, and biological activity assessed using assays for phosphatase and urease. Phosphatase activities were measured using p-nitrophenyl phosphate substrate (Tabatabai and Bremner, 1969). Urease activities were measured using the indophenol blue method (Kandeler and Gerber, 1988).

Statistical analysis of data

All analyses were carried out using R v4.3. For continuous response variables (shoot length, trunk increment, fruit weight, enzymatic activities) linear mixed-effects models were fitted using lmer (package lme4) with the fixed effects treatment, year, and their interaction, and with random intercepts for orchard and for block nested within orchard, plus a random intercept for tree to account for repeated measurements on the same tree: lmer(response ~ treatment * year + (1|orchard) + (1|orchard:block) + (1|orchard:block:tree)). For binomial response data (tree-level disease incidence) generalized linear mixed models were fitted with a logit link, using glmer and the same random structure. Denominator degrees of freedom and *P* values for LMMs were estimated using the Satterthwaite approximation implemented in lmerTest. Likelihood-ratio tests (χ^2, df), and, where appropriate, Wald Z statistics, are reported for GLMMs.

Pathogen identification – a methodological limitation

Isolations and identification of *Phytophthora* species from infected tissues or soil were not carried out at the onset of this study, due to practical limitations in field sample handling and laboratory capacity at the time. Therefore, while observed symptoms (gum exudation, trunk cankers, root necroses) resembled those caused by *Phytophthora* species (Cacciola and Magnano di San Lio, 2008), the causal agent(s) could not be confirmed in the surveyed orchards. This omission is mitigated by prior peer-reviewed surveys that have confirmed the presence of *P. nicotianae* and *P. citrophthora* as the dominant citrus gummosis pathogens in semi-arid Middle Eastern and Mediterranean citrus-growing regions comparable to Jahrom and Qir (Hamdan *et al.,* 1995; Cacciola and Magnano di San Lio, 2008). This indicates the regional likelihood of *Phytophthora* etiology. Consequently, the present study results describe the management of "citrus gummosis syndrome" rather than disease caused by confirmed *Phytophthora* species. The authors acknowledge that this as a significant limitation in the present study (see Discussion).

RESULTS

Disease incidence and severity

During two consecutive growing seasons (in 2023 and 2024), the integrated management strategy reduced incidence and severity of citrus gummosis across all the 12 orchards studied (Table 1; Figure 1). At baseline (month 0, prior to any interventions), disease incidence among the 15 to 20-year-old assessed trees did not differ between the two groups (controls: mean = 65 ± 5%; IDM =65 ± 4%; n = 240 trees per treatment), confirming that both groups began in the experiments from equivalent disease levels. Within the IDM group, 47 of the 240 enrolled trees (19.6%) subsequently exceeded the

Table 1. Mean disease gummosis incidence proportions (%) and severity scores for citrus trees in orchards either maintained without treatment (Control), or where integrated disease management was applied, during 2023 and 2024.

Season	Parameter	Control	Integrated Management	Reduction (%)	*P*-value
2023 (6 months)	Disease incidence (%)	65 ± 5	20 ± 3	69.2	< 0.01
2024 (12 months)	Disease incidence (%)	66 ± 4	18 ± 2	72.7	< 0.01
2023 (6 months)	Severity (0 to 5 scale)	3.8 ± 0.2	1.1 ± 0.1	71.1	< 0.01
2024 (12 months)	Severity (0 to 5 scale)	3.9 ± 0.3	1.2 ± 0.1	69.2	< 0.01

Data are presented as orchard-level means ± SE (n = 12 orchards). For tree-level analyses, 240 trees per treatment (control and IDM) were enrolled at baseline across the 12 orchards, consistent with the number reported in Table 2; this n is reported consistently in all tables and text.

A total of 47 of the 240 IDM trees (19.6%) exceeded the >30% collar infection threshold, and were uprooted and removed during this study; the 2024 (12-month) IDM values in this table are therefore based on the 193 surviving IDM trees, while control values remain based on all 240 control trees (no removals occurred in the untreated control).

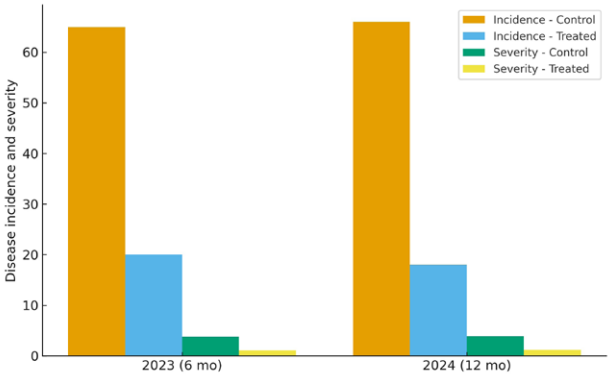

Figure 1. Graphical representation of the decline in disease incidence and severity in 12 citrus orchards following the integrated disease management (IDM) treatment used in this study.

predefined 30% collar-circumference infection threshold (see below), and were uprooted and removed. The remaining 193 IDM trees (80.4%) each had <30% collar involvement, underwent bark sanitation treatments, and were retained for all following assessments. Because the removed trees were, by definition, the most severely diseased, their exclusion is conservative with respect to the reported treatment effects, and likely underestimates true disease pressure that would have persisted in the IDM group without removal. No removals were carried out in the untreated control groups (n = 240 throughout). Consistent with this design, disease incidence declined significantly from the 65% baseline to 20 ± 3% at 6 months and 18 ± 2% at 12 months in the surviving IDM trees, compared with a stable 65 to 66% in the control (GLMM treatment effect: $\chi^2(1) = 48.3$, $P < 0.001$; Table 1). Severity of gum exudation, rated on the 0 to 5 scale, declined significantly from a baseline mean of 3.8 ± 0.2 (moderate-to-severe symptoms) to 1.1 ± 0.1 (mild symptoms) at 6 months (LMM treatment effect: $F_{1,22} = 41.2$, $P < 0.001$), reflecting substantial improvements in tree health. Consistent with prior research, the overall reduction in disease pressure observed here is best interpreted as a combined effect of the full IDM package (systemic fungicides, collar excavation, improved drainage via drip irrigation, manure mulching, and wound sanitation) rather than from fungicide applications alone.

Vegetative growth

Statistically significant improvements in vegetative growth parameters were recorded in the IDM-treated trees compared with untreated controls (Table 2). Mean shoot lengths increased by 40% (from 55 cm to 77 cm), and mean trunk diameters increased by 38% (from 8 mm yr^{-1} to 11 mm yr^{-1}). Leaf chlorophyll content, measured via SPAD readings, increased by 25%, indicating greater relative leaf greenness and consistent with improved tree physiological status.

Fruit yields, and soil physical properties and aeration dynamics

Integrated management increased fruit yields, and enhanced soil enzyme activity (Table 3). Mean fruit yields were 15 ± 2 kg $tree^{-1}$ from the control trees, and 25 ± 3 kg $tree^{-1}$ from the IDM treatments, a mean difference of 10.0 kg $tree^{-1}$ (95% CI: 6.2–13.8 kg; $P < 0.001$) estimated from the mixed model contrasts (95% CI, calculated via emmeans). Soil phosphatase activity increased by 45%, and urease activity by 32% for the IDM treatments, indicating enhanced biological activity and nutrient cycling capacity in the tree rhizospheres from these treatments.

The IDM approach also improved soil physical conditions around the tree collar zones (Table 4). Rather than reducing overall soil water contents, which addition of organic manure and conversion to drip irrigation would be expected to increase, the IDM interventions reduced the duration of surface soil saturation (waterlogging) at the tree collars by 35%, consistent with reduced water pooling under the drip-irrigation

Table 2. Mean vegetative growth parameters of citrus trees receiving integrated disease management (IDM) or remaining untreated.

Parameter	Control	IDM treated	Change (%)	*P*-value
Shoot length (cm)	55 ± 3	77 ± 4	+40	< 0.01
Trunk diameter increment (mm yr^{-1})	8.0 ± 0.6	11.0 ± 0.8	+38	< 0.01
Leaf chlorophyll (SPAD)	42 ± 2	52 ± 2	+25	< 0.05

Values are means ± SE. Baseline enrollment was 20 trees per orchard × 12 orchards = 240 trees per treatment. Control values are based on all 240 control trees (no removals). Treated (IDM) post-treatment values are based on the 193 IDM trees surviving after removal of the 47 trees that exceeded the 30% collar-infection threshold. The reduction in n is accounted for in tree-level mixed models, which accommodated unbalanced group sizes.

Table 3. Mean citrus fruit yields and soil biological activities for control and integrated disease management trees.

Parameter	Control	Integrated Management	Improvement (%)	*P*-value
Mean fruit yield (kg tree^{-1})	15 ± 2	25 ± 3	+66.7	< 0.001
Mean phosphatase activity (μmol P g^{-1} h^{-1})	100 ± 8	145 ± 10	+45	< 0.05
Mean urease activity (μmol NH_4^+ g^{-1} h^{-1})	120 ± 9	158 ± 11	+32	< 0.05

Table 4. Mean soil physical conditions near citrus plant collar zones for untreated (Control) plants, and those treated with integrated disease management (IDM).

Parameter	Control	IDM treated	Change (%)	*P*-value
Surface saturation / waterlogging duration at tree collars (% of monitoring days)	28 ± 3	18 ± 2	–35	< 0.01
Soil porosity (0–30 cm)	42 ± 2	50 ± 3	+19	< 0.05

system. This reduced saturation window reduces the favourable environment for *Phytophthora* spp. survival and infection. Meanwhile, soil porosity in the 0–30 cm layer increased by 19% following the integrated management intervention, consistent with improved soil aeration and drainage.

Efficacy of sanitation practices

Of the 193 IDM trees with <30% collar circumference affected by gummoses that underwent careful bark removal, all recovered fully within 4 weeks, with no further spread of symptoms. In contrast, the 47 trees exhibiting >30% collar involvement were removed according to the predefined management protocol; these observations do not independently validate the 30% threshold. Application of protective copper sulfate–lime paste to treated wounds prevented re-infection in 185 of the 193 sanitized trees (95.9%; 95% CI: 92.3–98.0%) during the 18 month monitoring period.

DISCUSSION

This study has demonstrated the effectiveness of integrated disease management (IDM) for mitigating citrus gummosis, likely associated with *Phytophthora* species under semi-arid conditions in southern Iran. The combined use of systemic fungicides, cultural practices, soil amendments, and host nutritional strategies was associated with reduced disease pressure, improved tree health, and enhanced fruit yields. As discussed below, however, because the IDM package was evaluated only against an untreated control, and pathogen identifications were not carried out, these results should be interpreted as preliminary evidence for the management package, rather than as proof of mechanism or independent contribution of any single component (see Limitations).

The reductions in disease incidence and severity observed in this study corroborate previous results for the curative and protective effects of systemic fungicides, such as metalaxyl and fosetyl-Al, against *Phytophthora* infections in citrus. In the semi-arid calcareous soils of southern Iran, fosetyl-Al was applied at 45 d intervals according to label guidance. The present study did not measure fungicide persistence or residual activities. Nonetheless, the risk of pathogen resistance to fungicides, particularly to metalaxyl/mefenoxam, remains a concern and warrants ongoing monitoring in long-term disease management programmes (Davidse *et al.,* 1983).

Reduced waterlogging duration at the tree collars probably suppressed *Phytophthora* proliferation, because zoospore movement depends on free water (Chaudhary *et al.,* 2016). These results support previous studies that have demonstrated that physical interventions, such as collar excavation and improved drainage, can help reduce soilborne diseases (Shrivastava and Kumar, 2015; Bhatt and Sharma, 2020; Brasier *et al.,* 2022; Fadli *et al.,* 2022; Sapkota *et al.,* 2023).

Soil amendments, including surface mulching with decomposed animal manure, improved soil physical properties such as porosity (+19%; Table 4) and were associated with increased enzyme activity, indicating enhanced biological activity and nutrient cycling capacity (Klein *et al.,* 2012). These improvements are consistent with mechanisms that may enhance soil suppressiveness (e.g., increased porosity, enzyme activities), but direct evidence – for example, quantification of *Phytophthora* soil inoculum or microbiome analyses – was not collected in this study; soil suppressiveness therefore remains

inferred rather than demonstrated, and should be confirmed by targeted pathogen-population monitoring conducted monthly for at least 24 months to cover two full citrus growing seasons and capture seasonal variation in disease pressure.

Foliar nutrition — monthly applications of humic acid–calcium chelate and amino acids (Section 2.2) — enhanced vegetative growth and chlorophyll content, underscoring the role of foliar biostimulants in improving plant metabolism, nutrient assimilation, and stress tolerance (da Silva *et al.,* 2021; de Moura *et al.,* 2023). Because these products were applied to the canopy rather than the soil in this study, we interpret their contribution as acting through plant physiology rather than through direct modulation of the soil microbiota; these physiological enhancements likely contributed indirectly to disease suppression by boosting overall tree vigor and increasing the capacity to withstand pathogen attack.

Sanitation of bark lesions and protective wound treatment proved highly effective in preventing reinfection, supporting the 30% collar-circumference threshold used to distinguish sanitation from removal in this study. This finding aligns with integrated management principles emphasizing timely wound treatment to disrupt pathogen entry and limit inoculum spread (Hajji-Hedfi *et al.,* 2024). Trees exceeding this threshold exhibited poor recovery, supporting its use as a removal criterion, in line with recommendations for managing *Phytophthora* trunk infection (Fadli *et al.,* 2022).

The integrated approach markedly enhanced fruit yield relative to what would be expected from single-method interventions reported elsewhere. The concurrent application of chemical, cultural, and nutritional practices underscores the potential value of integrated strategies in plant disease management, particularly in regions challenged by water scarcity and persistent pathogens.

This study highlights that, in semi-arid environments, reducing waterlogging at the collar and improving root-zone aeration are critical components of effective citrus gummosis management. Integrating multiple management tactics reduces pathogen pressure and enhances tree resilience while promoting sustainable production practices.

While the results are promising, further long-term studies are essential to evaluate the sustainability of IDM strategies, particularly concerning potential fungicide resistance, optimization of organic amendment protocols, and economic feasibility for commercial growers. Cost–benefit analyses and region-specific adaptations will be crucial for the widespread adoption of these integrated practices.

Limitations

Two methodological limitations of this study should be highlighted. First, the IDM package was compared only to an untreated control. The observed effects therefore represent the combined outcome of multiple simultaneous interventions – (i) the shift from flood to drip irrigation, (ii) the change from soil to foliar fertilization, (iii) manure mulching, (iv) trunk surgery and sanitation, and (v) fungicide applications – and our design does not allow us to quantify the independent contribution of each component to disease suppression or yield improvement. We did not quantify pathogen population density in soil before or after the intervention, so mechanisms such as "soil suppressiveness" remain inferred rather than demonstrated. Future studies should use factorial or other appropriately structured multi-treatment designs that separately manipulate the major cultural, chemical, nutritional, and sanitation components, allowing their individual and interaction effects to be estimated.

Second, we did not perform molecular or cultural confirmation of *Phytophthora* species at the onset of the study (Section 2.5). While the symptoms were typical of *P. nicotianae* or *P. citrophthora* – the dominant species reported in semi-arid citrus orchards of the wider region (Hamdan *et al.,* 1995; Cacciola and Magnano di San Lio, 2008) – we cannot rule out the involvement of other *Phytophthora* species or other oomycete pathogens. This uncertainty means our IDM package may have been effective against a pathogen complex, not necessarily *P. nicotianae* alone. Future studies must include species-level identification (via PCR or sequencing) before and after intervention to establish a causal link between management practices and specific pathogen suppression.

In conclusion, over the two seasons of this trial the integrated management strategy reduced disease incidence and improved tree health and productivity under the specific environmental conditions of the studied orchards. Extrapolation to broader claims of robustness and sustainability across other semi-arid regions requires replicated multi-year trials, pathogen population monitoring, and formal cost–benefit analyses (economic analysis horizon ≥ 5 years). The IDM model presented here provides a practical starting framework for managing citrus gummosis under the semi-arid orchard conditions evaluated, pending this further validation.

LITERATURE CITED

Amerian M., Palangi A., Gohari G., Ntatsi G., 2024. Humic acid and grafting as sustainable agronomic practices for increased growth and secondary metab-

olism in cucumber subjected to salt stress. *Scientific Reports* 14: 15883. https://doi.org/10.1038/s41598-024-66677-8

Bhatt B., Sharma G., 2020. Metalaxyl resistance in Phytophthora infestans: An overview. International *Journal of Chemical Studies* 8(4): 3047–3054. https://doi.org/10.22271/chemi.2020.v8.i4ak.10114

Bittner R.J., Sweigard J.A., Mila A.L., 2017. Assessing the resistance potential of *Phytophthora nicotianae*, the causal agent of black shank of tobacco, to oxathiopropalin with laboratory mutants. *Crop Protection* 102: 63–71. https://doi.org/10.1016/j.cropro.2017.08.002

Brasier C.M., Scanu B., Cooke D.E.L., Jung T., 2022. Phytophthora: An ancient, historic, biologically and structurally cohesive and evolutionarily successful generic concept in need of preservation. *IMA Fungus* 13(1): 12. https://doi.org/10.1186/s43008-022-00097-z

Cacciola S.O., Magnano di San Lio G., 2008. Management of citrus diseases caused by Phytophthora spp. In: *Integrated Management of Diseases Caused by Fungi, Phytoplasma and Bacteria.* (Ciancio A., Mukerji K.G., ed.), Springer, Dordrecht, The Netherlands, 61–84. https://doi.org/10.1007/978-1-4020-8571-0_4

Chaudhary S., Kusakabe A., Melgar J.C., 2016. Phytophthora infection in flooded citrus trees reduces root hydraulic conductance more than under non-flooded condition. *Scientia Horticulturae* 202: 107–110. https://doi.org/10.1016/j.scienta.2016.02.031

Chaudhary S., Laughlin D.A., Setamou M., da Graça J.V., Kunta M., Ancona V., 2020. Incidence, severity, and characterization of Phytophthora foot rot of citrus in Texas and implications for disease management. *Plant Disease* 104(9): 2455–2461. https://doi.org/10.1094/PDIS-07-19-1493-RE

da Silva M.S.R.A., dos Santos B.M.S., da Silva C.S.R.A., Antunes L.F.S., dos Santos R.M., Rigobelo E.C., 2021. Humic substances in combination with plant growth-promoting bacteria as an alternative for sustainable agriculture. *Frontiers in Microbiology* 12: 719653. https://doi.org/10.3389/fmicb.2021.719653

Davidse L.C., Danial D.L., van Westen C.J., 1983. Resistance to metalaxyl in Phytophthora infestans in the Netherlands. *Netherlands Journal of Plant Pathology* 89: 1–20. https://doi.org/10.1007/BF01974440

de Moura O.V.T., Berbara R.L.L., Torchia D.F. de O., da Silva H.F.O., de Castro T.A.T., García A.C., 2023. Humic foliar application as sustainable technology for improving the growth, yield, and abiotic stress protection of agricultural crops: A review. *Journal of the Saudi Society of Agricultural Sciences* 22(8): 493–513. https://doi.org/10.1016/j.jssas.2023.05.001

Ennab H.A., Mohamed A.H., El-Hoseiny H.M., Omar A.A., Hassan I.F., Alam-Eldein S.M., 2023. Humic acid improves the resilience to salinity stress of drip-irrigated Mexican lime trees in saline clay soils. *Agronomy* 13(7): 1680. https://doi.org/10.3390/agronomy13071680

Fadli A., Benyahia H., Hussain S., Khan R.I., Rao M.J., Khalid M.F., 2022. Phytophthora-citrus interactions and management strategies: A review. *Turkish Journal of Agriculture and Forestry* 46(5): 730–742. https://doi.org/10.55730/1300-011X.3038

Farooq Q.U.A., McComb J., Hardy G.E.S.J., Burgess T.I., 2024. Soil amendments for management of Phytophthora root rot in avocado and their impact on the soil microbiome. *Journal of Plant Pathology* 106: 439–455. https://doi.org/10.1007/s42161-024-01604-4

Gilardi G., Baudino M., Moizio M., Pugliese M., Garibaldi A., Gullino M.L., 2013. Integrated management of *Phytophthora capsici* on bell pepper by combining grafting and compost treatment. *Crop Protection* 53: 13–19. https://doi.org/10.1016/j.cropro.2013.06.008

Hajji-Hedfi L., Khlif A., Hlaoua W., Rhouma A., Dali S., Chhipa H., 2024. Plant diseases: Pathogenicity and integrated management overview. *Microbial Biosystems* 9(2): 41–57. https://doi.org/10.21608/mb.2024.307263.1134

Hamdan A.H.Y.A., Ali-Shtayeh M.S., Jones M.G., Mortimer A.M., 1995. *Phytophthora citrophthora* and P. nicotianae in two contrasting citrus plantations in the West Bank, Middle East. *Journal of Plant Diseases and Protection* 102(2): 151–163. http://www.jstor.org/stable/43386391

Hussain T., Legrifi I., El Maguri S., Abdellatif E., Besselma N., Lahlali R., 2025. Phytophthora spp.'s effect on citrus industry: Current status, challenges, and emerging control strategies. *CABI Reviews: Perspectives in Agriculture, Veterinary Science, Nutrition and Natural Resources* 20(1): 0020. https://doi.org/10.1079/cabireviews.2025.0020

Ippolito A., Schena L., Nigro F., Soleti Ligorio V., Yaseen T., 2004. Real-time detection of Phytophthora nicotianae and P. citrophthora in citrus roots and soil. *European Journal of Plant Pathology* 110: 833–843. https://doi.org/10.1007/s10658-004-5571-9

Islam T., Danishuddin, Tamanna N.T., Matin M.N., Barai H.R., Haque M.A., 2024. Resistance mechanisms of plant pathogenic fungi to fungicide, environmental impacts of fungicides, and sustainable solutions. *Plants* 13(19): 2737. https://doi.org/10.3390/plants13192737

Kandeler E., Gerber H., 1988. Short-term assay of soil urease activity using colorimetric determination of ammonium. *Biology and Fertility of Soils* 6: 68–72. https://doi.org/10.1007/BF00257924

Kim K.D., Nemec S., Musson G., 1997. Effects of composts and soil amendments on soil microflora and Phytophthora root and crown rot of bell pepper. *Crop Protection* 16(2): 165–172. https://doi.org/10.1016/S0261-2194(96)00074-9

Klein E., Katan J., Gamliel A., 2012. Soil suppressiveness to Meloidogyne javanica as induced by organic amendments and solarization in greenhouse crops. *Crop Protection* 39: 26–32. https://doi.org/10.1016/j.cropro.2012.02.013

Lahlali R., Taoussi M., Laasli S.-E., Gachara G., Ezzouggari R., Ait Barka E., 2024. Effects of climate change on plant pathogens and host-pathogen interactions. *Crop and Environment* 3(3): 159–170. https://doi.org/10.1016/j.crope.2024.05.003

Leoni C., Ghini R., 2006. Sewage sludge effect on management of *Phytophthora nicotianae* in citrus. *Crop Protection* 25(1): 10–22. https://doi.org/10.1016/j.cropro.2005.03.004

Markwell J., Osterman J.C., Mitchell J.L., 1995. Calibration of the Minolta SPAD-502 leaf chlorophyll meter. *Photosynthesis Research* 46: 467–472. https://doi.org/10.1007/BF00032301

Massi F., Torriani S.F.F., Borghi L., Toffolatti S.L., 2021. Fungicide resistance evolution and detection in plant pathogens: *Plasmopara viticola* as a case study. *Microorganisms* 9(1): 119. https://doi.org/10.3390/microorganisms9010119

Mekonen M., Ayalew A., Weldetsadik K., Seid A., 2015. Assessing and measuring of citrus gummosis (*Phytophthora* spp.) in major citrus growing areas of Ethiopia. *Journal of Horticulture* 2(4): 154. https://doi.org/10.4172/2376-0354.1000154

Moreira R.R., Smirne R.A.G., Pereira R.G., Machado F.J., Behlau F., Junior G.J.S., 2023. Duration of fungicide spray program for the control of citrus black spot in sweet orange based on cultivar maturation and orchard age. *Crop Protection* 172: 106303. https://doi.org/10.1016/j.cropro.2023.106303

Núñez-Zofío M., Larregla S., Garbisu C., 2011. Application of organic amendments followed by soil plastic mulching reduces the incidence of *Phytophthora capsici* in pepper crops under temperate climate. *Crop Protection* 30(12): 1563–1572. https://doi.org/10.1016/j.cropro.2011.08.020

Ramírez-Gil J.G., Morales-Osorio J.G., 2020. Integrated proposal for management of root rot caused by *Phytophthora cinnamomi* in avocado cv. Hass crops. *Crop Protection* 137: 105271. https://doi.org/10.1016/j.cropro.2020.105271

Razdan V.K., Sabitha M., 2009. Integrated disease management: Concepts and practices. In: *Integrated Pest Management: Innovation-Development Process*. (Peshin R., Dhawan A.K., ed.) Springer, Dordrecht, The Netherlands, 369–389. https://doi.org/10.1007/978-1-4020-8992-3_15

Rovetto E.I., La Spada F., Aloi F., Riolo M., Pane A., Garbelotto M., Cacciola S.O., 2024. Green solutions and new technologies for sustainable management of fungus and oomycete diseases in the citrus fruit supply chain. *Journal of Plant Pathology* 106: 411–437. https://doi.org/10.1007/s42161-023-01543-6

Sapkota S., Burlakoti R.R., Punja Z.K., Gerbrandt E.M., 2023. Influence of cultivar, environmental conditions, and fungicides on development of Phytophthora root rot and wilt on red raspberry. *Crop Protection* 172: 106347. https://doi.org/10.1016/j.cropro.2023.106347

Shrivastava P., Kumar R., 2015. Soil salinity: A serious environmental issue and plant growth promoting bacteria as one of the tools for its alleviation. *Saudi Journal of Biological Sciences* 22(2): 123–131. https://doi.org/10.1016/j.sjbs.2014.12.001

Tabatabai M.A., Bremner J.M., 1969. Use of p-nitrophenyl phosphate for assay of soil phosphatase activity. *Soil Biology and Biochemistry* 1(4): 301–307. https://doi.org/10.1016/0038-0717(69)90012-1

Phytopathologia Mediterranea
The international journal of the
Mediterranean Phytopathological Union

Firenze University Press
www.fupress.com/pm

Research Papers

Identification and characterization of *Aspergillus* species associated with Aspergillus vine canker of table grapes in Spain

Adnan ALI, Maela LEÓN, Mónica BERBEGAL, Josep ARMENGOL*

Instituto Agroforestal Mediterráneo, Universitat Politècnica de València, Camino de Vera S/N, 46022-Valencia, Spain
*Corresponding author. E-mail: jarmengo@eaf.upv.es

Summary. In the summer of 2024, table grape plants (*Vitis vinifera*, "Sweet Celebration") in Cieza (Murcia province, southeastern Spain) exhibited wood cankers and dieback symptoms consistent with Aspergillus vine canker (AVC). This study aimed to determine the aetiology of the disease and characterize the associated pathogens. Multi-locus phylogenetic analyses using *cal* and *tub* loci, combined with morphological characterization, identified *Aspergillus niger* and *A. tubingensis* from symptomatic plants. Mycelium growth patterns in response to temperature were similar for both species, with optimal growth between 30 and 33 °C, and no growth above 40 °C. Temperature also strongly influenced conidium germination. No germination occurred at 10 °C, and rapid and full germination occurred between 30 and 40 °C. Pathogenicity tests on table grape 'Alphonse Lavallée' showed that both species were pathogenic to grapevine wood, with *A. niger* exhibiting greater virulence. Inoculations on green leaves showed that both species colonized foliar tissues. These results confirm the association of *A. niger* and *A. tubingensis* with table grape cankers in southeastern Spain, and also highlight the ability of these fungi to develop at high temperatures, and pose potential threats to grape and wine production under warm Mediterranean conditions.

Keywords. *Aspergillus niger*, *A. tubingensis*, Grapevine trunk diseases, pathogenicity, *Vitis vinifera.*

OPEN ACCESS

Citation: Ali, A., León, M., Berbegal, M. & Armengol, J. (2026). Identification and characterization of *Aspergillus* species associated with Aspergillus vine canker of table grapes in Spain. *Phytopathologia Mediterranea* 65(2): 319-332. doi: 10.36253/phyto-17479

Accepted: August 30, 2026

Published: September 10, 2026

© 2026 Author(s). This is an open access, peer-reviewed article published by Firenze University Press (https://www.fupress.com) and distributed, except where otherwise noted, under the terms of the CC BY 4.0 License for content and CC0 1.0 Universal for metadata.

Data Availability Statement: All relevant data are within the paper and its Supporting Information files.

Competing Interests: The Author(s) declare(s) no conflict of interest.

Editor: Akif Eskalen, University of California, Davis, CA, United States.

ORCID:
AA: 0009-0008-9055-1338
ML: 0000-0003-0693-6988
MB: 0000-0002-5773-3104
JA: 0000-0003-3815-8578

INTRODUCTION

Grapevine (*Vitis vinifera* L.) is a crop of major socioeconomic importance in Spain, reinforcing this country's position as a world leader in grape production, with about 919,000 ha cultivated (OIV, 2026). However, the sustainability of Spanish viticulture is increasingly threatened by Grapevine Trunk Diseases (GTDs) caused by fungi, which pose challenges to vineyard health, longevity, and productivity (Gramaje Pérez *et al.*, 2020).

In many international table grape and wine producing regions, GTDs are among the main causes of vine decline and mortality, often leading to vine removal 10 to 15 years earlier than the expected 30 to 35 years lifespans. This premature replacement increases production costs and disrupts long-term

vineyard sustainability (Gramaje and Armengol, 2011; Mondello *et al*., 2018; Fontaine *et al*., 2025). Vineyards of all ages are susceptible to GTDs pathogens infections, which can originate as early as the nursery stage or occur later in established vineyards (Mondello *et al*., 2018).

Aspergillus vine canker (AVC), caused by *Aspergillus* spp., is a GTD affecting wine and table grapes (Fontaine *et al*., 2025). This disease has been reported in warm grape-growing regions, as *Aspergillus* spp. are favoured by hot and dry environmental conditions (Marquès *et al*., 2025). DNA-based methods have enabled inclusion of AVC within the GTD group, allowing reliable identification and classification of *Aspergillus* spp., and thus resolving previously ambiguous reports (Hong *et al*., 2005; Houbraken *et al*., 2020; Fontaine *et al*., 2025). Recent studies have shown that AVC is a distinct component within the GTD complex, rather than being a minor disease (Vitale *et al*., 2012; Bustamante *et al*., 2024, Rangel-Montoya and Hernández-Martínez, 2024; Fontaine *et al*., 2025).

AVC was first described in 1989 in the San Joaquin Valley (California, United States of America), and was later associated with reduced vine performance and canopy longevity in commercial vineyards. Follow-up studies reported that 2 to 6.1% of vines required retraining in following season, highlighting the re-establishment costs (Bustamante *et al*., 2024). In Italy, surveys conducted in southeastern Sicily (in Catania and Ragusa, between 2007 and 2009) recorded up to 18% of incidence AVC, with 2 to 4 cankers per vine persisting annually through 2010 (Vitale *et al*., 2012). In Mexico, the first national report of AVC documented up to 5% incidence, and the cultivar 'Cotton Candy' was the most susceptible, while 'Prime Seedless' was the least affected (Rangel-Montoya and Hernández-Martínez, 2024).

Infections caused by *Aspergillus* spp. on grapevines begin when conidia land on exposed or wounded tissues, particularly on fresh pruning cuts. Conidia germinate, and hyphae penetrate host plant woody tissues, typically between the cordons and the trunk of vines. Elongated, sunken cankers develop at or just below pruning or training wounds (Bustamante *et al*., 2024). Cross-sections of infected vines reveal brown to dark brown necroses spreading inward into nearby tissues, with the advancing lesions often appearing soft or spongy (Vitale *et al*., 2012; Rangel-Montoya and Hernández-Martínez, 2024). Severe lesions may girdle vascular tissues, restricting nutrient transport and leading to premature canopy decline, reduced vine vigour, and delayed budbreak (Bustamante *et al*., 2024). At the advancing margins beneath vine bark, the pathogenic fungi can produce dry black conidia, the main primary inoculum, which are dispersed in vineyards throughout growing seasons (Bustamante *et al*., 2024).

Management of AVC is due to pathogen latent infections that delay symptom detection, and the lack of effective treatments once the disease is established. Prevention of the disease using chemical, cultural, and biological measures is important (Bustamante *et al*., 2024). Pruning should avoid warm, dry conditions, and instead be performed during cool, humid periods, ensuring the removal of diseased tissues by making pruning cuts 10 to15 cm below visible symptoms. Recommended sanitation protocols include disinfecting pruning tools before, during, and after use, and protecting exposed grapevine tissues (Vitale *et al*., 2012). A key part of managing the GTD complex is protecting fresh pruning wounds with fungicides or biological control agents (e.g. *Trichoderma* spp.) immediately after pruning (Mondello *et al*., 2018; Fontaine *et al*., 2025). Trunk renewal from healthy wood can restore grape production, if applied early and followed by wound protection (Mondello *et al*., 2018).

In the summer of 2024, grapevine plants (cv. Sweet Celebration) in a table grape vineyard located in Cieza (Murcia province, southeastern Spain) exhibited cankers and dieback symptoms consistent with those described for AVC. The objectives of the present study were to determine the aetiology of the disease, and to characterize the associated pathogens.

MATERIALS AND METHODS

Sampling and fungal isolations

Four symptomatic grapevines were sampled, were cut into sections and then transported to the laboratory for fungal isolations. Wood sections (3 cm long) showing cankers were washed under running tap water, surface-sterilized using 70% ethanol, and flamed. Small internal wood chips (3–4 mm long) were then placed in Petri plates containing malt extract agar (MEA) supplemented with 0.5 g L^{-1} of streptomycin sulfate (Sigma-Aldrich) (MEAS). The plates were then incubated at 25 °C in the dark for 5 to 10 d. All emerging colonies were subcultured onto potato dextrose agar (PDA), and the subculture plates were incubated in the same conditions.

Four representative isolates (GIHF-506, GIHF-507, GIHF-508 and GIHF-509) were selected for molecular analysis, phenotypic characterization and pathogenicity tests. Single conidium isolates of each of the isolates were obtained using the serial dilution method (Dhingra and Sinclair, 2019). For long-term storage, mycelial plugs were stored at -80 °C in 1.5 mL cryovials containing 15% glycerol solution, at the fungal collection of the

Instituto Agroforestal Mediterráneo of the Universitat Politècnica de València, Spain.

Molecular identifications

Mycelium was scraped from 8-d-old PDA cultures of isolates GIHF-506, GIHF-507, GIHF-508 and GIHF-509. Total fungal DNA of each isolate was extracted using the E.Z.N.A. Plant DNA Kit (Omega Bio-tek), following the manufacturer's short protocol instructions.

Partial fragments of beta-tubulin (*tub*) and calmodulin (*cal*) genes were amplified and sequenced. Amplifications were carried out in total volumes of 20 µL using Speedy Supreme NZYTaq 2× Green Master Mix (NZYtech), according to the manufacturer's instructions, on a Peltier Thermal Cycler-200 (MJ Research). Each reaction included 10 µL of Speedy Supreme NZYTaq 2× Green Master Mix, 0.6 µL of each primer (10 µM), 1 µL of purified template DNA, and 7.8 µL of nuclease-free water. The thermal cycle consisted of an initial step of 5 min at 94 °C, followed by 35 cycles each of denaturation at 94 °C for 2 s, annealing for 5 s, and elongation at 72 °C for 5 s. A final extension was performed at 72 °C for 2 min. The primer pairs and the annealing temperatures (Ta) for each locus were as follows: BT2a and BT2b for *tub* (Ta = 55 °C) (Glass and Donaldson, 1995), and CMD5 and CMD6 for *cal* (Ta = 58 °C) (Samson *et al*., 2014). PCR products were visualized by 1.2% agarose gel electrophoresis, purified by illustra™ ExoProStar™ S (cytiva, GE Healthcare), and sequenced by the IBMCP-UPV sequencing service (Valencia, Spain). Chromatograms were checked using Sequencher software 5.0 (Gene Codes Corp.).

Sequences generated were compared with sequences in the GenBank nucleotide database, to determine the closest relatives for phylogenetic studies. For each genomic region (*tub* and *cal*), the DNA sequences obtained in the present study were aligned with reference sequences retrieved from GenBank (Table 1), using the ClustalW algorithm included in the MEGA7 soft-

Table 1. List of *Aspergillus* section *Nigri* isolates and their sequence numbers included in the phylogenetic analyses. Isolates in bold were obtained in this study from table grape samples.

Species	Isolate	Host	Country	GenBank	
				tub	*cal*
A. niger	NRRL 326 ^{T}	Tannin-gallic acid fermentation	USA	EF661089	EF661154
	CBS 101883	*Coffea robusta*	Sumatra	AY819998	EU163270
	IHEM 21604	Outdoor air	Cuba	MH614478	MH644996
	CBS 139.54	*Welwitschia mirabilis*	Namibia	FJ629291	KC480196
	IHEM 3090	Soil	Mauritius	MH614487	MH644884
	IHEM 18080	Soil of riverside	France	MH614513	MH644969
	ITAL 47.456	Surface of grape berries	Brazil	MN583579	MN583580
	GIHF-508	*Vitis vinifera*	Spain	PZ885810	PZ885814
A. brasiliensis	CBS 101740 ^{T}	Soil	Brazil	FJ629272	FN594543
	ITEM 6139	Grapes	Portugal	AM295185	AM295176
A. carbonarius	NRRL 369 ^{T}	Paper	USA	EF661099	EF661167
	NRRL 346	Unknown	Honduras	EF661098	EF661166
A. eucalypticola	DTO 53-A2 ^{T}	Soil	India	EU482435	EU482433
	NRRL 62632	*Eucalyptus* leaves	Australia	KC796360	KC796376
A. luchuensis	KACC 46772 ^{T}	Awamori-koji	Japan	JX500062	JX500071
	IHEM 25486	Human trimming liquid	France	MH614563	MH644862
A. tubingensis	NRRL 4875 ^{T}	Unknown	Unknown	EF661086	EF661151
	CBS 134.48	Unknown	Unknown	AY820007	AJ964876
	NRRL 62634	Mangrove water	Venezuela	KC796361	KC796377
	IHEM 22394	Conjunctivitis-human eye	India	MH614544	MH644870
	GIHF-506	*Vitis vinifera*	Spain	PZ885808	PZ885812
	GIHF-507	*Vitis vinifera*	Spain	PZ885809	PZ885811
	GIHF-509	*Vitis vinifera*	Spain	PZ885807	PZ885813
A. vadensis	CBS 113365 ^{T}	Dead plant tissue	Unknown	AY585531	FN594560
	IHEM 26351	Human sputum	France	MH614547	MH644878

^{T}Indicates the ex-type isolates.

ware package (Kumar *et al*. 2016). The alignments were analyzed and adjusted manually when necessary. Ambiguous sequences at either end of alignments were excluded prior to analyses. Concatenated datasets were built in Sequence Matrix v.1.8 (Vaidya *et al*., 2011).

Phylogenetic analyses were carried out using maximum parsimony (MP) and maximum likelihood (ML) approaches. Maximum parsimony analyses were carried out in MEGA X (Kumar *et al*., 2018), employing the tree Bisection and reconnection (TBR) algorithm, where gaps were treated as missing data. Topology robustness was evaluated by 1,000 bootstrap replications (Felsenstein, 1985). Measures for maximum parsimony, as tree length (TL), consistency index (CI), and retention index (RI), were also calculated. Maximum likelihood analyses were carried out using IQ-TREE v.3.1.2 (Wong *et al*., 2026). The concatenated dataset was partitioned into the *tub* and *cal* genomic regions, and the best-fit evolutionary models were selected using ModelFinder (Kalyaanamoorthy *et al*., 2017), based on the Bayesian information criterion (BIC). HKY+I was selected for *tub*, and HKY+G4 for *cal*. Branch support was assessed using 1,000 ultrafast bootstrap (UFBoot) replicates, and 1,000 SH-like approximate likelihood ratio test (SH-aLRT) replicates.

Morphological characterizations

Isolates GIHF-506 and GIHF-508 were used for morphological characterizations. Petri plates containing PDA or Czapek agar (CZA; 30.0 g L^{-1} sucrose, 2.0 g L^{-1} $NaNO_3$, 0.5 g L^{-1} KCl, 0.5 g L^{-1} Mg-glycerophosphate, 0.35 g L^{-1} K_2SO_4, 0.01 g L^{-1} $FeSO_4$, 12.0 g L^{-1} agar) were inoculated with 5 mm mycelium plugs taken from actively growing margins of a 7-d-old cultures. After 7 d of incubation at 25 °C in darkness, colony morphologies were recorded, including; obverse and reverse colours, texture (e.g., velvety *vs*. granular/fluffy), and margin appearance (smooth to slightly lobed). Microscopic features were assessed from 4- to 7-d old cultures. Mycelium and black conidia were mounted in Shear's fluid (50 mL of 2% potassium acetate, 20 mL glycerol, 30 mL of 95% ethanol), and examined at 10 ×, 20 ×and 40 × magnifications, using a Nikon Eclipse Ni microscope equipped with NIS-Elements-D imaging software. Vesicle and conidium diameters were measured for 50 replicates per structure and per isolate.

Mycelium growth at different temperatures

Isolates GIHF-506, GIHF-507, GIHF-508 and GIHF-509 were grown on PDA in 90 mm diam. Petri plates (~20 mL per plate). For each assay plate, a 5 mm diam mycelium plug was taken from the active margin of a 7-d-old culture, and placed (mycelium side down) in the centre of a fresh PDA plate. Growth was evaluated at 10, 15, 20, 25, 30, 35, 40, or 45 °C. For each isolate-temperature combination, four replicates were prepared. The experiment was repeated (two independent runs), resulting in a total of eight replicates per isolate–temperature combination. Inoculated plates were sealed with parafilm, randomized inside incubators, and kept for 7 to 21 d (depending on the temperature) in the dark. When the diameter (D, mm) of a colony on the medium reached 60-70% of the Petri dish diameter, it was measured along two perpendicular axes and averaged once uniform growth was established. The time elapsed from inoculation to measurement (t, d) was recorded. The average radial growth rate was calculated as:

$$\text{Growth rate (mm d}^{-1}) = [(D - 5\text{ mm}) / 2] / t;$$

where (D – 5 mm) / 2 was the radial increase from each inoculum plug edge to the colony edge. If no growth was observed by the endpoint, the rate was recorded as 0 mm d^{-1}.

The data obtained were rescaled to 0 to 1, by dividing each datum by the maximum datum obtained in each experiment. Rescaled data were regressed against temperature, and nonlinear regression equations were compared based on data representation. A beta equation was fitted to the data in the following form (Analytis, 1977):

$$y = [a \times \text{Teq}^b \times (1 - \text{Teq})]^c;$$

where: y = rescaled daily growth (0 to 1); Teq = temperature equivalent calculated as Teq = (T − T min) / (T max– T min): where T = temperature (°C); T min and T max = minimum and maximum temperatures for mycelium growth; and *a* to *c* = the equations parameters. T min for mycelium growth was 9 °C and T max was 44 °C, (Gougouli and Koutsoumanis, 2010). All data analyses were performed using R version 4.6.1 via RStudio version 2026.07.1 (Posit Team, 2026).

Equation parameters were estimated using the function *nls* included in the package "stats" (Wickman, 2019). Goodness-of-fit of the equations was evaluated based on the adjusted R^2, the concordance correlation coefficient (CCC), and the root mean square error (RMSE) (Lin, 1989). Linear regressions were carried out between the observed and the predicted data, to estimate the adjusted R^2, using the *lm* function of the R "stats" package. The CCCs were obtained using the *epi.ccc* function of the R

"epiR" package (Carstensen *et al*., 2022). The RMSEs, were obtained using the *rmse* function of the R "modelr" package (Wickham, 2019). According to Analytis (1977), the optimum temperatures (T opt) for daily mycelium growth were calculated as follows:

$$T\ opt = [(b \times c) / (b \times c + c)] \times (T\ max - T\ min) + T\ min;$$

where b and c are equation parameters, and T max and T min are as described above.

Conidium germination at different temperatures and time periods

Isolates GIHF-506 and GIHF-508 were used for this study. Conidium suspensions were obtained from 7-d-old PDA cultures by gently flooding respective colonies with sterile water containing a non-ionic surfactant (~ 0.01% Tween), loosening the conidia with a sterile loop, and filtering the resulting conidium suspensions through sterile gauze to remove hyphal fragments. Conidium concentrations were adjusted to 10^5 conidia mL^{-1} using hemocytometer counts. For each isolate-temperature-time combination, two 20 µL drops of conidium suspension were deposited onto the surface of a fresh 90 mm diam PDA plate, and the plates were incubated in the dark at the respective specified temperatures. Conidium germination was assessed at 6, 12, 18, 24, 36, and 48 h after plating. The experiment was repeated (two independent runs, with four replicates per run). At the end of each incubation period, conidium germination was determined by examining 100 conidia per drop using a microscope (× 40 magnification). A conidium was considered germinated when the length of the germtube exceeded the length of the conidium. Mean germination percentages were then calculated for each treatment, and statistical analyses were not carried out because this experiment was intended to be descriptive.

Pathogenicity test on table grape plants

For pathogenicity tests, rooted cuttings of table grape 'Alphonse Lavallée' were transplanted into 3 to 5 L capacity pots that were maintained in a greenhouse until inoculation, allowing a single shoot to develop on each cutting. Isolates GIHF-506 and GIHF-508 were tested using four plants per isolate, with an equal number of non-inoculated plants as inoculation controls. Inoculum consisted of 6 mm mycelium plugs taken from the advancing margins of 3 to 7-d-old PDA cultures. On each plant, a 6 mm diam. circular wound was made to the cambium at an internode of the main shoot, using a sterile cork borer. A mycelium plug was inserted (mycelium facing the cambium), was then covered with moist cotton, and then sealed with Parafilm to prevent desiccation. Plants were then arranged randomly in a greenhouse under semi controlled conditions (~35 °C day / 25 °C night), were irrigated as needed, and then inspected weekly for external symptoms. The experiment was performed twice (n = 8 plants per isolate in total).

The necrotic lesion length (mm) developed on each shoot was measured 50 d after inoculation, and mean lesion lengths were calculated. Small wood chips from lesion margins were surface-disinfected, and then plated on MEAS to assess completion of Koch's postulates. All emerging colonies were transferred to PDA plates and incubated at 25 °C in darkness until sporulation. The effect of the inoculated isolate, the experiment and the interaction on lesion length was analyzed using a generalized linear model (GLM) with a Gamma distribution and a log link function. The dispersion and residuals of the models were tested by using the function *simulateResiduals* of the "DHARMa" package. Once significance of factors was assessed pairwise comparisons of adjusted means were performed using the "emmeans" package (Lenth and Piaskowski, 2026) with Bonferroni correction adjustment and grouping letters were generated using the *cld* function with "multcomp" package (Hothorn *et al*., 2008).

Pathogenicity on leaves

The pathogenicity of isolates GIHF-506 and GIHF-508 was evaluated on detached leaves of table grape cv. 'Alphonse Lavallée' following the methods described by Rangel-Montoya and Hernández-Martínez (2024). Mature, healthy leaves without visible symptoms, wounds, or insect injury were collected, then gently rinsed with sterile water, and air-dried. For each isolate, eight leaves were inoculated, while an additional eight leaves served as non-inoculated controls.

Conidium suspensions were prepared from 3-d-old PDA cultures, and were adjusted to 10^5 conidia mL^{-1} in sterile water using a hemocytometer. For inoculation, each leaf was positioned abaxial side up. The petiole-lamina junction was punctured once with a sterile entomological needle, and a 10 µL droplet of conidium suspension was applied to the wound, to facilitate capillary entry and ensure uniform inoculation. Non-inoculated control leaves received 10 µL droplets of sterile water following the same procedure.

Inoculated and non-inoculated control leaves (four per isolate) were placed in humid chambers (sealed plas-

tic boxes containing moistened sterile filter paper) to maintain high relative humidity (>95%). These were kept for 10 d in an incubator at 25 °C with a 12 h light, 12 h darkness daily cycle. The filter paper was re-moistened periodically to maintain humidity, ensuring no direct water contact with the leaf surfaces. The experiment was performed twice.

Disease severity was visually assessed at the end of the incubation period, using a 0–5 scale (Montoya and Hernández-Martínez, 2024), where: 0 = no symptoms; 1 = slight wilting; 2 = red necrotic lesions; 3 = mycelium growth; 4 = conidium presence; 5 = mycelial growth and conidium presence. Severity data was transformed using the McKinney Index (MKI), a widely applied disease severity index for ordinal data (McKinney, 1923; Bock *et al*., 2024). The effect of the inoculated isolate and the experiment on disease severity were analyzed using Kruskal–Wallis rank-sum test by *kruskal_test* function of the "rstatix" package (Kassambara, 2026). Once significance of effects was assessed, pairwise comparisons were performed using Dunn's test with Bonferroni adjustment.

RESULTS

Sampling and fungus isolations

Symptoms observed in the table grape orchard are shown in Figure 1 A. Affected plants exhibited wilting and decay, along with cankers on the main trunks, and internal wood necroses (Figure 1, B and C). Isolations from symptomatic tissues consistently recovered *Aspergillus* colonies, characterized by rapid radial growth and profuse dark sporulation (Figure 1 D). From these primary cultures, the four representative isolates (GIHF-506, GIHF-507, GIHF-508, GIHF-509) were selected.

Molecular identifications

PCR amplification of the β-tubulin (*tub*) and calmodulin (*cal*) gene regions yielded single, well-defined amplicons of, respectively, approx. 550 bp and 600 bp, for all four fungal isolates. Purified PCR products were sequenced, and chromatograms were manually inspected. BLASTn analyses of the obtained sequences against the NCBI GenBank database showed ≥99% similarities with *A. tubingensis* and *A. niger*.

Multi-locus phylogenetic analyses of concatenated *tub* and *cal* alignments were conducted using the Maximum Parsimony (MP) method in MEGA X and the Maximum Likelihood (ML) method in IQ-TREE v.3.1.2

Figure 1. Field symptoms associated with *Aspergillus* infections in grapevines. (A) Decline symptoms in a vineyard. (B) External discolouration and tissue damage on a trunk. (C) Trunk cross sections showing internal necroses. (D) Colonies of *Aspergillus* isolated from infected grapevine tissues.

(Figure 2). The analyses included 25 taxa: 19 reference taxa representing the six species within section Nigri of *Aspergillus*, the four isolates analyzed in this study, and two *A. carbonarius* isolates used as the outgroup. The combined dataset comprised 975 positions including gaps (488 from *tub* and 487 from *cal*), of which 258 (26.5%) were parsimony-informative. MP analyses yielded nine most-parsimonious trees (TL = 372, CI = 0.89, RI = 0.99); one of which is shown in Figure 2. The resulting phylogeny resolved the six species into the three main phylogenetic lineages of section Nigri. Three of the isolates from the present study (GIHF506, GIHF507, and GIHF509) clustered unambiguously within the *A. tubingensis* species clade, which forms part of the *A. tubingensis* lineage, and isolate GIHF508 clustered within the *A. niger* species clade. The ML analysis produced a topology highly congruent with the MP analysis, confirming the same three major phylogenetic lineages and placement of the four isolates within the *A. tubingensis* and *A. niger* species clades (Figure 2).

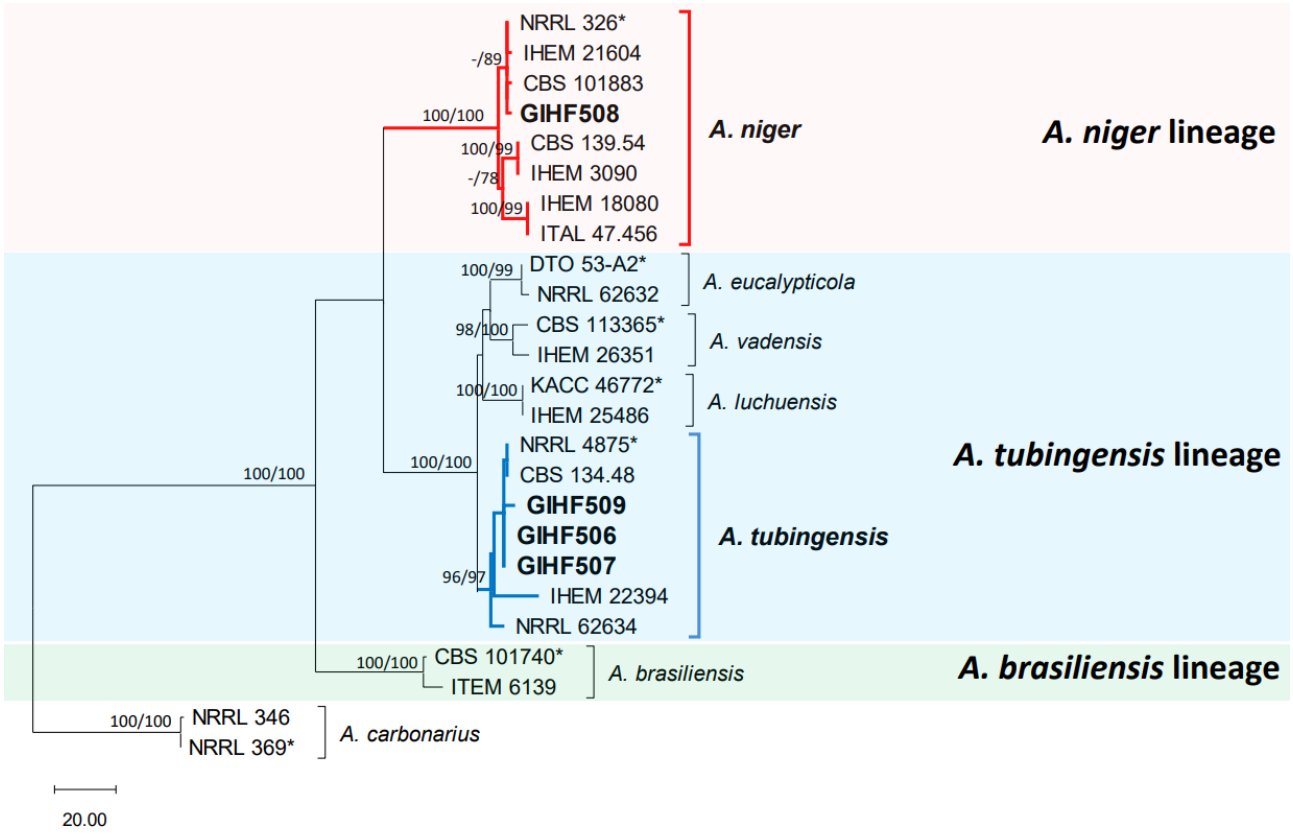

Figure 2. One of nine most parsimonious trees obtained from the analysis of the combined sequence data of two loci (beta-tubulin and calmodulin) of 25 *Aspergillus* isolates. Scale bar shows 20 changes, and bootstrap support values from 1,000 replicates for Maximum Likelihood (ML) and Maximum Parsimony (MP) analyses are indicated at the tree nodes (ML/MP). Values below 95% for ML and 70% for MP are not shown. The ex-type isolates are labelled with an asterisk, and the *Aspergillus* spp. isolated in the present study are highlighted in bold font. The tree was rooted to *A. carbonarius* (NRRL 369 and NRRL 346).

Morphological characterizations

After 4 to 7 d incubation at 25 °C in darkness, distinct colony characteristics were observed on CZA and PDA media for the representative isolates of *A. niger* (GIHF-508) and *A. tubingensis* (GIHF-506). On CZA, *A. niger* maintained dense black sporulation, with reverse pigmentation ranging from colourless to pale yellow. In contrast, *A. tubingensis* showed more variable sporulation intensity, and had yellowish reverse pigmentation. On PDA, the *A. niger* isolate developed colonies with intense black sporulation, granular texture, and well-defined white margins, while *A. tubingensis* had olive-green to black sporulation, with floccose aerial mycelium and well-defined white margins. Microscope examination revealed that both *A. niger* and *A. tubingensis* produced globose to subglobose conidia and spherical vesicles, typical of section Nigri, and had typical biseriate conidium structures. *Aspergillus niger* displayed robust conidiophores with prominent vesicles, dense conidium chains, and black, strongly echinulate, conidia. *Aspergillus tubingensis* developed less robust conidiophores, less compact conidium chains, and brown finely roughened conidia. Both fungi produced globose conidium heads. Conidium diameters of *A. niger* ranged from 3.05 to 4.75 µm (mean = 3.90 ± 0.42 µm), while those of *A. tubingensis* ranged from 2.85 to 4.65 µm (mean = 3.74 ± 0.38 µm). Vesicle diameters for *A. niger* varied from 36.39 to 73.39 µm (mean = 54.06 ± 8.37 µm), and from 41.30 to 61.17 µm (mean = 51.48 ± 6.12 µm) for *A. tubingensis*.

Mycelium growth at different temperatures

Curves that fit the temperature response to daily mycelium growth rates are shown in Figure 3. Equation parameters with their standard errors and goodness-of-fit coefficients are summarized in Table 2. In general, mycelium growth occurred between 15 and 40 °C, with radial expansion increasing with temperature, from 15 °C up

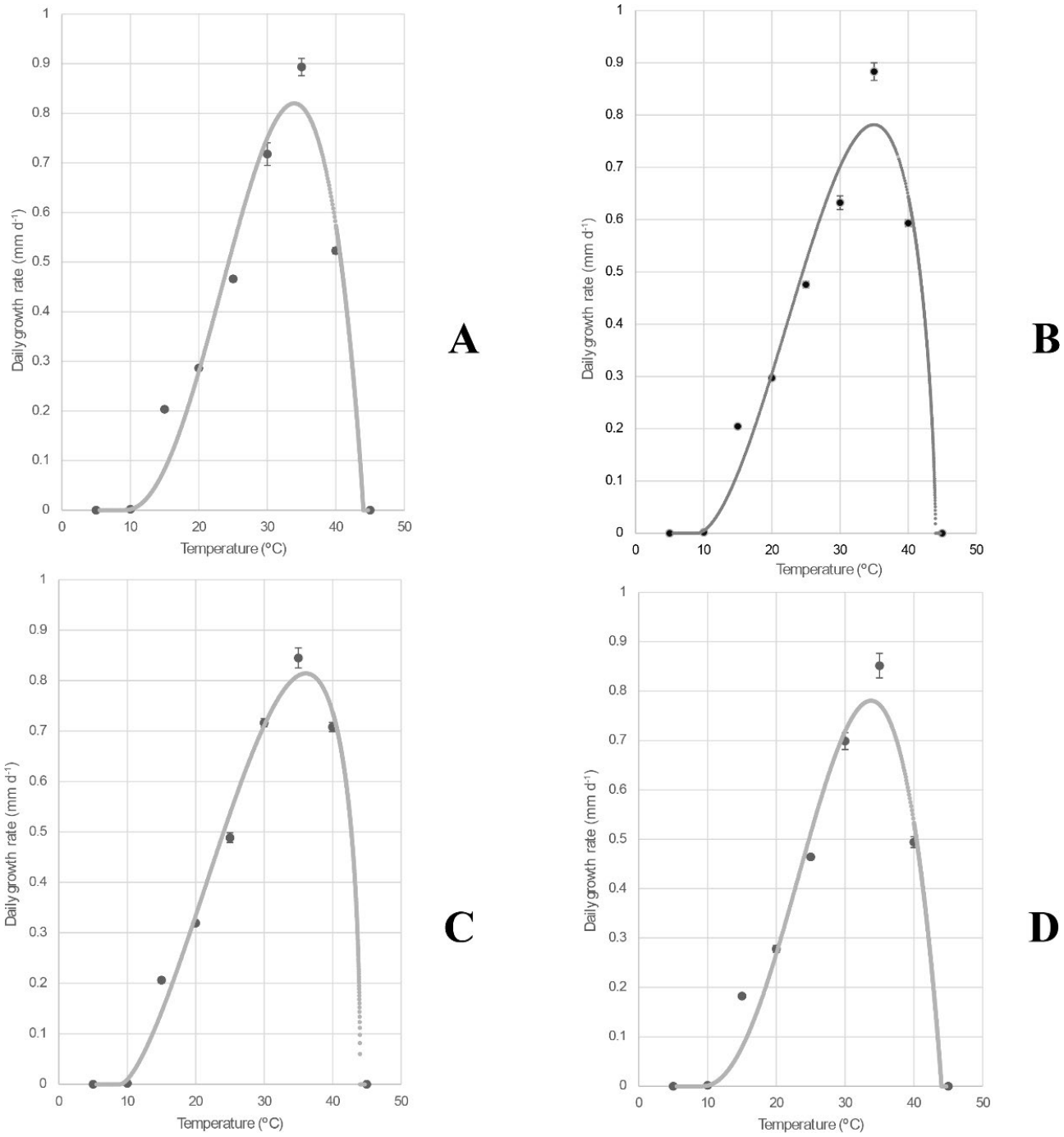

Figure 3. Mean mycelium growth rates of *Aspergillus* isolates at different temperatures. (A) Isolate GIHF-506, (B) GIHF-507, (C) GIHF-508, and (D) GIHF-509. Observed mean daily growth rates (points) are shown together with the fitted temperature response model (gray lines).

to a peak between 30 °C and 35 °C, followed by a sharp decline. At 15 °C, colony development was very slow (≤ 1 mm day^{-1}), and increased with increasing temperature, reaching mean radial rates of approx. 1.5 to 3.5 mm d^{-1} at 20–25 °C, while the greatest rates (6 to 8 mm d^{-1}) were recorded at 30 to 35 °C. At 40 °C, growth was substantially reduced (≤ 1 mm d^{-1}) and no mycelium growth occurred at 45 °C. Calculated optimum temperatures for growth ranged from 30.2 °C to 33.4 °C. The lower optimum temperature was recorded for *A. niger* isolate GIHF-

Table 2. Parameters and goodness-of-fit coefficients for equations used to describe the effect of temperature on daily mycelial growth of *Aspergillus niger* (GIHF-508) and *A. tubingensis* (GIHF-506, GIHF-507 and GIHF-509) isolates.

Isolate	Topt[a]	Estimated parameters ± SE			Goodness-of-fit		
		a	b	c	Adjusted R^{2b}	CCC[c]	RMSE[d]
GIHF-506	33.4	5.70 ± 3.14	2.30 ± 0.53	0.93 ± 0.27	0.9456	0.9759	0.0631
GIHF-507	31.2	3.15 ± 1.56	1.82 ± 0.47	0.63 ± 0.24	0.9404	0.9744	0.0623
GIHF-508	30.2	2.36 ± 0.61	1.54 ± 0.24	0.45 ± 0.12	0.9823	0.9925	0.0349
GIHF-509	33.4	5.67 ± 2.84	2.32 ± 0.48	0.96 ± 0.25	0.9535	0.9795	0.0559

[a]: Predicted optimal temperature (Analytis, 1977); [b]: adjusted coefficient of determination; [c]: concordance correlation coefficient; [d]: root mean square error.

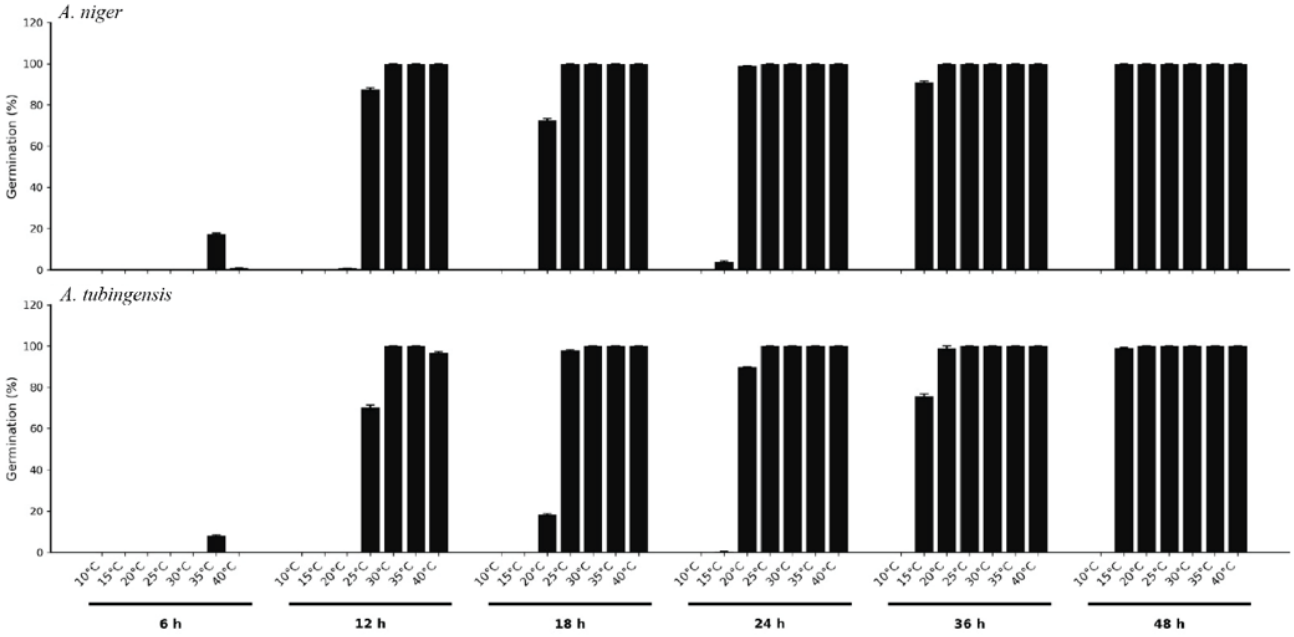

Figure 4. Mean conidium germination (%) of *Aspergillus niger* (upper histogram) and *A. tubingensis* (lower) at different temperatures (10 to 40 °C) over time intervals of 6, 12, 18, 24, 36, or 48 h). Bars accompanying each symbol represent standard error.

508 (Table 2). In general, the growth response equations provided a good fit of data, with adjusted R^2 values ranging from 0.9404 to 0.9823, and RMSE ranging from 0.0349 to 0.0631 (Table 2). CCC values were 0.99 for the equation describing the growth of the *A. niger* isolate, and 0.97 for the equations of *A. tubingensis* isolates.

Conidium germination at different temperatures and time periods

Conidium germination was influenced by temperature and incubation time, with *A. niger* generally initiating germ tube emergence slightly earlier than *A. tubingensis* (Figure 4). No germination occurred at 10 °C even after 48 h of incubation, indicating that this temperature was below the physiological threshold for germination. Consequently, responses are described for 15 to 40 °C.

After 6 h, no germination was observed between 15 °C and 30 °C for either species. At 35 °C, *A. niger* reached 17% germination, and *A. tubingensis* reached 8% germination, while only 1% germination was recorded for *A. niger* at 40 °C. After 12 h, conidia remained dormant at 15 °C. At 20 °C, *A. niger* showed 1% germination, whereas at 25 °C germination rates were greater (86% in *A. niger*; 73% in *A. tubingensis*). Complete germination (100%) was achieved at 30 to 35 °C for both species, and nearly so (96%) at 40 °C. After 18 h, while no germination occurred at 15 °C, *A. niger* reached 75%, and *A. tubingensis* 21%, at 20 °C. Both isolates attained 100%

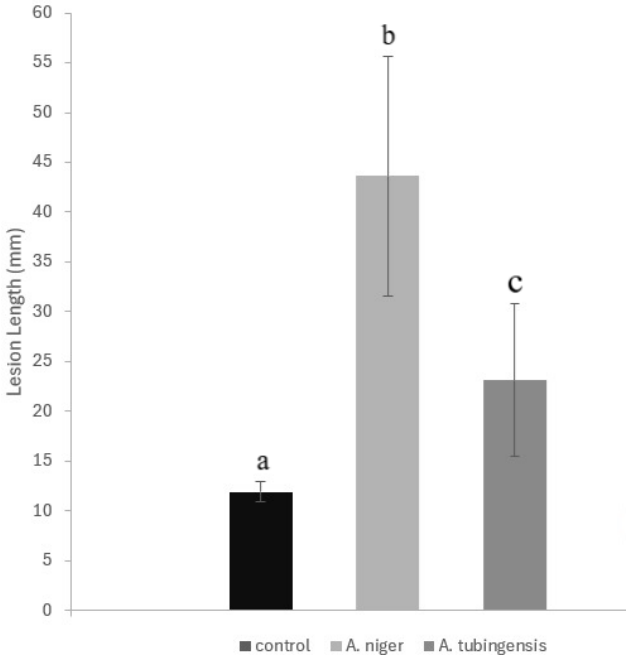

Figure 5. Mean lesion lengths in grapevine stems caused by *Aspergillus niger* and *A. tubingensis* isolates, compared with non-inoculated controls. Bars accompanying each mean represent standard errors, and different letters indicate statistically significant differences between the means, as shown by Bonferroni-adjusted pairwise comparisons of the means.

conidium germination between 25 and 40 °C. After 24 h germination was initiated at 15 °C (3% in *A. niger*, 1% in *A. tubingensis*), while at 20 °C, *A. niger* reached 100%, and *A. tubingensis* 90%. After 36 h, germination at 15 °C reached of 92% for *A. niger* and 79% for *A. tubingensis*. After 48 h, complete germination (100%) was achieved at all temperatures from 15 to 40 °C.

Pathogenicity test on grapevine plants

After 50 d incubation, both *A. niger* and *A. tubingensis* induced characteristic AVC symptoms on the inoculated grapevine shoots, while non-inoculated control plants remained symptomless. Necrotic lesions developed around the inoculation sites and extended longitudinally along the internodes. Darkened vascular tissues and black conidium masses were evident beneath the bark of inoculated plants.

The inoculated fungi were successfully re-isolated from all symptomatic tissues (100% re-isolation frequency), thereby fulfilling Koch's postulates. Mean lesion lengths differed significantly among the inoculated isolates (Figure 5), with the longest lesions produced by *A. niger* (43.62 ± 12.01 mm), followed by *A. tubingensis* (23.12 ± 7.65 mm). The non-inoculated control plants had limited discolourations around the wound sites (11.87 ± 1.02 mm).

Statistical analyses of lesion length data showed statistically significant effects on lesion development. However, no significant effect was observed for the experiment or the experiment × isolate interaction, indicating consistent symptom development across the two experimental repetitions. *Post hoc* comparisons showed significant differences among the isolates (Figure 5). and both inoculated isolates of *Aspergillus* spp. produced larger lesions than for the non-inoculated controls.

Pathogenicity test on grapevine leaves

Pathogenicity tests conducted on detached leaves of cv. 'Alphonse Lavallée' revealed significant differences in disease severity among inoculated isolates after 10 d of incubation (Figures 6 and 7). While most non-inoculated control leaves had no visible symptoms, one leaf exhibited slight wilting (severity = 1), resulting in a mean severity index of 0.12. In contrast, inoculated leaves developed characteristic red necrotic lesions and sporulation at the infection sites, consistent with *Aspergillus* infections.

Leaves inoculated with *A. niger* exhibited variable responses, with symptom severity ranging from 0 to 5 (mean severity index = 2.63), Red-necrotic lesions and localized mycelium growth were frequently observed, and some leaves developed black conidium masses at the inoculation sites. *Aspergillus tubingensis* induced the most severe symptoms, with seven out of the eight inoculated leaves reaching the maximum severity score (5), characterized by extensive mycelium growth and abundant conidium formation. The mean severity index for *A. tubingensis* was 4.38.

Statistical analyses confirmed a significant effect ($P < 0.001$) of the inoculations on leaf symptom severity relative to the non-inoculated controls. However, no effect ($P = 0.596$) was observed for the experiment. *Post hoc* comparisons indicated that while both *Aspergillus* species caused greater disease severity than the non-inoculated controls, the differences between the two fungal species were not statistically significant (Figure 7).

DISCUSSION

This study provides the first report of Aspergillus vine canker (AVC) affecting table grapevine in Spain. Etiology of this disease was established through morphological and molecular pathogen characterization, *in*

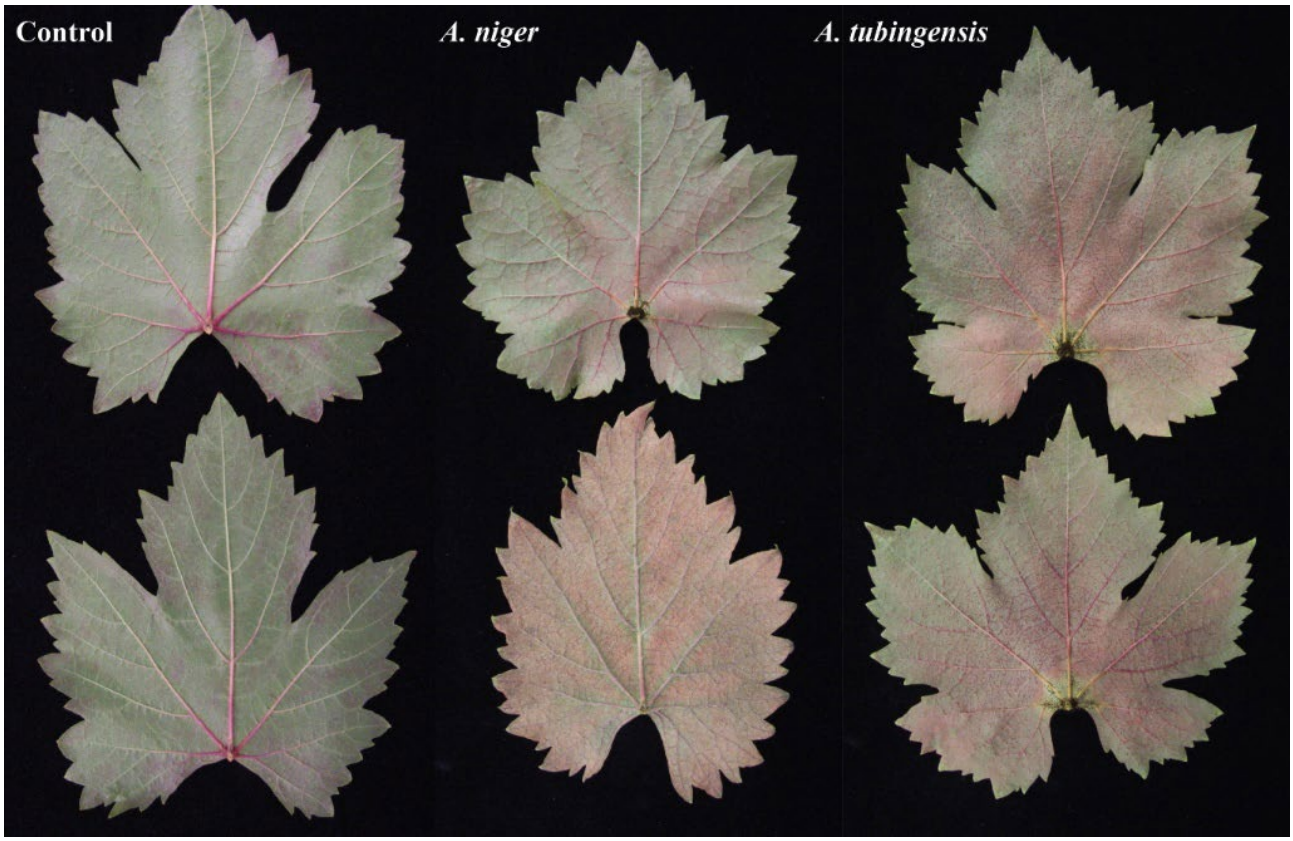

Figure 6. Grapevine leaf symptoms caused by *Aspergillus niger* or *A. tubingensis*, compared with symptomless non-inoculated control leaves (left).

vitro assays assessing mycelium growth and conidium germination of *Aspergillus* isolates under varying temperatures, and their pathogenicity to grapevine plants and leaves.

These results identified *A. niger* and *A. tubingensis* associated with AVC symptomatic plants. The combined use of *cal* and *tub* loci were effective for precise species level identifications within *Aspergillus* section Nigri, enabling differentiation of closely related taxa (Vitale *et al*., 2012). Morphological analyses also provided differentiation between these two species, confirming the results of the molecular identification. *Aspergillus tubingensis* was the predominant species, accounting for most isolates recovered from symptomatic table grape cankers, while *A. niger* occurred less frequently, indicating its coexistence with *A. tubingensis* in the AVC complex.

These results are consistent with those from other grape-producing regions. In Sicily, *A. tubingensis* and *A. niger* were identified as the main species associated with AVC, both capable of inducing lesions on woody grapevine tissues (Vitale *et al*., 2012). Bustamante *et al*., (2024) also reported *A. tubingensis* as the dominant species responsible for AVC and summer bunch rot in California, whereas *A. niger* was detected at lower frequency. Similar results were observed in Mexico, where *A. tubingensis* and *A. niger* were confirmed as the causal agents of AVC in several table grape cultivars (Rangel-Montoya and Hernández-Martínez, 2024).

Regarding effects of temperature on mycelium growth, both species showed similar patterns, but *A. niger* consistently had slightly faster radial growth than the *A. tubingensis* isolates across most temperatures assessed. The optimal growth temperatures were between 30 and 33 °C, and no growth occurred above 40 °C, which aligns with previously described thermal profiles for *Aspergillus* species involved in AVC (Vitale *et al*., 2012; Bustamante *et al*., 2024; Rangel-Montoya and Hernández-Martínez, 2024). Temperature also strongly influenced conidium germination of both species. The absence of germination at 10 °C showed that this temperature was below the physiological threshold, while the rapid and complete germination between 30 and 35 °C identified the optimum range, corresponding to observations of temperature effects on mycelium growth.

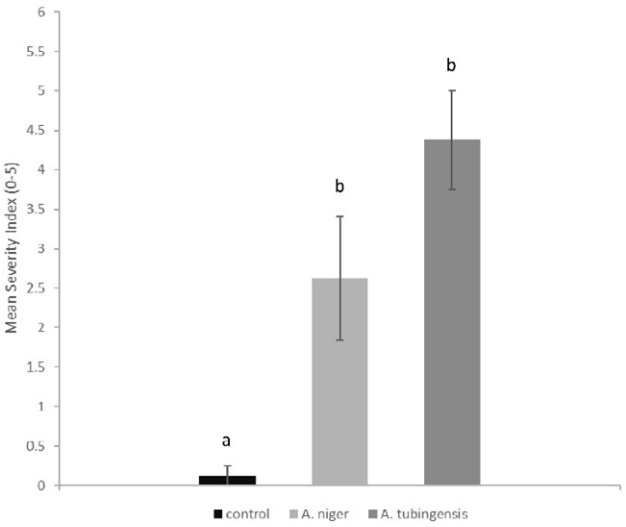

Figure 7. Mean severity indices for grapevine leaves inoculated with *Aspergillus* isolates. Mean severity index (0 to 5 scale) was recorded for leaves following plant inoculations with *A. niger* or *A. tubingensis*, compared with the non-inoculated controls. Bars represent mean severty index ± standard errors. Different letters indicate differences ($P \leq 0.05$), according to Bonferroni-adjusted pairwise comparisons of means.

The ability of conidia to germinate at 40 °C demonstrated high thermal tolerance in the isolates assessed.

These results indicate that *A. niger* and *A tubingensis* are both adapted to periods of elevated environmental temperatures typical of Mediterranean and semi-arid summers (Houbraken *et al*., 2020; Rangel-Montoya and Hernández-Martínez, 2024), and are consistent with previous findings. In Italy and California, *A. niger* and *A. tubingensis* were confirmed as the main agents of AVC, and were shown to thrive in warm, semi-arid vineyards (Vitale *et al*., 2012; Bustamante *et al*., 2024). Mexican isolates (*A. tubingensis*, *A. niger* and *A. welwitschiae*) survived temperatures of up to 40 to 50 °C (Rangel-Montoya and Hernández-Martínez, 2024). Seasonal aerobiology studies carried out by Bustamante *et al.* (2024) revealed sustained, warm season conidium production. Traps placed in table grape vineyards in Kern County, California, from late spring through summer, repeatedly captured *Aspergillus*, indicating that airborne inoculum can persist for weeks to months rather than appearing in brief pulses.

The pathogenicity tests performed on table grape plants cv. 'Alphonse Lavallée' demonstrated that both *A. niger* and *A. tubingensis* are pathogenic to grapevine wood, with *A. niger* exhibiting greater virulence than *A. tubingensis*, which is consistent with reports from Italy (Vitale *et al*., 2012), California (Bustamante *et al*., 2024), and Mexico (Rangel-Montoya and Hernández-Martínez, 2024). Grapevine leaf inoculations with *A. niger* and *A. tubingensis* also showed that both species can colonize grapevine leaf tissues. Development of necroses, mycelium growth, and black conidial masses on inoculated leaves, corroborates results of foliar inoculations reported in previous studies in Mexico (Rangel-Montoya and Hernández-Martínez, 2024), confirming the ability of these species to infect woody and green grapevine tissues.

Overall, the present study results confirm that *A. niger* and *A. tubingensis* are associated with table grape cankers in southeastern Spain, and highlight the ability of these fungi to develop under high temperatures, posing potential threats to grape and wine production under warm Mediterranean climatic conditions.

ACKNOWLEDGMENTS

This research was funded by the European Union. Views and opinions expressed are however those of the author(s) only and do not necessarily reflect those of the European Union or the European Education and Culture Executive Agency (EACEA). Neither the European Union nor EACEA can be held responsible for them.

LITERATURE CITED

Analytis S., 1977. On the relation between biological development and temperature of some plant pathogenic fungi. *Journal of Phytopathology* 90: 64–76. https://doi.org/10.1111/j.1439-0434.1977.tb02886.x

Bock C.H., Del Ponte E.M., Chiang K.-S., 2024. The nuances of plant disease severity estimation using quantitative ordinal scales—Lessons learned over four decades. *Phytopathology* 114(6): 1157–1159. https://doi.org/10.1094/phyto-11-23-0435-le

Bustamante M.I., Elfar K., Kuzmenko J., Zaninovich T., Arreguin M., ... Eskalen A., 2024. Reassessing the etiology of Aspergillus vine canker and summer bunch rot of table grapes in California. *Plant Disease* 108(4): 941–950. https://doi.org/10.1094/PDIS-06-23-1137-RE

Carstensen B., Plummer M., Laara E., Hills M., 2022. Epi: A Package for Statistical Analysis in Epidemiology. https://CRAN.R-project.org/package=Epi

Dhingra O.D., Sinclair J.B., 2019. Basic Plant Pathology Methods. 2nd edition. CRC Press, Boca Raton, Florida, USA. https://doi.org/10.1201/9781315138138

Felsenstein J., 1985. Confidence limits on phylogenies: An approach using the bootstrap. Evolution 39:

783–791. https://doi.org/10.1111/j.1558-5646.1985.tb00420.x

Fontaine F., Trouillas F.P., Armengol J., Eskalen A., 2025. Fungal trunk diseases: A global threat to grapevines. *Annual Review of Phytopathology* 63: 577–602. https://doi.org/10.1146/annurev-phyto-121323-022259

Glass N.L., Donaldson G.C., 1995. Development of primer sets designed for use with the PCR to amplify conserved genes from filamentous ascomycetes. *Applied and Environmental Microbiology* 61(4): 1323–1330. https://doi.org/10.1128/AEM.61.4.1323-1330.1995

Gougouli M., Koutsoumanis K.P., 2010. Modelling growth of *Penicillium expansum* and *Aspergillus niger* at constant and fluctuating temperature conditions. *International Journal of Food Microbiology* 140(2–3): 254–262. https://doi.org/10.1016/j.ijfoodmicro.2010.03.021

Gramaje D., Armengol J., 2011. Fungal trunk pathogens in the grapevine propagation process: Potential inoculum sources, detection, identification, and management strategies. *Plant Disease* 95(9): 1040–1055. https://doi.org/10.1094/PDIS-01-11-0025

Gramaje Pérez D., Armengol Fortí J., Barajas Tola E., Berbegal Martínez M., Chacón Vozmediano J.L., … Sagüés Sarasa A., 2020. Guía sobre las enfermedades fúngicas de la madera de la vid. Ministerio de Agricultura, Pesca y Alimentación (MAPA), Madrid, Spain.

Hong S.-B., Go S.-J., Shin H.-D., Frisvad J.C., Samson R.A., 2005. Polyphasic taxonomy of *Aspergillus fumigatus* and related species. *Mycologia* 97(6): 1316–1329. https://doi.org/10.1080/15572536.2006.11832738

Hothorn T., Bretz F., Westfall P., 2008. Simultaneous Inference in General Parametric Models. *Biometrical Journal* 50: 346–363. https://doi.org/10.1002/bimj.200810425

Houbraken J., Kocsubé S., Visagie C.M., Yilmaz N., Wang X.-C., … Frisvad J.C., 2020. Classification of *Aspergillus*, *Penicillium*, *Talaromyces* and related genera (Eurotiales): An overview of families, genera, subgenera, sections, series and species. *Studies in Mycology* 95: 5–169. https://doi.org/10.1016/j.simyco.2020.05.002

Kalyaanamoorthy S., Minh B.Q., Wong T.K., Von Haeseler A., Jermiin L. S., 2017. ModelFinder: fast model selection for accurate phylogenetic estimates. *Nature methods*, 14: 587–589. https://doi.org/10.1038/nmeth.4285

Kassambara, A. Rstatix: Pipe-Friendly Framework for Basic Statistical Tests Available online: https://cran.r-project.org/web/packages/rstatix/index.html (accessed on 31 August 2026).

Kumar S., Stecher G., Tamura K., 2016. MEGA7: Molecular evolutionary genetics analysis version 7.0 for bigger datasets. *Molecular Biology and Evolution* 33(7): 1870–1874. https://doi.org/10.1093/molbev/msw054

Kumar S., Stecher G., Li M., Knyaz C., Tamura K., 2018. MEGA X: Molecular evolutionary genetics analysis across computing platforms. Molecular *Biology and Evolution* 35: 1547–1549. https://doi.org/10.1093/molbev/msy096

Lenth R., Piaskowski J., 2026. emmeans: Estimated Marginal Means, aka Least-Squares Means. https://rvlenth.github.io/emmeans/

Lin L.I., 1989. A concordance correlation coefficient to evaluate reproducibility. *Biometrics* 45:255-268.

Marquès J., Castellà G., Bragulat M.R., Cabañes F.J., 2025. Diversity of *Aspergillus* section Nigri species from vineyards with different agro-climatic conditions in Catalonia, Spain. International *Journal of Food Microbiology* 430: 111049. https://doi.org/10.1016/j.ijfoodmicro.2024.111049

McKinney H.H., 1923. Influence of soil temperature and moisture on infection of wheat seedlings by *Helminthosporium sativum*. *Journal of Agricultural Research* 26: 195–217. https://doi.org/10.5555/19241100488

Mondello V., Songy A., Battiston E., Pinto C., Coppin C., … Fontaine F., 2018. Grapevine trunk diseases: A review of fifteen years of trials for their control with chemicals and biocontrol agents. *Plant Disease* 102(7): 1189–1217. https://doi.org/10.1094/PDIS-08-17-1181-FE

OIV, 2026. State of the world wine sector in 2025. International Organisation of Vine and Wine, Dijon, France: 25 pp.

Posit Team. 2026. RStudio: Integrated Development Environment for R. Posit Software, PBC, Boston, Massachusetts, USA. Available at: http://www.posit.co/

Rangel-Montoya E.A., Hernández-Martínez R., 2024. Identification and pathogenicity of *Aspergillus* species associated with vine canker in Mexico. *Journal of Plant Pathology* 106: 1311–1324. https://doi.org/10.1007/s42161-024-01686-0

Samson R.A., Visagie C.M., Houbraken J., Hong S.-B., Hubka V., … Frisvad J.C., 2014. Phylogeny, identification and nomenclature of the genus *Aspergillus*. *Studies in Mycology* 78: 141–173. https://doi.org/10.1016/j.simyco.2014.07.004

Vaidya G., Lohman D.J., Meier R., 2011. SequenceMatrix: Concatenation software for the fast assembly of multi-gene datasets with character set and codon information. *Cladistics* 27: 171–180. https://doi.org/10.1111/j.1096-0031.2010.00329.x

Vitale A., Cirvilleri G., Panebianco A., Epifani F., Perrone G., Polizzi G., 2012. Molecular characterisation and pathogenicity of *Aspergillus* Sect. Nigri causing Aspergillus vine canker of table grapes in Italy. *European Journal of Plant Pathology* 132: 483–487. https://doi.org/10.1007/s10658-011-9906-z

Wickham H., 2019. Modelr: Modelling functions that work with the pipe. https://rdrr.io/cran/modelr/man/modelr-package.html

Wong T.K., Ly-Trong N., Ren H., Demotte P., Baños H., ... Minh, B. Q., 2026. IQ-TREE 3: phylogenomic inference software using complex evolutionary models. *Molecular Biology and Evolution* 43: 1–6. https://doi.org/10.1093/molbev/msag117

Phytopathologia Mediterranea
The international journal of the
Mediterranean Phytopathological Union

Firenze University Press
www.fupress.com/pm

Research Papers

Two genetic groups of *Orobanche cumana* Wallr. in Moldova show contrasting regional affinities

Lidia DEL MORAL[1], Begoña PÉREZ-VICH[1], Steliana CLAPCO[2], Maria DUCA[2], Leonardo VELASCO[1,*], Angela PORT[2]

[1] *Institute for Sustainable Agriculture (IAS-CSIC), Córdoba, Spain*
[2] *Moldova State University, Chișinau, Republic of Moldova*
*Corresponding author. E-mail: lvelasco@ias.csic.es

Summary. Broomrape (*Orobanche cumana* Wallr.) is a parasitic plant of sunflower which is racially evolving and geographically expanding across most sunflower-growing regions. In the Republic of Moldova, broomrape has been present since 1937. Genetic diversity and structure of seven Moldovan broomrape populations, and reference populations from neighbouring Türkiye, Bulgaria, Romania and Serbia, were analysed using a set of 90 single nucleotide polymorphism (SNP) markers. Genetic diversity was moderate but highly variable among Moldovan populations, with appreciable unbiased expected heterozygosity and Shannon's index values in several populations. Observed heterozygosity was consistently low relative to expected heterozygosity, a pattern consistent with the predominantly selfing broomrape mating system. Population structure analyses, based on STRUCTURE, principal coordinates analysis (PCoA) and Neighbor-Joining clustering, consistently revealed the presence of two main genetic groups within Moldova. These groups had different affinities with populations from neighbouring countries, with genetic group G1 close to Romanian populations and genetic group G2 close to populations from Türkiye and Bulgaria, indicating a geographical component underlying the observed genetic differentiation. Analysis of molecular variance (AMOVA) indicated that most of the genetic variation was explained by differences among populations, confirming strong broomrape population structuring within Moldova.

Keywords. Genetic diversity, parasitic weed, SNP markers, virulence, population structure.

OPEN ACCESS

Citation: Del Moral, L., Pérez-Vich, B., Clapco, S., Duca, M., Velasco, L. & Port, A. (2026). Two genetic groups of *Orobanche cumana* Wallr. in Moldova show contrasting regional affinities. *Phytopathologia Mediterranea* 65(2): 333-342. doi: 10.36253/phyto-17407

Accepted: August 20, 2026

Published: September 10, 2026

© 2026 Author(s). This is an open access, peer-reviewed article published by Firenze University Press (https://www.fupress.com) and distributed, except where otherwise noted, under the terms of the CC BY 4.0 License for content and CC0 1.0 Universal for metadata.

Data Availability Statement: All relevant data are within the paper and its Supporting Information files.

Competing Interests: The Author(s) declare(s) no conflict of interest.

Editor: Maurizio Vurro, National Research Council, (CNR), Bari, Italy.

ORCID:
LDM: 0009-0005-7291-7234
BPV:0000-0002-7085-5173
SC:0000-0001-7147-2740
MD: 0000-0002-5855-5194
LV: 0000-0003-4998-9406
AP: 0000-0003-3994-8918

INTRODUCTION

Sunflower (*Helianthus annuus* L.) is an important oilseed crop, but its production is severely constrained by the root holoparasitic weed *Orobanche cumana* Wallr. The parasite has rapidly expanded its distribution in recent decades, particularly in Eastern Europe and the Mediterranean basin, where the intensification of sunflower cultivation has favoured emergence and spread of highly virulent populations able to overcome

resistance genes deployed in commercial sunflower hybrids (Cvejić *et al*., 2020).

Understanding the genetic structure and diversity of *O. cumana* populations is essential for interpreting evolutionary dynamics of the parasite, and its capacity to adapt to resistant sunflower genotypes. High levels of genetic diversity may enhance the adaptive potential of the species, facilitating occurrence of new virulence profiles, and breakdowns of host resistance. Although *O. cumana* is a predominantly self-pollinating species, several studies have reported substantial levels of cross-fertilization and gene flow between populations (Rodríguez-Ojeda *et al*., 2013a; Pineda-Martos *et al*., 2014). The existence of cross-fertilization, together with efficient seed dispersal that may lead to multiple introductions into particular areas (Nabloussi *et al*., 2023), and admixture of populations (Fernández-Melero *et al*., 2023), may contribute to increasing genetic diversity within populations, and to reduced geographic differentiation among populations compared with expectations for a predominantly autogamous species (Duca and Bivol, 2023).

Several studies have analysed population diversity of *O. cumana* using different types of molecular markers, including RAPD, ISSR, AFLP, SSR, and, more recently, SNPs (Gagne *et al*., 2000; Pineda Martos *et al*., 2013; Guchetl *et al*., 2014; Molinero-Ruiz *et al*., 2014; Martin-Sanz *et al*., 2016; Malek *et al*., 2017; Jebri *et al*., 2017; Ari *et al*., 2022; Duca and Bivol, 2023; Fernández-Melero *et al*., 2023; Nabloussi *et al*., 2023; Dedić *et al*., 2026). In the Black Sea basin, which is a main centre of *O. cumana* distribution, several studies have described the genetic relationships among populations from countries such as Bulgaria, Romania, Türkiye and Moldova. Analyses based on ISSR and SSR markers have generally shown substantial genetic differentiation among populations, although with weak geographic structuring and a tendency for Eastern European populations to share broadly related genetic backgrounds (Guchetl *et al*., 2014; Duca *et al*., 2019; Duca and Bivol, 2023; Duca *et al*., 2024).

Moldova is a relevant but still poorly characterised region for *O. cumana* population genetics. Previous studies evaluated Moldovan populations using limited numbers of ISSR or SSR markers (Duca *et al*., 2019; Duca *et al*., 2022; Duca and Bivol, 2023). Although these studies detected genetic differentiation among populations, they did not clearly resolve whether Moldovan populations shared one regional genetic background, or comprised differentiated genetic groups with distinct affinities to populations from neighbouring areas of the Black Sea region. Consequently, the internal subdivision of Moldovan populations and their regional genetic relationships remain only partially understood. The resolution of ISSR and SSR markers for detailed analyses of inter- and intrapopulation genetic diversity is limited and may be insufficient to detect fine scale population structure or recent divergence processes (Dossa *et al*., 2025). In contrast, single nucleotide polymorphism (SNP) markers provide increased resolution for detecting genetic variation, population structure, and admixture patterns (Morin *et al*., 2004; Helyar *et al*., 2011). Therefore, the use of a denser panel of locus-specific SNP markers may help to clarify the fine scale genetic structure of *O. cumana* populations within Moldova, and their affinities with populations from neighbouring regions.

The objectives of the present study were to determine whether *O. cumana* populations from the Republic of Moldova comprise differentiated genetic groups, and to examine their relationships with reference populations from neighbouring countries, using SNP markers.

MATERIALS AND METHODS

Sunflower broomrape populations

The study focused on seven Moldovan broomrape populations that were previously characterized using ISSR and SSR markers (Duca *et al*., 2022; Duca and Bivol, 2023). These populations were selected because archived DNA of sufficient quality was available for several individuals, whereas DNA from the remaining populations was too degraded for reliable SNP genotyping. The selected populations were from a broad geographical range within Moldova, although they should not be considered an exhaustive representation of the genetic diversity present in this country (Figure 1). They included: RM4 (Soroca), RM6 and RM7 (Bălți) in northern Moldova; RM12 (Căzănești) in the central part of the country; RM9 (Grigorievca) in south-eastern Moldova; and RM2 (Svetlii) and RM13 (Congaz) in southern Moldova.

The reference populations were selected to place the genetic variation observed in Moldova within a broader regional context. The assessments included most of the previously analysed Bulgarian (B2 to B4), Turkish (T1, T2, T3, T5), and Romanian (R1) populations, together with the Moldovan populations analysed by Duca and Bivol (2023), allowing direct comparison with the earlier ISSR-based study. Two additional previously characterized populations, and representatives of well-known gene pools, were also included as reference populations, including OCCS010 from Braila, Romania and OCCS009, from North Bačka County in Vojvodina, Serbia (Dedić *et al*., 2026). Selection was therefore based primarily on geographical relevance, continuity with previous studies, and available information on popula-

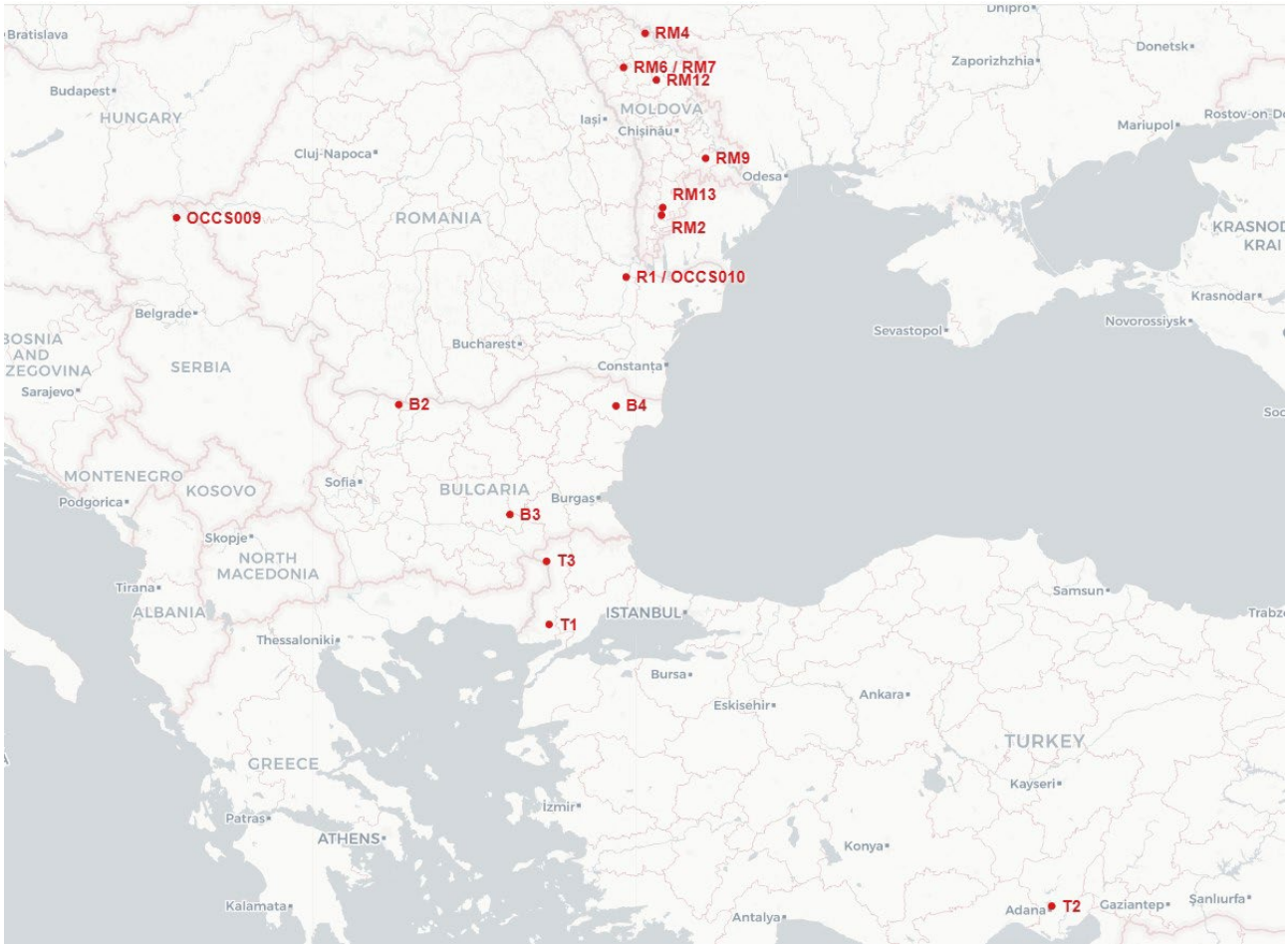

Figure 1. Geographic origins of the Moldovan and reference populations of *Orobanche cumana* analysed in this study. Population codes correspond to those used in the text and tables of this paper.

tion genetic relationships, rather than on virulence classification.

The numbers of individuals per population are provided in Table 1 for the Moldovan populations. For the reference populations, the numbers of individuals ranged from five in T3 to 14 in OCCS009 and OCCS010. Because the study was based on archived biological material, the numbers of successfully genotyped individuals were small and unequal among populations. Consequently, estimates of allele frequencies and intrapopulation diversity, particularly for populations represented by four to six individuals, should be interpreted cautiously.

Plant genotyping

DNA of individual plants, and in some cases SNP genotyping data, were available from the previous studies mentioned above. Genotyping of individual broomrape plants was carried out using 96 *O. cumana* SNP markers selected from the set reported and mapped by Calderón-González *et al.* (2019). After removing the markers with more than 10% missing data, the assessments were carried out with 90 SNP markers (Supplementary Table S1).

Genetic diversity and population structure analyses

Genetic diversity within populations was assessed using GenAlEx v.6.5 (Peakall and Smouse, 2012). For each population, intrapopulation diversity was described by estimating the percentage of polymorphic loci (P), observed heterozygosity (Ho), expected heterozygosity (He), unbiased expected heterozygosity (uHe), the fixation index (F), and Shannon's diversity index (I). Mean values and standard errors were calculated across loci. Because of the small and unequal

Table 1. Intrapopulation genetic diversity parameters of seven *Orobanche cumana* populations from Moldova, including the number of individuals analysed (N), percentage of polymorphic loci (P), observed heterozygosity (Ho), expected heterozygosity (He), unbiased expected heterozygosity (uHe), fixation index (F), and Shannon's diversity index (I).

Population	No.	P (%)	Ho (± SE)	He (± SE)	uHe (± SE)	F (± SE)	I (± SE)
RM2	6	66.67	0.11 ± 0.02	0.25 ± 0.02	0.27 ± 0.02	0.47 ± 0.05	0.37 ± 0.03
RM4	4	56.67	0.02 ± 0.01	0.23 ± 0.02	0.27 ± 0.03	0.94 ± 0.04	0.34 ± 0.03
RM6	9	74.44	0.09 ± 0.01	0.26 ± 0.02	0.27 ± 0.02	0.56 ± 0.05	0.38 ± 0.03
RM7	8	22.22	0.02 ± 0.01	0.03 ± 0.01	0.03 ± 0.01	0.09 ± 0.04	0.06 ± 0.01
RM9	10	58.89	0.01 ± 0.01	0.20 ± 0.02	0.21 ± 0.02	0.96 ± 0.03	0.30 ± 0.03
RM12	7	1.11	0.01 ± 0.01	0.01 ± 0.01	0.01 ± 0.01	—[a]	0.01 ± 0.01
RM13	5	56.67	0.00 ± 0.00	0.27 ± 0.03	0.29 ± 0.03	0.98 ± 0.02	0.37 ± 0.04

[a]The fixation index (F) was not reported for RM12, because it was based on a single polymorphic locus and was therefore not considered informative at population level.

population sample sizes, differences among population-level diversity estimates were interpreted descriptively, but were not subjected to formal significance tests. Nei's unbiased genetic distance was also computed between pairs of populations. The resulting distance matrix was used to construct a Neighbor-Joining (NJ) tree. The analysis was carried out using MEGA12 software (Kumar *et al*., 2024), with default parameters. The NJ tree was used to visualize patterns of genetic similarity among populations.

Population relationships were further explored by principal coordinates analysis (PCoA), carried out in GenAlEx v.6.5 using a matrix of pairwise codominant genotypic distances among individuals, and calculated across the 90 SNP loci. Graphical representation of PCoA results was produced using OriginPro 2023b (OriginLab Corporation).

Population structure was inferred with STRUCTURE v.2.3.4 (Pritchard *et al*., 2000), using an admixture model with correlated allele frequencies (Falush *et al*., 2003). The number of genetic clusters (K) tested ranged from 1 to 10, with ten independent runs performed for each K value. Each run consisted of 100,000 Markov chain Monte Carlo (MCMC) iterations, following a burn-in period of 10,000 iterations. The most likely number of clusters was determined using Structure Selector (https://lmme.ac.cn/StructureSelector/). Cluster alignments across runs were carried out with CLUMPP v.1.1.2b (Jakobsson and Rosenberg, 2007), using the FullSearch algorithm. Following the STRUCTURE analysis, individuals were assigned to clusters based on membership coefficients, and the two principal coordinates of PCoA were replotted, with the individuals from Moldova separated into those assigned to the genetic groups 1 (G1) and 2 (G2), based on more that 95% membership, and those admixed (A), having less than 95% membership to both genetic groups.

Analyses of molecular variance (AMOVA) were carried out using GenAlEx v.6.5 (Peakall and Smouse, 2012) to partition genetic variation among and within populations. This analysis was restricted to the Moldovan populations. Statistical significance of variance components were assessed using permutation tests implemented in the software.

RESULTS

Genetic diversity within Moldovan broomrape populations showed considerable variation among populations (Table 1). Percentages of polymorphic loci (P) ranged widely, from 1.11% in RM12 to 74.44% in RM6. Most populations exhibited moderate levels of polymorphism, with values greater than 50%, whereas RM7 (22.22%) and particularly RM12 (1.11%) showed low polymorphism. Observed heterozygosity (Ho) was consistently low across all the populations, ranging from 0.00 in RM13 to 0.11 in RM2. Expected heterozygosity (He) and unbiased expected heterozygosity (uHe) followed similar patterns. RM7 and RM12 had very low uHe values of, respectively, 0.03 and 0.01, consistent with their low P values, while the remaining populations had values between 0.21 and 0.29 (Table 1). The fixation index (F) was positive in all populations for which it had been reported, ranging from 0.09 in RM7 to 0.98 in RM13. Particularly high values were observed in RM4 (0.94), RM9 (0.96) and RM13 (0.98), indicating marked deficits of heterozygotes. Shannon's diversity indices (I) followed a similar pattern to the expected heterozygosity, with the lowest values in RM12 (I = 0.01) and RM7 (I = 0.03), while the remaining populations had values ranging from 0.30 to 0.38.

Analysis of molecular variance (AMOVA) showed that most of the genetic variation was explained by dif-

Table 2. Analysis of molecular variance (AMOVA) for *Orobanche cumana* populations from Moldova, based on SNP markers, showing the partitioning of genetic variation among populations, among individuals within populations, and within individuals.

Source	df	SS	MS	Estimated Variance	%
Among Populations	6	971.753	161.959	10.508	53
Among Individuals	42	707.696	16.850	7.547	38
Within Individuals	49	86.000	1.755	1.755	9
Total	97	1765.449		19.810	100

ferences among populations (53%), followed by variation among individuals within populations (38%), whereas variation within individuals was low (9%) (Table 2).

Figure 2 shows the biplots of the three principal coordinates obtained from the PCoA. The first three principal coordinates accounted for 53.5% of the total genetic variation (respectively, 23.6, 18.6 and 11.3%). Therefore, the biplots provide a partial representation of the multilocus variation, and were interpreted together with the STRUCTURE, Neighbor-Joining, and AMOVA results. In the plot of PCo1 *vs.* PCo2, some Moldovan individuals were located close to individuals from Romania, whereas the remaining individuals were positioned close to those from Türkiye and Bulgaria. A similar pattern was observed in the PCo1 *vs.* PCo3 plot. The plot of PCo2 *vs.* PCo3 did not provide additional information.

STRUCTURE analyses identified two main genetic groups (G1 and G2) within the Moldovan broomrape populations. The ΔK statistic showed a pronounced maximum at K = 2, providing strong support for this subdivision, whereas the secondary peak at K = 5 was considerably smaller (Figure 3). Most populations showed predominant assignment to one of the two groups, although admixed individuals were detected in several cases (Table 3). Populations RM2, RM4, RM7 and RM13 were mainly associated with G1, showing high mean membership coefficients and considerable proportions of individuals with assignment values above 95%. In contrast, RM9 and RM12 were clearly assigned to G2, with most individuals showing high membership to this group. Population RM6 displayed a more heterogeneous pattern, with individuals assigned to both groups, and a relatively high proportion of admixed genotypes. The Neighbor-Joining tree based on Nei's genetic distance (Figure 4) supported the genetic structure inferred by STRUCTURE. The Moldovan populations were separated into two main clusters, largely consistent with their assignment to G1 and G2. Populations associated with G1 tended to cluster together, and showed close relationships with reference populations from Romania (R1 and OCCS010), whereas those associated

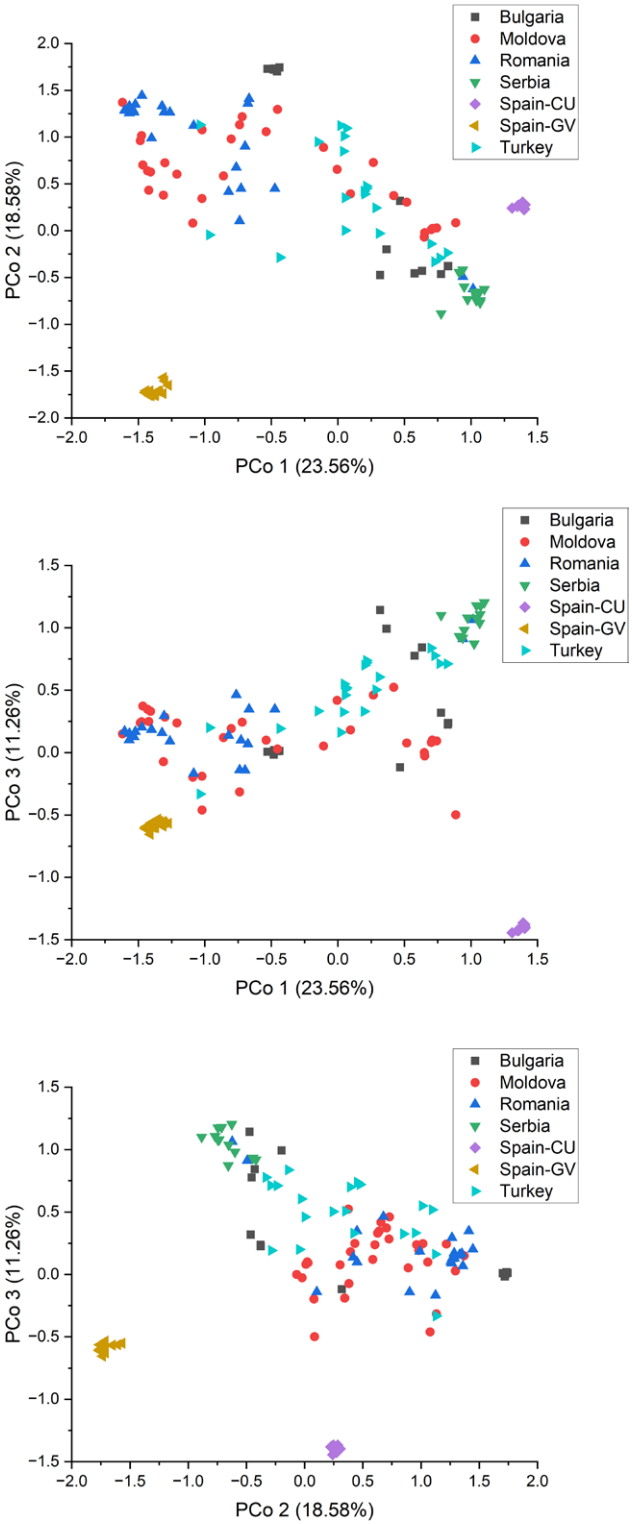

Figure 2. Principal coordinates analysis of 49 *Orobanche cumana* individuals from seven populations from the Republic of Moldova, together with 147 individuals from Bulgaria, Türkiye, Romania and Serbia used as references. Biplots with axes one and two, one and three, and two and three are shown. The percentage of variation explained by each principal coordinate is indicated in the axis titles.

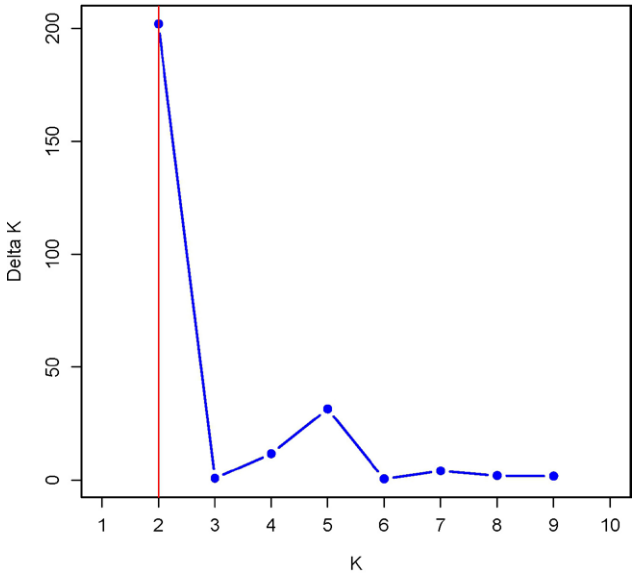

Figure 3. Delta K for values of K in the analysis of genetic structure of the *Orobanche cumana* populations from Moldova evaluated in this study.

Table 3. Genetic structures of sunflower broomrape populations from Moldova, showing the mean membership coefficients (q) in genetic groups G1 and G2, the number of individuals assigned to each group, and the number of admixed individuals. Individuals with q > 0.95 for either group were assigned to that group, whereas those with q ≤ 0.95 for both groups were classified as admixed.

Population	Mean q, G1	Mean q, G2	G1 (n)	G2 (n)	Admixed
RM2	0.82	0.18	2	0	4
RM4	0.87	0.13	2	0	2
RM6	0.63	0.37	4	1	4
RM7	0.98	0.02	7	0	1
RM9	0.07	0.93	0	8	2
RM12	0.00	1.00	0	7	0
RM13	0.85	0.15	3	0	2

with G2 were more closely related to populations from Türkiye (T1–T3, and T5), Bulgaria (B2–B4), and Serbia (OCCS009).

Figure 5 shows the PCoA (axes 1 and 2), replotted according to the STRUCTURE-based classification of Moldovan individuals. A clear correspondence was apparent between the distance-based PCoA and STRUCTURE analysis, with individuals assigned to each genetic group generally located at opposite extremes of the distribution of Moldovan samples, and admixed individuals occupying intermediate positions.

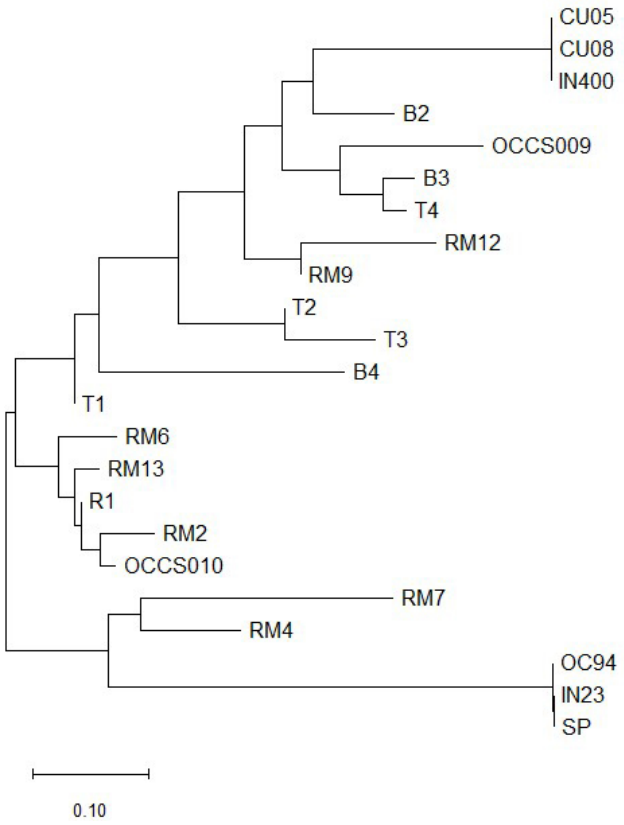

Figure 4. Neighbor-Joining (NJ) tree showing genetic relationships among *Orobanche cumana* populations based on Nei's unbiased genetic distance. The tree illustrates the genetic similarity among populations from Moldova and with reference populations from other countries. The scale bar represents genetic distance.

DISCUSSION

The present study has shown that the Moldovan broomrape populations analysed did not constitute a single homogeneous regional genetic background, but comprised at least two differentiated groups with contrasting affinities within the Black Sea region. This pattern was consistently supported by STRUCTURE, PCoA, and distance-based clustering analyses, indicating that the observed structure was robust across different analytical approaches, and has consistent biological relevance. Nevertheless, because only seven populations and a limited number of individuals were available, extrapolation of this pattern to the full diversity of *O. cumana* in Moldova requires caution.

Previous studies have also reported the existence of two differentiated *O. cumana* gene pools at country levels. This was the case, for example, of countries outside the main centre of distribution of the parasite, such as in Spain (Pineda-Martos *et al.*, 2013) and Morocco

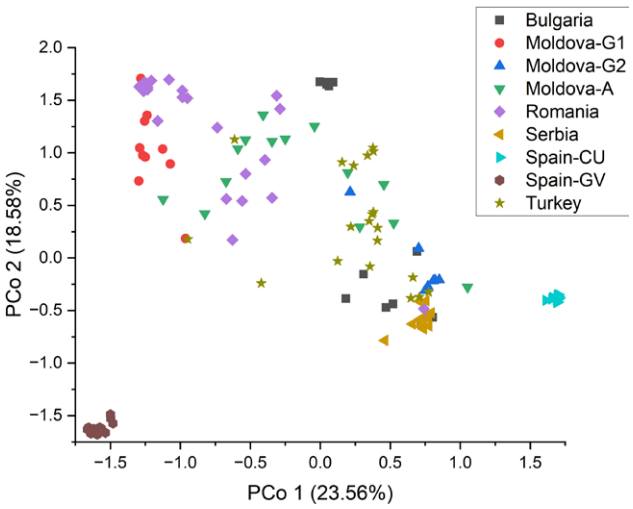

Figure 5. Principal coordinates plot (PCo 1 vs. PCo 2) of 49 *Orobanche cumana* individuals from seven populations from the Republic of Moldova, separated into those assigned to the genetic groups 1 (G1) and 2 (G2), based on more that 95% membership, and those admixed (A), having less than 95% membership to both genetic groups, together with 147 individuals used as references, from Bulgaria, Türkiye, Romania and Serbia. The percentage of variation explained by each principal coordinate is indicated in the axis titles.

(Nabloussi *et al*., 2023). However, in both of these countries, absence of genetic diversity within populations pointed to separate introductions followed by founder effects, rather than to local evolutionary processes of broomrape populations (Pineda-Martos *et al*., 2013; Nabloussi *et al*., 2023). In contrast, Dedić *et al.* (2026) identified two contrasting genetic groups in Serbia, associated with separate evolutionary histories and probably different introduction events. The pattern observed in Moldova in the present study is probably consistent with different introductions, as the two identified genetic groups have affinities with populations from neighbouring countries, Romania for genetic group G1, and Türkiye and Bulgaria for genetic group G2. This indicates that the differentiation observed in Moldovan populations may reflect historical processes of diversification and gene flow within the Black Sea region.

The contrasting affinities of G1 and G2 are compatible with the contribution of at least two historical regional sources for the present Moldovan populations. The relationship of G1 with Romanian populations may reflect connections with the Lower Danube region, whereas the affinities of G2 with Bulgarian and Turkish populations point to genetic connections with the western and southern sectors of the Black Sea basin. Movement of the very small broomrape seeds through contaminated host seed lots, in soil transported by agricultural machinery, or from other agricultural exchanges, could have contributed to these regional connections, followed by local multiplication and differentiation under predominant self-pollination. Nevertheless, the present set of reference populations is insufficient to establish direction or timing of broomrape dispersal.

AMOVA results showed that most of the genetic variation was explained by differences among populations (53%), providing quantitative support for strong population structuring in sunflower broomrape populations from Moldova. Previous studies based on ISSR and SSR markers that included some of the Moldovan populations analysed here, together with populations from other countries, also showed strong genetic structuring in *O. cumana* populations (Duca *et al*., 2022; Duca and Bivol, 2023). However, in those studies AMOVA was conducted on broader datasets than assessed in the present study, including populations from Romania, Türkiye, Serbia, Bulgaria and China, with the variance partitioned among countries, among populations within countries, and within populations. Therefore, the results are not directly comparable with those from the present study. Nevertheless, the present results demonstrate that strong population structuring is already evident when considering Moldovan populations alone. AMOVA has rarely been used to partition genetic variation among and within populations of *O. cumana* at country or regional levels. In a study based on *O. cumana* populations growing on wild hosts in the Black Sea region of Bulgaria, Pineda-Martos *et al.* (2014) reported 59.5% of variance among populations and 40.5% within populations, values consistent with those obtained in the present study. Other studies have applied AMOVA mainly to compare gene pools (Guchetl *et al*., 2014), or to assess genetic variation among countries and regions (Molinero-Ruiz *et al*., 2014).

The predominance of among-population variation is biologically consistent with the mating system of *O. cumana*. Predominant self-pollination reduces effective gene flow and recombination among local populations, favours the maintenance of homozygous genotypes, and allows genetic drift and founder effects to generate marked differentiation among geographically separated populations (Nybom, 2004). The consistently low observed heterozygosity and the small within individual component of AMOVA support this interpretation. Local selection imposed by the sunflower genotypes cultivated in each area could further contribute to differentiation, if populations have been exposed to different resistance genes (Pérez-Vich *et al*., 2013). However, information on the historical composition of sunflower cultivars at the collection

sites assessed in the present study was not available, and the relative contribution of host-mediated selection cannot here be separated from demographic processes.

The two *O. cumana* genetic groups identified in this study should not be interpreted as distinct virulence groups. According to previously reported race classifications, G1 includes populations classified as race H (RM2, RM4, RM6 and RM7) and race E (RM13), whereas G2 includes one race H population (RM9) and one race E population (RM12) (Duca and Bivol, 2023). Therefore, the available information does not indicate that virulence is simply associated with the genetic groups revealed by the SNP analysis. This is biologically plausible, because virulence may be determined by variation at one or a few avirulence loci, and may therefore differ among populations that otherwise share similar overall genetic backgrounds (Rodríguez-Ojeda *et al.*, 2013b; Fernández-Melero *et al.*, 2023).

The overall level of genetic diversity observed within Moldovan *O. cumana* populations was moderate, but was highly variable among populations. Observed heterozygosity was consistently low compared to expected heterozygosity, and the positive fixation index recorded in all populations for which these indices were reported (Table 1) indicated a marked deficit of heterozygotes. This pattern is consistent with the predominantly self-pollinating mating system of *O. cumana* (Rodríguez-Ojeda *et al.*, 2013a), and with the low intrapopulation variability and strong genetic differentiation among populations previously reported for the species (Gagne *et al.*, 1998). The presence of populations with very low diversity, such as RM12 and to a lesser extent in RM7, may reflect founder effects or recent bottlenecks (Cvejić *et al.*, 2020).

The results of the present study provide additional insights compared with previous research in the region. Duca *et al.* (2022) and Duca and Bivol (2023), using SSR and ISSR markers on a set of populations that included those analysed in the present study, also detected substantial genetic structuring among *O. cumana* populations from Moldova and other countries. However, the increased resolution provided by SNP markers in the present study allowed a clearer identification of two differentiated genetic groups within Moldovan populations. While SSR and ISSR markers are useful for detecting overall genetic variability and population differentiation, their capacity to resolve fine scale genetic structure is limited (Özbek, 2024). Despite the reduced number of populations and individuals analysed compared with the previous studies, the use of SNP markers allowed clear resolution of genetic structure. This indicates that marker resolution may be more important than sample size for detecting fine scale population structures, although both aspects remain important. Low sampling intensity may limit detection of low frequency variants, and therefore the present results should be interpreted within this context.

The SNP panel used in this study also provided a baseline for future molecular surveillance of *O. cumana* in the Black Sea region. Comparison of newly collected populations with the G1 and G2 reference profiles could help to identify new introductions, monitor changes in admixtures, and allow tracing of regional spread of emerging populations. Molecular surveillance should be combined with standardized virulence phenotyping to assess race composition of new populations. Integration of both types of information could support selection of populations for resistance screening, early detection of changes in virulence, and coordinated regional deployment and diversification of host resistance sources.

CONCLUSIONS

Combined evidence from diversity indices, AMOVA, STRUCTURE, PCoA and distance-based analyses indicates that the studied Moldovan populations of *O. cumana* comprise at least two genetic groups with distinct regional affinities: G1 with Romanian populations, and G2 with Bulgarian and Turkish populations. These results provide a genetic baseline for monitoring the regional dispersal and admixture of sunflower broomrape populations in Moldova. Integration of SNP-based surveillance with standardized virulence phenotyping may contribute to early detection of emerging populations, and to allow informed regional deployment of resistant sunflower hybrids.

FUNDING

This study was supported by subprogram 011101 Genetic and biotechnological approaches to the management of agroecosystems in the conditions of climate change, State Program 20.80009.5107.01, Genetic-molecular and biotechnological studies of the sunflower in the context of sustainable management of agricultural ecosystems, funded by the Ministry of Education and Research, Republic of Moldova. Funding was also provided by Consejería de Transformación Económica, Industria, Conocimiento y Universidades, Junta de Andalucía, Spain, and EU FEDER, grant number QUAL21_023 IAS.

LITERATURE CITED

Ari T., Demirbaş S., Bilgen B.B., 2022. Assessment of the genetic structure and diversity of *Orobanche cumana* populations from Türkiye using simple sequence repeat markers. *International Journal of Innovative Approaches in Agricultural Research* 6: 303–317. https://doi.org/10.29329/ijiaar.2022.506.2.

Calderón-González, A., Pouilly N., Muños S., Grand X., Coque M., Velasco L., Pérez-Vich B., 2019. A SSR-SNP linkage map of the parasitic weed *Orobanche cumana* Wallr. including a gene for plant pigmentation. *Frontiers in Plant Science* 10: 797. https://doi.org/10.3389/fpls.2019.00797.

Cvejić S., Radanović A., Dedić B., Jocković M., Jocić S., Miladinović D., 2020. Genetic and genomic tools in sunflower breeding for broomrape resistance. *Genes* 11: 152. https://doi.org/10.3390/genes11020152.

Dedić B., Martin-Sanz A., Sayago A., Pérez-Vich B., Velasco L., Cvejić S., 2026. Population genetics and virulence patterns of sunflower broomrape populations from Serbia. *Weed Research* 66: e70072. https://doi.org/10.1111/wre.70072.

Dossa A.F., Tchokponhoué D.A., Houdegbe A.C., Achigan-Dako E.G., 2025. SNP markers revealed the genetic diversity and population structure of *Mesosphaerum suaveolens* (L.) Kuntze Syn. *Hyptis suaveolens* (L.) Poit accessions collected in Benin. *PLoS One* 20(9): e0331702. https://doi.org/10.1371/journal.pone.0331702.

Duca M., Joiţa-Păcureanu M., Port A., Martea R., Boicu A., Rîşnoveanu L., Clapco S., 2019. Genetic diversity analysis of sunflower broomrape populations from Republic of Moldova using ISSR markers. *Romanian Agricultural Research* 37: 3–11.

Duca M., Bivol I., 2023. Genetic diversity of broomrape (*Orobanche cumana* Wallr.) populations from different geographical origins assessed by ISSR markers. *Helia* 79: 187–200. https://doi.org/10.1515/helia-2023-0014.

Duca M., Bivol I., Mutu A., Port A., Clapco S., 2024. Genetic relationships between broomrape populations from different countries using ISSR markers. *Notulae Botanicae Horti Agrobotanici Cluj-Napoca* 52(1): 13590. https://doi.org/10.15835/nbha52113590.

Duca M., Clapco S., Mutu A., Bivol I., 2022. Analysis of genetic variability in some broomrape populations with different geographical origin. *Bulletin of the Academy of Sciences of Moldova. Life Sciences* 2(346): 39–47. https://doi.org/10.52388/1857-064X.2022.2.04.

Falush D., Stephens M., Pritchard J.K., 2003. Inference of population structure using multilocus genotype data: linked loci and correlated allele frequencies. *Genetics* 164: 1567–1587. https://doi.org/10.1093/genetics/164.4.1567.

Fernández-Melero B., Martín-Sanz A, Del Moral L, Pérez-Vich B, Velasco L., 2023. A novel sunflower broomrape race with unusual virulence potentially caused by a mutation. *Frontiers in Plant Science* 14: 1236511. https://doi.org/10.3389/fpls.2023.1236511.

Gagne G., Roeckel-Drevet P., Grezes-Besset B., Shindrova P., Ivanov P., Grand-Ravel C., Vear F., Tourvieille de Labrouhe D., Charmet G., Nicolas P., 1998. Study of the variability and evolution of *Orobanche cumana* populations infesting sunflower in different European countries. *Theoretical and Applied Genetics* 96: 1216–1222. https://doi.org/10.1007/s001220050859.

Gagne G., Roeckel-Drevet P., Grezes-Besset B., Shindrova P., Ivanov P., Grand-Ravel C., Vear F., Charmet G., Nicolas P., 2000. Amplified fragment length polymorphism (AFLP) as suitable markers to study *Orobanche cumana* genetic diversity. *Journal of Phytopathology* 148: 457–459. https://doi.org/10.1046/j.1439-0434.2000.00528.x.

Guchetl S., Antonova T.S., Tchelustnikova T., 2014. Genetic similarity and differences between the *Orobanche cumana* Wallr. populations from Russia, Kazakhstan, and Romania revealed using the markers of Simple Sequence Repeat. *Russian Agricultural Sciences* 40: 326–330. https://doi.org/10.3103/S1068367414050103.

Helyar S.J., Hemmer-Hansen J., Bekkevold D., Taylor M.I., Ogden R., Limborg M.T., Cariani A., Maes G.E., Diopere E., Carvalho G.R., Nielsen E.E., 2011. Application of SNPs for population genetics of non-model organisms: new opportunities and challenges. *Molecular Ecology Resources* 11 (Suppl 1): 123–136. https://doi.org/10.1111/j.1755-0998.2010.02943.x.

Jakobsson M., Rosenberg N.A., 2007. CLUMPP: A cluster matching and permutation program for dealing with label switching and multimodality in analysis of population structure. *Bioinformatics* 23: 1801–1806. https://doi.org/10.1093/bioinformatics/btm233.

Jebri M., Ben Khalifa M., Fakhfakh H., Pérez-Vich B., Velasco L., 2017. Genetic diversity and race composition of sunflower broomrape populations from Tunisia. *Phytopathologia Mediterranea* 56: 421–430. https://doi.org/10.14601/Phytopathol_Mediterr-20839.

Kumar S., Stecher G., Suleski M., Sanderford M., Sharma S., Tamura K., 2024. MEGA12: Molecular Evolutionary Genetic Analysis version 12 for adaptive and

green computing. *Molecular Biology and Evolution* 41 (12): msae263. https://doi.org/10.1093/molbev/msae263.

Malek J., Del Moral L., Fernández-Escobar J., Pérez-Vich B., Velasco L., 2017. Racial characterization and genetic diversity of sunflower broomrape populations from Northern Spain. *Phytopathologia Mediterranea* 56, 70–76. https://doi.org/10.14601/Phytopathol_Mediterr-19163.

Martín-Sanz A., Malek J., Fernández-Martínez J.M., Pérez-Vich B., Velasco L., 2016. Increased virulence in sunflower broomrape (*Orobanche cumana* Wallr.) populations from Southern Spain is associated with greater genetic diversity. *Frontiers in Plant Science* 7: 589. https://doi.org/10.3389/fpls.2016.00589.

Molinero-Ruiz M.L., García-Carneros A.B., Collado-Romero M., Raranciuc S., Domínguez J., Melero-Vara J.M., 2014. Pathogenic and molecular diversity in highly virulent populations of the parasitic weed *Orobanche cumana* from Europe. *Weed Research* 54: 87–96. https://doi.org/10.1111/wre.12056.

Morin P., Luikart G., Wayne R.K., 2004. SNPs in ecology, evolution and conservation. *Trends in Ecology & Evolution*, 19: 208–216. https://doi.org/10.1016/j.tree.2004.01.009.

Nabloussi A., Pérez-Vich B., Velasco L., 2023. Virulence, genetic diversity, and putative geographical origin of sunflower broomrape populations from Morocco. *Phytopathologia Mediterranea* 62: 65–72. https://doi.org/10.36253/phyto-13948.

Nybom H., 2004. Comparison of different nuclear DNA markers for estimating intraspecific genetic diversity in plants. *Molecular Ecology* 13: 1143–1155. https://doi.org/10.1111/j.1365-294X.2004.02141.x.

Özbek Ö., 2024. Molecular markers used to reveal genetic diversity and phylogenetic relationships in crop plants. *OBM Genetics* 8: 274. https://doi.org/10.21926/obm.genet.2404274.

Peakall R., Smouse, P.E., 2012. GenAlEx 6.5: genetic analysis in Excel. Population genetic software for teaching and research-an update. *Bioinformatics* 28: 2537–2539. https://doi.org/10.1093/bioinformatics/bts460.

Pérez-Vich B., Velasco L., Rich P.J., Ejeta G., 2013. Marker-assisted and physiology-based breeding for resistance to root parasitic Orobanchaceae. In: Parasitic Orobanchaceae: Parasitic Mechanisms and Control Strategies (D.M. Joel, J. Gressel, L.J. Musselman, ed.), Springer, Berlin, Heidelberg, Germany, 369–391. https://doi.org/10.1007/978-3-642-38146-1_21.

Pineda-Martos R., Velasco L., Fernández-Escobar J., Fernández-Martínez J.M., Pérez-Vich B., 2013. Genetic diversity of *Orobanche cumana* populations from Spain. *Weed Research* 53: 279–289. https://doi.org/10.1111/wre.12022.

Pineda-Martos R., Pujadas-Salvà A.J., Fernández-Martínez J.M., Stoyanov K., Velasco L., Pérez-Vich B., 2014. The genetic structure of wild *Orobanche cumana* Wallr. (Orobanchaceae) populations in Eastern Bulgaria reflects introgressions from weedy populations. *The Scientific World Journal* 150432. https://doi.org/10.1155/2014/150432.

Pritchard J.K., Stephens M., Donnelly P., 2000. Inference of population structure using multilocus genotype data. *Genetics* 155: 945–959. https://doi.org/10.1093/genetics/155.2.945.

Rodríguez-Ojeda M.I., Fernández-Martínez J.M., Velasco L., Pérez-Vich B., 2013a. Extent of cross-fertilization in *Orobanche cumana* Wallr. *Biologia Plantarum* 57: 559–562. https://doi.org/10.1007/s10535-012-0301-1.

Rodríguez-Ojeda, M.I., Pineda-Martos R., Alonso L.C., Fernández-Escobar J., Fernández-Martínez J.M., Pérez-Vich B., Velasco L., 2013b. A dominant avirulence gene in *Orobanche cumana* triggers *Or5* resistance in sunflower. *Weed Research* 53: 322-327. https://doi.org/10.1111/wre.12034.

Phytopathologia Mediterranea
The international journal of the
Mediterranean Phytopathological Union

Firenze University Press
www.fupress.com/pm

Research Papers

Genetic diversity and pathogenicity of *Fusarium* and *Neocosmospora* associated with cultivated and wild *Asparagus officinalis* in The Netherlands

Marcelo SANDOVAL-DENIS[1,*], Mark ZWART[2], Roel BROUWER[1], Johannes Z. GROENEWALD[1], Wilfried JONKERS[3], Diana KATSCHNIG[3], Wietse DE BOER[2], Paolina GARBEVA[2], Pedro W. CROUS[1]

[1] *Westerdijk Fungal Biodiversity Institute, Uppsalalaan 8, 3584 CT, Utrecht, The Netherlands*
[2] *Netherlands Institute of Ecology (NIOO-KNAW), 6708 PB, Wageningen, The Netherlands*
[3] *Bejo Zaden B.V., 1749 CZ, Warmenhuizen, The Netherlands*
*Corresponding author. E-mail: m.sandoval@wi.knaw.nl

Summary. Fusarium crown and root rot is one of the main threats to asparagus production worldwide. The aetiology of the disease, attributed to several species of *Fusarium* and *Neocosmospora*, has not been re-evaluated in the context of recent advances in *Fusarium* taxonomy, and relevant studies in The Netherlands are scarce and outdated. *Asparagus officinalis* plants and associated soil samples were assessed from 38 cultivated fields and one location where this plant naturally occurs in The Netherlands. A total of 164 specimens were obtained yielding 551 fungal strains. Fungal identification according to DNA sequencing and phylogenetic analyses based on fragments of the translation elongation factor 1-alpha (*tef1*) and the DNA-directed RNA polymerase II second largest subunit (*rpb2*) showed that these isolates belonged to 20 taxa (*Fusarium acuminatum*, *F. annulatum*, *F. avenaceum*, *F. carminascens*, *F. celtidicola*, *F. clavus*, *F. cugenangense*, *F. culmorum*, *F. equiseti*, *F. flagelliforme*, *F. flocciferum*, *F. inflexum*, *F. nirenbergiae*, *F. odoratissimum*, *F. oxysporum*, *F. redolens*, *F. vanleeuwenii*, *Neocosmospora geoasparagicola*, *N. solani* and *N. stercicola*), of which 11 species (*Fusarium avenaceum*, *F. carminascens*, *F. celtidicola*, *F. clavus*, *F. cugenangense*, *F. flagelliforme*, *F. flocciferum*, *F. inflexum*, *F. odoratissimum*, *F. vanleeuwenii* and *N. stercicola*) are first reports on *A. officinalis*. These results, and testing of Koch's postulates on *A. officinallis* plantlets, showed that *F. annulatum*, *F. culmorum*, *F. redolens*, *F. nirenbergiae* and *N. solani* were the most prevalent and aggressive species. In contrast, although *F. oxysporum* is pathogenic to *A. officinalis*, it was among the least prevalent species encountered in this study.

Keywords. *Asparagaceae*, fungal diversity, fusarioid, pathogens, phylogeny.

OPEN ACCESS

Citation: Sandoval-Denis, M., Zwart, M., Brouwer, R., Groenewald, J. Z., Jonkers, W., Katschnig, D., De Boer, W., Garbeva, P. & Crous, P. W. (2026). Genetic diversity and pathogenicity of *Fusarium* and *Neocosmospora* associated with cultivated and wild *Asparagus officinalis* in The Netherlands. *Phytopathologia Mediterranea* 65(2): 343-358. doi: 10.36253/phyto-17513

Accepted: August 30 2026

Published: September 10, 2026

© 2026 Author(s). This is an open access, peer-reviewed article published by Firenze University Press (https://www.fupress.com) and distributed, except where otherwise noted, under the terms of the CC BY 4.0 License for content and CC0 1.0 Universal for metadata.

Data Availability Statement: All relevant data are within the paper and its Supporting Information files.

Competing Interests: The Author(s) declare(s) no conflict of interest.

Editor: Lizel Mostert, Faculty of AgriSciences, Stellenbosch, South Africa.

ORCID:
MS-D: 0000-0001-6832-0252
MZ: 0000-0003-4361-7636
JZG: 0000-0002-9474-6246
WJ: 0000-0002-4154-5475
WdB: 0000-0002-5380-2993
PG: 0000-0002-2359-5719
PWC: 0000-0001-9085-8825

INTRODUCTION

Asparagus officinalis has historically been cultivated in The Netherlands, and at present remains an economically significant crop. Primarily grown as a cash crop in the southern-most provinces of Limburg and Noord-Brabant (CBS, 2025), wild plants also occur in sandy and loamy soil on the dunes of South and North Holland and Zeeland provinces. Dutch asparagus production has fluctuated between 13.3 to 17.5 million kg p. a. over the past 11 years, and at its lowest production in 2024 (CBS, 2025). Currently, both world market value and production of asparagus are increasing, and despite a decline in Dutch cultivation, most of the country's local asparagus production is still destined for external markets. Almost 60% of the total 14.5 million kg produced in 2023 was exported, valued at US$68.22 million (CBS, 2025; World Integrated Trade Solution, 2025).

Fusarium crown and root rot pose a significant threat to asparagus production, both in The Netherlands and elsewhere. The disease is caused by diverse species of *Fusarium* or related fusarioid taxa, and is characterized by vascular discolourations with typical red-brown elliptical lesions affecting asparagus root systems, and sometimes extending to the crowns. Asparagus plants can be infected through various routes, including root, root tip, or stem wounds, and insect transmission, such as by the asparagus miner (*Ophiomyia simplex*, *Agromyzidae*, *Diptera*) (Elmer, 2015), while seed contamination can occur during harvesting when seeds are washed with water contaminated with diseased host tissues (Block and Bollen, 1995). Plants can be affected at any growth stage, although disease symptoms are more commonly observed in established fields (Elmer *et al*., 1997; Elmer, 2015). The disease leads to stunted ferns with a gradual decline in productivity, and plants show progressive yellow discolourations, followed by necroses and stem death (Elmer, 2015; Aegerter *et al.,* 2016). Due to a lack of effective countermeasures, preventive measures are the only available option for disease management. However, finding pathogen-free substrates for asparagus cultivation is challenging due to the biology of the fungal pathogens, being able to persist in the soil for decades by producing highly resistant and resilient propagules (Block and Bollen, 1995). Wind-blown pathogen infested soil, rain splash, soil movement and contamination of tools and machinery can easily spread the disease and compromise neighbouring fields or glasshouses (Block and Bollen, 1995). Presence of the fungi in seeds and crowns can also spread the disease to distant localities (Corpas-Hervias *et al*., 2006; Elmer, 2015).

Fungal species traditionally associated with fusarium root rot of asparagus include *Fusarium acuminatum*, *F. annulatum*, *F. oxysporum* (*F. oxysporum* f. sp. *asparagi*), and *F. redolens* (*F. redolens* f. sp. *asparagi*), with *F. redolens* also commonly associated with spear rot, and *Neocosmospora solani* (*F. solani*); while *F. culmorum* often causes stem base and crown rot (Van Bakel and Krom-Kerstens, 1974; Baayen *et al*., 2000; Corpas-Hervias *et al*., 2006; Borrego-Benjumea *et al*., 2014; Elmer, 2015). All these species are soil-borne, cosmopolitan, and plant pathogenic, and are known to occur in The Netherlands. However, not all these species have been associated with asparagus disease in this country.

Recent advances in the taxonomy of *Fusarium* and related taxa, particularly in *F. oxysporum* and *Neocosmospora*, suggest that a larger number of pathogenic species could be involved as asparagus pathogens (Lombard *et al*., 2019; Sandoval-Denis *et al*., 2019; Crous *et al*., 2022). This is due to the known genotype diversity of relevant *formae speciales* (Baayen *et al*., 2000; Corpas-Hervias *et al*., 2006; Elmer, 2015).

This present study aimed to identify and report fusarioid fungal species associated with root-rot of cultivated and wild *A. officinalis* in The Netherlands, and to determine the ability of these fungi to cause disease under controlled laboratory conditions.

MATERIALS AND METHODS

Specimen collection

Asparagus plants and adjacent soil samples were collected from 38 asparagus fields in Limburg, The Netherlands. Wild asparagus plants, soils and rhizosphere samples were also collected from the Berkheide dune area, Hollandse Duinen National Park, Wassenaar, South Holland (Table 1). Additionally, 123 fusarioid isolates were obtained from working collections of two laboratories belonging to Bejo Zaden B.V. (Warmenhuizen, The Netherlands). These isolates were from numerous *Asparagus* spp. tissues, including 44 isolates originating from *Asparagus* spp. seeds (Supplementary Table S1). Plant material and soils were deposited in sterile plastic bags and maintained at 10 °C until processing.

Fungal isolations

Plant material was washed thoroughly under running tap water to remove any soil remnants. Different plant tissues (*i.e*., crowns, roots, or stems) were processed independently. Seeds and fragments (ca. 5 × 5

Table 1. Origins and characteristics of sampled *Asparagus officinalis* plants.

Plant	Location	Variety	Plant age (years)	Origin of the variety
1	Limburg, Kessel	Backlim	3	Netherlands, Limseeds B.V.
2	Limburg, Kessel	Backlim	3	Netherlands, Limseeds B.V.
3	Limburg, Kessel	Grolim	3	Netherlands, Limseeds B.V.
4	Limburg, Kessel	Grolim	3	Netherlands, Limseeds B.V.
5	Limburg, Kessel	Grolim	3	Netherlands, Limseeds B.V.
6	Limburg, Kessel	Canticus	3	Netherlands, Bejo Zaden B.V.
7	Limburg, Kessel	Cumulus	3	Netherlands, Bejo Zaden B.V.
8	Limburg, Kessel	Cygnus	3	Netherlands, Bejo Zaden B.V.
9	Limburg, Kessel	Gynlim	3	Netherlands, Limseeds B.V.
10	Limburg, Kessel	Inbred breeding cross	3	Netherlands, Bejo Zaden B.V.
11	Limburg, Kessel	Inbred breeding cross	3	Netherlands, Bejo Zaden B.V.
12	Limburg, Kessel	Inbred breeding cross	3	Netherlands, Bejo Zaden B.V.
13	Limburg, Kessel	Grolim	3	Netherlands, Limseeds B.V.
14	Limburg, Kessel	Guelph Millenium	3	Canada, University of Guelph
15	Limburg, Kessel	Herkolim	3	Netherlands, Limseeds B.V.
16	Limburg, Kessel	Inbred breeding cross	3	Netherlands, Bejo Zaden B.V.
17	Limburg, Kessel	Inbred breeding cross	3	Netherlands, Bejo Zaden B.V.
18	Limburg, Kessel	Inbred breeding cross	2	Netherlands, Bejo Zaden B.V.
19	Limburg, Kessel	Prius	2	Netherlands, Bejo Zaden B.V.
20	Limburg, Kessel	Roem van Brunswijk	2	Germany
21	Limburg, Kessel	Schneekopf	2	Germany
22	Limburg, Kessel	Inbred breeding cross	2	Netherlands, Bejo Zaden B.V.
23	Limburg, Kessel	Interspecific cross	1	Netherlands, Bejo Zaden B.V.
24	Limburg, Kessel	Interspecific cross	1	Netherlands, Bejo Zaden B.V.
25	Limburg, Kessel	Interspecific cross	1	Netherlands, Bejo Zaden B.V.
26	Limburg, Kessel	Interspecific cross	1	Netherlands, Bejo Zaden B.V.
27	Limburg, Kessel	Cygnus	Unknown	Netherlands, Bejo Zaden B.V.
28	Limburg, Kessel	Cygnus	Unknown	Netherlands, Bejo Zaden B.V.
29	Limburg, Kessel	Inbred breeding cross	2	Netherlands, Bejo Zaden B.V.
30	South Holland, Berkheide	Wild	Unknown	Not applicable
31	South Holland, Berkheide	Wild	Unknown	Not applicable
32	South Holland, Berkheide	Wild	Unknown	Not applicable
33	South Holland, Berkheide	Wild	Unknown	Not applicable
34	Limburg, Kessel	Prius	8	Netherlands, Bejo Zaden B.V.
35	Limburg, Kessel	Bacchus	8	Netherlands, Bejo Zaden B.V.
36	Limburg, Kessel	Gynlim	8	Netherlands, Bejo Zaden B.V.
37	Limburg, Kessel	Backlim	8	Netherlands, Bejo Zaden B.V.
38	Limburg, Kessel	Grolim	8	Netherlands, Bejo Zaden B.V.
39	Limburg, Kessel	Cumulus	8	Netherlands, Bejo Zaden B.V.
40	Limburg, Kessel	Erasmus	8	Netherlands, Bejo Zaden B.V.
41	Limburg, Kessel	Cygnus	8	Netherlands, Bejo Zaden B.V.

mm) of symptomatic and asymptomatic tissues were excised, surface-sterilized by immersion in 10% sodium hypochlorite solution for 1 min, followed by immersion in 70% ethanol for 30 s, and rinsing three times in sterilised distilled water. Tissue fragments were then dried using sterilised paper towels, and up to five fragments were aseptically distributed on medium surfaces of 9 cm diam. Petri dishes containing different culture media, including: Malt Extract agar (MEA; Crous *et al.*, 2019), MEA amended with 2% chloramphenicol (MEA + CAF), Synthetic Nutrient Poor agar (SNA; Nirenberg, 1976), and Pentachloronitrobenzene agar (PCNB; Crous *et al.*, 2021). Plates were incubated at room temperature (approx. 24 °C) in darkness, checked daily for fungal

growth, and single conidium cultures were obtained by transferring individual germinating conidia onto Oatmeal agar plates (OA; Crous *et al*., 2019) with the aid of low magnification microscopy. Soil and rhizosphere samples were processed with a modification of the protocol of Groenewald *et al.* (2018). Samples were aseptically sieved to remove any plant remains and other large debris, and were deposited in open 9 cm diam. Petri dishes and were then left to dry under a laminar flow cabinet. One g of dry soil was then serially diluted from 10^{-2} to 10^{-4} in water containing 0.5 g L^{-1} agarose, and 1 mL of each dilution was spread over the surface of solid MEA + CAF or PCNB agar in Petri plates. The plates were then incubated and single conidium isolations were carried out as described above.

Fungal identifications

All isolates were subjected to total DNA extraction, using the Wizard® Genomic DNA Purification Kit (Promega), following the manufacturer's instructions, from mycelium scraped from colonies grown on MEA for 3 to 5 d at 24 °C in darkness. Fragments of two genomic regions, the translation elongation factor 1-alpha (*tef1*) and the DNA-directed RNA polymerase II second largest subunit (*rpb2*), were then PCR amplified using the primer pairs EF-1/EF-2 (O'Donnell *et al*., 1998) and RPB2-5f2/fRPB2-7cr (Liu *et al*., 1999), using the PCR protocols according to Crous *et al.* (2021). Amplicons were sequenced in both directions using the primers indicated above on a Hitachi 3730xl DNA analyser (Applied Biosystems Inc.). Consensus sequences were assembled from forward and reverse sequences using Geneious Prime v. 2023.2.1 (Biomatters Inc.). Sequences generated in this study were deposited in GenBank (Supplementary Table S1).

Sequences from each locus newly generated in the present study, as well as type and reference sequence data retrieved from Fusarioid-ID (www.fusarium.org) and GenBank (Supplementary Table S2), were aligned using MAFFT v. 7 (Katoh and Standley, 2013) Multiple Sequence Alignment (MSA) as provided by the EMBL's European Bioinformatics Institute website (www.ebi.ac.uk/jdispatcher/msa/mafft), were exported and manually corrected in MEGA v. 6.06 (Tamura *et al*., 2013), and individual loci datasets were combined using SequenceMatrix v. 1.9 (Vaidya *et al*., 2011).

Phylogenetic analyses were carried out using Maximum-Likelihood (ML) and Bayesian (BI) algorithms. For ML, RAxML-HPC2 was used on XSEDE v. 8.2.12 (Stamatakis, 2006) as implemented in the CIPRES Science Gateway (Miller *et al*., 2010), and additional calculations were made using IQ-TREE multicore v. 2.1.2 COVID-edition (Minh *et al*., 2020). For RAxML runs, the default best-fit model (General Time Reversible) and parameters were retained, and branch support was calculated using 1,000 non-parametric bootstrap inferences. Evolutionary models for IQ-TREE were calculated for each partition according to the TESTNEW option of ModelFinder (Kalyaanamoorthy *et al*., 2017) as implemented in IQ-TREE, and branch support was estimated with 1,000 replicates of ultrafast bootstrap approximation (UFBoot; Hoang *et al*., 2018). For BI, evolutionary models were calculated for each gene partition in MrModelTest v. 2.3 (Posada and Crandall, 1998; Nylander, 2004), selected according to the Akaike information criterion. The BI analyses were set up on MrBayes v. 3.2.7a (Ronquist *et al*., 2012) as implemented in the CIPRES Science Gateway, and included 5 M generations with the stop-rule option on, including four incrementally heated MCMC chains. Trees were sampled every 1,000 generations and runs were checked for convergence by average standard deviation of split frequencies below 0.01. Consensus trees (50%) and posterior probabilities (PP) were calculated after discarding 25% of the initial samples as the burn-in fraction. Alignments, phylogenetic trees and supplementary data were deposited in www.figshare.com (doi: https://doi.org/10.6084/m9.figshare.33269964).

Pathogenicity testing

To test Koch's Postulates, an *in vitro* method was developed by adapting and optimizing the protocols of Blok and Bollen (1995), Wong and Jeffries (2006), Corpas-Hervias *et al.* (2006) and Borrego-Benjumea *et al.* (2014). Seeds of *Asparagus officinalis* "Cumulus F1" (Bejo Zaden B.V.) were surface sterilized by immersion in a solution of 5% sodium hypochlorite and 0.05% Tween 20 for 1 min under constant agitation, followed by five rinses in abundant sterilized distilled water. The sterilized seeds were then aseptically placed in moisture chambers, and incubated at 27 °C in darkness, and were checked daily for 7 to 8 d until a 2 to 5 mm long radicle from each seed was visible. Once germinated, the seeds were placed onto 2.2 g L^{-1} Murashige and Skoog agar (MS; Sigma-Aldrich) amended with 5 g L^{-1} sucrose, with 8 mL of MS per glass test tube (18 mm diam.). Plantlets were then incubated for 1 to 2 weeks under a day/night cycle (23 °C for 16 h under cool fluorescent light, followed by 18 °C for 8 h in darkness) until root systems and 3 to 4 cm long shoots had developed. These plants were then inoculated by transferring an agar plug (*ca.* 5 × 5 mm from an OA plate containing a 7 to 14-d-old, well-spor-

ulated fungal culture, incubated at 24 °C under constant near UV light (nUV), located on the agar surface), near the base of the roots. Quantification experiments showed that this inoculum was equivalent to 1×10^5 conidia mL^{-1}. Challenged plants were then incubated for up to 21 d in a day/light cycle (as indicated above). Five replicates (plants) were used for each fungal isolate. Control plants were inoculated with sterile OA plugs. Presence/absence and extent of root lesions were observed daily, and pathogenicity was scored according to observed symptom severity as: 0 (absence of symptoms), 1 = browning of roots without evident lesions; 2 = presence of few (< 10) discernible lesions on primary roots, with restricted secondary roots; 3 = abundant (> 10) lesions on primary roots, with severely restricted secondary roots; and 4 = plant death. Severity scores were used to calculate the disease incidence (I = [N affected plants/N plants examined] × 100) and disease severity index (DSI = [sum of numerical ratings/(N examined plants × maximum possible grade)] × 100). To exclude duplicate isolates from the pathogenicity experiments and to avoid data repetition, a selection of 487 unique fusarioid isolates was carried out by comparing the isolate origin and *tef1* haplotypes of all strains where this information was available.

Pathogenicity results were statistically analysed using one-way ANOVA, followed by Student´s t-test assuming equal variances, with Bonferroni´s correction for multiple comparisons, using the data analysis module in MS Excel v. 2019. Adjusted *P* values (P_{adj}) are shown after each comparison in Results (below). Graphs were made using the same software and coloured using Adobe Illustrator v. 30.0.

RESULTS

Samples and fungal isolation

Plant material and soil samples were obtained from 38 cultivated fields in Limburg, plus one location where wild *A. officinalis* naturally occurs (Table 1). A total of 41 plants were dug and processed, corresponding to 13 different commercial asparagus varieties (Bacchus, Backlim, Canticus, Cumulus, Cygnus, Erasmus, Grolim, Guelph Millenium, Gynlim, Herkolim, Prius, Roem van Brunswijk, and Schneekopf), seven breeding crosses, four interspecific crosses, and wild *A. officinalis* plants. The age of the sampled plants varied from 1- to 8-years-old for cultivated fields while for wild asparagus it was undetermined. A total of 551 fungal isolates were obtained belonging to the fusarioid genera *Fusarium* or *Neocosmospora*. Exclusion of identical isolates from one origin based on *tef1* haplotypes resulted in 487 unique isolates.

Fusarioid fungi were recovered from every type of sample studied. Most fusarioid isolates were obtained from asparagus tissues (380; 68.9%), including: from roots (243 isolates; 44%), crowns (55; 10%), seeds (44; 8%), seedlings (32; 6%), or from stems (six; 1%). Soil (112 isolates; 20.3%) and rhizosphere (59 isolates; 10.7%) accounted for a third of the total number of fungal strains (Table 2).

Twenty species were identified based on molecular data, 17 of which belonged to seven *Fusarium* species complexes (SC), namely: *F. celtidicola* in the *Fusarium celtidicola* SC (FCCSC); *F. annulatum* in the *F. fujikuroi* SC (FFSC); *F. clavus*, *F. equiseti* and *F. flagelliforme* in the *F. incarnatum-equiseti* SC (FIESC); *F. carminascens*, *F. cugenangense*, *F. inflexum*, *F. nirenbergiae*, *F. odoratissimum*, *F. oxysporum* and *F. vanleeuwenii* in the *F. oxysporum* SC (FOSC); *F. redolens* in the *F. redolens* SC (FRSC), *F. culmorum* in the *F. sambucinum* SC (FSAMSC), *F. acuminatum*, *F. avenaceum* and *F. flocciferum* in the *F. tricinctum* SC (FTSC); and three species in the genus *Neocosmospora* (formerly the *F. solani* SC; *N. geoasparagicola*, *N. solani* and *N. stercicola*) (Figure 1, Table 2). The most prevalent species was *Fusarium nirenbergiae* (34%), which was also the only species found in all the sample types, and was the most prevalent species from every origin except from seeds or soil. The second most prevalent species was *Fusarium redolens* (23%), being the predominant species in soil and the second most common fusarioid species in roots. This fungus was recovered with less frequency from rhizospheres, crown tissues, and seedlings, but was not recovered from seeds or stems. The third most prevalent species, *Fusarium annulatum* (15%), was the most common fusarioid fungus isolated from seeds (95% of the total isolations from seeds), but was also found in every other sample type except from stems. This species was one of the most common isolates found in plant tissues and soils from cultivated asparagus in this study, but was not found associated with asparagus in the wild environment. The fourth and fifth most isolated species were *Neocosmospora solani* and *Fusarium culmorum*, comprising, respectively, 7.6% and 4% of the total isolations. These two fungi were mostly isolated from roots and soil (*N. solani*), and seedlings (*F. culmorum*).

Less commonly isolated species included: *F. carminascens* (19 isolates), *N. stercicola* (16 isolates), *F. avenaceum* (10 isolates), *F. vanleeuwenii* (eight isolates), *N. geoasparagicola* (seven isolates), *F. acuminatum* and *F. flagelliforme* (six isolates each), *F. inflexum* (three isolates), *F. clavus*, *F. odoratissimum* and *F. oxysporum* (two isolates each), and *F. cugenangense, F. equiseti*, *F. celtidicola* and *F. flocciferum* (one isolate each) (Table 2).

Table 2. Origins of fusarioid fungal isolates, according to asparagus plant or soil sample type.

Fungus name	Origin (number of isolates)							
	Crown	Rhizosphere	Root	Seed	Seedling	Soil	Stem	Total
Fusarium acuminatum	2				4			6
Fusarium annulatum	10	10	20	42	1	3		86
Fusarium avenaceum	1	2	4		3			10
Fusarium carminascens		3	9			7		19
Fusarium celtidicola							1	1
Fusarium clavus						2		2
Fusarium cugenangense		1	0					1
Fusarium culmorum	3	2	2		10	3	1	21
Fusarium equiseti						1		1
Fusarium flagelliforme			1		3	2		6
Fusarium flocciferum						1		1
Fusarium inflexum			3					3
Fusarium nirenbergiae	27	22	97	1	10	28	4	189
Fusarium odoratissimum			2					2
Fusarium oxysporum	1		1					2
Fusarium redolens	5	11	78		1	33		128
Fusarium vanleeuwenii	1		4	1		2		8
Neocosmospora geoasparagicola						7		7
Neocosmospora solani	2	7	17			16		42
Neocosmospora stercicola	3	1	5			7		16
Total	55	59	243	44	32	112	6	551

Pathogenicity testing

In vitro pathogenicity testing of 487 unique isolates showed that a majority (408; 84%) could induce lesions on asparagus seedling roots and crowns. Disease incidence (% of affected replicates) ranged from 20 to 100%, with 43% (209 isolates) inducing lesions in all five plant replicates. The degree of root damage was, in general, highly variable, with most challenges resulting in either absence of root lesions (severity score 0; 35% of isolates) or great compromise of the entire root system resulting in plant death (severity score 4; 33.3% of isolates). Intermediate severity scores (1 to 3) were observed in, respectively, 6, 12.8 or 12.6% of the total assays (Figures 2 and 3).

Among the most prevalent fungal species in the dataset, 99% of isolates of *F. annulatum*, 95% of *F. culmorum*, 92% of *F. redolens*, 89% of *F. nirenbergiae*, and 67% of *N. solani* induced symptoms in asparagus plantlets, affecting either root or crown tissue alone, or as combinations of both. According to calculated I and DSI indices, the two most pathogenic and aggressive species were *F. culmorum* (I = 78%; DSI = 64%) and *F. annulatum* (I = 67%; DSI = 55%) (Figure 2). Seventy-seven percent of all *in vitro* asparagus inoculations with *F. culmorum*, and 37% of inoculations with *F. annulatum*, led to plant death at the end of the trial, in both cases mostly due to effects on the host plant crowns, with minimal presence or absence of root lesions. No statistically significant differences in pathogenicity were observed between these two species. However, both species were associated to significantly more aggressive disease *in vitro* than most of the common asparagus pathogens tested here, including *F. redolens*. This species (I = 74%; DSI = 44%) differed significantly from *F. annulatum* in both incidence (P_{adj} = 0.01) and disease severity (P_{adj} = 1.89×10^{-8}). Incidence of *F. redolens* was comparable to that of *F. culmorum* (P_{adj} = 0.59), although disease severity was significantly less (P_{adj} = 3.03×10^{-7}). *Fusarium nirenbergiae* (I = 69%; DSI = 44%) did not differ from *F. redolens* in either parameter, and showed greater incidence than *F. annulatum* (P_{adj} = 1.59×10^{-4}), but not than *F. culmorum* (P_{adj} = 0.26). Disease severity was significantly lower in *F. nirenbergiae* than that from *F. redolens* (P_{adj} = 6.72×10^{-9}) or from *F. annulatum* (P_{adj} = 6.96×10^{-7}). *Neocosmospora solani* caused the least disease incidence and severity (I = 28%; DSI = 18%), differing significantly from all the other fungi mentioned above in both parameters ($P_{adj} \leq 3.86 \times 10^{-5}$ for incidence, $\leq 1.22 \times 10^{-21}$ for disease severity). Less represented species induced varied levels of disease, among which *F. oxyspo-*

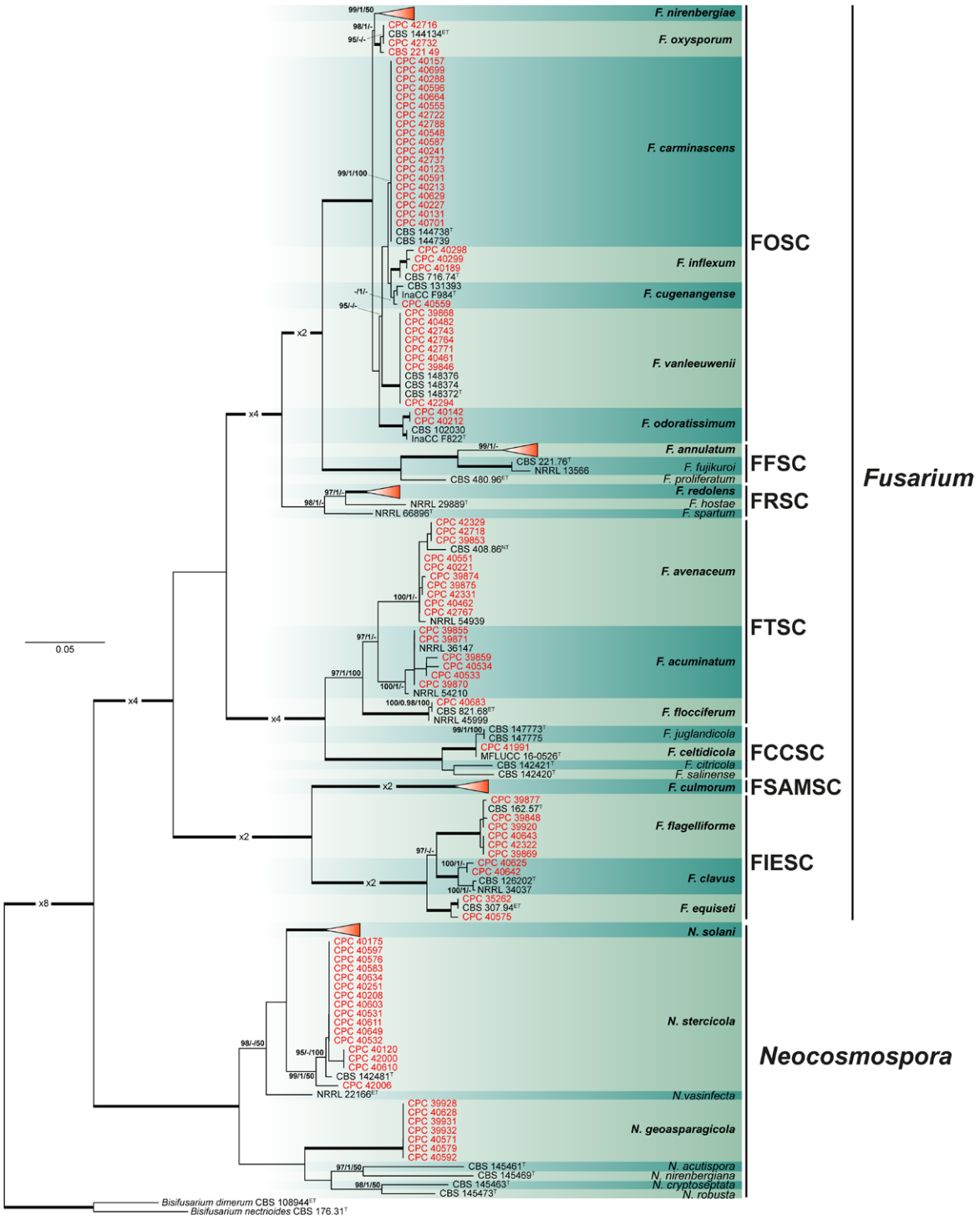

Figure 1. Maximum Likelihood (IQ-TREE) phylogram inferred from combined *rpb2* and *tef1* datasets of representative isolates of *Fusarium* and *Neocosmospora*, plus 551 fungal isolates obtained from asparagus tissues and soils. Numbers at nodes indicate support values (IQ-TREE-BS / BI-PP / RAxML-BS) greater than 70 % (BS) and 0.95 (PP). Thickened branches indicate full support (BS = 100, PP = 1). The tree is rooted to *Bisifusarium dimerum* CBS 108944 and *B. nectrioides* CBS 176.31. Due to the abundance of strains, clades representing *F. annulatum*, *F. culmorum*, *F. nirenbergiae*, *F. redolens* and *N. solani* were collapsed to facilitate display. Culture collection abbreviations are listed in Supplementary Table S2. Ex-epitype, ex-neotype or ex-type strains are indicated by, respectively, ET, NT or T. *Fusarium* species complexes (SC) are abbreviated as: FCCSC = *F. celtidicola* SC, FFSC = *F. fujikuroi* SC, FIESC = *F. incarnatum-equiseti* SC, FOSC = *F. oxysporum* SC, FRSC = *F. redolens* SC, FSAMSC = *F. sambucinum* SC, and FTSC = *F. tricinctum* SC.

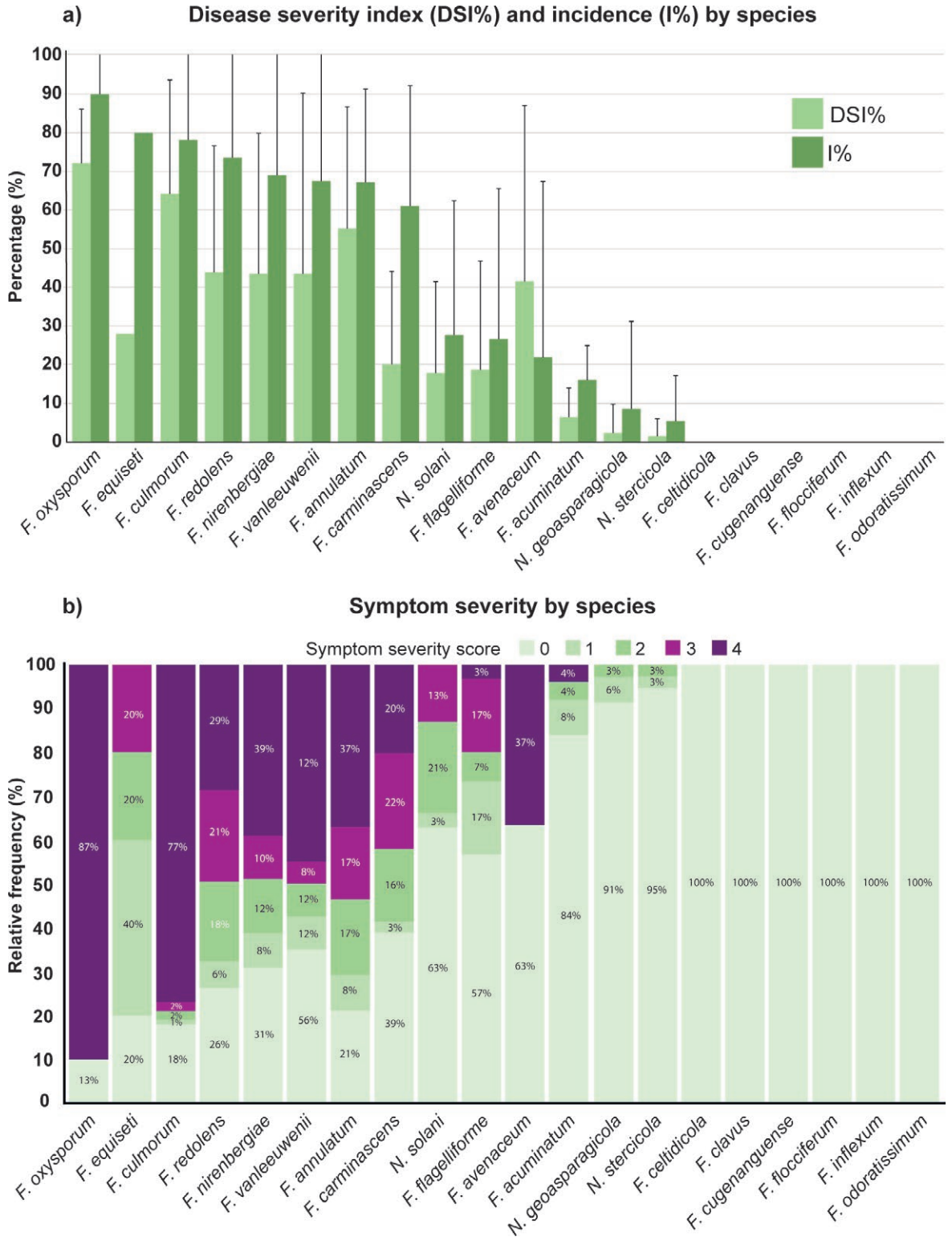

Figure 2. a: Calculated mean Disease Severity Indices (DSI%) and incidences (I%) per species, for fungal taxa ordered according to their indices, from high (left) to low (right). Lines above bars indicate standard deviations. b: Observed symptom severity scores per species, as: 0 = no symptoms, 1 = browning of roots, without evident lesions; 2 = few discernible lesions on primary roots, with restricted secondary roots; 3 = abundant lesions on primary roots, with severely restricted secondary roots; 4 = plant death. Fungal species are ordered alphabetically from left to right.

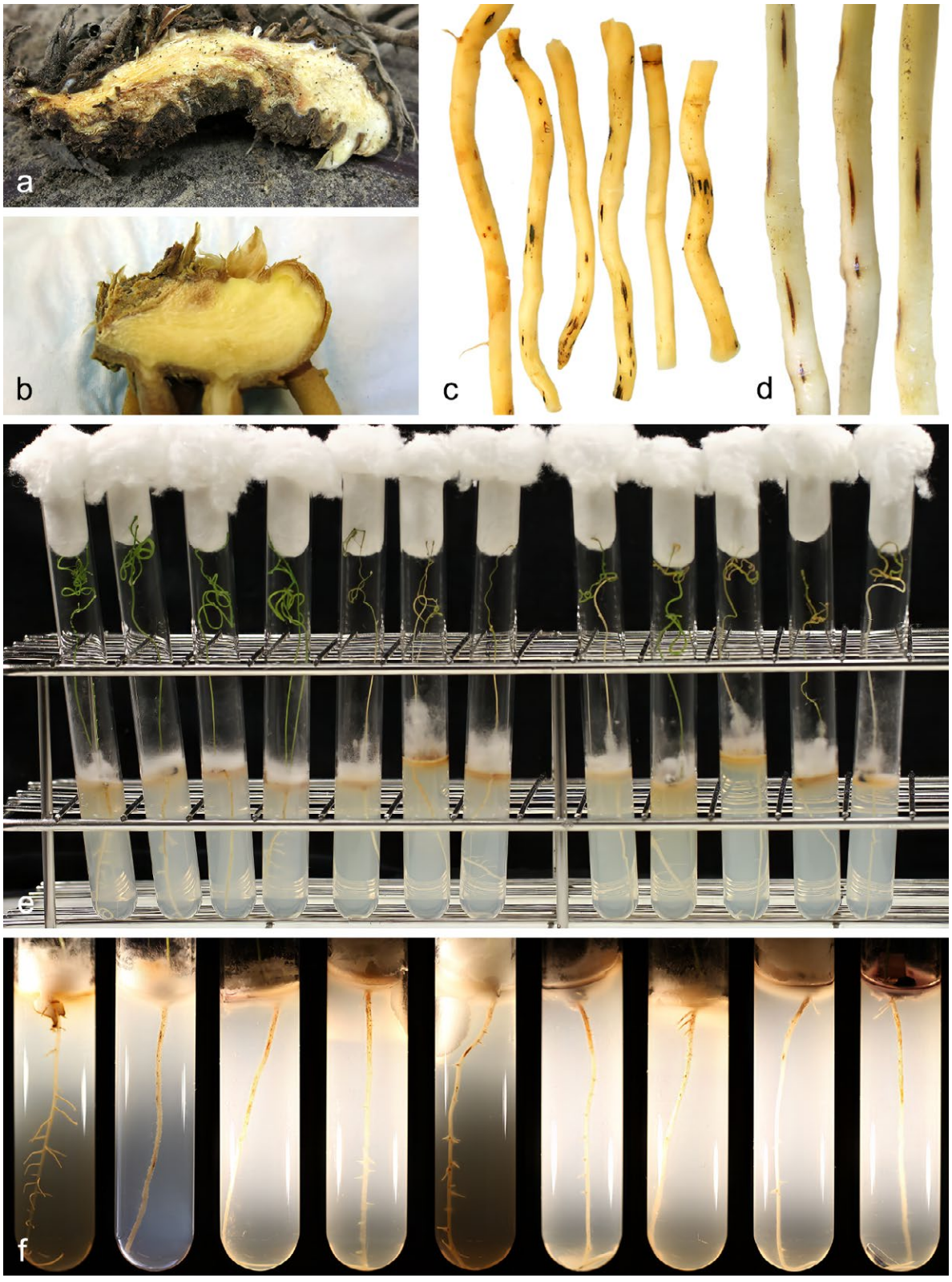

Figure 3. Asparagus lesions attributed to fusarioid species. a, b: naturally occurring crown lesions on cultivated *Asparagus officinalis*. c, d: typical root lesions on a cultivated plant (c) and a wild plant (d). e: experimental setup showing diverse symptoms on infected *A. officinalis* plantlets. f: detail of different degrees of root symptoms on infected *A. officinalis* plantlets.

rum and other members of the FOSC (*i.e.*, *F. carminascens*, *F. vanleeuwenii, F. cugenangense*), and *F. equiseti* from the *Fusarium incarnatum-equiseti* species complex (FIESC) caused high incidences (I = 56 to 100%). Despite its low isolation frequency (two isolates), *Fusarium oxysporum* also showed high aggressiveness (DSI = 72%, and causing 87% plant death with extensive crown symptoms, but without root lesions). However, these observations are not statistically supported, due to the limited number of isolates in this dataset. *Fusarium avenaceum* (belonging to the *Fusarium tricinctum* species complex, FTSC) gave relatively low disease incidence (I = 22%), and did not attack the asparagus root systems. This fungus, however, was an aggressive crown pathogen (DSI = 42%), with 37% of inoculations leading to plant death. Isolates of *F. acuminatum*, *N. stercicola* and *N. geoasparagicola* were only associated with mild root and crown symptoms (I ≤ 16%; DSI ≤ 6%). None of the *F. celtidicola*, *F. clavus*, *F. flocciferum*, *F. inflexum*, or *F. odoratissimum* isolates induced symptoms on inoculated asparagus seedlings.

A subset of 37 isolates (*N. solani* n = 13, *N. stercicola* n = 8, *F. redolens* n = 4, *F. carminascens*, *F. flagelliforme* and *F. nirenbergiae* each n = 3 each, *F. annulatum* n = 4, and *F. culmorum* n = 1) was associated with enhanced asparagus growth in the bioassays, producing taller, thicker and greener stalks than the inoculation controls. This phenotype was constant between repetitions and had no apparent association with fungal species or strain origin (see isolate details in Table S1).

DISCUSSION

Twenty species of *Fusarium* and *Neocosmospora* were isolated from *Asparagus officinalis* tissues and associated soils, and were identified by using multilocus phylogenetic analysis, and their pathogenicity was assessed using an *in vitro* system. The present study is the most extensive in terms of fusarioid diversity to have been carried out on asparagus.

Fusarium nirenbergiae was the most frequently encountered species in this dataset, and until recently was an unnamed phylogenetic lineage, hidden within a too comprehensive concept of *F. oxysporum sensu lato* (*s. l.*) (Snyder and Hansen 1940). After its formal description (Lombard *et al.* 2019), *F. nirenbergiae* has emerged as a ubiquitous species in the FOSC (Crous *et al.* 2021, Wang *et al.* 2022, Han *et al.* 2023). Nevertheless, its host range and pathogenicity, including against *A. officinalis*, remains to be determined and contrasted against historical data for *F. oxysporum s. l.* Previous studies on the prevalence of fusarioid asparagus pathogens in The Netherlands date from the 1990s, and were based on old taxonomic concepts (Blok and Bollen, 1995; Baayen *et al.*, 2000). Similarly, modern studies from asparagus producing countries, although based on molecular data, have often relied on outdated *Fusarium* taxonomy. This is of particular relevance when assessing the most prevalent asparagus pathogens, most of which have recently undergone important taxonomic changes (Lombard *et al.*, 2015, 2019; Sandoval-Denis *et al.*, 2019; Crous *et al.*, 2021). Nevertheless, as observed here, the distribution of the most common species is, in general, congruent with previous reports in The Netherlands and elsewhere (Block and Bollen, 1995; Elmer *et al.*, 1997; Wong and Jeffries, 2006; Farr *et al.*, 2023; Buitrago-Acosta *et al.*, 2025). However, and contrary to previous indications, *F. oxysporum* was not the most commonly associated species on cultivated asparagus and was found on one crown and one root sample in the present study.

Previous knowledge about asparagus-related *F. oxysporum* is, without exception, based on old species concepts. The name *F. oxysporum s. l.* has traditionally and erroneously been employed as a wild card to classify a genetically diverse group of different species with very similar phenotypes (O'Donnell *et al.*, 2004; Lombard *et al.*, 2019; McTaggart *et al.*, 2021), therefore perpetuating the incorrect application of the name *F. oxysporum*. Conversely, the widespread availability of sequence data has recently accelerated species descriptions within FOSC, occasionally resulting in the recognition of poorly delimited or taxonomically redundant taxa that complicate identification and the interpretation of phylogenetic analyses (Lombard *et al.*, 2019; Tan and Conroy, 2024; Tan and Shivas, 2024). Such taxa were therefore not adopted in the identification of isolates in the present study. However, isolates potentially assignable to these entities and their phylogenetic relationships are documented in the extended phylogenetic analysis available in FigShare (doi:10.6084/m9.figshare.33269964). The alternative classification of this group of pathogens according to the f. sp. nomenclature (*e.g.*, *F. oxysporum* f. sp. *asparagi*, Cohen and Heald (1941)) has resulted in a similar problem since they do not cluster in monophyletic groups, when compared to formal taxonomic ranks, grouping different entities here demonstrated to be different species. Most of these species have only recently been formally described, and were shown in the present study to induce asparagus disease (Lombard *et al.*, 2019). As demonstrated here, the traditional concepts of *F. oxysporum s. l.* and *F. oxysporum* f. sp. *asparagi* encompass a series of distinct species (*F. nirenbergiae*, *F. carminascens*, *F. cugenangense*, *F. vanleeuwenii*, *F. inflexum*, *F. odoratissimum*, and *F. oxyspo-*

rum sensu stricto [*s. st.*]), all belonging to the FOSC and virtually indistinguishable morphologically. The relevance of the reassessment of *Fusarium* taxonomy is highlighted by the markedly different levels of pathogenicity of these fungi towards *A. officinalis*.

Fusarium redolens, the second most prevalent species in the present study, was for a long time treated either as a synonym or a variety of *F. oxysporum* (Snyder and Hansen, 1940; Gordon, 1952; Bilai, 1955; Block and Bollen, 1995; Baayen *et al*., 2000). This species is a recognized asparagus pathogen commonly isolated from fields in Western and Northern Europe, including The Netherlands (Baayen *et al*., 2000; Schroers *et al*., 2004; Wong and Jeffries, 2006), and North America (Vujanovic *et al*., 2006; Borrego-Benjumea *et al*., 2014). Similarly, the third most isolated species in this series, *F. annulatum*, is also a documented asparagus pathogen with broad distribution that includes Argentina (Lori *et al*., 1998), Australia and New Zealand (Elmer *et al*., 1997), Canada, and the United States of America (Elmer, 1990; Baayen *et al*., 2000; Vujanovic *et al*., 2006; Borrego-Benjumea *et al*., 2014), Japan (Nahiyan *et al*., 2011), The Netherlands (Baayen *et al*., 2000), South Africa (Schreuder *et al*., 1995), Spain (Wong and Jeffries, 2006) and the United Kingdom (Wong and Jeffries, 2006).

Fusarium annulatum has often been erroneously reported as *F. proliferatum*, due to the confusing taxonomic history of these two species. These two taxa, both segregates of *F. moniliforme s. l.* (Seifert *et al*., 2003) and previously considered synonyms, are now confined to two genealogically exclusive clades, of which the one representing the widely distributed and well-recognised plant pathogenic species is now assigned to *F. annulatum* (Yilmaz *et al*., 2021). Despite being a cosmopolitan species, only one report has mentioned isolation of *F. annulatum* (as *F. proliferatum*) from asparagus fields in The Netherlands (Baayen *et al*., 2000;), with no clear indication of its origin. The apparent absence of this species from Dutch soils was probably due to low soil temperatures, because this species is more commonly isolated in warm regions, and does not survive well in soils without plant hosts (Block and Bollen, 1996). This species was one of the most commonly found in the present study in plant tissues and soils from cultivated asparagus, but was not found associated with asparagus in the wild environments, suggesting introduction and spread through agricultural practices, or indicating a level of environmental adaptation.

The fourth most isolated species, *N. solani*, is commonly associated with soil-borne root diseases of several hosts (Sandoval-Denis *et al*., 2019), including *A. officinalis*, with reports from Brazil (Mendes *et al*., 1998), Europe, including the United Kingdom, The Netherlands, and Spain (Block and Bollen, 1996; Corpas-Hervias *et al*., 2006; Wong and Jeffries, 2006; Brizuela *et al*., 2020), Malaysia (Chehri *et al*., 2014), Canada and the United States of America (Damicone and Manning, 1985; Borrego-Benjumea *et al*., 2014), and South Africa (Schreuder *et al*., 1995). However, this species was non-to weakly aggressive to asparagus in the present study. *Neocosmospora* (previously the *Fusarium solani* SC) is another example of radical taxonomic change, particularly the segregation of this group to a separate genus based on molecular and morphological evidence (Lombard *et al*., 2015; Sandoval-Denis *et al*., 2019), and the epitypification and confinement of its historically most notorious species *N. solani* to a discrete phylogenetic lineage (Schroers *et al*., 2016). The name *N. solani* is no longer applicable to cover multiple phylogenetic entities (Snyder and Hansen, 1941).

Contrary to all the species discussed above, there is a broad taxonomic consensus regarding *F. culmorum*, the fifth most commonly isolated species in the present study. This species is a notable asparagus pathogen with wide distribution including Brazil (Mendes *et al*., 1998), China (Tai, 1979; Zhuang, 2005), Europe, including Italy (Richardson, 1990), The Netherlands (Block and Bollen, 1996), Spain (Brizuela *et al*., 2020) and the United Kingdom (Wong and Jeffries, 2006); and New Zealand (Pennycook, 1989).

While the above-mentioned species were approx. 85% of the total isolations in the present study, the remaining 15% of isolations were a heterogeneous assemblage of species with reduced isolation frequencies, from which only three taxa (*F. acuminatum*, *F. equiseti*, and *F. oxysporum s. st.*) are previously known from *Asparagus* spp. (Elmer *et al*., 1997; Vujanovic *et al*., 2006; Brizuela *et al*., 2020). The remaining 12 species (*i.e*., *F. avenaceum*, *F. carminascens*, *F. celtidicola*, *F. clavus*, *F. cugenangense*, *F. flagelliforme*, *F. flocciferum*, *F. inflexum*, *F. odoratissimum*, *F. vanleeuwenii*, *N. geoasparagicola*, and *N. stercicola*) are here reported for the first time in association with cultivated *A. officinalis*. In addition, a species novel to science, *N. geoasparagicola*, was discovered during this study, and has since been published elsewhere (Crous *et al*., 2022). This species was found only in soil samples from five cultivated fields; associated with five asparagus cultivars (Cygnus, Grolim, Guelph-Millenium, Schneekopf, plus an unidentified cultivar). It was recovered from asparagus-associated soils in two independent occasions separated by almost 2 years, and has since also been isolated from other types of soil in Limburg and Noord-Brabant (ARISE project, Westerdijk Fungal Biodiversity Institute, personal communication).

Verifications of Koch's postulates in this study largely agree with previous reports. However, the pathogenicity assays conducted in this study were designed as an initial screening, to identify potentially pathogenic *Fusarium* species under strictly controlled conditions. Consequently, the present results should be interpreted as evidence of pathogenic potential, while further validation under more representative cultivation conditions (mature asparagus plants under greenhouse or field conditions) remains warranted. Apart from slight regional evidence variations, pathogenicity data tend to allocate *Fusarium* species as the most relevant in terms of pathogenicity and virulence against asparagus (Elmer *et al*., 1997; Wong and Jeffries, 2006; Nahiyan *et al*., 2011; Borrego-Benjumea *et al*., 2014; Brizuela *et al*., 2020). However, as previously noted by Blok and Bollen (1995), the present study experimental set up could have overestimated the virulence of *F. culmorum*. Though in this dataset *F. culmorum* was isolated from every type of sample except asparagus seeds, unlike other species tested here, *F. culmorum* has been typically associated with stem base lesions leading to plant death (Van Bakel and Krom-Kerstens, 1974; Blok and Bollen, 1995). Due to the thin stem bases of young asparagus plants, and the inoculation method employed, these plant tissues are easy targets for this pathogen, which can quickly kill plantlets.

This is the first report of *F. avenaceum* from *A. officinalis*, However, this fungus has been reported in association with *Puccinia ranulipes* on *Asparagus laricinus* in South Africa (Doidge, 1950; Farr *et al*., 2023). Here this species was shown to induce moderate root symptoms on asparagus seedlings, yet when plant crowns were impacted, it can lead to plant death *in vitro*. Nevertheless, its behaviour under field conditions remains to be tested. Previous reports have shown moderate aggressiveness of *F. acuminatum* (Borrego-Benjumea *et al*., 2014) or no pathogenicity (Brizuela *et al*., 2020) against asparagus *in vitro*, which coincides with the present study observations. However, this species is a known plant root pathogen, and has a host range including *Asparagaceae* (*Ophiopogon japonicus*) (Tang *et al*., 2021). Conversely, none of the isolates of *F. celtidicola*, *F. clavus*, *F. flocciferum*, *F. inflexum*, or *F. odoratissimum* induced symptoms on inoculated asparagus. While none of the latter species have been previously reported from *Asparagus* spp., and are probably non-pathogenic, *F. flocciferum*, *F. inflexum* and *F. odoratissimum* are well-known pathogens of several plant species, particularly in *Fabaceae*, *Musaceae* and *Poaceae* (Farr *et al*., 2023).

Thirty-seven isolates belonging to seven *Fusarium* species (*i.e*., *F. redolens* [four isolates]), *F. carminascens*, *F. flagelliforme* and *F. nirenbergiae* [three isolates each], *F. annulatum* [two isolates]; and *F. culmorum* [one isolate], and particularly to two *Neocosmospora* species (*i.e*., *N. solani* [13 isolates], and *N. stercicola* [eight isolates]) were associated with improved plant growth in the present study bioassays. These isolates induced much taller, thicker and greener asparagus stalks compared to the controls, irrespective of the presence of root lesions on infected plants, which was a paradoxical phenomenon that seemed to not respond to any particular fungal species or isolate origin (data not shown). These experiments were not designed to test for beneficial effects of fungi, so further research will be required to confirm this effect, determine its magnitude, and consider underlying mechanisms.

CONCLUSIONS

The aetiology of asparagus fusarium disease is more complex than previously thought, with several species reported here as potential pathogens. Some of these species, despite being internationally ubiquitous, and known from several host species, are here reported for the first time from asparagus. Given the abilities of these fungi to induce asparagus disease *in vitro*, their importance for international asparagus global industries needs to be studied further. Several taxa recovered from lesions can also be isolated from healthy (or apparently healthy) asparagus plants, and several isolates obtained from healthy plants were able to induce symptoms in the *in vitro* assays. This demonstrates the plasticity and variety of adaptations known for fusarioid species (Ulaszewski *et al*., 2025), the complexity of host-fungal interactions, and the role of stochastic processes in the occurrence of disease. Furthermore, the presentation of asparagus disease is also known to vary in response to abiotic factors, which were not assessed here, while *in vitro* pathogenicity testing can be highly influenced by the age of the tested host plants (Elmer, 2015; Brizuela *et al*., 2020).

In terms of fungal diversity and despite limited sampling, this study has identified the greatest number of species isolated and tested for pathogenicity against *A. officinalis*. This diversity reflects improved species identification due to refined *Fusarium* taxonomy (Crous *et al*., 2021), and explains the differences in pathogenicity observed here with respect to traditionally encountered taxa (*F. oxysporum s. l.*). Re-evaluations of pathogen distribution and virulence, according to modern techniques and updated taxonomic concepts and classifications, will lead to increased understanding of species biology, which is fundamental for designing specific disease control measures, managing quarantine, and interpreting research data.

ACKNOWLEDGMENTS

The Authors thank Bart Arends (Bejo Zaden B.V., Kessel, The Netherlands) and co-workers for their invaluable assistance to dig-up and organize asparagus plants for sampling. Laurens Kroon (Bejo Zaden B.V., The Netherlands) is thanked for providing MTAs. Casper Zuyderduyn (Staatsbosbeheer) provided collection permits for the Coepelduynen and Berkheide dune area, Hollandse Duinen National Park, Wassenaar, South Holland (permit number 2020/45), and Raymond Duindam and Margot Holland (PWN) provided collection permits for the Kennemerduinen Nature Reserve, Zuid-Kennemerland National Park, North Holland (permit number 6807), although collections in this zone were unproductive. Maria Hundscheid (NIOO, Wageningen, The Netherlands), Lorenzo Lombard, Marian Figge and Michel de Vries (Westerdijk Fungal Biodiversity Institute, Utrecht, The Netherlands) are thanked for technical assistance during several steps of this study. This research was funded by the Royal Netherlands Academy of Arts and Sciences (KNAW), to stimulate collaboration between the Netherlands Institute of Ecology (NIOO-KNAW), and Westerdijk Fungal Biodiversity Institute (WI-KNAW), under the Academy Institutes fund scheme, project BDO/1257.

LITERATURE CITED

Aegerter B.J., Davis R.M., Natwick E.T., Smith R.F., Baldwin R.A., 2016. Fusarium crown and root rot. In: *Pest Management Guidelines:* Asparagus. (Aegerter B, Davis R, Natwick E, *et al*., ed.). *UC ANR Publication 3435*. Davis, California, USA.

Baayen R.P., van den Boogert P.H.J.F., Bonants P.J.M., Poll J.T.K, Blok W.J., Waalwijk C., 2000. *Fusarium redolens* f. sp. *asparagi*, causal agent of asparagus root rot, crown rot and spear rot. *European Journal of Plant Pathology* 106: 907–912. https://doi.org/10.1023/A:1008766707266

Bilai V.I., 1955. *The fusaria (biology and systematics)*. Akademia Naukwe Ukrainskii, SSR, Kiev.

Blok W.J., Bollen G.J., 1995. Fungi on roots and stem bases of asparagus in the Netherlands: species and pathogenicity. *European Journal of Plant Pathology* 101: 15–24. https://doi.org/10.1007/BF01876090

Blok W.J., Bollen G.J., 1996. Etiology of asparagus replant-bound early decline. *European Journal of Plant Pathology* 102: 87–98. https://doi.org/10.1007/BF01877119

Borrego-Benjumea A., Basallote-Ureba M.J., Melero-Vara J.M., Abbasi P.A., 2014. Characterization of *Fusarium* isolates from *Asparagus* fields in southwestern Ontario and influence of soil organic amendments on Fusarium crown and root rot. *Ecology and Epidemiology* 104(4): 403–415. https://doi.org/10.1094/PHYTO-08-13-0231-R

Brizuela A.M., De la Lastra E., Marín-Guirao J.I., Gálvez L., de Cara-García M., … Palmero D., 2020. *Fusarium* consortium populations associated with asparagus crop in Spain and their role on field decline syndrome. *Journal of Fungi* 6(4): 336. https://doi.org/10.3390/jof6040336

Buitrago-Acosta M.C., Minier D.H., Getson S., Medina-Mora C.M., Hausbeck M.K., 2025. *Fusarium* spp. associated with asparagus crowns and the influence of the preplant fumigant metam-sodium in Michigan crown nurseries. *Annals of Applied Biology* 186(3): 323–333. https://doi.org/10.1111/aab.12971

Centraal Bureau voor de Statistiek (CBS), 2025. *Vegetables; yield and cultivated area per kind of vegetable*. Retrieved November 19, 2025, from https://www.cbs.nl/en-gb/figures/detail/37738ENG

Chehri K., Salleh B., Zakaria L., 2014. *Fusarium virguliforme*, a soybean sudden death syndrome fungus in Malaysian soil. *Australasian Plant Disease Notes* 9(1): 1–7 https://doi.org/10.1007/s13314-014-0128-z

Cohen S.I., Heald F.D., 1941. A wilt and root rot of asparagus caused by *Fusarium oxysporum* Schlecht. *Plant Disease Reporter* 25: 50–509.

Corpas-Hervias C., Meloro-Vara J., Molinero-Ruiz M., Zurera-Muñoz C., Basallote-Ureba M.J., 2006. Characterization of isolates of *Fusarium* spp. obtained from *Asparagus* in Spain. *Plant Disease* 90: 1441–1451. https://doi.org/10.1094/PD-90-1441

Crous P.W., Lombard L., Sandoval-Denis M., Seifert K.A., Schroers H-J., … Thines M., 2021. *Fusarium*: more than a node or a foot cell. *Studies in Mycology* 98: 100116. https://doi.org/10.1016/j.simyco.2021.100116

Crous P.W., Sandoval-Denis M., Costa M.M., Groenewald J.Z., van Iperen A.L., … Thines M., 2022. *Fusarium* and allied fusarioid taxa (FUSA). 1. *Fungal Systematics and Evolution* 9: 161–200 https://doi.org/10.3114/fuse.2022.09.08

Crous P.W., Verkley G.J.M., Groenewald J.Z., Houbraken J., 2019. *Fungal Biodiversity*. Utrecht, The Netherlands: Westerdijk Fungal Biodiversity Institute.

Damicone J.P., Manning W.J., 1985. Frequency and pathogenicity of *Fusarium* spp. isolated from first-year asparagus grown from transplants. *Plant Disease* 69: 413–416 https://doi.org/10.1094/PD-69-413

Elmer W.H., 1990. *Fusarium proliferatum* as a causal agent in fusarium crown and root rot of asparagus. *Plant Disease* 74: 938. https://doi.org/10.1094/PD-74-0938E

Elmer W.H., Summerell B.A., Burgess L.W., Backhouse D., Abubaker A.A., 1997. *Fusarium* species associated with asparagus crowns and soil in Australia and New Zealand. *Australasian Plant Pathology* 26: 255–261. https://doi.org/10.1071/AP97041

Elmer W.H., 2015. Management of Fusarium crown and root rot of asparagus. *Crop Protection* 73: 2–6. https://doi.org/10.1016/j.cropro.2014.12.005

Farr D.F., Rossman A.Y., Castlebury L.A., 2023. United States national fungus collections fungus-host dataset. Ag Data Commons. Retrieved 2023-09-15, from https://fungi.ars.usda.gov/

Gordon W.L., 1952. The occurrence of *Fusarium* species in Canada. II. Prevalence and taxonomy of *Fusarium* species in cereal seed. *Canadian Journal of Botany* 30(2): 209–251. https://doi.org/10.1139/b52-018

Groenewald M., Lombard L., de Vries M., Giraldo A., Smith M., Crous PW., 2018. Diversity of yeast species from Dutch garden soil and the description of six novel Ascomycetes. *FEMS Yeast Research* 18(7): foy076. https://doi.org/10.1093/femsyr/foy076

Han S.L., Wang M.M., Ma Z.Y., Raza M., Zhao P., … Cai L., 2023. *Fusarium* diversity associated with diseased cereals in China, with an updated phylogenomic assessment of the genus. *Studies in Mycology* 104: 87–148. https://doi.org/10.3114/sim.2022.104.02

Hoang D.T., Chernomor O., von Haeseler A., Minh B.Q., Vinh L.S., 2018. UFBoot2: improving the ultrafast bootstrap approximation. *Molecular Biology and Evolution* 35(2): 518–522. https://doi.org/10.1093/molbev/msx281

Kalyaanamoorthy S., Minh B.Q., Wong T.K.F., von Haeseler A., Jermiin L.S., 2017. ModelFinder: fast model selection for accurate phylogenetic estimates. *Nature Methods* 14(6): 587–589. https://doi.org/10.1038/nmeth.4285

Katoh K., Standley D.M. 2013. MAFFT multiple sequence alignment software version 7: improvements in performance and usability. *Molecular Biology and Evolution* 30(4): 772–780. https://doi.org/10.1093/molbev/mst010

Liu Y.J., Whelen S., Hall B.D., 1999. Phylogenetic relationships among ascomycetes: evidence from an RNA polymerse II subunit. *Molecular Phylogenetics and Evolution* 16(12): 1799–1808. https://doi.org/10.1093/oxfordjournals.molbev.a026092

Lombard L., Sandoval-Denis M., Lamprecht S.C., Crous P.W., 2019. Epitypification of *Fusarium oxysporum*: clearing the taxonomic chaos. *Persoonia* 43: 1–47. https://doi.org/10.3767/persoonia.2019.43.01

Lombard L., van der Merwe N.A., Groenewald J.Z., Crous P.W., 2015. Generic concepts in *Nectriaceae*. *Studies in Mycology* 80: 189–245. https://doi.org/10.1016/j.simyco.2014.12.002

Lori G., Wolcan S., Mónaco, C.I., 1998. *Fusarium moniliforme* and *F. proliferatum* isolated from crown and root rot of asparagus and their association with asparagus decline in Argentina. *Plant Disease* 82(12): 1405. https://doi.org/10.1094/PDIS.1998.82.12.1405A

McTaggart A.R., James T.Y., Shivas R.G., Drenth A., Wingfield B.D., … Duong T.A., 2021. Population genomics reveals historical and ongoing recombination in the *Fusarium oxysporum* species complex. *Studies in Mycology* 99: 100132. https://doi.org/10.1016/j.simyco.2021.100132

Mendes M.A.S., da Silva V.L., Dianese J.C., Ferreira, M.A.S.V, dos Santos C.E.N., … Castro C., 1998. *Fungos em Plantas no Brasil*. Embrapa-SPI/Embrapa-Cenargen, Brasilia

Miller M.A., Pfeiffer W., Schwartz T., 2010. Creating the CIPRES Science Gateway for inference of large phylogenetic trees. *Proceedings of the Gateway Computing Environments Workshop (GCE)*, 14 Nov. 2010, New Orleans, LA pp. 1–8.

Minh B.Q., Schmidt H.A., Chernomor O., Schrempf D., Woodhams M.D., … Lanfear R., 2020. IQ-TREE 2: New models and efficient methods for phylogenetic inference in the genomic era. *Molecular Biology and Evolution* 37: 1530–1534. https://doi.org/10.1093/molbev/msaa015

Nahiyan A.S.M., Boyer L.R., Jeffries P., Matsubara Y., 2011. PCR-SSCP analysis of *Fusarium* diversity in asparagus decline in Japan. *European Journal of Plant Pathology* 130: 197–203. https://doi.org/10.1007/s10658-011-9745-y

Nylander J.A.A., 2004. MrModeltest v2. Program distributed by the author. Evolutionary Biology Centre, Uppsala University.

Nirenberg H.I., 1976. Untersuchungen über die morphologische und biologische differenzierung in der *Fusarium*-Sektion *Liseola*. *Mitteilungen der Biologischen Bundesanstalt für Land- und Forstwirtschaft Berlin-Dahlem* 169: 1–117.

O'Donnell K., Cigelnik E., Nirenberg H.I., 1998. Molecular systematics and phylogeography of the *Gibberella fujikuroi* species complex. *Mycologia* 90(3): 465–493. https://doi.org/10.1080/00275514.1998.12026933

O'Donnell K., Sutton D.A., Rinaldi M.G., Magnon K.C., Cox P.A., … Robinson J.S., 2004. Genetic diversity of human pathogenic members of the *Fusarium*

oxysporum complex inferred from multilocus DNA sequence data and amplified fragment length polymorphism analyses: Evidence for the recent dispersion of a geographically widespread clonal lineage and nosocomial origin. *Journal of Clinical Microbiology* 42(11): 5109–5120. https://doi.org/10.1128/jcm.42.11.5109-5120.2004

Pennycook S.R., 1989. *Plant Diseases Recorded in New Zealand.* Plant Disease Division, D.S.I.R., Auckland.

Posada D., Crandall K.A., 1998. MODELTEST: testing the model of DNA substitution. *Bioinformatics* 14(9): 817–818. https://doi.org/10.1093/bioinformatics/14.9.817

Richardson M.J., 1990. *An Annotated List of Seed-borne Diseases, 4th Edition.* The International Seed Testing Association, Bassersdorf, Switzerland, 338 pp.

Ronquist F., Teslenko M., van der Mark P., Ayres D.L., Darling A., … Huelsenbeck J.P., 2012. MrBayes 3.2: efficient Bayesian phylogenetic inference and model choice across a large model space. *Systematic Biology* 61(3): 539–542. https://doi.org/10.1093/sysbio/sys029

Sandoval-Denis M., Lombard L., Crous P.W., 2019. Back to the roots: a reappraisal of *Neocosmospora*. *Persoonia* 43: 90–185. https://doi.org/10.3767/persoonia.2019.43.04

Schreuder W., Lamprecht S.C., Marasas W.F.O., Calitz F.J., 1995. Pathogenicity of three *Fusarium* species associated with asparagus decline in South Africa. *Plant Disease* 79: 177–181. https://doi.org/10.1094/PD-79-0177.

Schroers H.J., Baayen R.P., Meffert J.P., de Gruyter J., Hooftman M., O'Donnell K., 2004. *Fusarium foetens*, a new species pathogenic to *Begonia elatior* hybrids (*Begonia* x *hiemalis*) and the sister taxon of the *Fusarium oxysporum* species complex. *Mycologia* 96(2): 393–406. https://doi.org/10.1080/15572536.2005.11832984

Schroers H-J., Samuels G.J., Zhang N., Short D.P.G., Juba J., Geiser D.M., 2016. Epitypification of *Fusisporium* (*Fusarium*) *solani* and its assignment to a common phylogenetic species in the *Fusarium solani* species complex. *Mycologia* 108(4): 806–819 https://doi.org/10.3852/15-255

Seifert K.A., Aoki T., Baayen R.P., Brayford D., Burgess L.W., … Waalwijk C., 2003. The name *Fusarium moniliforme* should no longer be used. *Mycological Research* 107(6): 643–644. https://doi.org/10.1017/S095375620323820X

Snyder W.C., Hansen H.N., 1940. The species concept in *Fusarium*. *American Journal of Botany* 27(2): 64–67.

Snyder W.C., Hansen H.N., 1941. The species concept in *Fusarium* with reference to section *Martiella*. *American Journal of Botany* 28(9): 738–742. https://doi.org/10.2307/2436658

Stamatakis A., 2006. RAxML-VI-HPC: maximum likelihood-based phylogenetic analyses with thousands of taxa and mixed models. *Bioinformatics* 22(21): 2688–2690. https://doi.org/10.1093/bioinformatics/btl446

Tai F.L., 1979. *Sylloge Fungorum Sinicorum*. Science Press, Academia Sinica, Peking.

Tamura K., Stecher G., Peterson D., Filipski A., Kumar S., 2013. MEGA6: Molecular Evolutionary Genetics Analysis version 6.0. *Molecular Biology and Evolution* 30(12): 2725–2729. https://doi.org/10.1093/molbev/mst197

Tan Y.P., Conroy J.R., 2024. Nomenclatural novelties. *Index of Australian Fungi* 45: 1–8. https://doi.org/10.5281/zenodo.13858562Tang T., Wang F., Guo J., Guo X., Duan Y., You J., 2021. *Fusarium acuminatum* associated with root rot of Maidong (*Ophiopogon japonicus*) in China. *Plant Disease* 105(6): 1860. https://doi.org/10.1094/PDIS-11-20-2344-PDN

Tan Y.P., Shivas R.G., 2024. Nomenclatural novelties. *Index of Australian Fungi* 31: 1–1. https://doi.org/10.5281/zenodo.10784072

Tang T., Wang F., Guo J., Guo X., Duan Y., You J., 2021. Fusarium acuminatum associated with root rot of maidong (*Ophiopogon japonicus*) in China. *Plant Disease* 105: 6. https://doi.org/10.1094/PDIS-11-20-2344-PDN

Ulaszewski B., Sandoval-Denis M., Groenewald J.Z., Costa M.M., Mishra B., … Thines M., 2025. Genomic features and evolution of lifestyles support the recognition of distinct genera among fusarioid fungi. *Mycological Progress* 24(1): 20. https://doi.org/10.1007/s11557-024-02025-4

Vaidya G., Lohman D.J., Meier R., 2011. SequenceMatrix: concatenation software for the fast assembly of multi-gene datasets with character set and codon information. *Cladistics* 27(2): 171–180. https://doi.org/10.1111/j.1096-0031.2010.00329.x

Van Bakel J.M.M., Krom-Kerstens J.J.A., 1974. Deal stem disease of asparagus caused by *Fusarium culmorum*. *Netherlands Journal of Plant Pathology* 80: 104–109. https://doi.org/10.1007/BF01980615

Vujanovic V., Hamel C., Yergeau E., St-Arnaud M., 2006. Biodiversity and biogeography of *Fusarium* species from northeastern North American asparagus fields based on microbiological and molecular approaches. *Microbial Ecology* 51(2): 242–255. https://doi.org/10.1007/s00248-005-0046-x

Wang M.M., Crous P.W., Sandoval-Denis M., Han S.L., Liu F., ... Cai L., 2022. *Fusarium* and allied genera from China: species diversity and distribution. *Persoonia* 48: 1–53. https://doi.org/10.3767/persoonia.2022.48.01

Wong J., Jeffries P., 2006. Diversity of pathogenic *Fusarium* populations associated with asparagus roots in decline soils in Spain and the UK. *Plant Pathology* 55(3): 331–342. https://doi.org/10.1111/j.1365-3059.2006.01360.x

World Integrated Trade Solution, 2025. *Netherlands asparagus, fresh or chilled exports by country in 2023*. Retrieved November 19, 2025, from https://wits.worldbank.org/trade/comtrade/en/country/NLD/year/2023/tradeflow/Exports/partner/ALL/product/070920

Yilmaz N., Sandoval-Denis M., Lombard L., Visagie C.M., Wingfield B.D., Crous P.W., 2021. Redefining species limits in the *Fusarium fujikuroi* species complex. *Persoonia* 46: 129–162. https://doi.org/10.3767/persoonia.2021.46.05.

Zhuang W.Y., 2005. *Fungi of Northwestern China*. Mycotaxon, Ltd., Ithaca, NY.

Mediterranean Phytopathological Union

Founded by Antonio Ciccarone

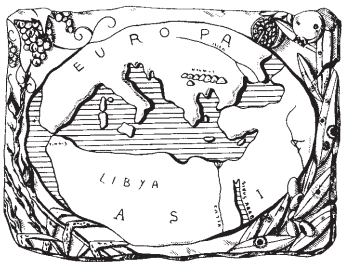

The Mediterranean Phytopathological Union (MPU) is a non-profit society open to organizations and individuals involved in plant pathology with a specific interest in the aspects related to the Mediterranean area considered as an ecological region.
The MPU was created with the aim of stimulating contacts among plant pathologists and facilitating the spread of information, news and scientific material on plant diseases occurring in the area. MPU also intends to facilitate and promote studies and research on diseases of Mediterranean crops and their control.
The MPU is affiliated to the International Society for Plant Pathology.

MPU Governing Board

President
Salah M. Abdel-Momen, Agricultural Research Center, Giza, Egypt,
E-mail: salah1993@yahoo.com

Immediate Past President
Dimitrios Tsitsigiannis, Agricultural University of Athens, Greece
E-mail: dimtsi@aua.gr

Board members
Nihal Buzkan, Faculty of Agriculture, Avşar Campus, 46100 Kahramanmaraş, Türkiye
Diana Fernandez, INRAE, Institute Agro, Montpellier, France
Juan A. Navas-Cortés, Institute for Sustainable Agriculture, Spanish National Research Council, Córdoba, Spain

Honorary President - Treasurer
Giuseppe Surico, DAGRI, University of Florence, Firenze, Italy
E-mail: giuseppe.surico@unifi.it

Secretary
Anna Maria D' Onghia, CIHEAM-Mediterranean Agronomic Institute of Bari, Valenzano, Bari, Italy – E-mail: donghia@iamb.it

Treasurer
Laura Mugnai, DAGRI, University of Florence, Firenze, Italy
E-mail: laura.mugnai@unifi.it

Coordinator of the Advisory Committee
Maria Do Céu Silva, University of Lisbon, Portugal,
E-mail: mariaceusilva@isa.ulisboa.pt

MPU National Society Members

Croatian Plant Protection Society
Egyptian Phytopathological Society (EPS)
French Society of Plant Pathology (SFP)
Hellenic Phytopathological Society (HPS)
Israeli Phytopathological Society (IPS)
Italian Association for Plant Protection (AIPP)
Italian Phytopathological Society (SIPAV)
Italian Nematological Society (SIN)
Palestinian Plant Production and Protection Society (PPPPS)
Plant Protection Society in Bosnia and Herzegovina
Plant Protection Society of Serbia
Plant Protection Society of Slovenia
Portuguese Phytopathological Society (PPS)
Spanish Phytopathological Society
Turkish Phytopathological Society (SEF)

MPU Affiliated Members

Arab Society of Plant Pathology
Euphresco
CIHEAM-Bari
International Mycotoxicology Society
International Society for Plant Pathology

2026 Information for authors of the Open Access journal *Phytopathologia Mediterranea*

Only MPU members are eligible to publish according to MPU membership categories (see https://oajournals.fupress.net/index.php/pm/about):

– All authors belonging to an MPU National Society Member (see list above) or to an MPU Affiliated Member (international organizations or networks), that signed a Memorandum of Understanding with MPU, are entitled to publish with a contribution to publication cost (https://oajournals.fupress.net/index.php/pm/about)

– All Individual Members (not in the above categories), including members of profit or non-profit entities, and physical person.

To become an Individual Member see www.mpunion.org or contact secretariat@mpunion.org

To receive the paper version of the journal please contact phymed@unifi.it

For information visit the MPU web site:
www.mpunion.org
or contact us at: Phone +39 39 055 2755861/862 – E-mail: phymed@unifi.it

Phytopathologia Mediterranea

Volume 65, August, 2026

Contents

Phytopathologia Mediterranea is an Open Access Journal published by Firenze University Press (available at www.fupress.com/pm/) and distributed under the terms of the Creative Commons Attribution 4.0 International License (CC-BY-4.0) which permits unrestricted use, distribution, and reproduction in any medium, provided you give appropriate credit to the original author(s) and the source, provide a link to the Creative Commons license, and indicate if changes were made.
The Creative Commons Public Domain Dedication (CC0 1.0) waiver applies to the data made available in this issue, unless otherwise stated.
Copyright © 2026 Authors. The authors retain all rights to the original work without any restrictions.
Phytopathologia Mediterranea is covered by AGRIS, BIOSIS, CAB, Chemical Abstracts, CSA, ELFIS, JSTOR, ISI, Web of Science, PHYTOMED, SCOPUS and more

Direttore responsabile: Giuseppe Surico • Autorizzazione del Tribunale di Firenze n. 4923 del 5-1-2000 • *Printed by* Logo S.r.l. - Padova, October 2026